

Copyright
by
Kory Lee Kirchner
2014

The Thesis Committee for Kory Lee Kirchner
Certifies that this is the approved version of the following thesis:

**Early Miocene high-pressure metamorphism in the
Nevado-Filabride Complex of the Betic Cordillera,
Spain: implications for subduction in the Western
Mediterranean**

APPROVED BY

SUPERVISING COMMITTEE:

Whitney Behr, Supervisor

Staci Loewy

Daniel Stockli

**Early Miocene high-pressure metamorphism in the
Nevado-Filabride Complex of the Betic Cordillera,
Spain: implications for subduction in the Western
Mediterranean**

by

Kory Lee Kirchner, B.S.

THESIS

Presented to the Faculty of the Graduate School of
The University of Texas at Austin
in Partial Fulfillment
of the Requirements
for the Degree of

MASTER OF SCIENCE IN GEOLOGICAL SCIENCES

THE UNIVERSITY OF TEXAS AT AUSTIN

August 2014

Dedicated to my parents, grandparents, and teachers.

Acknowledgments

I would like to first thank my advisor, Dr. Whitney Behr for accepting me as one of her first graduate students and for composing and refining the goals of this thesis project. Whitney was always available and willing to answer questions and help solve problems throughout the course of my studies. She provided numerous opportunities for me to learn in the field, in the classroom, and at conferences. Whitney's positivity and enthusiasm for geology kept me motivated throughout the completion of the project.

Committee members Dr. Staci Loewy and Dr. Daniel Stockli provided helpful feedback and were instrumental in developing the methodology for my thesis. Staci devoted countless hours to developing the methods, along with Dr. Ben Byerly, and was extremely patient while teaching me how to do geochemistry. Danny provided world-class lab facilities for my research, valuable feedback on my thesis, and took me and my fellow students to see world-class rocks in the field.

I greatly appreciate the generosity of the Jackson School of Geosciences as a whole for accepting me into the program. Support from the Ronald K. DeFord field scholarship and a JSG seed grant facilitated all aspects of my research. Graduate Program Coordinator Phillip Guerrero cheerfully helped me navigate the logistics of graduate school. I am immensely grateful for the

financial support that allowed me to focus my attention on my education while living well in Austin, Texas.

Whitney, Dr. John Platt, and Jason Williams assisted me with my field work and taught me a great deal about the geology of southern Spain. Dr. Juan Ignacio Soto at the Universidad de Granada answered questions and provided useful discussion. Donggao Zhao, Rudra Chatterjee, Eric Kelly, Stephanie Moore, and George Morgan taught me how to use the electron microprobe and assisted in data collection for my thesis. Bill Carlson provided helpful discussion on garnet x-ray map interpretations. Staci and Spencer Seman helped me with mass spectrometry and Dr. John Lassiter and Danny Stockli provided the lab facilities necessary. Fawwaz Aziz helped me hand pick mineral grains. It would have taken a lifetime for me to learn every method utilized in this project were it not for everyone who helped me!

I am most grateful for the opportunities to teach and mentor others while at UT. I would like to thank Dr. Mark Helper for giving me the amazing opportunity to assist him in teaching three classes, including field camp, while at UT. I thoroughly enjoyed teaching geology in the field with Mark, Dr. Randy Marrett, Dr. Tip Meckel, Dr. David Mohrig, Dr. Peter Flaig, Dr. Lesli Wood, Dr. Charlie Kerans, Dr. Greg Frebourg, Dr. Kirt Kempter, Dr. Whitney Behr, Dr. Tim Diggs, Dr. Rich Ketcham, Dr. Brian Horton, and Dr. Jim Gardner. I'd also like to thank my fellow TAs, Meredith Bush, Mike Prior, Maren Mathisen, Ali MacNamee, Kate Atakturk, Rob Dennen, Becky Simon, Edgardo Pujols, Joel Lunsford, Doug Barber, and Nikki Seymour for

enriching my teaching experience. I'd like to thank the students (especially the Honey Badgers) for having great attitudes and being stoked to learn. I also want to thank all of my professors who I had the privilege to learn from over the course of my studies at the Jackson School.

I want to thank everyone who helped me through the stresses of school and gave me opportunities to adventure: Brendan Murphy, Peter Gold, Paul Betka, Rachel Bernard, Dan Arnost, Anine Pedersen, Kenzie Day, Patrick Gustie, Owen Callahan, John Swartz, Bud Davis, Sebastien Ramirez, Dr. Ian Dalziel, Dr. Larry Lawver, Miguel Cisneros, Jake Jordan, Jackie Rambo, Tyler Schulze, Kilian Ashley, Alex Wood, Greg Olson, Nate Duray, Kyle Timblin, Jake Grissom, Alex Cheifetz, Barry and Ethan Dale, Kevin Rayes, and many others.

Finally I must thank my whole family for giving me the opportunities early in life to learn the value of self-assurance and hard work and my parents for inspiring me to pursue geology and explore the Earth. Cheers!

Early Miocene high-pressure metamorphism in the Nevado-Filabride Complex of the Betic Cordillera, Spain: implications for subduction in the Western Mediterranean

Kory Lee Kirchner, M.S. Geo. Sci.
The University of Texas at Austin, 2014

Supervisor: Whitney Behr

The Betic Cordillera of southern Spain is an orogen formed in response to convergence between Africa and Iberia, from the late Mesozoic to the present. The orogen consists of three main tectonic complexes, two of which have been subducted to depth, then exhumed back to the surface over short timescales. Subduction in the structurally higher of these complexes is relatively well constrained to the Eocene, but the timing of high-pressure metamorphism in the structurally lower complex, known as the Nevado-Filabride Complex, has been a topic of debate for several years due to conflicting geochronological data. Several proposed tectonic models for the Nevado-Filabride Complex are based on ages of single mineral phases. For example, models based primarily on $^{40}\text{Ar}/^{39}\text{Ar}$ dating on white mica in high-pressure schists require that the Nevado-Filabride and the overlying tectonic unit, the Alpujarride Complex, were coevally subjected to high-pressure metamorphism in the Eocene,

and subsequently exhumed at different rates. More recent models, based on Lu-Hf dating on prograde garnets in eclogites, separate the timing of high-pressure metamorphism of the Nevado-Filabride Complex from the Alpujaride Complex by at least 10 m.y. We examine the viability of these models using multimineral Rb-Sr dating of blueschist and eclogite facies rocks in the Nevado-Filabride Complex. The multimineral isochron method uses the whole high-pressure mineral assemblage rather than a single phase, which allows testing for isotopic disequilibrium. Statistically valid Rb-Sr ages of two schists and one eclogite from the Nevado-Filabride Complex yield ages of 15.78 ± 0.47 , 15.8 ± 1.1 , and 17.6 ± 1.1 Ma, respectively. The early Miocene Rb-Sr ages are in agreement with garnet Lu-Hf ages and zircon U-Pb ages for high-pressure conditions in the Nevado-Filabride Complex. The new ages imply that two episodes of subduction, punctuated by a period of extension and exhumation, occurred in the Western Mediterranean.

Table of Contents

Acknowledgments	v
Abstract	viii
List of Tables	xii
List of Figures	xiii
Chapter 1.	1
1.1 Introduction	1
1.2 Tectonic Setting	5
1.3 Overview of the Nevado-Filabride Complex	8
1.4 Previous Geochronology in the NFC	11
1.4.1 Ar-Ar Dating	13
1.4.2 U-Pb Dating	14
1.4.3 Lu-Hf Dating	14
1.4.4 Whole Rock Rb-Sr Dating	14
1.5 Conflicting Tectonic Models	15
1.6 Rb-Sr Multimineral Dating Method	19
1.6.1 Sample Selection	19
1.6.2 Microstructural Descriptions of Selected Samples . .	23
1.6.3 Electron Microprobe Analyses	26
1.6.4 Mineral Separation	48
1.6.5 Rb-Sr Measurements using Inductively Coupled Plasma and Thermal Ionization Mass Spectrometry	48
1.7 Results	51
1.8 Discussion	55
1.8.1 Problem Samples	55
1.8.2 Timing of HP metamorphism in the NFC	58

1.8.3	Comparison to other geochronologic data from the NFC	59
1.8.4	Tectonic Implications	62
1.9	Conclusions	66
Chapter 2.	Supplementary Information	68
2.1	Detailed methods	68
2.2	Supplementary Electron Microprobe Data: Cameca SX-50 and JEOL JXA-8200 Analyses	81
Appendix		82
Bibliography		152
Vita		166

List of Tables

1.1	Rock samples collected from the Nevado-Filabride Complex. . .	20
1.2	Mineral composition data for garnet in eclogite and blue schist facies rocks of the Nevado-Filabride Complex, measured by electron microprobe.	33
1.3	Mineral composition data for white mica in eclogite and blueschist facies rocks of the Nevado-Filabride Complex, measured by electron microprobe.	34
1.4	Mineral composition data for omphacites and amphiboles in eclogite facies rocks of the Nevado-Filabride Complex, measured by electron microprobe.	36
1.5	Rb-Sr analytical data.	53

List of Figures

1.1	Regional map of the Alboran Domain and the Betic Cordillera (modified from Comas et al., 1999).	6
1.2	Geologic map of the Nevado-Filabride Complex in southern Spain. Map shows the primary tectonic units of the NFC. The units of interest to this study, the Bedar-Macael and the Calar Alto, are shown in purple and dark blue, respectively. The overlying Alpujarride Complex is shown in red. Starred locations are localities for dated samples in this study: CC: Cortijo del Camarate, RP: Rio Poqueira, and EC: El Chive. Modified from Martínez-Martínez et al. (2002).	9

1.3	Geochronological and stratigraphic age data from the NFC. Bars represent method, mineral used and dated P-T domains. Age data are from: 1. Multimineral Rb-Sr: This study. 2. Lu-Hf: Platt et al. (2006). 3. Ar-Ar: Andriessen et al. (1991); Monie et al. (1991); Augier et al. (2005a); Platt et al. (2005). 4. Rb-Sr on Phengite: Andriessen et al. (1991). 5. Fission Track (FT): Johnson et al. (1997) . 6. Stratigraphic Constraints: Montenat and Ott (1999); Briend et al. (1990); Mora (1993); Vissers et al. (1995); Montenat and Ott (1999); Poisson et al. (1999); Weijermars et al. (1985). 7. U-Pb: Sanchez-Vizcaino et al. (2001). Modified from Augier et al. (2005a).	12
1.4	P-T-t paths showing both coeval and separate subduction of the NFC and AC and slightly different exhumation paths for each complex. Modified from Augier et al. (2005a)	17
1.5	Two conflicting tectonic models for the subduction and exhumation histories of the NFC and AC. Model 1 after Behr and Platt (2012) corresponds with P-T-t path B in Figure 1.4. Model 2 after Vergés and Fernandez (2012) corresponds with P-T-t path A from Figure 1.4.	18

1.6	Sample KB20. A) Photograph of hand sample. B) Photomicrograph of phengite grain in garnet pressure shadow in cross-polarized light (XPL). C and D) Photomicrographs of garnet porphyroblast in a matrix of phengite and omphacite. C was taken in XPL and D was taken in plane polarized light (PPL).	28
1.7	Sample WB163. A and B) Photomicrographs of garnet porphyroblasts in a matrix of white mica, amphibole and omphacite. Garnets are rimmed by amphibole. C and D) Photomicrographs of garnet porphyroblasts rimmed by amphibole and crosscut by late mineralized fractures.	29
1.8	Sample WB164. A and B) Photomicrographs of a garnet porphyroblast in a matrix of white mica, amphibole, rutile, and omphacite. C and D) Photomicrographs of garnet porphyroblasts. Porphyroblasts are the smaller of the bimodal grain size distribution of garnet (photos A and B exemplify the larger component) in the sample and occur in domains oriented parallel to foliation defined by amphibole.	30
1.9	Sample WB137. A and B) Photomicrographs of a euhedral garnet in a matrix of phengite. Inclusions in garnet are quartz and phengite.	31

1.10	Sample KB2. A and B) Photomicrographs of garnet porphyroblasts in a matrix of foliated quartz and white mica. C and D) A closer view of a garnet shown in A and B. E) Field photograph of sample KB2, looking perpendicular to foliation. Kyanite is present in quartz veins throughout the outcrop.	32
1.11	A retrogressed garnet porphyroblast from Sample WB159 – a mylonitized ecogite. A and B) photomicrograph of euhedral garnet in matrix of foliated white mica, amphibole, omphacite and rutile. C) WDS major element map of Mn concentration in garnet (hot colors indicate higher relative concentrations than cool colors). Change in concentration towards the rim suggests two episodes of growth. D) Backscattered electron (BSE) image of garnet showing evidence for two episodes of growth.	37
1.12	EPMA data summary for prograde garnets analyzed in sample KB20. Ternary diagram shows change in garnet composition from more pyrope-rich to more almandine+spessartine-rich from rim to core. WDS maps (hot colors indicate higher relative concentrations than cool colors) for Mn, Mg, Ca, and Fe are shown next to quantitative analyses of their respective oxide weight percents, taken from EPMA transects across garnets.	38
1.13	Ternary diagram shows white mica compositions for each dated sample.	39

1.14	Composition diagram for omphacites in each dated eclogite.	40
1.15	EPMA data summary for garnets analyzed in sample WB163. Ternary diagram shows change in garnet composition from more pyrope-rich to more almandine+spessartine-rich from rim to core. WDS maps (hot colors indicate higher relative concen- trations than cool colors) for Mn and Mg are shown next to quantitative analyses of their respective oxide weight percents, taken from EPMA transects across garnets.	42
1.16	EPMA data summary for garnets analyzed in sample WB164. Ternary diagram shows change in garnet composition from more pyrope-rich to more almandine+spessartine-rich from rim to core. WDS maps (hot colors indicate higher relative concen- trations than cool colors) for Mn, Mg, Ca, and Fe are shown next to quantitative analyses of their respective oxide weight percents, taken from EPMA transects across garnets.	43
1.17	EPMA data summary for prograde garnets analyzed in sam- ple WB137. Ternary diagram shows change in garnet composi- tion from more pyrope-rich to more almandine+spessartine-rich from rim to core. WDS maps (hot colors indicate higher rela- tive concentrations than cool colors) for Mn, Mg, Ca, and Fe are shown next to quantitative analyses of their respective oxide weight percents, taken from EPMA transects across garnets.	45

1.18	A) Photomicrograph of folded white micas in sample WB137. B) BSE image showing density contrast between differing mica compositions. Dark grains are paragonite, lighter grains are phengite. Table 1.2 summarizes characteristic mica compositions in the sample.	46
1.19	EPMA data summary for garnets analyzed in sample KB2. Ternary diagram shows change in garnet composition from more grossular+andradite-rich to more almandine+spessartine-rich from rim to core. WDS maps (hot colors indicate higher relative concentrations than cool colors) for Mn, Mg, Ca, and Fe are shown next to quantitative analyses of their respective oxide weight percents, taken from EPMA transects across garnets. .	47
1.20	Isochrons for all dated samples, calculated with Isoplot software Ludwig (1999). All collected data (Table 1.5) is plotted, but preferred isochrons are shown. Data-point error crosses are 2σ .	54

Chapter 1

1.1 Introduction

Dating eclogite and blueschist-facies metamorphic events is key to determining the timing of subduction in exhumed orogens, but is often fraught with challenges. The most commonly used isotopic systems for high pressure (HP) rocks are for single minerals: for example, $^{40}\text{Ar}/^{39}\text{Ar}$ on phengitic white mica (e.g. Hacker and Wang, 1995; Ring and Layer, 2003), Lu-Hf and Sm-Nd on garnet (e.g. Kylander-Clark et al., 2007; Anczkiewicz et al., 2004), and U-Pb on metamorphic zircon (e.g. Duchêne and Lardeaux, 1997; Rubatto et al., 1998; Zhang et al., 2007). The Ar system may be unreliable because excess Ar is commonly incorporated during HP metamorphism and can be difficult to detect (e.g. Arnaud and Kelley, 1995; de Jong et al., 2001; Sherlock and Kelley, 2002; de Jong, 2003). The Lu-Hf system can be problematic due to Hf-bearing mineral inclusions (e.g. zircon), or due to multiple, temporally distinct stages of garnet growth: for example, late, spessartine-rich rims formed during decompression (Bakker et al., 1989; Scherer et al., 2000; Dempster et al., 2008). The U-Pb system in zircon can also be challenging because the timing of zircon growth is often difficult to constrain; for example, it is not always obvious whether the zircon grew during peak temperatures or peak pressures of metamorphism (Rubatto, 2002; Platt et al., 2006), and the two may not be

coincident in time.

These challenges are exemplified by geochronologic data from high pressure metamorphic rocks in the Betic Cordillera of southern Spain, where debate over the timing of high pressure metamorphism has continued for over a decade (Monie et al., 1991; de Jong, 2003; Augier et al., 2005a; Sanchez-Vizcaino et al., 2001; Whitehouse and Platt, 2003; Platt et al., 2006; Behr and Platt, 2012; Gomez-Pugnaire et al., 2012). The Betic Cordillera formed as a result of slow convergence between Africa and Iberia since the late Mesozoic. Geochronologic data from exhumed high pressure rocks has yet to resolve the complex subduction history of the region. Accuracy in dating strongly affects tectonic models and interpretations of 3-D mantle tomography for the Western Mediterranean because the models hinge on the timing of high pressure metamorphism in the structurally lowest tectonic unit of the Cordillera: the Nevado-Filabride Complex (NFC). The timing of high pressure metamorphism in the NFC has been interpreted to be Eocene (Monie et al., 1991; Augier et al., 2005a) or Miocene (Sanchez-Vizcaino et al., 2001; Platt et al., 2006; Gomez-Pugnaire et al., 2012). Acceptance of an Eocene age for high pressure metamorphism in the NFC leads to models that suggest a single, continuous phase of subduction followed by large-scale exhumation and heating in the Miocene (e.g. Monie et al., 1991; Augier et al., 2005a; Aerden and Sayab, 2008; Vergés and Fernandez, 2012). Alternatively, the acceptance of a Miocene age for high pressure metamorphism suggests a two-stage subduction history, in which subduction was punctuated in time by a pulse of large-scale

exhumation and heating (e.g. Platt et al., 2006; Behr and Platt, 2012).

A geochronologic technique that has recently achieved greater success in constraining the timing of high pressure metamorphism in other orogens is Rb-Sr multi-mineral isochron dating (Sherlock et al., 1999; Glodny et al., 2005, 2008). Although the Rb-Sr system has been used for several decades, new analytical precision allows dating of individual minerals by micro-drilling (Müller et al., 2000), or by bulk mineral separation from carefully selected, small (cm-size) samples (Glodny et al., 2005). This makes the technique well-suited to dating high-pressure metamorphic mineral assemblages, because 1) it allows one to identify and select specific regions within a sample that can be shown to be in textural equilibrium, and to avoid those regions that show patchy retrogression and disequilibrium; and 2) it allows one to quantitatively test for disequilibrium by dating several Sr-bearing minerals that should lie on a single isochron within the analytical uncertainties. The technique has proven invaluable to deciphering the timing of HP metamorphism in several similarly complex metamorphic terranes throughout the Mediterranean region, including in regions where other isotopic systems (e.g. Ar/Ar) yield ambiguous results (Glodny et al., 2005, 2007, 2008; Rosenbaum et al., 2012).

In this thesis, I apply the Rb-Sr multi-mineral isochron technique to equilibrium assemblages within HP metamorphic rocks (blueschists and eclogites) in the Nevado-Filabride Complex, in an effort to resolve the timing of subduction in this unit, and its implications for large-scale tectonics in the Western Mediterranean region. I will demonstrate that the Rb-Sr multi-mineral tech-

nique applied to mafic eclogites and blueschist facies graphitic mica schists yields very similar ages to the Lu-Hf system in garnet for this Complex— a testament to the viability of both systems as geochronometers for high-pressure metamorphism. In the following sections, I begin with an overview of the tectonic setting of the Betic Cordillera and the Nevado-Filabride Complex (Sections 1.2 and 1.3). In Sections 1.4 and 1.5 I discuss the previous geochronologic data from the Complex and the conflicting tectonic models that have arisen from it. Section 1.6 focuses on the methods used to select and date samples using the multi-mineral Rb-Sr technique. In Section 1.7 I present the new geochronologic data for the HP metamorphic event in the Nevado-Filabride Complex, and in Section 1.8 I conclude with a discussion of the implications of these new data for the tectonics of the Western Mediterranean region. The research presented in this thesis will be submitted for publication in Fall, 2014. The citation information for the manuscript will be:

Kirchner, K., Behr, W.M., Loewy, S., Stockli, D., Early Miocene subduction in the Western Mediterranean: constraints from Rb-Sr multi-mineral isochron geochronology.

Disclosure of contributions to this work by other authors. In accordance with the University of Texas at Austin Graduate School rules, I am disclosing the contributions to this thesis by the other authors of future publications discussed above. Whitney Behr composed and refined the direction of research and broad motivation for this research topic. Staci Loewy, Daniel

Stockli, and I refined the techniques used in the research. The main sources of funding for this work were Whitney Behr's start-up fund, a Jackson School of Geosciences seed grant to Whitney Behr, and the Ronald K. DeFord Field Scholarship at the Jackson School of Geosciences. Whitney Behr helped me collect samples and take measurements in the field. Laboratory facilities used in this study were provided by Daniel Stockli (ICPMS), John Lassiter (TIMS), Donggao Zhao (EPMA at UT), and George Morgan (EPMA at OU). Additionally, Whitney Behr, Staci Loewy, Donggao Zhao, George Morgan, Eric Kelly, Stephanie Moore, Ben Byerly, Spencer Seman, and Fawwaz Aziz assisted me in the laboratory. Ideas, interpretations, results, and models were discussed and refined with the help of Whitney Behr. George Morgan and I collected EPMA data for several samples at the OU electron probe laboratory.

1.2 Tectonic Setting

The Betic Cordillera of southern Spain is an orogen formed in response to several million years of slow convergence between Africa and Iberia, from the late Mesozoic to the present (Figure 1.1). The Cordillera is a prime example of late-stage orogenic extension superimposed on an earlier contractional orogeny (Platt and Vissers, 1989). The Cordillera comprises two distinct zones that are defined by their respective stratigraphies, degrees of metamorphism and deformational styles. Significantly shortened, but unmetamorphosed Mesozoic and Tertiary sedimentary rocks characterize the external zone, whereas medium- to high-grade, polydeformed metamorphic rocks are present within

the internal zone, also known as the Alboran domain (Vissers et al., 1995; Martínez-Martínez et al., 2002). Most of the structures exposed in the Alboran domain are extensional, but two of three main tectonic complexes also preserve remnants of early HP/low-temperature metamorphism formed during earlier contraction (Vissers et al., 1995).

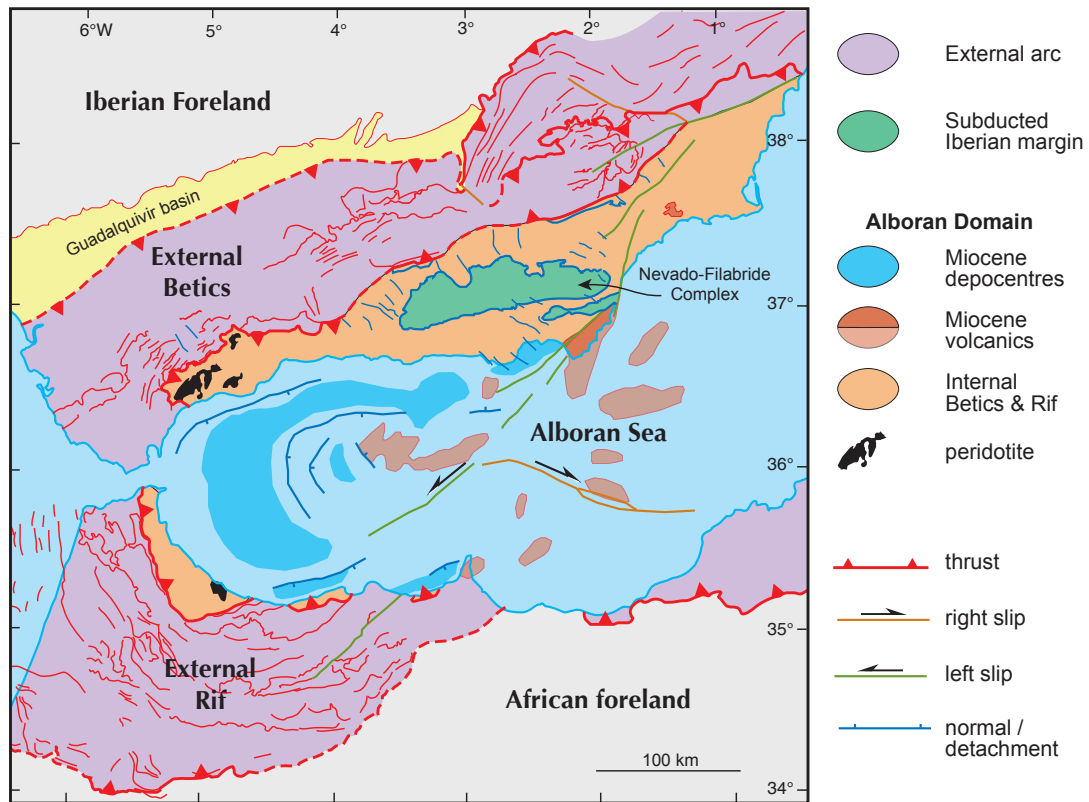


Figure 1.1: Regional map of the Alboran Domain and the Betic Cordillera (modified from Comas et al., 1999).

The Alboran domain's three main tectonic complexes, from structurally highest to lowest, are: 1) the Malaguide Complex (MC), 2) the Alpujaride Complex (AC), and 3) the Nevado-Filabride Complex (NFC). The MC

protolith was a sequence of Silurian to Oligocene marine sedimentary rocks (Chalouan and Michard, 1990). The AC protoliths were a sequence of Paleozoic pelitics and Triassic carbonates (Goffé et al., 1989; Balanya et al., 1997). The NFC protoliths were a Paleozoic sequence of pelitic and psammitic rocks overlain by brecciated, late-Triassic dolostones, as well as discontinuous lenses of basic and ultramafic rocks interpreted to represent a disrupted ophiolite complex (Puga et al., 1999; Platt et al., 2013).

The three complexes are distinguished by sharp increases in metamorphic grade across their contacts with increasing structural depth. These contacts are interpreted to represent large-scale extensional detachments that have cut or reactivated earlier contractional structures (Martínez-Martínez et al., 2002). Rocks of the NFC show greenschist facies metamorphism in the lower tectonic units and amphibolite facies metamorphism in the uppermost unit, with some lenses of blueschist and eclogite facies material interspersed (De Roever and Nijhuis, 1964; Puga, 1971; Puga and Díaz de Federico, 1978; Vissers, 1981; Gomez-Pugnaire and Fernández-Soler, 1987; Bakker et al., 1989). The AC shows pervasive amphibolite to greenschist facies metamorphism that has overprinted low- temperature, high-pressure fabrics (Goffé et al., 1989; Vissers et al., 1995; Azañón and Goffé, 1997; Balanya et al., 1997). The MC rocks are mostly unmetamorphosed but preserve some Variscan orogenic features of low metamorphic grade (Tubía et al., 1992; Vissers et al., 1995).

The timing of subduction in the Alpujarride Complex (AC) is con-

strained to the Eocene, although the exact timing within that period is unknown. Ar-Ar ages from white micas in highly deformed and recrystallized AC rocks suggest HP/high-temperature metamorphism occurred in the complex from 50-30 Ma (Platt et al., 2005). Zircon U-Pb crystallization ages and rare-earth element analyses suggest that a high-temperature event occurred during decompression at 21 Ma (Platt et al., 2003b). Zircon and apatite fission track analysis documents rapid cooling in early Miocene time (19-16 Ma) (Platt et al., 2005). The timing of HP metamorphism in the NFC is debated, and is the focus of this study.

1.3 Overview of the Nevado-Filabride Complex

The NFC is the lowest structural unit within the Betic Cordillera, exposed in the Sierra Nevada-Sierra de los Filabres and the Sierra Alhamilla-Sierra Cabrera culminations (Figure 1.2). The NFC is separated from the overlying AC by brittle detachment faults, which formed along earlier ductile shear zones collectively referred to as the Betic Movement Zone (BMZ) (Platt et al., 1984). The NFC is exposed in the cores of elongated, east-west trending, antiformal dome structures (Figure 1.2), with exposures of AC rocks along the dome margins (Martínez-Martínez et al., 2002). Martínez-Martínez et al. (2002) describe the NFC as having been exhumed by a series of low-angle detachments and refer to the collective mountain ranges as the Sierra Nevada core complex.

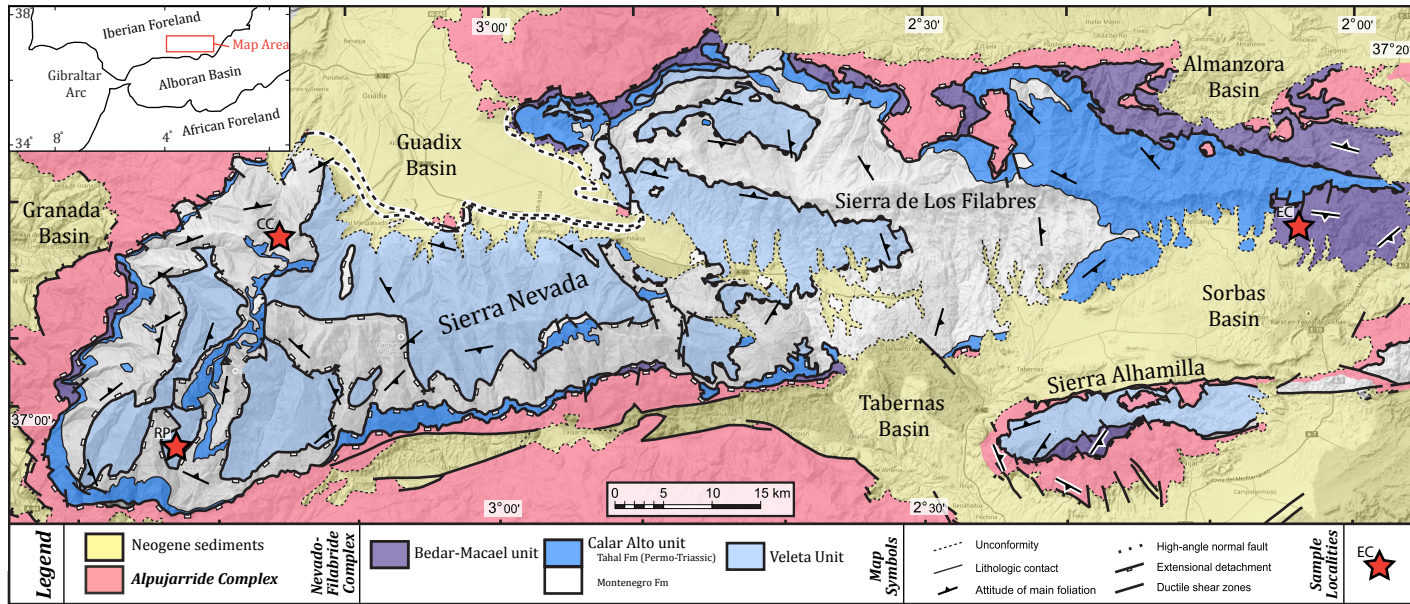


Figure 1.2: Geologic map of the Nevado-Filabride Complex in southern Spain. Map shows the primary tectonic units of the NFC. The units of interest to this study, the Bedar-Macael and the Calar Alto, are shown in purple and dark blue, respectively. The overlying Alpujarride Complex is shown in red. Starred locations are localities for dated samples in this study: CC: Cortijo del Camarate, RP: Rio Poqueira, and EC: El Chive. Modified from Martínez-Martínez et al. (2002).

The NFC comprises two units: the lower Ragua (also known as Veleta) and the upper Mulhacen (Martínez-Martínez et al., 2002). The Ragua unit is composed of thick (kilometer scale) Paleozoic graphitic mica schists with quartzite beds and graphitic marble lenses (Priem et al., 1966). The exposures of the Mulhacen unit in the Sierra Nevada-Sierra de los Filabres are the focus of this project; they are further divided into the Bedar-Macael and Calar Alto units. The Calar Alto unit is composed of folded Permo-Triassic schists and Paleozoic graphitic-mica-schists that are overlain by a sequence of light schists, quartzites, metaconglomerates, and marbles (Martínez-Martínez, 1984, 1986; Martínez-Martínez et al., 2002). The Bedar-Macael unit is a similar, but thinner sequence of metamorphic rocks that have been folded, thrust, and intruded by Permian metagranites (Priem et al., 1966; García-Dueñas et al., 1988). Vissers et al. (1995) note that the mylonites in the BMZ, along which the NFC was exhumed, show a progressive, counterclockwise change of motion from north in the Sierra Alhamilla to southwest in the western Sierra Nevada (Figure 1.2). (Jabaloy et al., 1993) established that top-to-the-west is the dominant sense of motion along the BMZ. Quartz c-axis fabrics and stretching lineation data from the Sierra Alhamilla provide evidence for a change in the dominant stretching direction in the NFC over time from northeast-southwest to east-west (Behr and Platt, 2012). Behr and Platt (2012) suggest a southeast subduction polarity, on the basis of the south-southwest shear sense indicators in the NFC.

Thermobarometric analyses done in various studies reveal an inverted

metamorphic gradient, i.e., higher temperatures were reached towards the structurally higher units of the NFC (Platt et al., 2006; Behr and Platt, 2012). This inverted gradient was interpreted by Behr and Platt (2012) to have formed during subduction of the NFC beneath the hot, thin, Alboran lithosphere. Other workers have interpreted the gradient as a result of a late-stage thermal overprint (De Roever and Nijhuis, 1964; Vissers, 1981; Bakker et al., 1989). Lenses of mafic eclogites and blueschist facies garnet-kyanite-mica schist are present throughout the Mulhacen unit, but are absent in the Ragua unit (Platt et al., 2006). These rocks preserve high pressure/moderate temperature mineral assemblages, in some localities overprinted by amphibolite to greenschist facies retrogression (Augier et al., 2005b). The unretrogressed mineral phases in these lenses record the early HP history of the NFC and their presence is of key importance to understanding the timing of subduction.

1.4 Previous Geochronology in the NFC

Numerous geochronological and thermochronological studies have been conducted in an effort to establish the timing of HP metamorphism in the NFC. Here I summarize each technique that has been applied previously and their outcomes. The geochronologic data for all of the NFC are compiled in Figure 1.3 for reference.

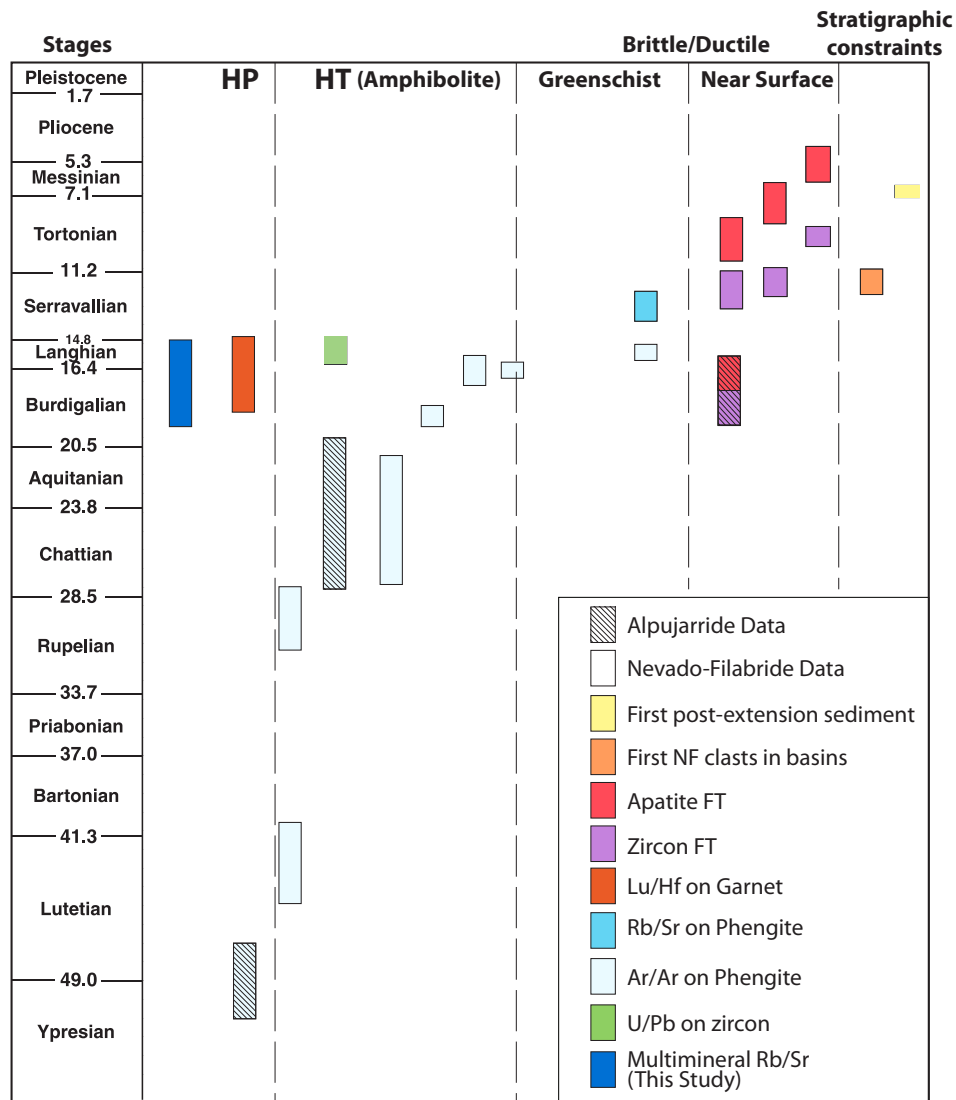


Figure 1.3: Geochronological and stratigraphic age data from the NFC. Bars represent method, mineral used and dated P-T domains. Age data are from: 1. Multimineral Rb-Sr: This study. 2. Lu-Hf: Platt et al. (2006). 3. Ar-Ar: Andriessen et al. (1991); Monie et al. (1991); Augier et al. (2005a); Platt et al. (2005). 4. Rb-Sr on Phengite: Andriessen et al. (1991). 5. Fission Track (FT): Johnson et al. (1997). 6. Stratigraphic Constraints: Montenat and Ott (1999); Briend et al. (1990); Mora (1993); Vissers et al. (1995); Montenat and Ott (1999); Poisson et al. (1999); Weijermars et al. (1985). 7. U-Pb: Sanchez-Vizcaino et al. (2001). Modified from Augier et al. (2005a).

1.4.1 Ar-Ar Dating

$^{40}\text{Ar}/^{39}\text{Ar}$ ages of HP rocks in the NFC obtained by Monie et al. (1991) and Augier et al. (2005a) suggest that HP metamorphism occurred during Oligocene or Eocene time (Figure 1.3). Monie et al. (1991) interpreted their Ar-system age on a barroisitic amphibole to be representative of early blueschist and eclogite facies metamorphism in the NFC at 48 Ma. On the basis of an $^{40}\text{Ar}/^{39}\text{Ar}$ age on phengite, they bracket the end of the HP event to the early Miocene at 25 Ma (Monie et al., 1991). (Augier et al., 2005a) collected *in situ* Ar/Ar data on white mica occurring in different microstructural contexts. Relict, large, porphyroclastic grains gave ages of between 43-25 Ma, whereas smaller, recrystallized grains in shear bands yielded younger ages ranging from 22-18 Ma and clustering around 14 Ma. (Augier et al., 2005a) interpreted the older micas to represent those that grew during the prograde phase of HP metamorphism, and the younger micas to represent progressive resetting of the Ar systematics during exhumation. Behr and Platt (2012) also collected Ar data from *in situ* white mica grains in different microstructural contexts, but found a much wider spread in their ages – they attributed their highly variable ages (180-8 Ma) to excess Ar in the NFC. de Jong (2003) used Ar-Ar dating on high pressure phengites from the NFC and found highly variable ages from ~66-17 Ma. de Jong (2003) attributed the age variability to incorporation of excess ^{40}Ar and isotopic inheritance under conditions of recrystallization and restricted fluid mobility.

1.4.2 U-Pb Dating

Sanchez-Vizcaino et al. (2001) interpreted the average age of HP metamorphism to be ~ 15 Ma for the NFC on the basis of Sensitive High Resolution Ion MicroProbe (SHRIMP) measurements of U-Pb ratios on zircon overgrowths in Mulhacen unit eclogites. These ages were corroborated by (Gomez-Pugnaire et al., 2012), who determined a more precise age of 17.3 ± 0.4 Ma for the NFC using the same methods as (Sanchez-Vizcaino et al., 2001).

1.4.3 Lu-Hf Dating

Platt et al. (2006) obtained Lu-Hf ages for garnet in NFC rocks ranging from ~ 18 -14 Ma. Two eclogites were dated from lenses within the Bedar-Macael and Calar Alto Units of the NFC. A garnet mica schist was dated from the Calar Alto Unit. The isochrons are defined by multiple garnet separates, apatite, and a clinopyroxene or whole rock separate. In addition to Lu-Hf, Platt et al. (2006) conducted Ar-Ar dating on eight samples from the NFC. Five of eight of their Ar-Ar ages corroborated the Lu-Hf ages, and the others (~ 75 -40 Ma) were interpreted to have been influenced by excess Ar.

1.4.4 Whole Rock Rb-Sr Dating

de Jong (2003) attempted to date metamorphic events in the NFC by measuring whole rock Rb-Sr ratios; these authors obtained variable ages between 66 to 14 Ma. They interpreted age variation in graphitic mica schists from the NFC to show evidence for open system behavior in the Rb-Sr iso-

topic system over time. Additionally, they speculated that graphite may have inhibited phengite from fully recrystallizing and thereby incorporating a representative Rb-Sr component during the metamorphic event shown to have occurred at 15 Ma by Sanchez-Vizcaino et al. (2001). In contrast, two whole rock Rb-Sr dates from quartz-rich, graphite-poor samples yielded 14 Ma and 17 Ma ages (de Jong, 2003). These ages correlate with U-Pb ages discussed above, but they are difficult to interpret due to the variability in age data from other samples in the de Jong (2003) study.

1.5 Conflicting Tectonic Models

The geochronologic data collected from the Betic Cordillera has a significant impact on tectonic models and interpretations of geophysical data from the western Mediterranean region, but several models conflict due to the ambiguity in interpreting the existing geochronologic data, particularly with respect to the timing of HP metamorphism. For example, an Eocene-Oligocene age for high pressure metamorphism, as suggested by Monie et al. (1991) and Augier et al. (2005a), would suggest that both the NFC and AC were subducted together and subsequently exhumed at different rates (Figure 1.4, A). The model proposed by Augier et al. (2005a), for instance, maintains that the NFC was subducted at ~ 30 Ma and exhumed from ~ 22 -18 Ma, close to, but shortly after the main exhumation event in the Alpujarride Complex. Additionally, a recent tectonic model proposed by Vergés and Fernandez (2012) suggests that slab break-off occurred below the Alboran Domain in the Early

Miocene, after which subduction ceased permanently.

In contrast to an Eocene-Oligocene age for HP metamorphism, acceptance of an early Miocene age in the Nevado-Filabride complex requires that the NFC was subducted after the AC was already exhumed to the surface. For example, Behr and Platt (2012) suggest a two phase subduction and exhumation model for the Betic Cordillera on the basis of the early Miocene Lu-Hf ages and thermal modeling of the NFC (e.g. Figure 1.4, B). Their model suggests that the NFC was subducted in the early Miocene beneath previously thinned Alboran lithosphere that was heated and attenuated during exhumation of the Alpujarride Complex. Subsequently, the NFC was exhumed in two stages: first along a subduction channel and later along a low-angle detachment fault, by ~ 7 Ma (Behr and Platt, 2012). Additionally, Bezada et al. (2013) interpret mantle tomography beneath the Alboran Domain as a continuous slab. This model contradicts the interpretations of Vergés and Fernandez (2012), who suggested that the slab was detached in the early Miocene. If the mantle tomography interpretations of Bezada et al. (2013) are correct, then a slab break-off event in the Early Miocene, as proposed by Vergés and Fernandez (2012) is impossible. Additionally, if the Early Miocene ages for high pressure metamorphism are correct, then slab breakoff in the Early Miocene is unlikely, because breakoff implies that subduction had ended. Figure 1.5 offers a visual summary of the two conflicting models.

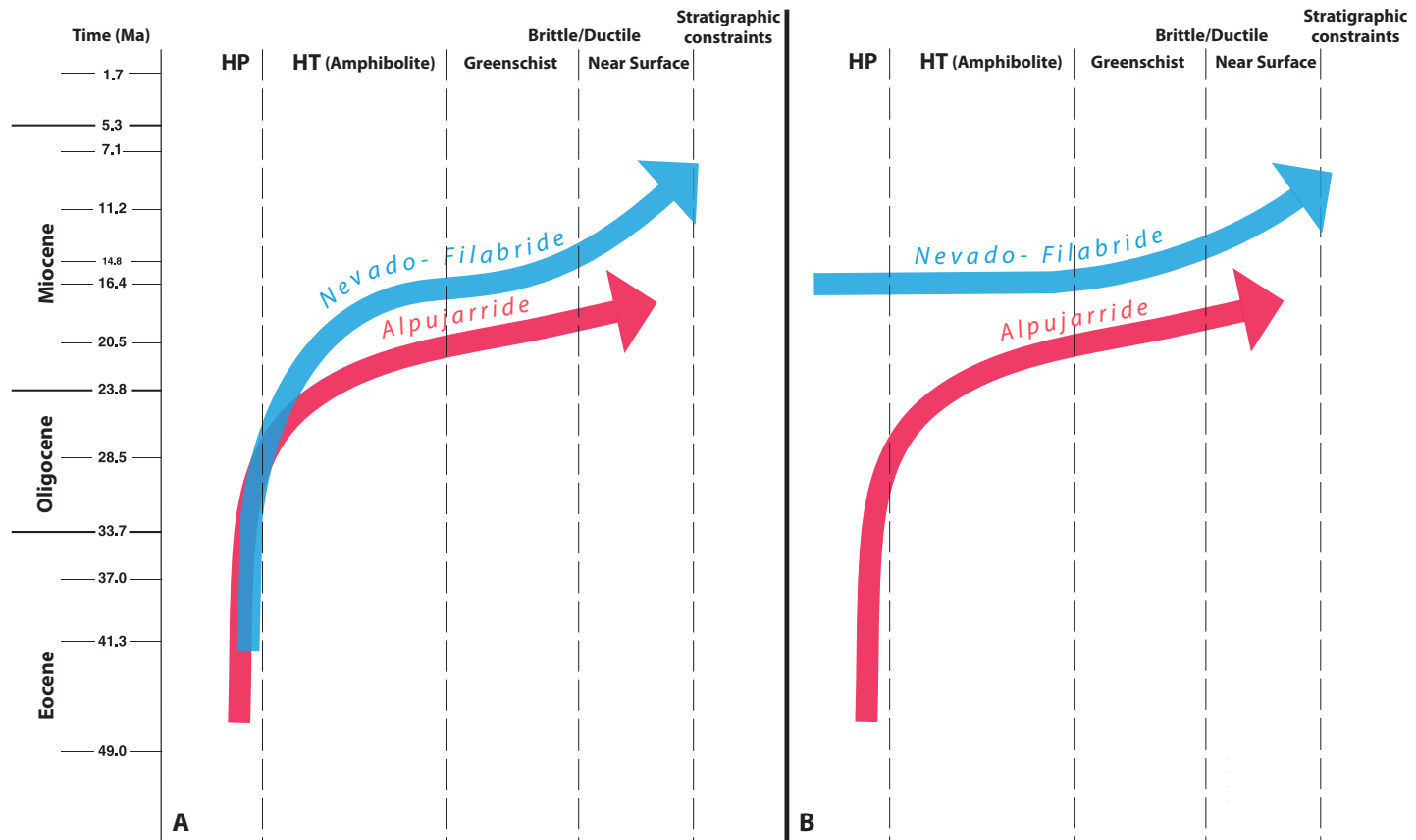


Figure 1.4: P-T-t paths showing both coeval and separate subduction of the NFC and AC and slightly different exhumation paths for each complex. Modified from Augier et al. (2005a)

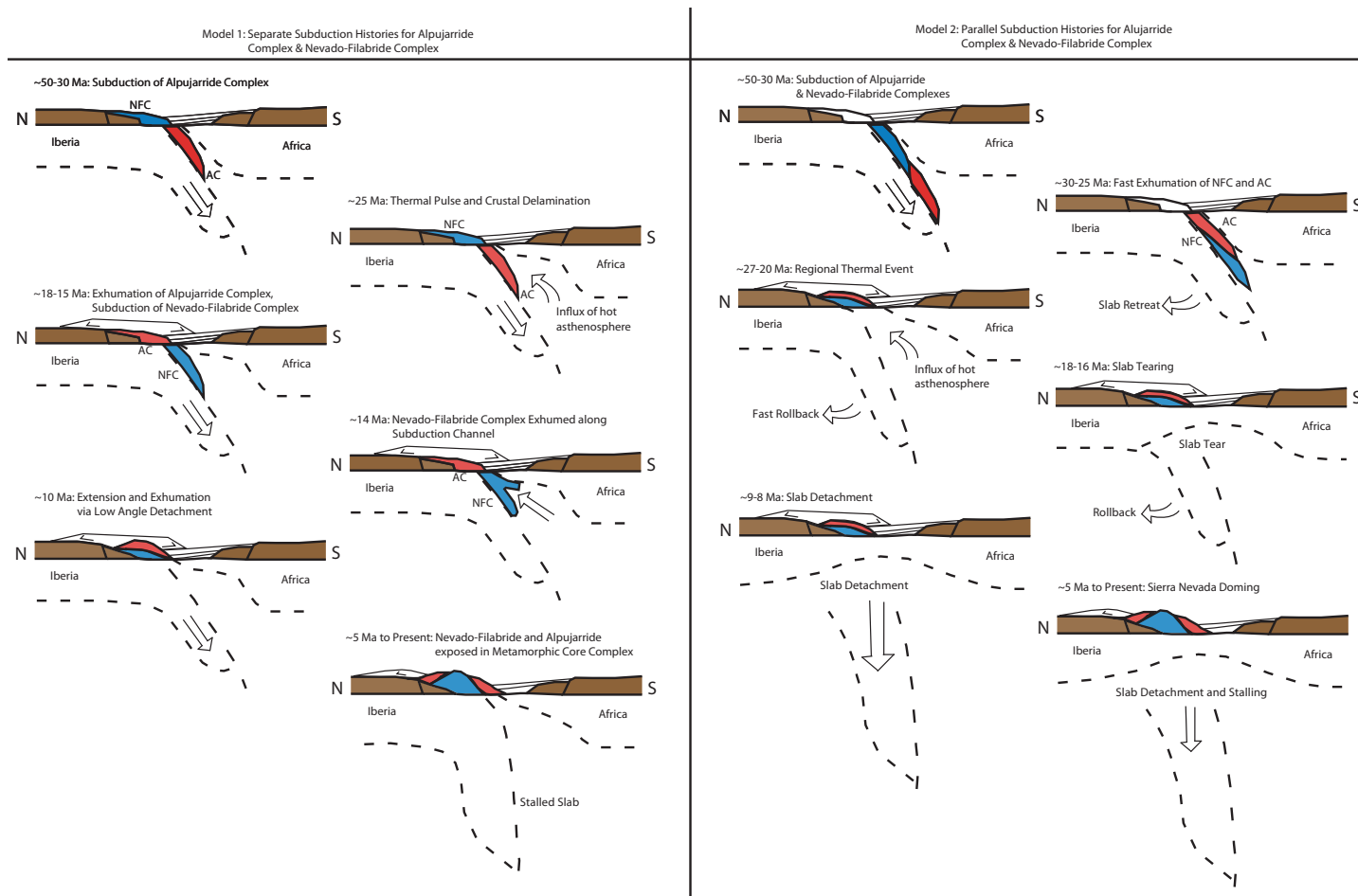


Figure 1.5: Two conflicting tectonic models for the subduction and exhumation histories of the NFC and AC. Model 1 after Behr and Platt (2012) corresponds with P-T-t path B in Figure 1.4. Model 2 after Vergés and Fernandez (2012) corresponds with P-T-t path A from Figure 1.4.

1.6 Rb-Sr Multiminerall Dating Method

Distinguishing between the tectonic models described above requires a more discriminant method of dating high pressure metamorphism in the NFC. The Rb-Sr multiminerall technique (e.g. Glodny et al., 2005, 2008) is a more discriminant method because 1) it allows one to identify and select specific regions within a sample that appear to be in textural equilibrium, and to avoid those regions that show patchy retrogression and disequilibrium; and 2) it allows one to quantitatively test for disequilibrium by dating several Sr-bearing minerals that should lie on a single isochron within the analytical uncertainties (e.g. Glodny et al., 2005), if formed during a single phase of metamorphism. Here we follow the methods outlined by Glodny et al. (2005) to select and date HP assemblages within the NFC in order to constrain the timing of HP metamorphism.

1.6.1 Sample Selection

Eclogite and blueschist facies rock samples were collected in the field from outcrop and subcrop of NFC rocks, as well as in drainages leading to known outcrops that were inaccessible due to snow cover. The primary sample localities are marked in Figure 1.2, and GPS coordinates of sample locations are provided in Table 1.1. Samples showing little to no evidence for retrogression were chosen for further analysis by optical and electron microscopy.

37 samples were collected in the field and examined in detail via an optical microscope. The samples can be subdivided into the following 5 categories

Table 1.1: Rock samples collected from the Nevado-Filabride Complex.

Sample Name	Rock Type	Category	Locality	GPS Coordinates
KB1	Altered gabbro	N/A	Other	N 37 15.872', W 2 12.571'
KB2	Garnet-kyanite schist	3	EC	N 37 11.149', W 2 4.501'
KB3	Metagabbro	N/A	Other	N 37 14.133', W 3 12.478'
KB4	Psammitic schist	5	CC	N 37 10.109', W 3 16.152'
KB5	Amphibolite	4	CC	N 37 9.956', W 3 16.443'
KB6	Graphitic schist	5	CC	N 37 9.964', W 3 16.428'
KB7	Amphibolitized eclogite	4	CC	N 37 10.007', W 3 16.477'
KB8	Amphibolitized eclogite	4	CC	N 37 10.006', W 3 16.479'
KB9	Amphibolitized eclogite	4	RP	N 36 55.651', W 3 24.925'
KB10	Eclogite	2	RP	N 36 59.489', W 3 20.991'
KB11	Amphibolitized eclogite	4	RP	N 37 0.864', W 3 20.020'
KB12	Amphibolitized eclogite	4	RP	N 37 0.864', W 3 20.020'
KB13	Metagabbro	N/A	RP	N 37 0.864', W 3 20.020'
KB14	Metagabbro	N/A	RP	N 37 0.864', W 3 20.020'
KB15	Amphibolite	4	RP	N 37 0.864', W 3 20.020'
KB16	Greenschist	5	RP	N 37 0.864', W 3 20.020'
KB17	Amphibolitized eclogite	4	RP	N 37 0.864', W 3 20.020'
KB18	Greenschist	5	RP	N 37 0.864', W 3 20.020'
KB19	Calc-schist	5	RP	N 37 0.864', W 3 20.020'
KB20	Eclogite	1	RP	N 37 0.864', W 3 20.020'
KB21	Amphibolitized eclogite	4	RP	N 37 0.864', W 3 20.020'
KB22	Schist	5	LQ	N 37 14.016', W 3 12.583'
KB23	Schist	5	LQ	N 37 14.016', W 3 12.583'
KB24	Graphitic schist	5	LQ	N 37 14.040', W 3 12.679'
KB25	Metagranite	N/A	LQ	N 37 14.070', W 3 12.686'
KB26	Amphibolite	4	LQ	N 37 14.069', W 3 12.685'
KB27	Amphibolitized eclogite	4	LQ	N 37 14.076', W 3 12.686'
KB28	Garnet schist	5	LQ	N 37 14.076', W 3 12.686'
KB29	Amphibolitized eclogite	4	LQ	N 37 14.076', W 3 12.686'
KB30	Amphibolitized eclogite	4	LQ	N 37 14.076', W 3 12.686'
WB137	Garnet schist	3	RP	N 36 55.604', W 3 24.922'
WB159	Mylonitic eclogite	2	CC	N 37 10.081', W 3 16.456'
WB160	Amphibolitized eclogite	4	CC	N 37 10.081', W 3 16.456'
WB161	Amphibolite	4	CC	N 37 10.081', W 3 16.456'
WB162	Amphibolite	4	CC	N 37 10.081', W 3 16.456'
WB163	Eclogite	1,2	CC	N 37 10.081', W 3 16.456'
WB164	Eclogite	2	CC	N 37 10.081', W 3 16.456'

based on their protoliths and apparent degrees of retrogression.

Category 1: mafic eclogites with little to no evidence for retrogression.

Mafic eclogites occur as lenses within the Mulhacen schist. Higher metamorphic grade rocks generally occur at the core of the lenses, and are enveloped in amphibolite to greenschist facies rocks. Because *in situ* outcrops are retrogressed and do not expose pristine eclogite, the best exposures of these rocks are found in resistant cobbles and boulders in drainages. The dated samples from this category were collected as float blocks in the Rio Poqueira and Cortijo del Camarate localities, downstream from known outcrops of eclogite (Figure 1.2, localities 'RP' and 'CC'). These rocks generally show an S1 fabric defined by omphacite and white mica with garnet porphyroblasts. Category 1 includes samples KB20 and WB163.

Category 2: mafic eclogites with minor evidence for retrogression.

Exposures of mafic eclogites observed in the field (Figure 1.2, locality 'CC') are commonly lens shaped, with an average long axis length of 5m and a short axis length of 2m. These rocks generally show an S1 fabric defined by omphacite, white mica, and amphibole with garnet porphyroblasts. Category 2 includes samples WB164 and WB159.

Category 3: mafic eclogites with strong microstructural evidence for retrogression and overprinting to amphibolite facies.

Exposures of retrogressed mafic eclogites observed in the field are commonly lens shaped, with an average long axis length of 5m and a short axis length of 2m. The retrogressed eclogites show strong S1 fabrics defined by amphibole and white mica with poorly preserved omphacite. No Category 3 samples were chosen for further analysis.

Category 4: garnet-kyanite schists with little evidence of retrogression.

Exposures of garnet-kyanite schists observed in the field near El Chive (Figure 1.2, locality 'EC') are commonly lens shaped with an average long axis length of 6m and short axis length of 3m. These rocks generally show an S1 fabric defined by white mica with garnet porphyroblasts. Category 3 includes sample KB2 and WB137.

Category 5: retrograde schists.

The most common rock type in the Nevado-Filabride Complex is a thick sequence of graphitic mica schists that contain no high pressure mineral assemblages. These rocks are commonly overprinted by F2 folds, contain abundant chlorite, relict kyanite (or absence of kyanite), low-Si micas (Behr and Platt, 2012) .

Out of the samples collected, we selected 6 from Categories 1, 2, and 4 for further analysis based on their microstructural relationships.

1.6.2 Microstructural Descriptions of Selected Samples

Sample KB20 – Eclogite (Category 1).

Sample KB20 was collected from float blocks in Rio Poqueira below known outcrops of eclogite in Mulhacen schist. This sample shows a consistent foliation defined by omphacite and white mica with abundant euhedral garnets. The mineral assemblage includes omphacite, white mica, garnet, and trace amphibole and apatite. Omphacite and white mica define an S1 fabric. Euhedral garnet porphyroblasts range from \sim 1-3 mm in diameter and have pressure shadows that contain quartz and white mica parallel to S1 (Figure 1.6). Inclusions of omphacite, white mica, epidote, rutile, and quartz are present in garnet and are roughly parallel to S1. Amphibole occurs in trace amounts along garnet rims.

Sample WB163 – Eclogite (Category 1-2).

Sample WB163 was collected from float blocks below lens-shaped outcrops of eclogite in Mulhacen schist near Cortijo del Camarate. The mineral assemblage consists of omphacite, white mica, garnet, amphibole, and apatite. Sample exhibits an S1 foliation defined by omphacite and white mica with abundant euhedral garnet porphyroblasts. Domains of larger grain sizes are present, parallel to the main foliation and contain white micas up to 2 mm

long and 1 mm wide. Aligned omphacites and amphiboles define a weak S1 foliation. Weakly aligned white micas occur in coarse-grained domains parallel to S1. Euhedral garnet porphyroblasts have diameters ranging from 0.5-3 mm and are commonly rimmed with amphibole. Inclusions of omphacite and white mica are present in garnet and show no preferred orientations. A set of micro-scale fractures crosscuts the S1 fabric and is defined by oxide minerals (Figure 1.7).

Sample WB164 – Mylonitic eclogite (Category 2).

Sample WB164 was collected from float blocks below lens-shaped outcrops of eclogite and amphibolite in Mulhacen schist near Cortijo del Camarate. Sample shows distinct domains of aligned amphiboles and omphacites, both interspersed with white mica and garnets. Euhedral garnet porphyroblasts have a bimodal grain size distribution (one population less than 1mm and one greater than 2mm in diameter) and have pressure shadows aligned parallel to foliation. The mineral assemblage consists of omphacite, white mica, garnet, amphibole, apatite, and trace rutile. Aligned omphacites and amphiboles define an S1 foliation. Amphibole rims garnet porphyroblasts. Rare rutile occurs parallel to S1.

Sample WB159 – Mylonitic eclogite (Category 2).

Sample WB159 was collected from float blocks below outcrops of eclogite in Mulhacen schist near Cortijo del Camarate. Sample shows foliation

defined by omphacite and white mica with abundant euhedral garnet porphyroblasts. The mineral assemblage consists of omphacite, white mica, garnet, amphibole, and apatite. Omphacite and white mica define an S1 fabric. Euhedral garnet porphyroblasts have diameters ranging from 0.5-2mm and contain inclusions of white mica. Rutile and amphibole are rare and commonly aligned with foliation.

Sample WB137 – Garnet-mica schist (Category 3).

Sample WB137 was collected from float blocks in Rio Poqueira below outcrops of the Tahal schist, a unit within the Mulhacen. White mica defines a strong foliation and euhedral garnet porphyroblasts range from 3-5 mm in diameter (Figure 1.9). Garnets include abundant inclusions of white mica and quartz. The assemblage consists of white mica, quartz, garnet, and apatite. White mica and quartz define an S1 foliation. A weakly developed set of F2 crenulations crosscuts S1 and is visible in hand sample. Limbs of F2 crenulations are composed of $\sim 250\text{-}500\ \mu\text{m}$ white mica grains whereas the white mica is partly recrystallized to a grain size of $\sim 125\ \mu\text{m}$ along the crenulation hinges.

Sample KB2 – Garnet-kyanite-mica schist (Category 3).

Sample KB2 was collected from an lens shaped outcrop of blueschist within the Mulhacen schist near El Chive. Radiating kyanite crystals are present in quartz veins throughout outcrop. Quartz and mica define a foliation

and euhedral garnet porphyroblasts range from \sim 1-3mm in diameter. Many garnets are slightly oxidized along fractures localized to garnet grains, visible in thin section (Figure 1.10). The assemblage consists of white mica, quartz, garnet, kyanite, and apatite. White mica and quartz define an S1 foliation.

1.6.3 Electron Microprobe Analyses

All quantitative mineral analyses, backscatter electron images and X-ray element maps were obtained by electron probe microanalysis (EPMA) at The University of Texas at Austin with a JEOL JXA-8200 and at The University of Oklahoma with a Cameca SX-50. Analyses of micas, amphiboles, and omphacites were performed with an accelerating voltage of 15 kV, a beam current of 12 nA and an electron beam of diameter 2 μ m. Mineral analyses of garnets were performed with an accelerating voltage of 15 kV, a beam current of 25 nA, and an electron beam of diameter 0 μ m. The dwell time for garnet maps was 25 ms. Obtained data were corrected for absorption, atomic number, fluorescence and background using the Phi-Rho-Z method. Albite (Na), adularia (K), forsterite (Mg), grossular (Si), spessartine (Mn), magnesiochromite (Cr), titanite glass (Ti), augite (Fe), phlogopite (Mg), labradorite (Al), rhodonite (Mn), anorthite (Al), enstatite (Si, Mg), fayalite (Fe), and pyrope (Mg) were used as primary standards. Augite and pyrope were used as secondary standards for Si, Al, Mg, Fe, Mn, and Ca. Characteristic composition data for minerals in each sample are displayed in Tables 1.2, 1.3, and 1.4. Detailed descriptions of procedures, standards used, and all data collected are

compiled in Section 2.2.

Our primary goal with the electron probe analysis was to identify and/or confirm the presence of prograde minerals, particularly garnet and white mica, which can also grow and/or be stable phases during retrogression. For prograde garnets, major element maps and quantitative analysis transects should show (a) CaO and MnO enrichment towards the core, (b) depletion of MgO towards the core, and (c) increasing Mg# from rim to core. Augier et al. (2005a) found phengite with high Si (3.0-3.40 c.p.f.u Si) in high pressure rocks from the NFC. Our criteria to identify phengite on with EPMA were high-Si, low-Na, and high-Fe in white mica grains. Table 1.3 summarizes the mica compositions used in the dated samples. Probe analyses were conducted for a total of six samples, and are described for each sample below.

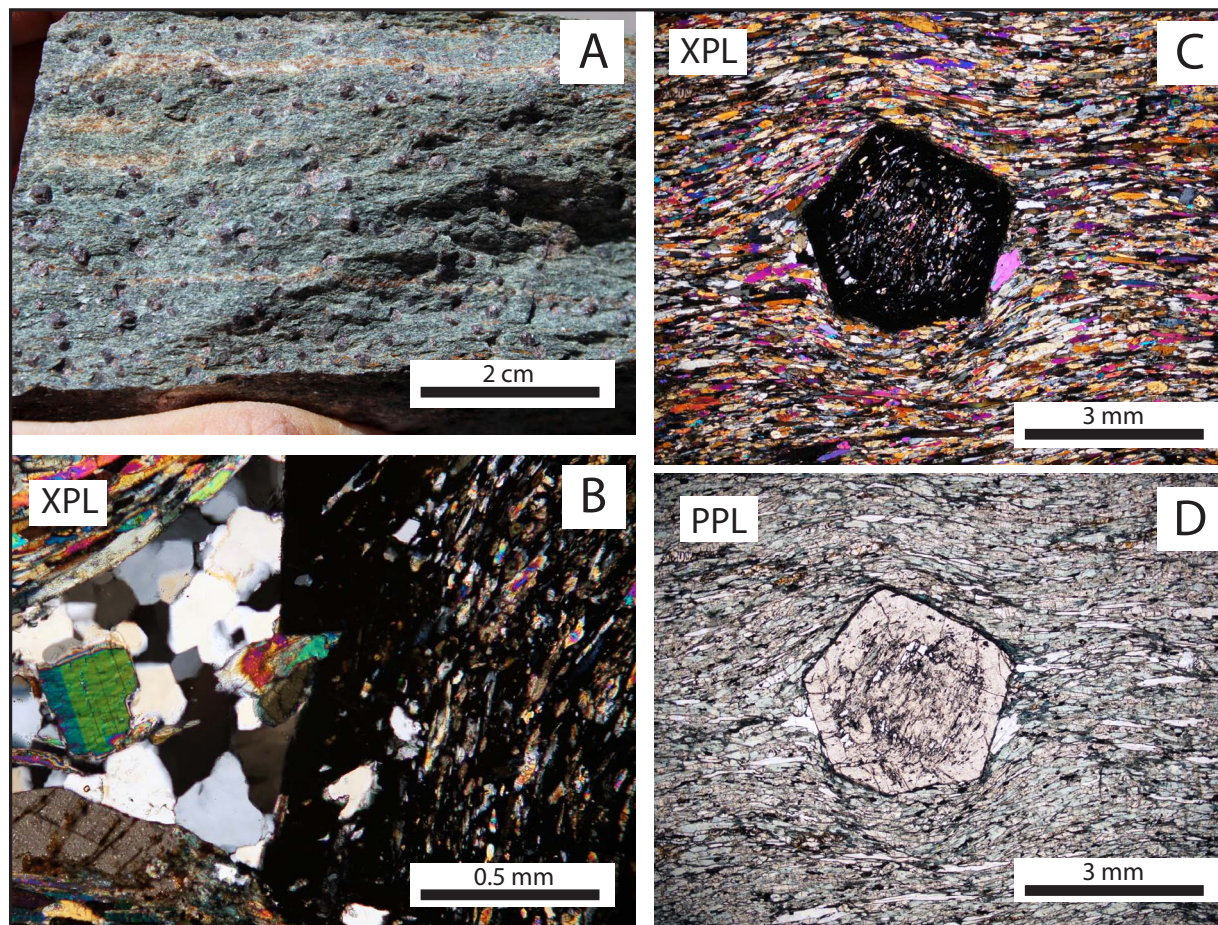


Figure 1.6: Sample KB20. A) Photograph of hand sample. B) Photomicrograph of phengite grain in garnet pressure shadow in cross-polarized light (XPL). C and D) Photomicrographs of garnet porphyroblast in a matrix of phengite and omphacite. C was taken in XPL and D was taken in plane polarized light (PPL).

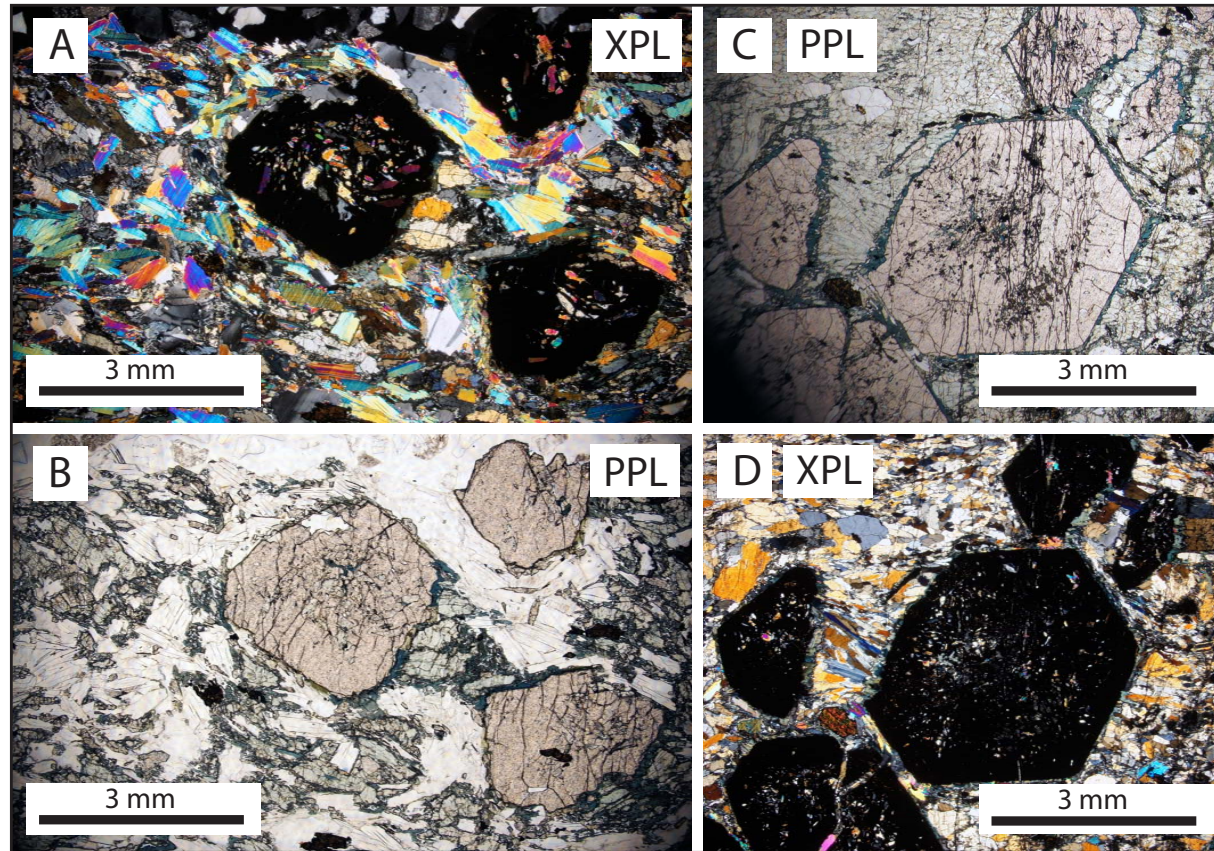


Figure 1.7: Sample WB163. A and B) Photomicrographs of garnet porphyroblasts in a matrix of white mica, amphibole and omphacite. Garnets are rimmed by amphibole. C and D) Photomicrographs of garnet porphyroblasts rimmed by amphibole and crosscut by late mineralized fractures.

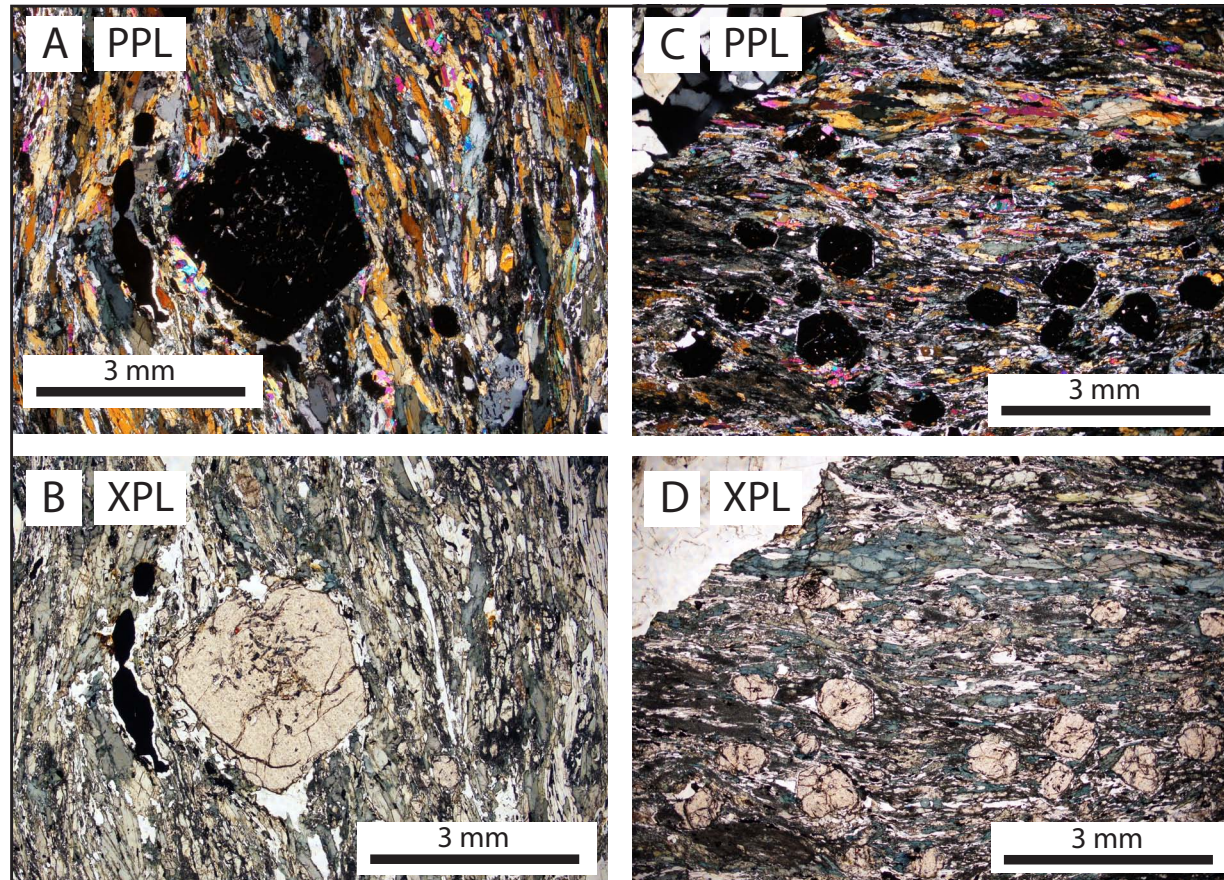


Figure 1.8: Sample WB164. A and B) Photomicrographs of a garnet porphyroblast in a matrix of white mica, amphibole, rutile, and omphacite. C and D) Photomicrographs of garnet porphyroblasts. Porphyroblasts are the smaller of the bimodal grain size distribution of garnet (photos A and B exemplify the larger component) in the sample and occur in domains oriented parallel to foliation defined by amphibole.

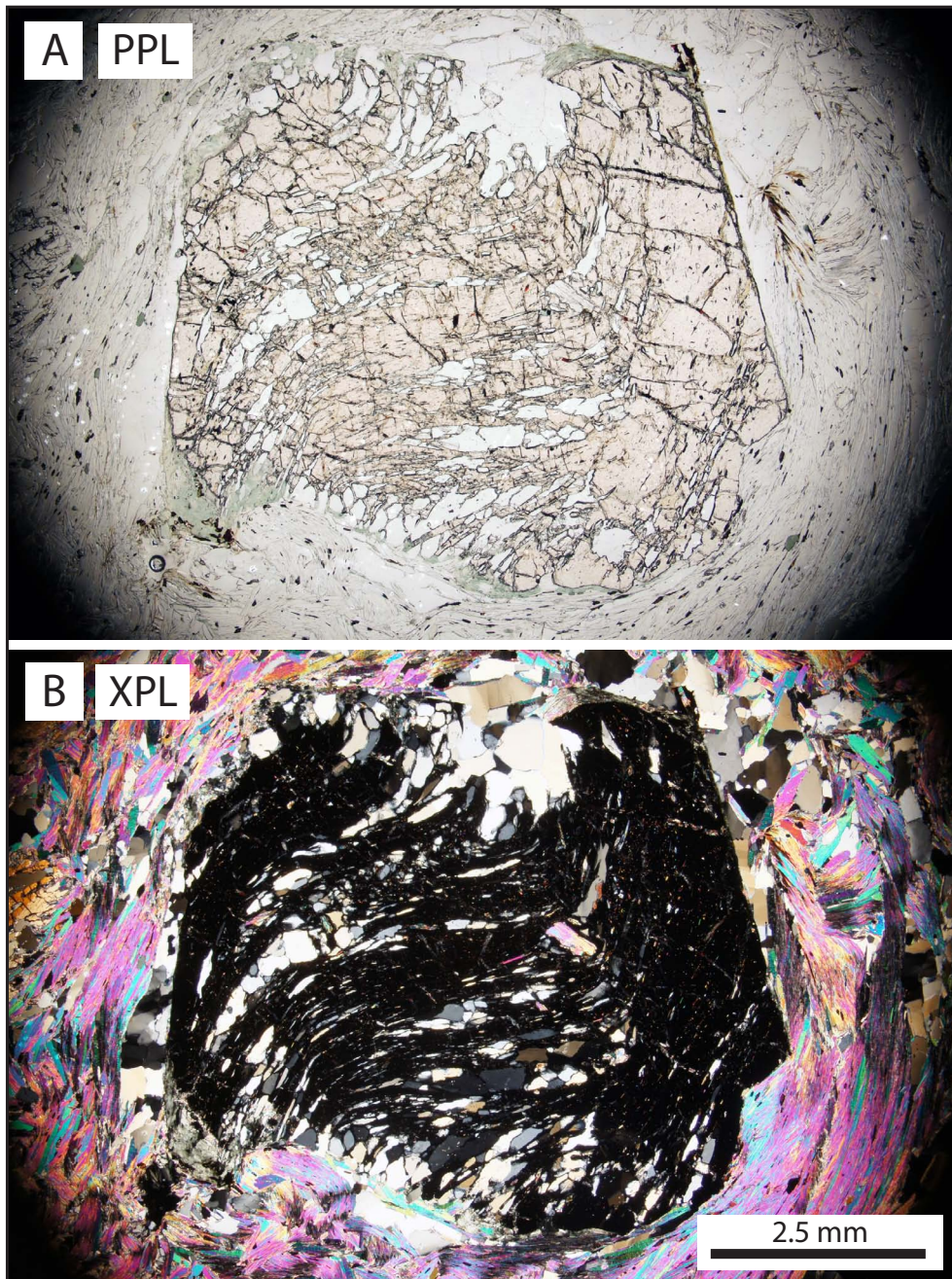


Figure 1.9: Sample WB137. A and B) Photomicrographs of a euheedral garnet in a matrix of phengite. Inclusions in garnet are quartz and phengite.

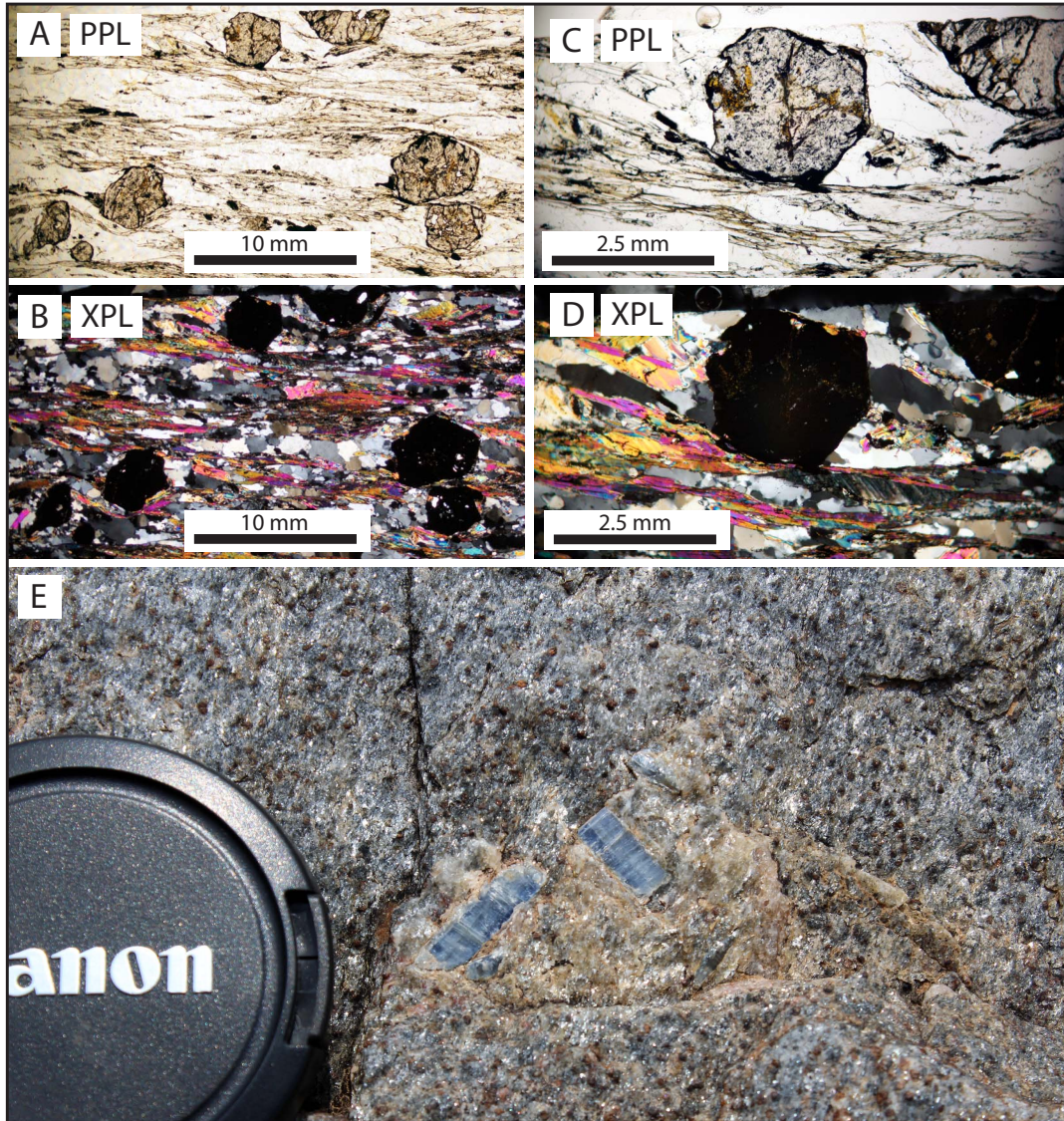


Figure 1.10: Sample KB2. A and B) Photomicrographs of garnet porphyroblasts in a matrix of foliated quartz and white mica. C and D) A closer view of a garnet shown in A and B. E) Field photograph of sample KB2, looking perpendicular to foliation. Kyanite is present in quartz veins throughout the outcrop.

Table 1.2: Mineral composition data for garnet in eclogite and blue schist facies rocks of the Nevado-Filabride Complex, measured by electron microprobe.

Sample	KB20	KB20	WB163	WB163	WB164	WB164	WB137	WB137	KB2	KB2
Mineral, Position	Gt, Core	Gt, Rim	Gt, Core	Gt, Rim	Gt, Core	Gt, Rim	Gt, Core	Gt, Rim	Gt, Core	Gt, Rim
SiO ₂	38.63	37.77	37.55	38.04	37.10	37.26	17.66	18.21	37.68	37.95
TiO ₂	0.14	0.05	0.02	0.10	0.16	0.08	nm	nm	0.11	0.10
Al ₂ O ₃	20.69	21.01	20.91	20.61	20.37	20.90	11.307	11.75	20.90	20.81
Cr ₂ O ₃	0.00	0.00	0.00	0.00	0.02	0.00	nm	nm	0.01	0.02
FeO	29.64	28.45	30.73	29.59	24.85	30.06	21.48	20.86	32.32	34.51
MnO	1.48	1.17	1.06	0.56	8.47	1.11	2.019	0.53	1.02	0.28
MgO	2.28	3.76	3.33	4.33	1.62	3.41	2.621	4.86	2.60	4.12
CaO	8.60	8.24	7.03	7.25	7.87	7.39	3.859	2.60	6.71	3.09
Na ₂ O	0.00	0.00	0.00	0.00	0.00	0.00	nm	nm	0.00	0.00
K ₂ O	0.00	0.00	0.00	0.01	0.00	0.00	nm	nm	0.01	0.00
Total	101.49	100.44	100.64	100.49	100.45	100.21	99.14	100.40	101.36	100.88
Si	3.03	2.98	2.98	3.00	2.97	2.96	3.00	2.30	2.98	3.00
Al iv	0.00	0.30	0.03	0.00	0.03	0.04	0.00	0.00	0.02	0.00
Al vi	1.91	1.93	1.92	1.91	1.90	1.92	2.00	2.00	1.93	1.94
Ti	0.01	bd	bd	bd	0.01	bd	nm	nm	bd	0.01
Cr	bd	0.00	0.00	0.00	bd	0.00	nm	nm	0.00	0.00
Fe3+	0.04	0.06	0.07	0.07	0.08	0.07	0.00	0.00	0.06	0.04
Fe2+	1.91	1.82	1.97	1.87	1.59	1.93	1.84	1.73	2.08	2.24
Mn	0.10	0.08	0.06	0.04	0.58	0.08	0.18	0.05	0.07	0.02
Mg	0.27	0.44	0.43	0.51	0.19	0.40	0.52	0.92	0.31	0.49
Ca	0.72	0.70	0.56	0.61	0.66	0.63	0.46	0.30	0.57	0.26
Total	7.99	8.02	8.02	8.02	8.02	8.03	8.00	8.00	8.02	8.00
Almandine	63	59	64	61	51	63	62	58	66	74
Andradite	2	3	3	4	4	3	0	0	3	2
Grossular	23	20	17	17	19	18	15	10	18	7
Pyrope	9	15	13	17	7	14	17	31	10	16
Spessartine	3	3	2	1	19	3	6	1	2	1
Uvarovite	0	0	0	0	0	0	0	0	0	0

Reformatted oxide percentages based on 12 oxygens and with Fe2+/Fe3+ calculated assuming full occupancy, *bd*, below detection limit of ~0.01%, *nm*, not measured

Table 1.3: Mineral composition data for white mica in eclogite and blueschist facies rocks of the Nevado-Filabride Complex, measured by electron microprobe.

Sample	WB137	WB137	WB137	WB137	KB2	KB2	KB20	KB20	WB163	WB164	WB164
Mineral Position	Phe (250-500 um) Matrix	Phe fold limb	Phe (125-250 um) Matrix	Pg fold hinge	Wm Matrix	Wm Matrix	Wm Matrix	Wm P shadow	Pg Matrix	Wm Matrix	Pg Matrix
SiO ₂	49.49	48.91	49.79	46.07	49.73	49.89	49.96	50.36	48.28	49.51	47.48
TiO ₂	0.32	0.18	0.45	0.16	0.31	0.28	0.53	0.36	0.18	0.52	0.12
Al ₂ O ₃	30.97	29.64	30.67	38.65	32.11	32.21	28.59	27.72	39.75	29.70	39.57
Cr ₂ O ₃	nm	nm	nm	nm	0.03	0.02	0.02	0.01	0.00	0.04	0.01
FeO	2.23	2.44	2.32	0.69	1.35	1.30	3.68	3.51	1.10	2.90	0.89
MnO	0	0.03	0	0.01	0.00	0.00	0.00	0.01	0.00	0.01	0.00
MgO	2.37	2.58	2.64	0.14	2.08	2.17	2.82	2.98	0.18	2.58	0.17
CaO	0	0	0.01	0.55	0.00	0.00	0.00	0.00	0.21	0.00	0.19
Na ₂ O	1.72	1.03	1.39	7.08	0.77	0.69	0.87	0.73	6.92	1.25	7.24
K ₂ O	8.96	9.49	9.19	0.76	8.78	8.90	9.85	10.10	1.00	9.31	0.76
Total	96.06	94.3	96.43	94.13	95.17	95.47	96.31	95.77	97.63	95.81	96.45
Si	3.26	3.29	3.27	2.99	3.27	3.27	3.32	3.36	3.02	3.29	3.00
Ti	0.02	0.01	0.02	0.01	0.02	0.01	0.03	0.02	0.01	0.03	0.01
Al	2.40	2.35	2.37	2.96	2.49	2.49	2.24	2.18	2.93	2.32	2.95
Cr	0.00	0.00	0.00	0.00	0.00	0.00	0.00	0.00	0.00	0.00	0.00
Fe	0.12	0.14	0.13	0.04	0.07	0.07	0.20	0.20	0.06	0.16	0.05
Mn	0.00	0.00	0.00	0.00	0.00	0.00	0.00	0.00	0.00	0.00	0.00
Mg	0.23	0.26	0.26	0.01	0.20	0.21	0.28	0.30	0.02	0.25	0.02
Ca	0.00	0.00	0.00	0.04	0.00	0.00	0.00	0.00	0.01	0.00	0.01
Na	0.22	0.13	0.18	0.89	0.10	0.09	0.11	0.09	0.84	0.16	0.89
K	0.75	0.81	0.77	0.06	0.74	0.74	0.83	0.86	0.08	0.79	0.06
Total	7.01	7.00	7.00	7.00	6.89	6.89	7.01	7.01	6.97	7.00	6.99
Mg/Mg+Fe	0.65	0.65	0.67	0.27	0.73	0.75	0.58	0.60	0.22	0.61	0.25
Na/K+Na	0.23	0.14	0.19	0.93	0.12	0.11	0.12	0.10	0.91	0.17	0.94

Oxide weight percentages of major elements, number of ions on the basis of 11 Oxygen atoms, *bd*, below detection limit of ~0.01%, *nm*, not measured

Sample WB159 – WDS x-ray mapping of garnet porphyroblasts reveals multiple growth stages for garnet in sample WB159. Figure 1.11 shows an example of a garnet with a rim that is distinctly different in composition from its core. It is likely that this indicates two stages of growth in garnets for the sample – an early prograde stage followed by growth of spessartine-rich garnet during retrogression. The sample was not chosen for dating due to the possibility of a time gap in between garnet growth stages. Composition data for minerals in sample WB159 are presented in the appendix.

Sample KB20 – Garnet, white micas, and omphacites were analyzed for sample KB20 and the compositions are summarized in Figures 1.12, 1.13, and 1.14, respectively. Figure 1.12 also shows 4 major element maps for a euhedral garnet. The zoning profiles suggest a transition from almandine+spessartine to pyrope-rich garnet from core to rim. These data suggest that the garnet grew during a single prograde metamorphic event. The phengitic mica composition (Figure 1.13) and high jadeite content omphacites (Figure 1.14) in the sample also suggest a prograde assemblage that remained in equilibrium through exhumation.

Table 1.4: Mineral composition data for omphacites and amphiboles in eclogite facies rocks of the Nevado-Filabride Complex, measured by electron microprobe.

Sample	KB20	WB163	WB163	WB164	WB163	WB164
Mineral	Omph	Omph	Omph	Omph	Amph	Amph
Position	Matrix	Matrix	Matrix	Matrix	Rimming Gt	Rimming Omph
SiO ₂	55.88	55.89	56.31	49.18	40.61	40.35
TiO ₂	0.10	0.10	0.10	0.38	0.22	0.24
Al ₂ O ₃	9.40	10.45	11.60	13.24	16.01	19.01
Cr ₂ O ₃	0.01	0.00	0.01	0.01	0.00	0.00
FeO	9.70	9.69	9.37	13.00	20.86	18.54
MnO	0.05	0.03	0.03	0.09	0.18	0.26
MgO	6.56	5.97	5.42	11.45	6.82	6.65
CaO	11.20	10.09	9.16	6.39	8.12	8.62
Na ₂ O	7.94	8.53	9.03	5.06	4.65	4.19
K ₂ O	0.00	0.00	0.00	0.35	0.88	0.92
Total	100.84	100.75	101.03	99.15	98.36	98.79
Atom per Formula Unit (6 oxygen basis)					Atom per Formula Unit (22 oxygen basis)	
Si	1.99	2.01	2.01	1.82	6.17	6.02
Ti	0.00	0.00	0.00	0.01	0.03	0.03
Al	0.39	0.44	0.49	0.58	2.87	3.34
Cr	0.00	0.00	0.00	0.00	0.00	0.00
Fe Total	0.29	0.29	0.28	0.40	2.65	2.31
Mn	0.00	0.00	0.00	0.00	0.02	0.03
Mg	0.35	0.32	0.29	0.63	1.54	1.48
Ca	0.43	0.39	0.35	0.25	1.32	1.38
Na	0.55	0.60	0.63	0.36	1.37	1.21
K	0.00	0.00	0.00	0.02	0.17	0.18
Total	4.00	4.06	4.05	4.07	16.14	15.98
Aegerine	17	18	16	35		
Jadeite	39	42	48	25		
Diopside	44	40	36	40		

Oxide wt. % of major elements, *bd*, below detection limit of ~0.01%, *nm*, not measured

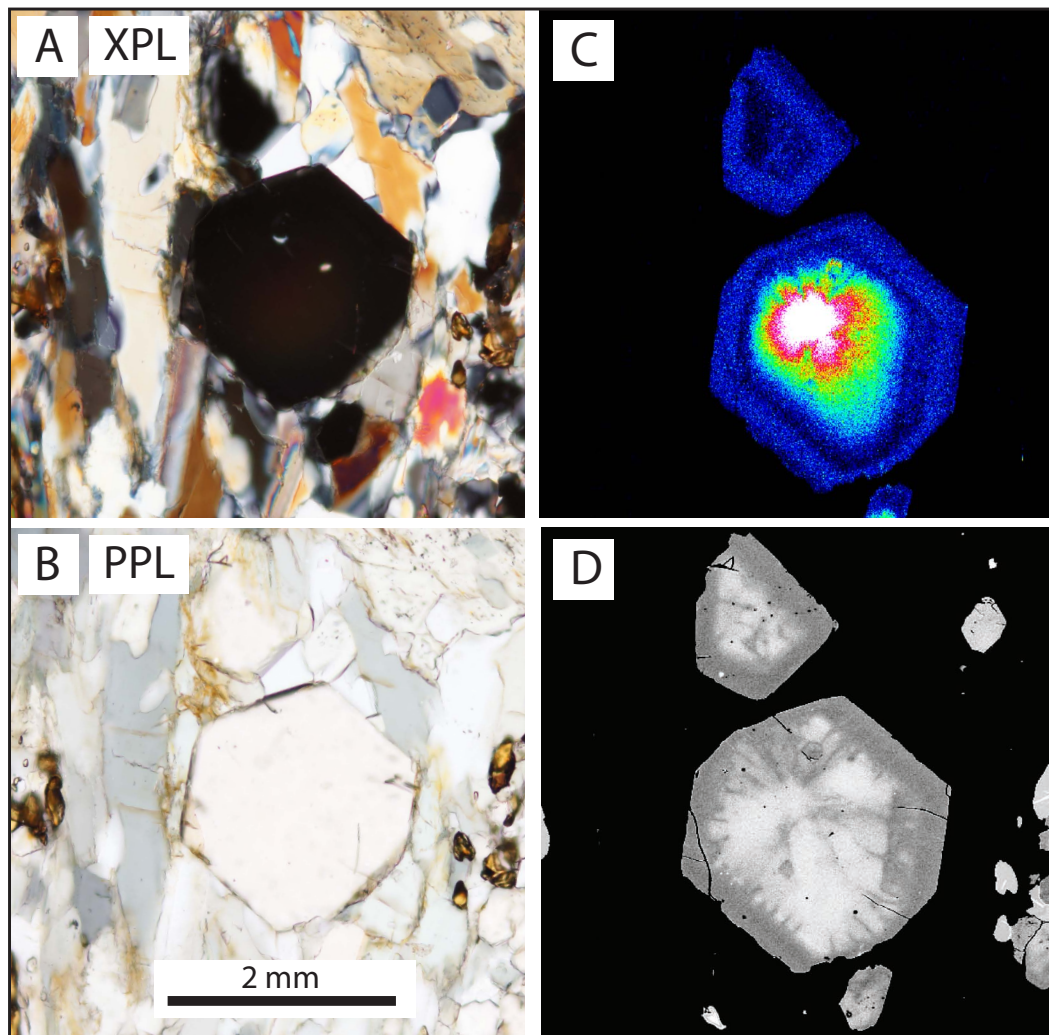


Figure 1.11: A retrogressed garnet porphyroblast from Sample WB159 – a mylonitized ecogite. A and B) photomicrograph of euhedral garnet in matrix of foliated white mica, amphibole, omphacite and rutile. C) WDS major element map of Mn concentration in garnet (hot colors indicate higher relative concentrations than cool colors). Change in concentration towards the rim suggests two episodes of growth. D) Backscattered electron (BSE) image of garnet showing evidence for two episodes of growth.

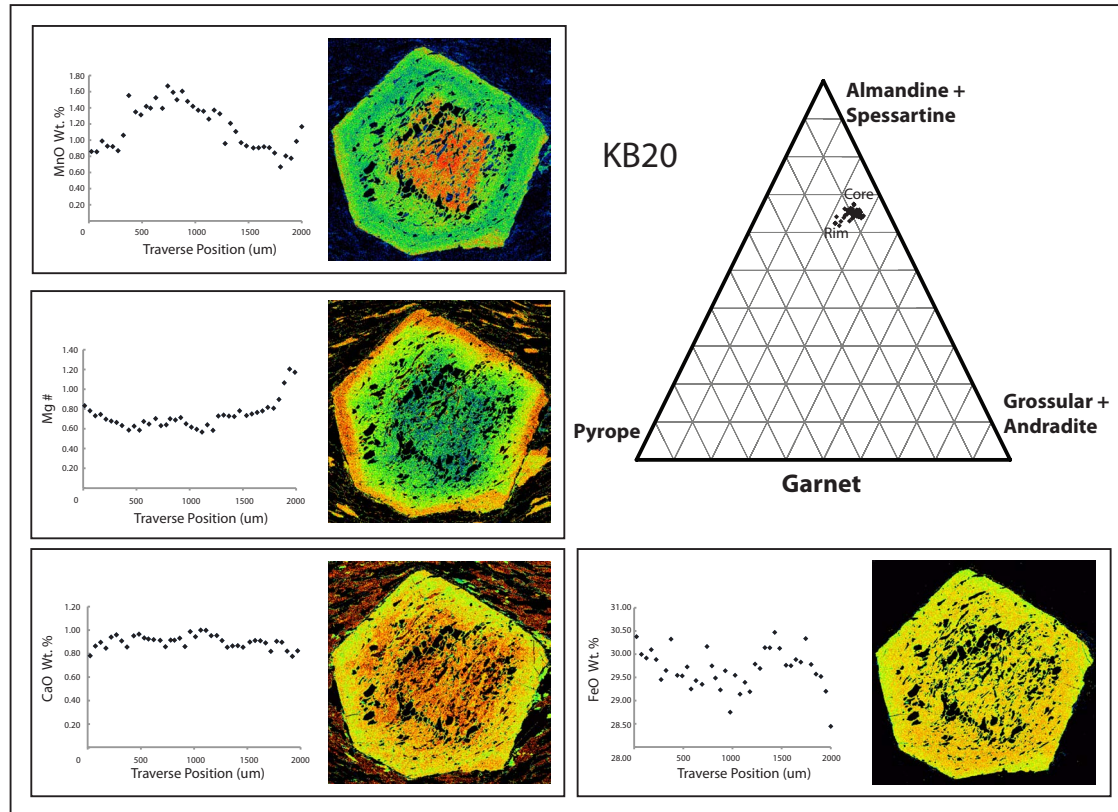


Figure 1.12: EPMA data summary for prograde garnets analyzed in sample KB20. Ternary diagram shows change in garnet composition from more pyrope-rich to more almandine+spessartine-rich from rim to core. WDS maps (hot colors indicate higher relative concentrations than cool colors) for Mn, Mg, Ca, and Fe are shown next to quantitative analyses of their respective oxide weight percents, taken from EPMA transects across garnets.

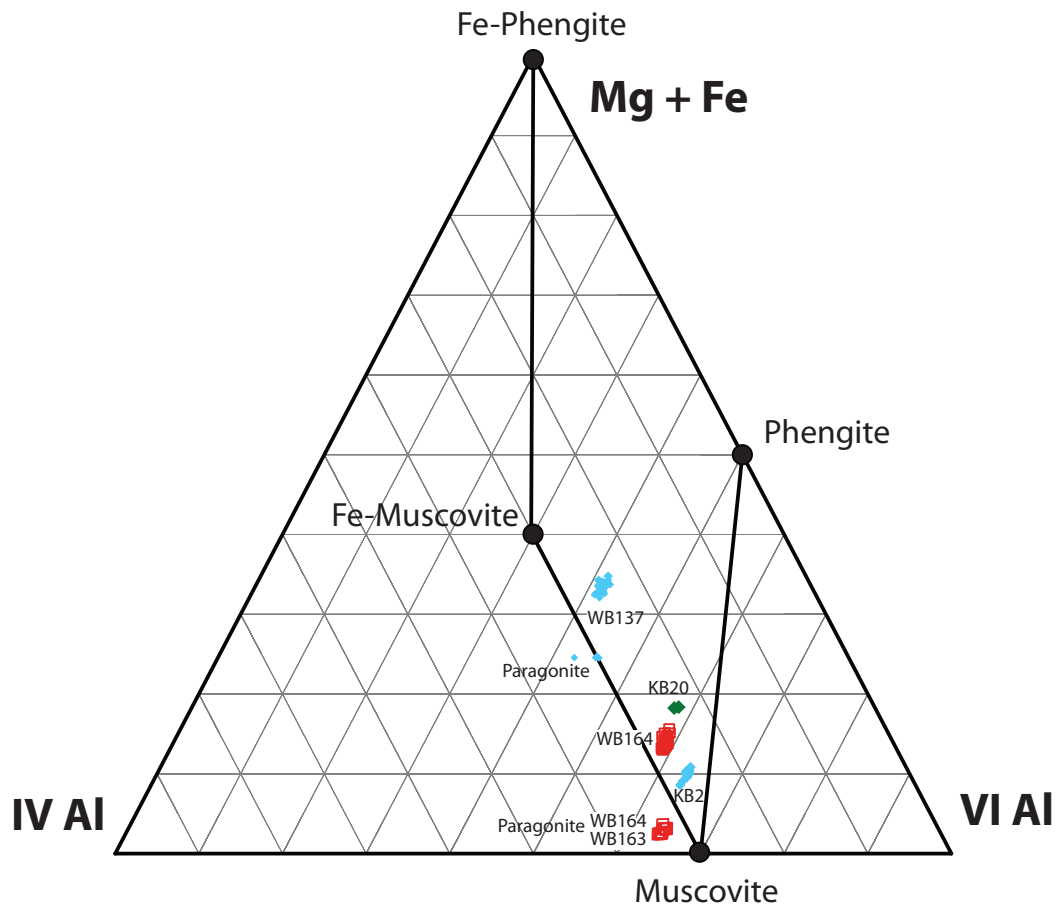


Figure 1.13: Ternary diagram shows white mica compositions for each dated sample.

Sample WB163 – Garnet, white micas, and omphacites were analyzed for sample WB163 and the compositions are summarized in Figures 1.15, 1.13, and 1.14, respectively. Figure 1.15 shows 2 major element maps for a euhedral garnet. The zoning profiles suggest a transition from almandine+spessartine to pyrope-rich garnet from core to rim. These data suggest that the garnet grew during a single prograde metamorphic event. The paragonitic mica com-

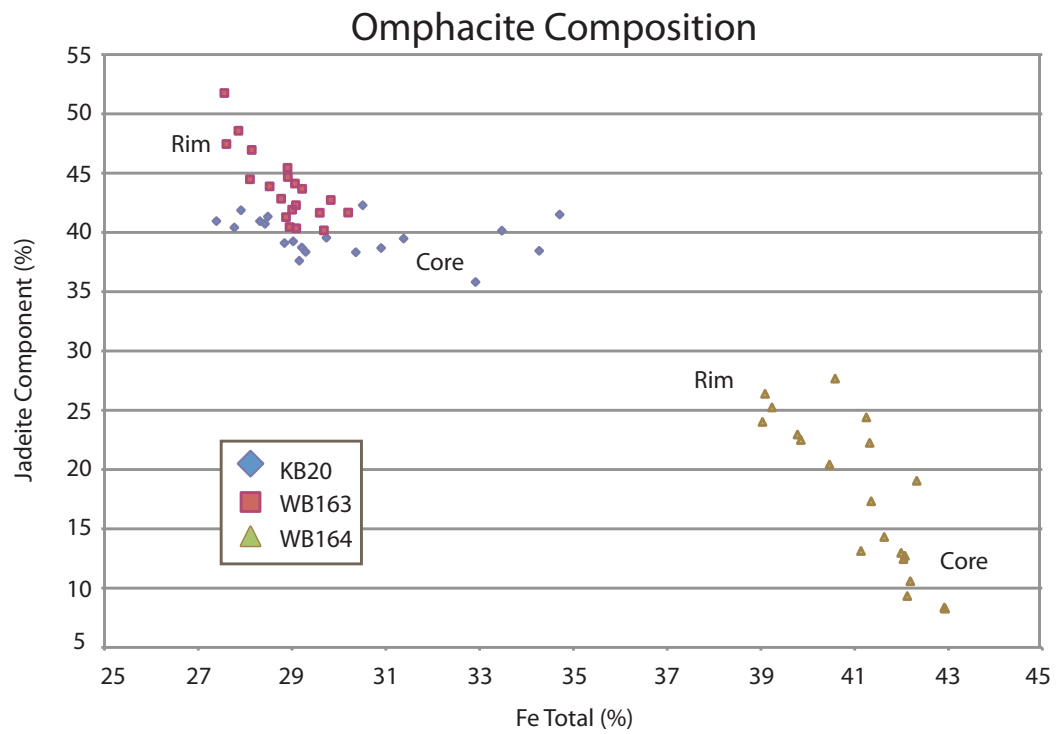


Figure 1.14: Composition diagram for omphacites in each dated eclogite.

position (Figure 1.13) and low jadeite content omphacites (Figure 1.14) in the sample suggest the sample may have been affected by a) diffusion during minor retrogression, b) difference in bulk composition, or c) different PT conditions compared to other similar lithologies. Paragonite grows as 250-500 μm grains within the matrix and is subparallel to the main foliation. The sample was chosen for dating to determine if it remained in isotopic equilibrium during amphibole growth.

Sample WB164 – Garnet, white micas, and omphacites were analyzed for sample WB164 and the compositions are summarized in Figures 1.16, 1.13, and 1.14, respectively. Figure 1.16 shows 4 major element maps for a euhedral garnet. The zoning profiles suggest a transition from almandine+spessartine to pyrope-rich garnet from core to rim. These data suggest that the garnet grew during a single prograde metamorphic event. Two populations of mica compositions exist in the sample: phengite and muscovite (Figure 1.13). High jadeite component omphacites (Figure 1.14) in the sample also suggest a prograde assemblage that remained in equilibrium through exhumation. The sample was chosen for dating to determine if it remained in isotopic equilibrium during amphibole growth.

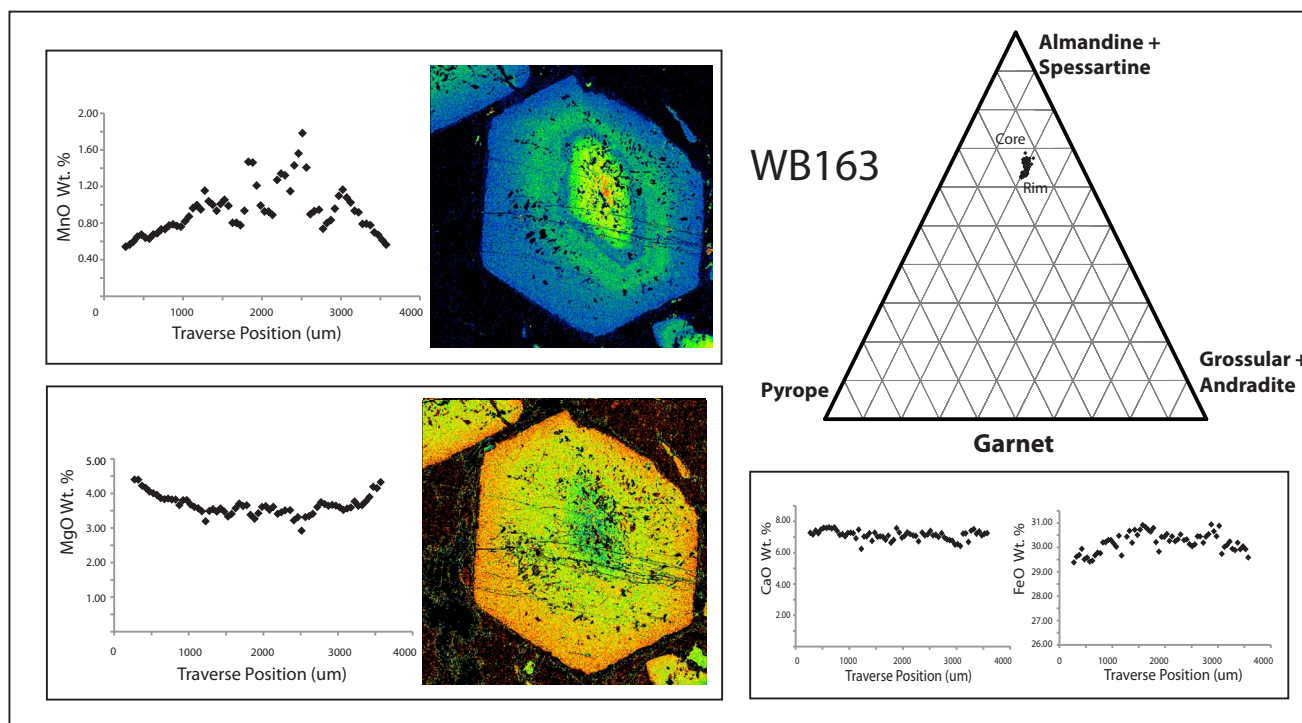


Figure 1.15: EPMA data summary for garnets analyzed in sample WB163. Ternary diagram shows change in garnet composition from more pyrope-rich to more almandine+spessartine-rich from rim to core. WDS maps (hot colors indicate higher relative concentrations than cool colors) for Mn and Mg are shown next to quantitative analyses of their respective oxide weight percents, taken from EPMA transects across garnets.

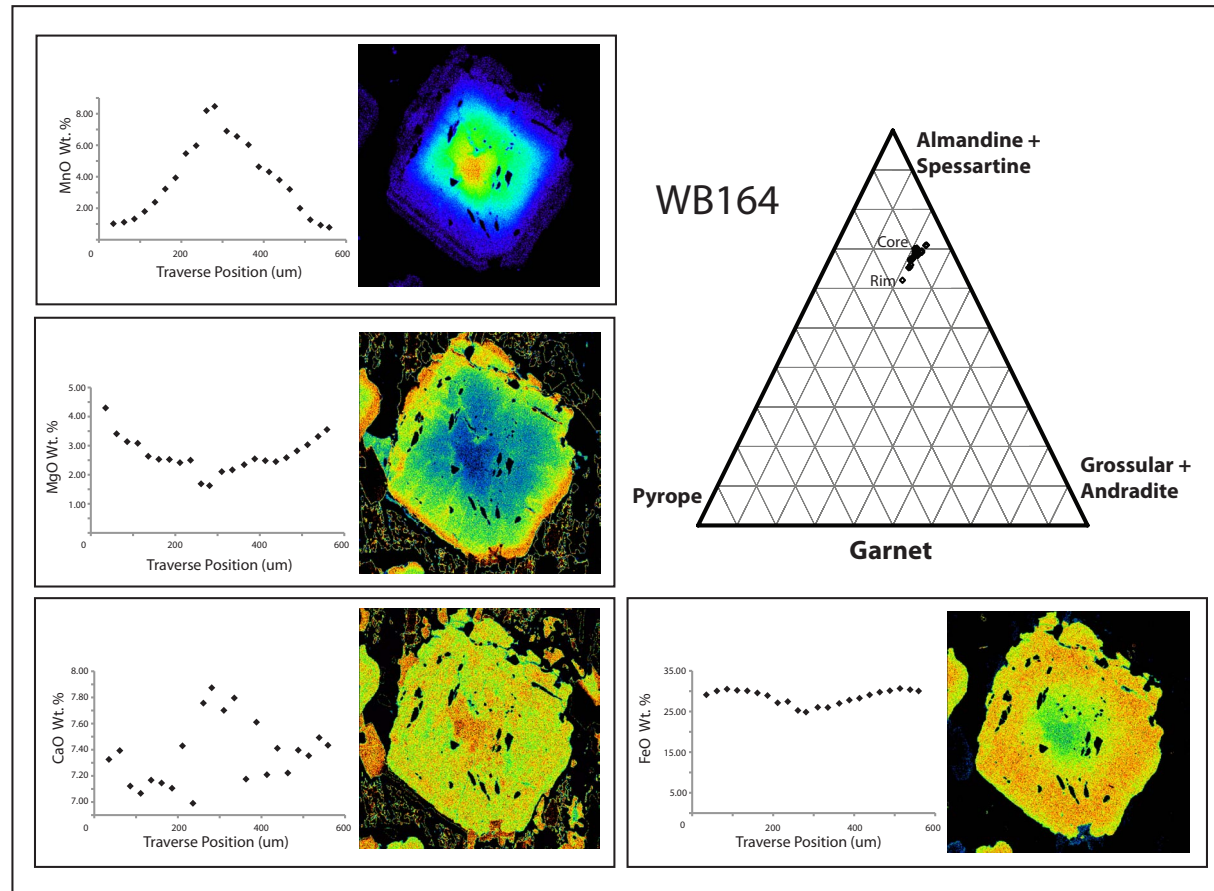


Figure 1.16: EPMA data summary for garnets analyzed in sample WB164. Ternary diagram shows change in garnet composition from more pyrope-rich to more almandine+spessartine-rich from rim to core. WDS maps (hot colors indicate higher relative concentrations than cool colors) for Mn, Mg, Ca, and Fe are shown next to quantitative analyses of their respective oxide weight percents, taken from EPMA transects across garnets.

Blueschist facies samples

Sample WB137 – Garnet and white micas were analyzed for sample WB137 and the compositions are summarized in Figures 1.17 and 1.13, respectively. Figure 1.17 shows 4 major element maps for a euhedral garnet. The zoning profiles suggest a transition from almandine+spessartine- to pyrope-rich garnet from core to rim. These data suggest that the garnet grew during a single prograde metamorphic event. The phengitic mica composition (Figure 1.13) in the sample also suggests a prograde assemblage that remained in equilibrium through exhumation. Fine-grained, recrystallized white mica in crenulation hinges turned out to be paragonitic in composition. Additionally, growth of paragonitic mica within folds of phengitic mica suggests that the fabric preserved in the sample formed during high pressure metamorphism (Figure 1.18).

Sample KB2 – Figure 1.19 shows 4 major element maps for a euhedral garnet. The zoning profiles suggest a transition from almandine+spessartine- to pyrope-rich garnet from core to rim. These data suggest that the garnet grew during a single prograde metamorphic event. The phengitic mica composition (Figure 1.13) in the sample also suggests a prograde assemblage that remained in equilibrium through exhumation. The sample was selected for dating to determine the timing of high pressure mineral growth.

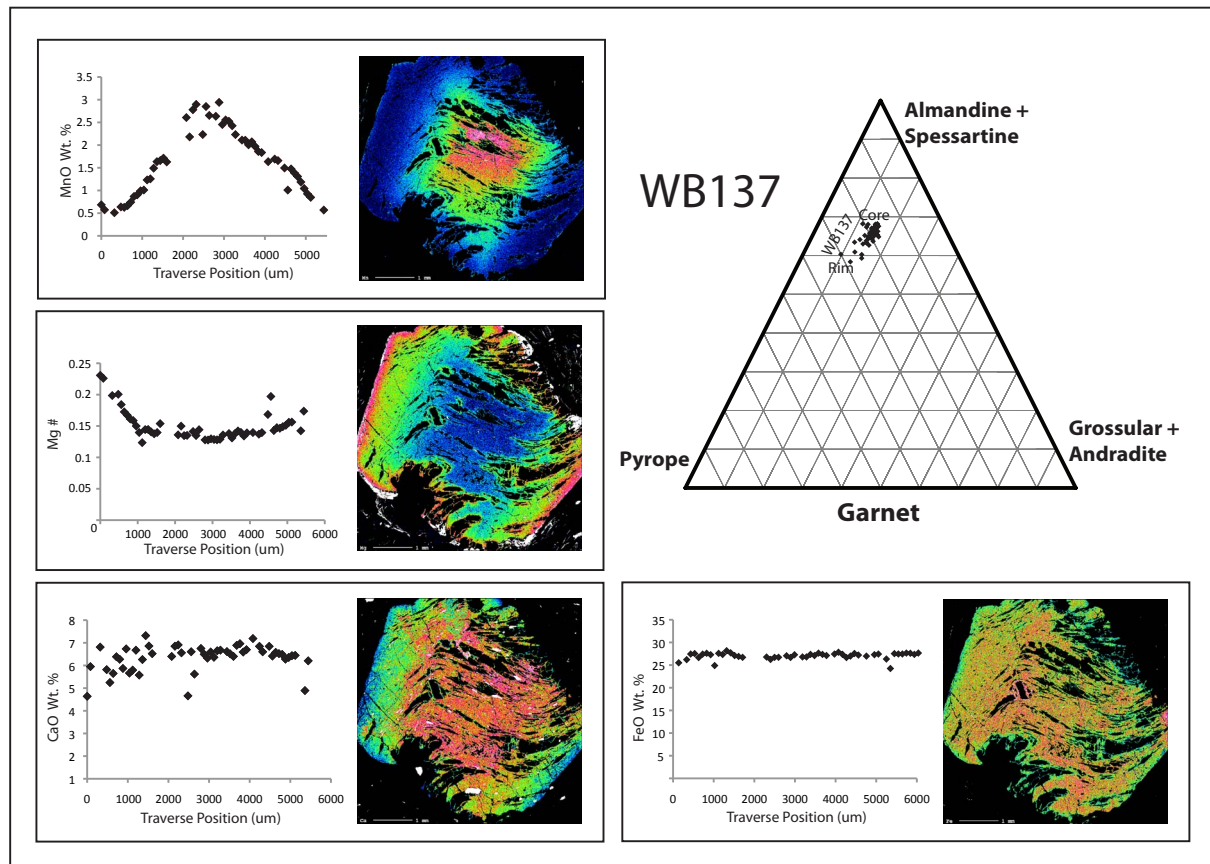


Figure 1.17: EPMA data summary for prograde garnets analyzed in sample WB137. Ternary diagram shows change in garnet composition from more pyrope-rich to more almandine+spessartine-rich from rim to core. WDS maps (hot colors indicate higher relative concentrations than cool colors) for Mn, Mg, Ca, and Fe are shown next to quantitative analyses of their respective oxide weight percents, taken from EPMA transects across garnets.

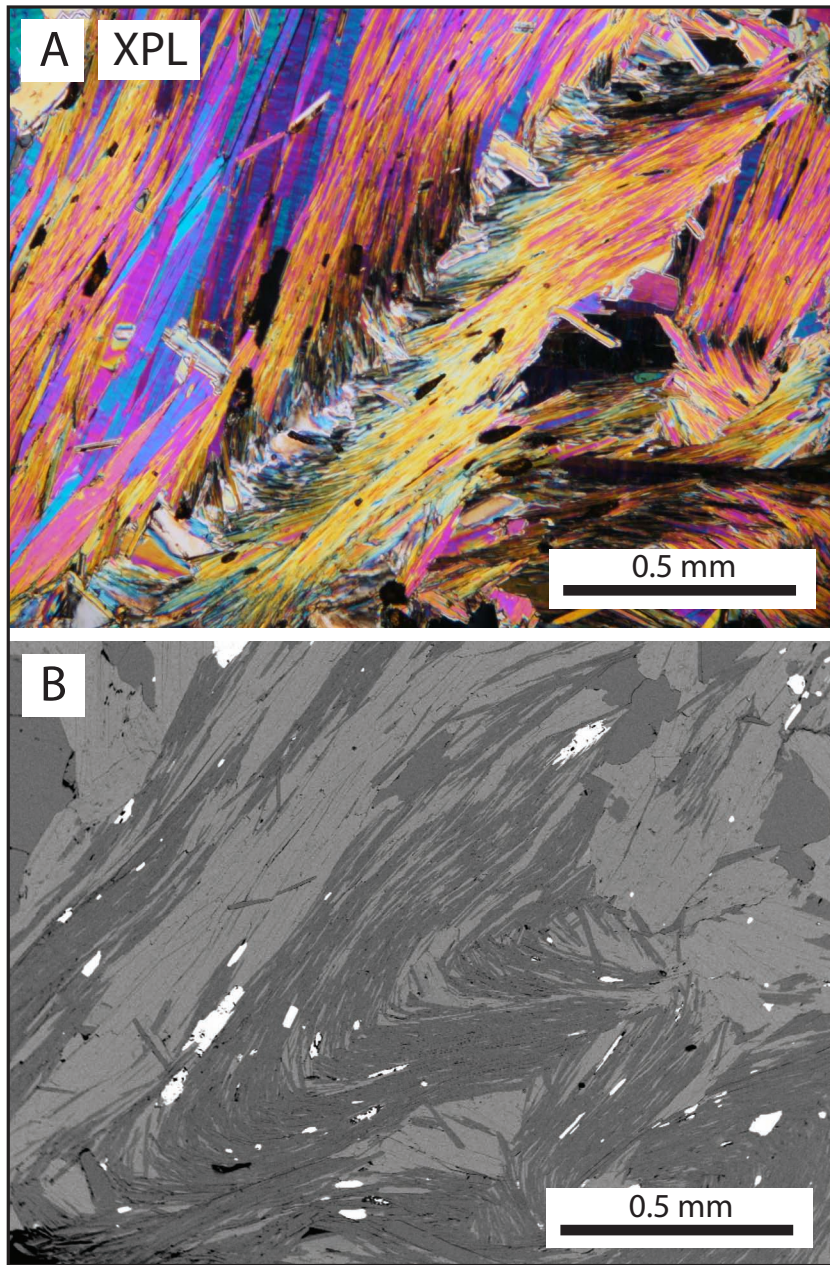


Figure 1.18: A) Photomicrograph of folded white micas in sample WB137. B) BSE image showing density contrast between differing mica compositions. Dark grains are paragonite, lighter grains are phengite. Table 1.2 summarizes characteristic mica compositions in the sample.

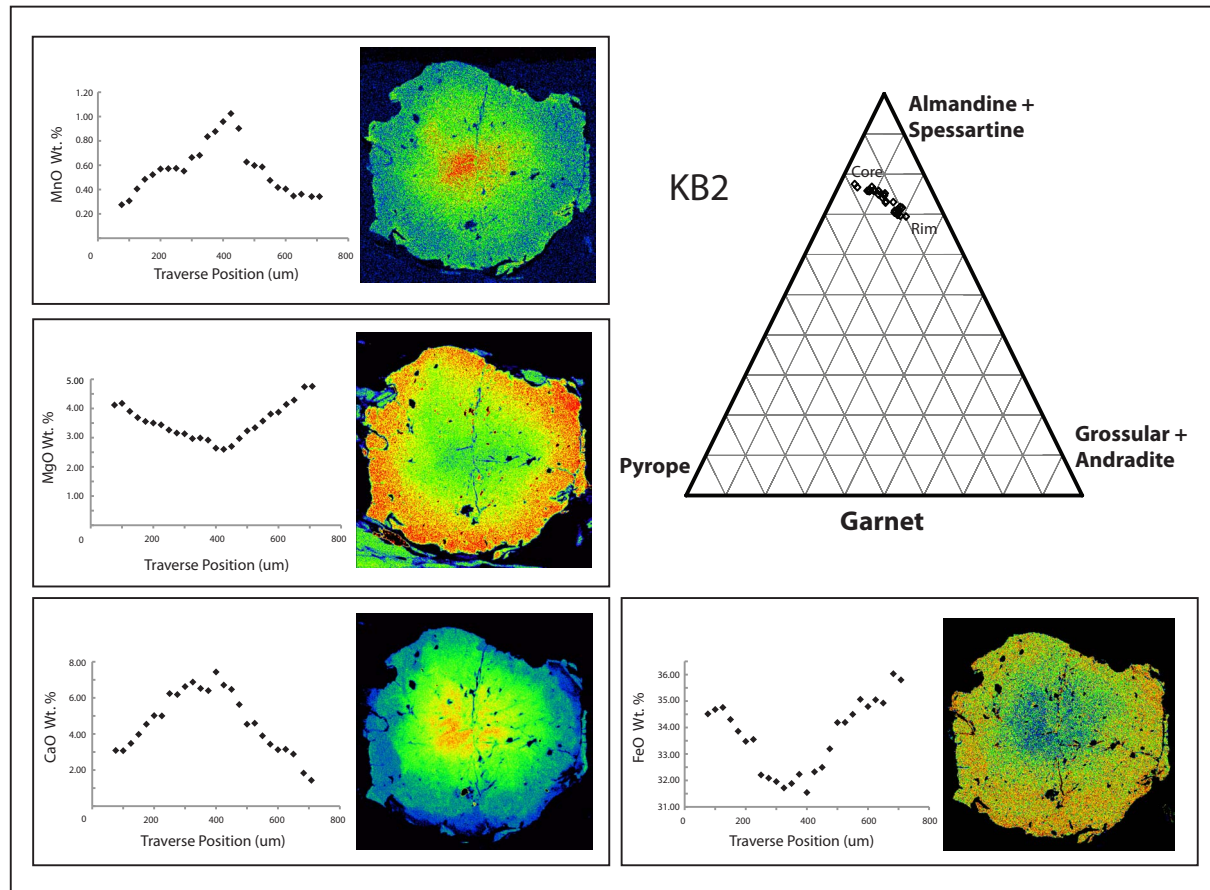


Figure 1.19: EPMA data summary for garnets analyzed in sample KB2. Ternary diagram shows change in garnet composition from more grossular+andradite-rich to more almandine+spessartine-rich from rim to core. WDS maps (hot colors indicate higher relative concentrations than cool colors) for Mn, Mg, Ca, and Fe are shown next to quantitative analyses of their respective oxide weight percents, taken from EPMA transects across garnets.

1.6.4 Mineral Separation

Samples were crushed by jaw crusher and disc mill, sieved, and separated using a Frantz magnetic separator. The smallest grain size (50-125 μm) was separated with bromoform to gather apatite. Individual minerals garnet, phengite, paragonite, amphibole, omphacite, and apatite were hand picked under a microscope following magnetic and heavy liquid separation procedures. Garnet grains were leached in 8% acetic acid prior to dissolution to remove inclusions of oxide minerals. Mica grains were crushed and sieved in ethanol prior to hand-picking to ensure selection of inclusion free grains. For Sample WB137, two distinct magnetic susceptibilities were observed for micas. The lower susceptibility mica fraction was interpreted to be paragonite on the basis of its relatively low Fe content compared with phengite. Consequently, the phengite had higher magnetic susceptibility and responded to lower amperages than paragonite separates. After various separation techniques, all minerals were hand picked to ensure inclusion-free sampling.

1.6.5 Rb-Sr Measurements using Inductively Coupled Plasma and Thermal Ionization Mass Spectrometry

All Rb and Sr isotope analyses were performed at the University of Texas at Austin. Sr was measured with a Thermo Scientific Triton thermal ionization mass spectrometer (TIMS). Rb was measured with a Thermo Scientific Element 2 inductively coupled plasma mass spectrometer (ICPMS). Samples were spiked using ^{87}Rb spike and ^{84}Sr spike that was calibrated against

multiple normal solutions to determine Rb and Sr concentrations by isotope dilution mass spectrometry (IDMS) and dissolved in a 4:1 HF:HNO₃ solution. Strontium was isolated using Eichrom Sr-specific resin and HNO₃. Many samples had high-K concentrations which reduced the effectiveness of the Sr-Spec resin for Sr. As such, in many high-Sr samples, Sr was found in the Rb cut after Sr isolation. To ensure pure Rb separates, the Rb cuts from Sr-Spec chemistry were run through the Sr-Spec columns a second time followed by purification of Rb from major cations using AG50wX8 100-200 mesh cation exchange resin with 1.25N HCl.

Strontium was loaded on to Re filaments with a TaF activator. Sr isotope ratios were obtained using static multi-collector analysis with internal exponential normalization to an $^{88}\text{Sr}/^{86}\text{Sr}$ value of 8.375209. In general, the reported isotopic ratios are the average of 160 determinations with 8 second integration time measured at an ^{88}Sr ion intensity of 8-10 V using 10^{11} ohm resistors. Uncertainties reported for each analysis are 2σ , based on in-run statistics. Repeat analysis of the NBS-987 Sr isotope standard during the period of analysis run under similar conditions as the samples yielded an average $^{87}\text{Sr}/^{86}\text{Sr}$ value of 0.710221 ± 0.000018 (2 std dev., $n = 8$). This value is 0.000027 lower than the accepted value of 0.710248 and all ratios were adjusted accordingly. Analyses of BHVO processed in this manner produced ratios of 0.703466 ± 0.000079 and concentrations of 383 ppm, in good agreement with accepted values of 0.703435 and 389 ± 23 ppm (Raczek et al., 2003; Wilson, 1997). Long term lab stability is demonstrated by the six month average of

replicate analysis of NBS987 of 0.710226 ± 0.000020 (2 std dev., n=26). Analyses were corrected for ^{87}Rb by simultaneously measuring ^{85}Rb and using the measured Rb ratios for each sample to calculate the amount of ^{87}Rb . The first procedural blank when running Sample WB137 was 64 pg Sr and the chemistry blank was 9 pg Sr. In the second round of samples (all other analyses except WB137 Round 1), the chemistry blank contained 3 pg Sr. All blanks are insignificant relative to the amount of Sr in each analyzed sample.

Rubidium separates were diluted to 10 ppb solutions in 5% HNO_3 for ICPMS analysis to obtain optimal signal intensities and minimize washout time between samples. Each sample was doped with 10 ppb Zr, to correct for exponential fractionation using the $^{92}\text{Zr}/^{90}\text{Zr}$ ratio of 0.33339 based on the methods of Waight et al. (2002). ^{87}Rb measurements were corrected for ^{87}Sr based on simultaneous measurement of ^{88}Sr and the measured Sr ratios for each sample. Rb, Zr and Sr isotopes were measured by peak hopping using electrostatic scanning in analog mode for 5 runs with 50 passes each, for a total of 250 measurements. Integration times on Rb, Zr and Sr isotopes were 0.25, 0.005 and 0.05 seconds, respectively. ^{95}Mo was monitored to correct for interference on ^{92}Zr , but no appreciable Mo was measured. Rb blanks were insignificant relative to the amount of Rb in each sample. Standard solutions of Rb were analyzed throughout analyses. Daily averages were 0.385771865 ± 0.0009 and were consistent with measured ratios for unspiked samples of USGS standard Hawaiian Basalt BHVO-2. Sample ratios were adjusted to correspond to the difference between the measured Rb ratios for the standards and the accepted

natural value of 0.3856. BHVO analyses processed in this way produced ratios in agreement with the natural ratio 0.3856 and with the accepted value of 9.8 ± 1.0 ppm Rb (Wilson, 1997). Uncertainties for Sr ratios were determined by the reproducibility of NBS987 during the analytical periods. ^{86}Sr concentration for the $^{87}\text{Rb}/^{86}\text{Sr}$ ratios were determined using natural abundances of Sr.

1.7 Results

Out of five total samples, statistically valid multimineral isochrons were obtained for one eclogite and two schist samples (Figure 1.3). Table 1.5 summarizes the Rb and Sr data measured by TIMS and ICPMS. Ages were calculated using Isoplot 4.1 software (Ludwig, 1999). Statistical validity is verified by MSWD values less than 2.5 for all regression calculations (cf. Kullerud, 1991).

WB163 – The isochron for this sample produced a statistically unreasonable age of 36 ± 23 Ma (MSWD = 1.2). Rb and Sr analyses on garnet, apatite and white mica were used to constrain the isochron. Initial amphibole and omphacite analyses failed to produce valid results due to faulty TIMS filament loading, so were not used to calculate the age. White micas exhibited uncharacteristically low Rb/Sr ratios compared to other samples because the sample contained paragonite (low Rb) rather than phengite (high Rb).

WB164 – The isochron for this sample produced a statistically unreasonable age of 13 ± 22 Ma (MSWD = 1.15). Rb and Sr analyses of garnet,

apatite, amphibole, omphacite, and white mica were used to constrain the isochron. However, garnet exhibited an uncharacteristically high ^{87}Rb content compared to the garnet in WB163. When garnet is removed from the isochron, it yields a more statistically reasonable, but still uncertain age of 10.1 ± 5.1 Ma (MSWD = 1.15). White micas exhibited uncharacteristically low Rb/Sr ratios compared to other samples because the sample contained paragonite (low Rb) rather than phengite (high Rb).

WB137 – The initial isochron for this sample produced a statistically valid age of 15.92 ± 0.66 Ma (MSWD = 0.70). This was the result of the first suite of mineral separates that were dated while calibrating the methods. Two populations of garnets, apatites, small phengites (125-250 μm), large phengites (250-500 μm), and paragonites were used to constrain the Rb and Sr ratios for the isochron. A second run of the procedure on a newly selected suite of mineral separates reproduced the Rb and Sr concentration data remarkably well, and when added to the data from the first suite of mineral separates, yields an age of 16.7 ± 1.7 Ma (MSWD = 11.8). Apatite on both runs consistently fell below the isochron. When it is excluded from the isochron, the age is 15.78 ± 0.47 Ma (MSWD=0.70).

KB2 – The isochron for this sample produced a statistically unreasonable age of 29 ± 110 Ma (MSWD = 1629). Garnet, two grain size populations of phengite (125-250 μm , 250-500 μm), and apatite were analyzed to obtain Rb-Sr ratios. As in sample WB164, garnet exhibited an uncharacteristically high ^{87}Rb content and low $^{87}\text{Sr}/^{86}\text{Sr}$ ratio. The analyses yield a statistically

valid age of 15.8 ± 1.1 (MSWD = 0.12) Ma when garnet is excluded from the isochron.

KB20 – The isochron for this sample produced a statistically valid age of 17.6 ± 1.1 Ma (MSWD = 0.22). Rb and Sr analyses on apatite, garnet, omphacite, and phengite were used to constrain the isochron.

Table 1.5: Rb-Sr analytical data.

Sample #, Analysis #	Material	Rb [ppm]	Sr [ppm]	$^{87}\text{Rb}/^{86}\text{Sr}$	$^{87}\text{Sr}/^{86}\text{Sr}$	$^{87}\text{Sr}/^{86}\text{Sr}$ 2σ [%]
<i>Schist Samples</i>						
WB137 Round 1 (16.6 ± 2.7 Ma, MSWD = 10.38, $\text{Sr}_1 = 0.72321 \pm 0.00018$)						
	Garnet	1.92	20.56	0.270444	0.723288	0.000006
	Apatite	0.00	599.53	0.000000	0.723056	0.000006
	Phengite, 125-250 μm	602.98	217.05	8.050360	0.725085	0.000007
	Phengite, 250-500 μm	562.73	233.08	6.995923	0.724831	0.000006
	Paragonite	40.93	604.99	0.196016	0.723331	0.000006
WB137 Round 2 (16.7 ± 4.5 Ma, MSWD = 285, $\text{Sr}_1 = 0.72314 \pm 0.00032$)						
	Garnet	1.92	24.81	0.176402	0.723315	0.000005
	Apatite	0.00	580.55	0.188430	0.722949	0.000006
	Phengite, 125-250 μm	602.98	210.43	8.147599	0.725087	0.000021
	Phengite, 250-500 μm	562.73	227.61	7.418941	0.724895	0.000008
	Paragonite	40.93	5983.77	0.052956	0.723262	0.000006
WB137 All Data (16.7 ± 1.7 Ma, MSWD = 11.8, $\text{Sr}_1 = 0.72318 \pm 0.00012$)						
WB137 All Data, No Apatite (15.78 ± 0.47 Ma, MSWD = 0.70, $\text{Sr}_1 = 0.723273 \pm 0.000036$)						
KB2 (29 ± 110 Ma, MSWD = 1629, $\text{Sr}_1 = 0.7236 \pm 0.0084$)						
KB2 No Garnet (15.8 ± 1.1 Ma, MSWD = 0.12, $\text{Sr}_1 = 0.725345 \pm 0.000061$)						
	Garnet	3.81	4.52	2.436858	0.721906	0.000129
	Apatite	0.13	2351.53	0.000165	0.725344	0.000062
	White Mica (mixed grain size)	554.76	217.97	7.363416	0.726982	0.000134
	White Mica 250-500 μm	556.48	237.14	6.789198	0.726887	0.000136
<i>Eclogite Samples</i>						
KB20 (17.6 ± 1.1 Ma, MSWD = 0.22, $\text{Sr}_1 = 0.703565 \pm 0.000042$)						
	Garnet	0.81	33.59	0.069581	0.703572	0.000066
	Apatite	12.13	669.70	0.052398	0.703602	0.000083
	White Mica	319.23	86.26	10.706794	0.706246	0.000170
	Omphacite	5.53	274.45	0.058289	0.703574	0.000077
WB163 (36 ± 23 Ma, MSWD = 1.2, $\text{Sr}_1 = 0.706254 \pm 0.000054$)						
	Garnet	1.16	49.40	0.067953	0.706260	0.000067
	Apatite	1.48	1892.92	0.002260	0.706279	0.000069
	White Mica	169.10	1558.11	0.313984	0.706423	0.000082
	Omphacite	0.45	no data	no data	no data	no data
	Amphibole	6.79	no data	no data	no data	no data
WB164 (13 ± 22 Ma, MSWD = 11.3, $\text{Sr}_1 = 0.70568 \pm 0.00021$)						
WB164 No Garnet (10.1 ± 5.1 Ma, MSWD = 1.15, $\text{Sr}_1 = 0.705750 \pm 0.000046$)						
	Garnet	1.00	25.51	0.113947	0.705527	0.000073
	Apatite	0.27	1802.98	0.000434	0.705786	0.000071
	White Mica	233.80	442.51	1.528622	0.705971	0.000100
	Omphacite	0.83	146.72	0.016441	0.705703	0.000089
	Amphibole	2.90	70.13	0.119602	0.705761	0.000082

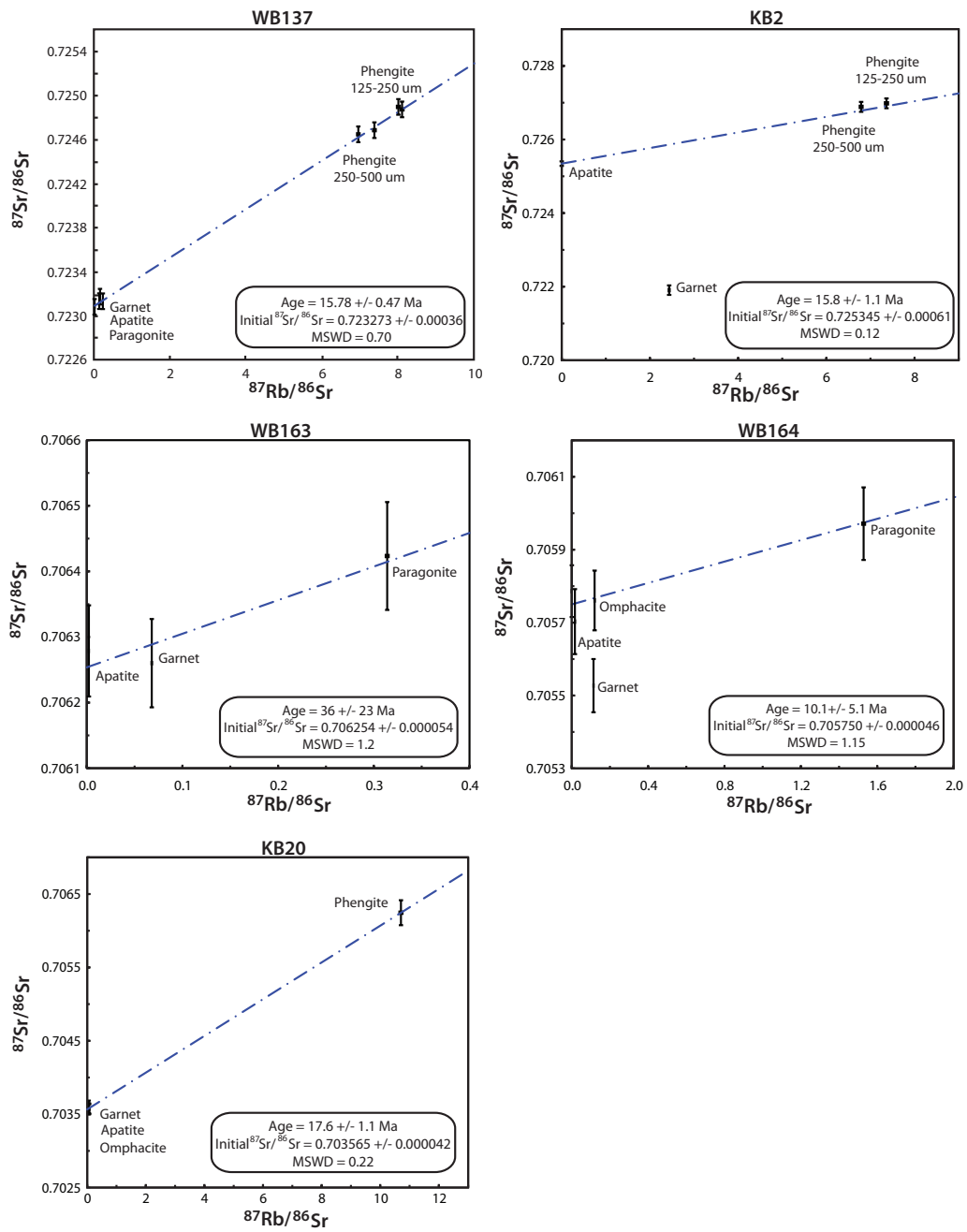


Figure 1.20: Isochrons for all dated samples, calculated with Isoplot software Ludwig (1999). All collected data (Table 1.5) is plotted, but preferred isochrons are shown. Data-point error crosses are 2σ .

1.8 Discussion

1.8.1 Problem Samples

Eclogite samples WB163 and WB164 produced Rb-Sr isochrons that are statistically scattered and inconsistent with the results of the other three samples dated in this study. Mineralogy and elemental geochemistry of WB163 and WB164 do not show significant evidence for retrogression, as shown earlier in Section 1.6.1. Given that these two samples are prograde eclogites with only minor evidence for retrogression, the high pressure mineral assemblage should still be in equilibrium, and should therefore produce an age that represents high pressure metamorphism. Due to the lack of evidence for retrogression, the spurious ages are may be a result of errors in methodology.

First, the garnet separates for both WB163 and WB164 were not leached in acetic acid, as was the garnet for WB137. Iron oxides or inclusions that would have dissolved out with leaching may have increased Rb or decreased Sr in the sample, elevating the final $^{87}\text{Rb}/^{86}\text{Sr}$ ratios and decreasing the $^{87}\text{Sr}/^{86}\text{Sr}$ ratios. The garnet analysis for WB164 was removed from the initial age calculation (13+/-22 Ma), which significantly decreased the margin of error for the calculated age (10.1+/-5.1 Ma). However, excluding garnet from the WB164 isochron produces an age that is slightly younger than the early Miocene ages produced for samples KB20, KB2, and WB137. Garnet was included for the WB163 isochron and has an $^{87}\text{Rb}/^{86}\text{Sr}$ ratio that is consistent with the measurements for garnet in KB20. It is possible that iron oxide inclusions in WB164 garnets influenced the $^{87}\text{Sr}/^{86}\text{Sr}$ ratio, which could

have been prevented by leaching the garnets prior to analysis. WB164 garnets are currently being re-analyzed after being leached in acetic acid to test for this. The acetic acid leach product is also being analyzed to determine whether it contains a component of Rb or Sr that would have influenced the initial analysis.

Second, paragonitic mica is abundant in WB164 and is present in WB163 (Table 1.3). Based on the relatively low Rb content of the analyzed white mica separates in WB163 and WB164 (Figure 1.20) compared to phengites in other samples, it is likely that WB163 and WB164 separates included either a mixture of paragonite and phengite or was dominantly paragonite. The low Rb in paragonite causes high uncertainty when calculating the slope of the isochron, and may therefore yield an inaccurate age. A more rigorous magnetic separation of mica grains from both samples yielded a distinct separation between a more magnetic and less magnetic fraction of mica. Based on the composition data in Table 1.3, the higher Fe-content (more magnetic) grains were interpreted to be phengite and selected for analyses. Pure phengite separates are currently being analyzed to add to the current isochrons for publication purposes.

The ages presented for WB163 and WB164 are inconclusive due to the questionable composition of the analyzed mica separates and lack of reliable data for other mineral phases. Initial analyses on amphibole and omphacite from WB163 failed due to user errors in filament loading and are being repeated to complete the isochron for publication. Analyses from WB164 gar-

net, phengite, WB163 omphacite, amphibole, and phengite will complete the dataset and should produce statistically valid ages for both samples.

Schist sample KB2 yields a statistically valid age of 15.8+/-1.1 Ma (MSWD = 0.12) when garnet is excluded from the isochron. Based on observed mineral textures and elemental composition data (Figures 1.10 and 1.19), the garnet in KB2 grew during prograde, high pressure metamorphism and is not retrogressed. However, the garnet separate results show an uncharacteristically high Rb content, compared to the garnet from WB137, which is of similar lithology. It is possible that the source of error in measurement for KB2 garnets can be attributed to errors in methodology.

Compared to other samples, which contained light pink, vitreous, and transparent garnets as observed under a picking microscope, many of the garnets in KB2 contained a powdery, rusty red and yellow film along the grain margins. We interpret this to represent significant oxidation. Unfortunately, these garnets were not leached prior to analyses. Oxide mineralization may have had a lower Sr isotopic ratio such that analysis of the combined garnet-oxide separate would have had a lower $^{87}\text{Sr}/^{86}\text{Sr}$ ratio. Since obtaining the original isochron, a second separate of KB2 was leached first in acetic acid, then in hydrochloric acid, and is now being re-analyzed. Both leach products were collected and are also being analyzed in order to determine the Rb and Sr isotopic compositions of the leached components.

The age presented here for KB2 is presently inconclusive due to the lack of reliable Rb and Sr data for garnet. However, the minerals that are

in equilibrium on the isochron suggest that the age does represent the timing of high pressure metamorphism. Based on the detailed characterization of the high pressure mineral assemblage outlined in earlier sections, and the age correlation with the highly reproducible WB137 age, we interpret the age from sample KB2 (excluding the garnet) to represent the timing of high pressure metamorphism in the NFC.

1.8.2 Timing of HP metamorphism in the NFC

The conclusions of this work hinge on the validity of ages obtained for samples KB2, KB20, and WB137. WB137 is the most robust of the ages, as the mineral separates for the sample were analyzed twice and produced nearly identical results. All mineral separates lie on a statistically valid isochron, with the exception of apatite. In order for the apatite to fall on the isochron in concordance with the other minerals, the radiogenic Sr content would need to be elevated. The lack of radiogenic Sr in apatite suggests that some mechanism must have influenced apatite following high pressure metamorphism or that the apatites were not fully in equilibrium with the other minerals when they formed.

Apatite in sample WB137 may have experienced later alteration that did not affect the Sr isotopic composition of the other minerals in the assemblage. If the apatites grew during high pressure metamorphism, it is possible that fluids rich in nonradiogenic Sr flowed through the Tahal Schist near the margins of the Betic Movement zone during exhumation of the NFC and in-

incorporated Sr into the apatite. Alternatively, if the apatites contain detrital components, their initial isotopic composition may not have been fully reset by high pressure metamorphism. Due to the uncertainty of the microstructural context of the apatites in the sample, we have elected to disregard the low $^{87}\text{Sr}/^{86}\text{Sr}$ ratio of apatite and attribute it to post-HP alteration. Based on the detailed characterization of the high pressure mineral assemblage outlined in earlier sections, we interpret the age from sample WB137 (excluding apatite) to represent the timing of high pressure metamorphism in the NFC.

Sample KB20 gives a statistically valid early Miocene age that represents growth of the eclogite mineral assemblage. The fact that all KB20 minerals lie on an isochron suggests that the HP mineral assemblage is in equilibrium. The evidence for a prograde mineral assemblage in equilibrium suggests that there was no redistribution of radiogenic Sr following the formation of the eclogite and that the age is geologically valid.

1.8.3 Comparison to other geochronologic data from the NFC

The conflicting tectonic models discussed above stem from the ambiguity in interpreting the significance of existing geochronologic data. The validity of the tectonic models proposed for the Betic Cordillera hinges on the geochronologic data collected in the NFC. The early Miocene Rb-Sr ages from this study agree with both the Lu-Hf ages (~ 18 - 14 Ma) of Platt et al. (2006) and the U-Pb ages (~ 17 - 15 Ma) of Sanchez-Vizcaino et al. (2001) and Gomez-Pugnaire et al. (2012). It is clear that the majority of the methods used to

constrain the timing of HP metamorphism have produced Early Miocene ages, with the exception of Ar-Ar (e.g. Monie et al., 1991; Augier et al., 2005a; Platt et al., 2006; Behr and Platt, 2012), which has produced highly variable ages ranging from \sim 220-8 Ma.

The Ar-system has proven to be reliable in the Alpujarride Complex, but other workers have shown that the system does not produce reliable age data within the NFC (e.g. Behr and Platt, 2012). Although Augier et al. (2005a) were able to correlate their data with specific grain sizes and deformational events in the NFC, their data do not correlate well with similarly collected Ar age data (Figure 1.3) from Monie et al. (1991) in the NFC. Additionally, contrary to Augier et al. (2005a), Behr and Platt (2012) observed no correlation between Ar-Ar ages of phengite crystals and grain size or microstructural context in the NFC. The correlation found by Augier et al. (2005a), may be a result of grain deformation dependence of excess Ar (e.g. Sherlock and Kelley, 2002).

The most likely explanation for the Ar system to be an effective dating technique in one complex and not the other is the contrast in P-T paths for these two units. The Alpujarride Complex exhibits a pervasive, late thermal pulse associated with decompression, which produced abundant sillimanite and andalusite, likely resetting the Ar system (Platt et al., 2005). The Nevado-Filabride, on the other hand, appears to have been cooled during decompression, and remained entirely in the kyanite stability field, so thermal resetting of the complex (and the Ar system) was likely not achieved (de Jong,

2003; Behr and Platt, 2012).

Other mechanisms for the incorporation of excess ^{40}Ar may include phengite recrystallization related to fluid flow or interaction with meteoric waters (de Jong et al., 2001). Due to the high variability in Ar ages and the conflict with age data obtained through other methods, it appears that the Ar system may not be the ideal recorder of the metamorphic events in the NFC. Therefore, the Ar-Ar ages should not be interpreted as the timing of high pressure metamorphism in the NFC.

Previous U-Pb zircon ages from NFC rocks were determined from vermicular metamorphic rims (Sanchez-Vizcaino et al., 2001). It is difficult to know at what point on the P-T path the zircons grew. It is possible the zircon grew late during decompression at peak temperature (e.g. Platt and Behrmann, 1986; Whitehouse and Platt, 2003), rather than at peak pressure. An age for HT metamorphism may not necessarily correlate with the age of HP metamorphism for the NFC.

Although Platt et al. (2006) interpret their Lu-Hf ages as evidence for early Miocene subduction of the NFC, there are reasons to believe that the ages may lack precision. It is possible that dissolution of zircon inclusions in garnets may affect the ages (Behr and Platt, 2012). Zircon dissolved along with garnet separates would increase the Hf concentration, thereby yielding younger ages (Scherer et al., 2000). However, Platt et al. (2006) selected inclusion-free garnets and dissolved them using a hot plate as opposed to HP, high temperature dissolution, which prevents zircon dissolution and therefore

contribution of excess Hf to the sample (Anczkiewicz et al., 2004). Additionally, garnets that have multiple stages of growth would yield spurious ages if included in the sample (Aerden and Sayab, 2008).

It appears unlikely that the whole-rock Rb-Sr ages from de Jong (2003) (66-14 Ma) are truly representative of one, prograde HP metamorphic event. Whole rock analyses include all minerals in the rock, including inherited detrital components and later retrograde minerals. It is more likely that the ages obtained with this method included components of Rb and Sr that were incorporated by a later episode of retrograde metamorphism.

The Rb-Sr technique used in this study specifically avoids sampling retrograde phases that would otherwise be incorporated with a whole-rock Rb-Sr technique. The rigorous sample characterization and selection of the multimineral Rb-Sr method ensures that only prograde mineral phases that formed in equilibrium with each other are dated. Based on the correlation of ages found in this study with Lu-Hf and U-Pb ages, the high pressure minerals in the NFC must have formed during high pressure metamorphism in the Early Miocene.

1.8.4 Tectonic Implications

The Early Miocene ages for WB137 and KB20 represent the timing of high pressure metamorphism in the NFC. Additionally, an Early Miocene age for sample KB2, excluding garnet, is promising, but not conclusive. These three new ages provide evidence that the NFC was subducted in the Early

Miocene, after the overlying Alpujarride Complex had already been exhumed. The age of the high pressure mineral assemblage in the NFC is vital to the understanding of the geologic history of the Betic Cordillera as a whole. Existing tectonic models rely upon the age of high pressure metamorphism in the NFC to constrain the subduction history of the western Mediterranean. It is impossible to accurately interpret mantle tomographic imagery beneath the western Mediterranean when the subduction history of the region is not well understood. Due to the conflicting geochronological data generated by workers in the NFC over the past few decades, multiple models have been proposed in the literature, following two main themes:

1) Coeval subduction of the Alpujarride and Nevado-Filabride Complexes

Primarily supported by Eocene-Oligocene Ar-Ar high pressure metamorphism ages for the NFC (e.g. Monie et al., 1991; Augier et al., 2005a), the coeval subduction model corresponds to Model 2 in Figure 1.5. The model requires that both the NFC and AC were subducted together at the same time, and subsequently exhumed along the subduction channel as slab rollback occurred (e.g. Vergés and Fernandez, 2012). The proposed mechanisms for extension and decompression for this model are westward slab rollback (e.g. Augier et al., 2005a) and slab detachment (Vergés and Fernandez, 2012). The interpretations of the slab activity beneath the Alboran rely on interpretations of mantle tomography for the region (e.g. Spakman and Wortel, 2004; Bezada et al., 2013), coupled with geochronologic constraints on metamorphic events

(e.g. Monie et al., 1991; Augier et al., 2005a).

This model generally requires an Early Miocene extension event that postdates the exhumation of both complexes and precludes subduction of the NFC in the Early Miocene. The Rb-Sr ages from this study are incompatible with the coeval subduction model because the new ages suggest an Early Miocene HP metamorphic event occurred in the NFC. The rocks formed by this HP metamorphic event could not have been exhumed to the surface after the Early Miocene if the subducting slab was detaching from the lithosphere during this time. If the Early Miocene Rb-Sr ages do represent HP metamorphism, as shown in this study, then the slab must have been continuously subducting during through the Early Miocene.

2) Multiple phases of subduction in the Betic Cordillera

The multiple subduction phase model is primarily supported by Early Miocene Lu-Hf and U-Pb ages for high pressure metamorphism in the NFC (e.g. Platt et al., 2006; Sanchez-Vizcaino et al., 2001; Gomez-Pugnaire et al., 2012). The model is illustrated in Model 1 of Figure 1.5. In contrast to the coeval subduction model, these ages require different metamorphic and tectonic histories for the two complexes. Fission track data suggest that the Alpujarride complex was exhumed by ~ 16 Ma (Platt et al., 2005). If the Alpujarride was subducted in the Eocene, then exhumed in the Early Miocene as the NFC was being subducted, a punctuated phase of extension between the two subduction events is required.

Metamorphic zircon from high-grade Alpujarride rocks yield ages of 23-21 Ma, and Ar-Ar ages and fission track data provide evidence for rapid cooling between 20-18 Ma (Monie et al., 1994; Sosson et al., 1998; Platt et al., 2003a). The rapid heating and cooling event between 23-18 Ma represents a period of decompression and extension in the Betic Cordillera that predates the subduction of the NFC. The heating was likely due to inflow of hot asthenosphere due to slab discontinuity beneath thinned Alboran crust (Platt et al., 1998, 2003a; Mancilla et al., 2013), however, the mechanism for thinning of the lithosphere is not certain. Possible mechanisms for asthenospheric inflow are slab break-off (Blanco and Spakman, 1993), lithosphere delamination (Calvert et al., 2000), or convective removal (Platt and Vissers, 1989).

Following the exhumation of the Alpujarride Complex, subduction would have resumed, subjecting NFC rocks to HP/LT metamorphism in the early Miocene. The NFC was then exhumed along a subduction channel, captured by a low-angle detachment fault, and brought to the surface in its present day configuration. Based on improved imaging of the mantle and beneath the Alboran, it is likely that the slab is currently stalled (Bezada et al., 2013).

The results of this study are compatible with the multiple phase subduction model discussed above. The multimineral Rb-Sr ages are identical to Lu-Hf and U-Pb ages for the HP event in the NFC. The coeval subduction model requires the NFC to have been subducted in the Eocene along with the AC, but the geochronology does not match up in favor of this model. Additionally, the NFC shows no evidence of being affected by the same de-

compressional heating event that occurred in the AC, as it remained within the kyanite stability field throughout its exhumation (Behr and Platt, 2012).

The question remains whether the subduction of the NFC represents renewed subduction after plate boundary reorganization or punctuated subduction and exhumation above a continuously subducting slab (Platt et al., 2013). The answer to this question depends upon the mechanism of lithospheric thinning before 18 Ma and the polarity of early subduction. Slab rollback and break-off allow for continuous subduction if the original subduction zone was oriented to the southeast (Vergés and Fernandez, 2012). Bezada et al. (2013), show a southeast subduction polarity for the onset of collision between Iberia and Africa. Bezada et al. (2013) suggest that the slab rolled back westward towards Gibraltar and is currently stalled beneath the Alboran domain.

1.9 Conclusions

Based on the three statistically valid ages from samples KB2, KB20, and WB137, HP metamorphism must have occurred in the NFC during the early Miocene, from ~ 18 -14 Ma. The ages corroborate other geochronological evidence suggesting that rocks in the Betic Cordillera record two punctuated stages of subduction and exhumation since at least 30 Ma. Figure 1.3 summarizes the new multimineral Rb-Sr ages in context with all other geochronological data from the Betic Cordillera. The results require a reevaluation of the tectonic evolution models proposed for the Alboran domain and the Betic

Cordillera. The data support the early Miocene garnet Lu-Hf ages of Platt et al. (2006) and the U-Pb ages of Sanchez-Vizcaino et al. (2001) and Gomez-Pugnaire et al. (2012). The new Rb-Sr ages suggest that the Nevado-Filabride Complex has a younger metamorphic and tectonic history than the overlying Alpujarride and Malaguide Complexes. The Nevado-Filabride Complex underwent prograde, high-pressure metamorphism during the early Miocene, at which point the overlying Alpujarride Complex had already been exhumed and cooled. Following the high pressure metamorphic event, the NFC was rapidly exhumed along a subduction channel and later captured by a low-angle detachment fault and brought to the surface in a metamorphic core complex geometry (Behr and Platt, 2012).

Chapter 2

Supplementary Information

2.1 Detailed methods

The following section is intended to benefit future students at The University of Texas at Austin who wish to use the technique developed over the course of this thesis project.

The Multimineral Rb-Sr Dating Method

1. Collect samples to be dated.
2. Make probe-quality thin sections.
3. Optical Microscope Analyses.
 - (a) If samples show little to no evidence for retrogression, move on to EPMA.
4. Electron Microprobe Analyses.
 - (a) Map out grains to be analyzed on thin section photographs
 - (b) Make WDS maps for representative garnets in sample
 - (c) Collect composition data for minerals to be dated

- i. Garnet
 - ii. Amphiboles
 - iii. Omphacites
 - iv. White Micas
5. If samples still show no evidence for retrogression, move on to mineral separation
6. Crush samples into small pieces with sledgehammer.
7. Crush samples with jaw crusher.
8. Crush samples with disc mills.
 - (a) Use approximately 1mm of separation between discs.
9. Sieve samples through 1 mm, 710 μm , 500 μm , 250 μm , 125 μm and 53 μm sieves. Collect and bag each grain size fraction.
10. Frantz magnetic separation of samples.
 - (a) Separate nonmagnetics from grain sizes by using high amperage setting:
 - i. 53-125 μm (bag the nonmagnetic fraction for later heavy liquid separation of apatite)
 - ii. 125-250 μm
 - iii. 250-500 μm

(b) Use various amperages to extract minerals from bulk sample.

11. Heavy liquid separation

(a) Run nonmagnetic 53-125um grain size fraction through bromoform

(b) Bag the heavy separate and collect apatite from it.

12. Hand pick the desired mineral grains for each sample.

13. Package samples in weigh paper.

14. Make foil boats to measure sample quantities on microgram scale.

15. Weigh out samples and standards.

16. Put samples into 15 mL beakers.

17. Calculate Rb and Sr spike amounts on basis of sample masses

18. Wash samples before spiking

(a) Add D2 H2O

(b) Ultrasonic for 10 minutes

(c) Pipette away the water

(d) Add more water

(e) Repeat 3 times

19. Weigh samples again

20. Add Rb Spike
21. Weigh samples
22. Add Sr
23. Weigh samples
24. Begin dissolution of samples and standards
 - (a) Add 1 mL of concentrated HF
 - (b) Add 100-250 of concentrated HNO₃
 - (c) Let samples dry down on hot plate at 120C overnight.
25. Remove samples from hotplate and continue dissolution process
 - (a) Add 1600 ul of concentrated HF
 - (b) Add 400 ul of concentrated HNO₃
 - (c) Let samples sit on hotplate for minimum 72 hours at 150C
26. Remove samples from hotplate to cool.
27. Return samples to hotplate (caps off) to dry down overnight.
28. Remove samples from hotplate when dry.
29. Add 2 ml of concentrated HNO₃
30. Let samples sit on hotplate (caps on) for 24 hours at 150C

31. *If there are still solids in solution, follow these steps (if there are no solids, move to step 32):*

- (a) Remove from hotplate to cool
- (b) Add 1 ml of concentrated HCl
- (c) Let samples sit on hotplate for 3 hours at 150C
- (d) Remove caps and let samples dry down overnight
- (e) Add 500 ul of concentrated HNO₃ to dry samples
- (f) Let samples sit in HNO₃ for a few hours on hotplate at 150C (caps on)
- (g) Remove caps and let samples dry down overnight on hotplate.
- (h) Once dry, add 300 ul of 3N HNO₃

32. *If no solids remain in solution, follow these steps:*

- (a) Let samples sit on hotplate overnight to dry down
- (b) Once dry, add 300 ul of 3N HNO₃ (day before Sr Chemistry)

33. Sr Column Chromatography

- (a) Preparation
 - i. Rinse Sr columns with D₂ H₂O
 - ii. Set up Sr columns on clean racks
 - iii. Add Sr-Spec Resin to columns, fill to top of small-diameter section

- iv. Heat up D2 H₂O on hotplate (1ml/column)
- v. Add 1ml D2 H₂O to each column, let drain
- vi. Transfer samples to centrifuge tubes
- vii. Centrifuge samples for 3 minutes
- viii. Condition the resin with 70 ul 3N HNO₃
- ix. Condition the resin with 70 ul 3N HNO₃

(b) Loading and Washing

- i. Wash beakers in 6N HCl, Label them as Rb separates
- ii. Place beakers underneath Sr Columns
- iii. Transfer samples from centrifuge tubes to columns
- iv. Wash with 50 ul 3N HNO₃
- v. Wash with 50 ul 3N HNO₃
- vi. Wash with 50 ul 3N HNO₃
- vii. Wash with 50 ul 3N HNO₃
- viii. Wash with 50 ul 3N HNO₃
- ix. Add 200 ul 3N HNO₃
- x. Add 300 ul 3N HNO₃
- xi. Add 450 ul 3N HNO₃
- xii. Cap Rb beaker and set aside

(c) Sr Collection – this collects 90% of Sr in sample

- i. Label clean 5ml beakers as Sr separates

- ii. Place Sr beakers underneath columns
 - iii. Add 70 ul 0.01N HNO₃
 - iv. Add 70 ul 0.01N HNO₃
 - v. Add 600 ul 0.01N HNO₃
 - vi. Cap Sr beakers and store for later processing.
- (d) Rb Purification – this removes the remaining 10% Sr from the sample
- i. Transfer Rb separate to centrifuge tube
 - ii. Centrifuge for 3 minutes
 - iii. Rinse Rb beaker with 6N HCl
 - iv. Place a waste beaker underneath Sr columns
 - v. Condition Resin with 70 ul 3N HNO₃
 - vi. Condition Resin with 70 ul 3N HNO₃
 - vii. Remove the waste beaker
 - viii. Place clean Rb beaker underneath columns
 - ix. Transfer sample from centrifuge tubes to columns
 - x. Wash with 50 ul 3N HNO₃
 - xi. Wash with 50 ul 3N HNO₃
 - xii. Wash with 50 ul 3N HNO₃
 - xiii. Wash with 50 ul 3N HNO₃
 - xiv. Wash with 50 ul 3N HNO₃

- xv. Add 200 ul 3N HNO₃
- xvi. Add 300 ul 3N HNO₃
- xvii. Add 450 ul 3N HNO₃
- xviii. Add a drop of 0.03M H₃PO₄
- xix. Cap the Rb beaker and store for later processing.

34. Preparation of Sr for TIMS analysis

- (a) Prepare Re filaments on centers
 - i. Weld strips of Re to clean centers
 - ii. Outgas the filaments for 3 hours
 - iii. Let filaments cool in outgasser for 3 hours
 - iv. Remove filaments from outgasser and let sit for 48 hours before loading samples
- (b) Dry down Sr samples
- (c) Add a drop of concentrated HNO₃ to the sample to destroy organic matter
- (d) Dry down Sr samples
- (e) Loading the TIMS Filaments
 - i. Add 1 ul H₃PO₄ to each sample
 - ii. Place filament on amplifier
 - iii. Turn on amplifier

- iv. Add 1 ul TaF solution to filament
- v. Turn off amplifier once TaF has partially dried
- vi. Pipette/mix up sample in H₃PO₄
- vii. Turn on amplifier
- viii. Add sample to drop of TaF in as many aliquots as possible
- ix. Let sample + TaF sit until dry
- x. Raise current by 0.1A/3 seconds until 2.1A, or when filament glows red
- xi. Once filament glows, turn down current immediately over about 10 seconds
- xii. Place filament/center onto Re-specific turret
- xiii. Place a clean center cover over filament

35. TIMS analysis of Sr

- (a) Place turret into TIMS the night before analysis start
- (b) Allow baking sequence to run for 12 hours
- (c) Start the TIMS
- (d) Add 4L of liquid nitrogen to the cryopump
- (e) Calibrate machine for Sr analyses

36. Running Sr Samples on TIMS

- (a) Calibrate the Baseline

- (b) Calibrate the Gains
- (c) Run standard NBS987 first
- (d) Allow 1.5 hours per sample analysis
 - i. Set turret position to desired sample (1-21)
 - ii. Bring filament current up to 1800 mA at a rate of 700mA/min
 - iii. Bring filament current up to 2100 mA at a rate of 700mA/min
 - iv. Bring filament current up to 2400 mA at a rate of 700mA/min
 - v. Open analyzer valve if pressure is good/constant @ 3.0×10^{-8}
 - vi. Peak center on ^{88}Sr in H4 (only necessary at start of run)
 - vii. Focus source lenses without wheel fine tuning once sample signal begins to level out after initial spike
 - viii. Increase filament current by 100mA at a time at rate 100mA/min
 - ix. Repeat previous step until filament temperature = 1475C
 - x. Focus source lens with wheel fine tuning option selected
 - xi. Increase filament current by 100mA at a time by rate 100mA/min
 - xii. Repeat previous step until signal intensity reaches 8.5 volts
 - xiii. If sample is not increasing intensity quickly, use wheel fine tuning focus again when filament current = 3000mA
 - xiv. Continue increasing filament current until intensity is 8.5V
 - xv. Run the sample in 8 blocks of 20 runs each with the manual Sr88 H4 method file.

- xvi. If sample signal is inconsistent, run with 16 blocks.
- (e) If leaving overnight before full analysis of turret
 - i. Set scan control-peak control to 6Li and cup C
 - ii. Check that field probe (magnet) is at 0 volts

37. Rb Column Chromatography

(a) Dissolution

- i. Place Rb separate from Sr separation step on hotplate overnight to dry down at 150C
- ii. Remove dry Rb salts from hotplate
- iii. Let beakers cool
- iv. Add 1ml 6N HCl to beakers
- v. Place capped beakers on hotplate 150C for 3 hours
- vi. Remove beakers to cool
- vii. Place beakers on hotplate 150C to dry down, caps off
- viii. Remove beakers to cool
- ix. Add 500 ul 1.25N HCl, let sit overnight

(b) Preparation

- i. Rinse Rb columns with D2 H2O
- ii. Set up Rb columns on clean racks
- iii. Place waste beakers beneath columns

- iv. Fill Rb columns with D2 H2O
- v. Fill Rb columns with AG50NX8 Resin to top of column
- vi. Condition column (half volume) with 6N HCl, let drain
- vii. Condition column (full volume) with 6N HCl, let drain
- viii. While waiting for column to drain, transfer samples to centrifuge tubes and centrifuge for 3 minutes at 10k RPM
- ix. Rinse column (half volume) with D2
- x. Condition with 500 ul 1.25N HCl
- xi. Condition with 2 ml 1.25N HCl

(c) Loading and Rb Collection

- i. Load sample (in 500 ul 1.25N HCl)
- ii. Wash in 500 ul 1.25N HCl
- iii. Wash in 1 ml 1.25N HCl
- iv. Wash in 9 ml 1.25N HCl
- v. Add 2 ml 1.25N HCl
- vi. Collect the 2 ml and label: Rb backup
- vii. Add 3.5 ml 1.25N HCl
- viii. Collect the 3.5 ml and label: Rb

38. Preparing the Rb separate for ICPMS analysis

- (a) Dry down the Rb separate (3.5 ml) on hotplate overnight 150C
- (b) Bring up in 500 ul Concentrated HNO3 for ICPMS

- (c) Let sit on hotplate 150C for 3 hours, caps ON
- (d) Dry down slowly on hotplate @ 2.5 setting
- (e) Add concentrated HNO₃ to dried Rb salt, such that a 10 ppb Rb solution can be attained in a 5% HNO₃ solution ? this depends on Rb concentration of sample
- (f) Pipette ?50-n? ul of HNO₃ into a clean centrifuge tube, where ?n? is the volume of sample+HNO₃
- (g) Pipette ?n? volume of sample sufficient to create a 10 ppb Rb solution into the centrifuge tub
- (h) Pipette 950 ul D2 H₂O into the centrifuge tube
- (i) Add 1 ul of Zr to 10 ppb Rb, 5% Nitric solution (should be 1 mL total)
- (j) Centrifuge the samples
- (k) Pipette the liquid portion of the centrifuged samples into clean centrifuge tubes for ICPMS analysis, leaving any solids behind.

39. ICPMS analysis with Finnigan Element 2

- (a) Turn on ICPMS
- (b) Tune ICPMS
- (c) Run standards
- (d) Run samples

(e) Budget 20 minutes per sample/standard

40. Perform data processing in MS Excel

41. Perform Isochron Calculation with Isoplot (MS Excel)

2.2 Supplementary Electron Microprobe Data: Cameca SX-50 and JEOL JXA-8200 Analyses

The following tables (located in the Appendix) of supplementary data were collected by the author and George Morgan. The analyses were conducted at the Electron Microprobe Laboratory at the University of Oklahoma in Norman, OK, using a Cameca SX-50. The data were collected in October, 2013. Albite, adularia, forsterite, grossular, spessartine, magnesiochromite, titanite glass, augite, phlogopite, labradorite, rhodonite, anorthite, enstatite, fayalite, and pyrope were used as standards for analyses on garnets and low-density silicates (omphacite, white mica, amphibole, epidote, and chlorite). The tables of supplementary data for Sample WB137 were collected by the author with assistance from Donggao Zhao. The analyses were conducted at the Electron Microprobe Laboratory at the University of Texas at Austin, using a JEOL JXA-8200. The data were collected in November 2012 and January 2013. Enstatite, Anorthite, Fayalite, Pyrope, Augite, Spessartine, and Ilmenite were used as standards for analyses on garnets and white mica.

Appendix

Pre-Run Standards for OU Cameca SX-50 October 11-12, 2013

Standard	Coordinates		Weight Percent Oxides										Total
	X	Y	SiO ₂	TiO ₂	Al ₂ O ₃	Cr ₂ O ₃	FeO*	MnO	MgO	CaO	Na ₂ O	K ₂ O	
AMAB-1	7527	-19291	68.36	0.00	18.82	0.00	0.00	0.00	0.00	0.21	11.56	0.19	99.14
AMAB-2	7604	-19291	67.85	0.00	18.64	0.01	0.01	0.01	0.00	0.25	11.67	0.23	98.66
AMAB-3	7963	-19313	68.62	0.00	18.57	0.01	0.00	0.01	0.00	0.25	11.71	0.21	99.38
AMAB-4	7947	-19053	67.92	0.00	18.51	0.00	0.01	0.02	0.00	0.25	11.72	0.24	98.65
FOSY-1	13078	-32821	42.15	0.00	0.01	0.05	0.02	0.00	57.47	0.01	0.00	0.00	99.71
FOSY-2	13153	-32881	42.21	0.00	0.00	0.01	0.01	0.01	57.35	0.01	0.00	0.00	99.61
FOSY-3	13017	-32936	41.46	0.01	0.00	0.03	0.01	0.00	57.16	0.01	0.00	0.00	98.69
FOSY-4	13017	-32855	41.74	0.01	0.01	0.04	0.01	0.00	57.45	0.00	0.00	0.01	99.27
VGRS-1	12125	-35478	39.18	0.40	20.84	0.48	0.08	0.71	0.52	35.62	0.00	0.00	97.82
VGRS-2	12165	-35482	39.03	0.39	20.80	0.46	0.07	0.74	0.51	35.32	0.00	0.00	97.33
VGRS-3	12151	-35505	39.09	0.41	20.85	0.44	0.04	0.71	0.54	35.50	0.01	0.00	97.59
VGRS-4	12151	-35537	39.00	0.42	20.78	0.47	0.07	0.71	0.53	35.60	0.00	0.00	97.58
VGRS-5	12139	-35557	39.06	0.41	20.88	0.46	0.04	0.71	0.53	35.51	0.00	0.00	97.60
VGRS-6	12143	-35618	38.86	0.38	20.97	0.43	0.06	0.73	0.55	35.66	0.01	0.00	97.65
SGKF-1	16208	-19176	64.16	0.00	17.48	0.00	0.01	0.01	0.00	0.00	1.26	14.76	97.67
SGKF-2	16208	-19121	64.69	0.00	17.77	0.01	0.02	0.00	0.01	0.01	1.29	14.91	98.71
SGKF-3	16176	-19044	64.00	0.00	17.48	0.00	0.01	0.00	0.00	0.01	1.26	14.74	97.50
SGKF-4	16277	-19044	64.06	0.00	17.45	0.00	0.00	0.00	0.00	0.00	1.30	14.73	97.55
TTNG-1	18702	-28352	30.37	40.01	0.01	0.00	0.04	0.00	0.00	27.43	0.05	0.05	97.96
TTNG-2	18792	-28352	30.54	40.17	0.00	0.02	0.06	0.00	0.00	27.66	0.02	0.04	98.51
TTNG-3	18769	-28189	30.06	40.30	0.00	0.00	0.05	0.00	0.00	27.57	0.02	0.05	98.06
TTNG-4	18711	-28109	30.20	40.21	0.01	0.00	0.07	0.02	0.00	27.65	0.04	0.04	98.24
MGCR-1	14905	-30485	0.03	0.00	0.08	79.86	0.04	0.00	20.66	0.00	0.00	0.00	100.67
MGCR-2	14938	-30446	0.04	0.01	0.09	79.95	0.04	0.00	20.57	0.00	0.00	0.00	100.69
MGCR-3	14793	-30446	0.03	0.00	0.08	79.97	0.07	0.00	20.75	0.00	0.00	0.01	100.91
MGCR-4	14766	-30347	0.03	0.00	0.08	80.34	0.08	0.00	20.81	0.00	0.00	0.00	101.35
SPSS-1	19472	-33026	36.02	0.01	19.60	0.00	6.23	37.10	0.00	0.85	0.00	0.00	99.81
SPSS-2	19522	-33078	36.35	0.02	19.66	0.00	6.21	37.62	0.00	0.85	0.00	0.00	100.72
SPSS-3	19536	-33155	35.88	0.01	19.63	0.00	6.36	36.91	0.00	0.88	0.00	0.00	99.67
SPSS-4	19536	-33155	36.15	0.00	19.78	0.00	6.32	37.13	0.00	0.86	0.00	0.00	100.24
SPSS-5	19575	-33160	36.51	0.01	19.80	0.00	6.28	37.76	0.00	0.81	0.00	0.00	101.18
AUGI-1	8971	-21042	47.66	0.45	0.69	0.00	29.44	0.76	1.19	19.54	0.19	0.01	99.93
AUGI-2	8966	-21042	47.92	0.43	0.65	0.00	29.49	0.74	1.23	19.48	0.18	0.01	100.14
AUGI-3	8956	-21042	47.90	0.44	0.67	0.02	30.07	0.75	1.16	18.82	0.21	0.00	100.05
AUGI-4	8951	-21042	47.60	0.45	0.68	0.02	29.81	0.77	1.21	19.32	0.19	0.00	100.06

Pre-Run Standards for OU Cameca SX-50

Atoms per 12 Oxygen

Standard	Si	Ti	Al	Cr	Fe	Mn	Mg	Ca	Na	K	Sum
AMAB-1	4.502	0.000	1.482	0.000	0.000	0.000	0.000	0.015	1.497	0.016	7.513
AMAB-2	4.513	0.000	1.461	0.001	0.000	0.000	0.000	0.018	1.505	0.020	7.518
AMAB-3	4.528	0.000	1.445	0.001	0.000	0.001	0.000	0.018	1.498	0.017	7.507
AMAB-4	4.517	0.000	1.451	0.000	0.000	0.001	0.000	0.018	1.524	0.020	7.530
FOSY-1	2.974	0.000	0.001	0.003	0.001	0.000	6.045	0.001	0.000	0.000	9.024
FOSY-2	2.980	0.000	0.000	0.001	0.001	0.001	6.036	0.001	0.000	0.000	9.019
FOSY-3	2.958	0.001	0.000	0.002	0.001	0.000	6.078	0.001	0.000	0.000	9.040
FOSY-4	2.960	0.001	0.001	0.002	0.001	0.000	6.073	0.000	0.000	0.001	9.039
VGRS-1	3.014	0.023	1.890	0.029	0.005	0.046	0.059	2.936	0.000	0.000	8.003
VGRS-2	3.017	0.023	1.895	0.028	0.005	0.048	0.059	2.925	0.000	0.000	7.999
VGRS-3	3.014	0.024	1.894	0.027	0.003	0.046	0.062	2.932	0.002	0.000	8.003
VGRS-4	3.009	0.024	1.890	0.029	0.005	0.046	0.061	2.943	0.000	0.000	8.007
VGRS-5	3.011	0.024	1.897	0.028	0.003	0.046	0.061	2.933	0.000	0.000	8.003
VGRS-6	2.997	0.022	1.907	0.026	0.004	0.048	0.063	2.947	0.001	0.000	8.015
SGKF-1	4.533	0.000	1.455	0.000	0.001	0.000	0.000	0.000	0.172	1.330	7.491
SGKF-2	4.523	0.000	1.465	0.000	0.001	0.000	0.002	0.001	0.175	1.330	7.497
SGKF-3	4.530	0.000	1.458	0.000	0.000	0.000	0.000	0.001	0.173	1.331	7.493
SGKF-4	4.532	0.000	1.455	0.000	0.000	0.000	0.000	0.000	0.178	1.329	7.494
TTNG-1	2.423	2.400	0.001	0.000	0.003	0.000	0.000	2.345	0.007	0.005	7.183
TTNG-2	2.423	2.397	0.000	0.001	0.004	0.000	0.000	2.351	0.003	0.004	7.183
TTNG-3	2.399	2.419	0.000	0.000	0.004	0.000	0.000	2.357	0.003	0.005	7.187
TTNG-4	2.406	2.409	0.001	0.000	0.005	0.002	0.000	2.360	0.006	0.004	7.191
MGCR-1	0.003	0.000	0.009	6.026	0.004	0.000	2.939	0.000	0.000	0.000	8.980
MGCR-2	0.004	0.001	0.010	6.032	0.003	0.000	2.926	0.000	0.000	0.000	8.975
MGCR-3	0.003	0.000	0.009	6.020	0.006	0.000	2.945	0.000	0.000	0.001	8.983
MGCR-4	0.003	0.000	0.009	6.022	0.007	0.000	2.941	0.000	0.000	0.000	8.982
SPESS-1	2.996	0.001	1.922	0.000	0.433	2.614	0.000	0.076	0.000	0.000	8.043
SPESS-2	2.999	0.002	1.912	0.000	0.428	2.629	0.000	0.075	0.000	0.000	8.044
SPESS-3	2.990	0.001	1.928	0.000	0.443	2.605	0.000	0.079	0.000	0.000	8.046
SPESS-4	2.993	0.000	1.931	0.000	0.437	2.604	0.000	0.076	0.000	0.000	8.041
SPESS-5	2.998	0.000	1.917	0.000	0.431	2.626	0.000	0.072	0.000	0.000	8.044
AUGI-1	3.934	0.028	0.067	0.000	2.032	0.053	0.147	1.728	0.030	0.001	8.020
AUGI-2	3.950	0.027	0.063	0.000	2.033	0.052	0.151	1.720	0.029	0.001	8.027
AUGI-3	3.949	0.027	0.065	0.001	2.074	0.052	0.143	1.663	0.033	0.000	8.007
AUGI-4	3.929	0.028	0.066	0.001	2.058	0.054	0.149	1.709	0.031	0.001	8.025

Pre-Run Standards for OU Cameca SX-50

Standard	K Numbers (=Ix/Istd)									
	Na	Mg	Al	Si	K	Ca	Ti	Cr	Mn	Fe
AMAB-1	1.0049	0.0000	0.8945	1.7176	0.0124	0.0057	0.0000	0.0000	0.0001	0.0000
AMAB-2	1.0144	0.0000	0.8855	1.7338	0.0153	0.0068	0.0000	0.0001	0.0001	0.0002
AMAB-3	1.0181	0.0000	0.8828	1.7581	0.0136	0.0068	0.0000	0.0001	0.0003	0.0000
AMAB-4	1.0179	0.0000	0.8783	1.7363	0.0158	0.0066	0.0000	0.0000	0.0004	0.0002
FOSY-1	0.0000	1.0025	0.0004	0.9258	0.0003	0.0002	0.0001	0.0005	0.0000	0.0006
FOSY-2	0.0000	1.0002	0.0001	0.9276	0.0000	0.0003	0.0000	0.0001	0.0003	0.0004
FOSY-3	0.0000	0.9955	0.0002	0.9085	0.0000	0.0002	0.0003	0.0004	0.0000	0.0003
FOSY-4	0.0000	1.0017	0.0003	0.9154	0.0009	0.0000	0.0002	0.0004	0.0000	0.0003
VGRS-1	0.0000	0.0076	1.0002	1.0091	0.0001	1.0029	0.0095	0.0053	0.0176	0.0025
VGRS-2	0.0001	0.0075	0.9985	1.0046	0.0002	0.9942	0.0093	0.0051	0.0183	0.0024
VGRS-3	0.0008	0.0079	1.0007	1.0064	0.0000	0.9993	0.0096	0.0050	0.0176	0.0014
VGRS-4	0.0000	0.0078	0.9972	1.0041	0.0000	1.0024	0.0098	0.0053	0.0176	0.0023
VGRS-5	0.0000	0.0078	1.0023	1.0053	0.0001	0.9997	0.0097	0.0052	0.0177	0.0014
VGRS-6	0.0005	0.0080	1.0065	0.9995	0.0000	1.0040	0.0090	0.0048	0.0182	0.0019
SGKF-1	0.1021	0.0000	0.8900	1.7389	0.9976	0.0001	0.0000	0.0000	0.0001	0.0004
SGKF-2	0.1050	0.0002	0.9050	1.7538	1.0083	0.0002	0.0001	0.0001	0.0001	0.0006
SGKF-3	0.1023	0.0000	0.8904	1.7337	0.9966	0.0002	0.0000	0.0000	0.0001	0.0002
SGKF-4	0.1058	0.0000	0.8882	1.7357	0.9957	0.0001	0.0001	0.0000	0.0000	0.0001
TTNG-1	0.0029	0.0000	0.0003	0.8536	0.0039	0.8345	0.9915	0.0000	0.0000	0.0014
TTNG-2	0.0013	0.0000	0.0000	0.8585	0.0030	0.8413	0.9958	0.0002	0.0000	0.0021
TTNG-3	0.0013	0.0000	0.0000	0.8447	0.0038	0.8394	0.9990	0.0000	0.0000	0.0017
TTNG-4	0.0023	0.0000	0.0003	0.8486	0.0030	0.8417	0.9968	0.0000	0.0006	0.0022
MGCR-1	0.0000	0.2245	0.0026	0.0006	0.0001	0.0000	0.0000	1.0052	0.0000	0.0014
MGCR-2	0.0000	0.2234	0.0029	0.0008	0.0003	0.0000	0.0003	1.0064	0.0000	0.0012
MGCR-3	0.0000	0.2256	0.0027	0.0007	0.0006	0.0000	0.0000	1.0069	0.0000	0.0023
MGCR-4	0.0000	0.2263	0.0028	0.0006	0.0000	0.0000	0.0000	1.0121	0.0000	0.0027
SPESS-1	0.0001	0.0000	0.8075	0.8519	0.0003	0.0251	0.0002	0.0001	0.9967	0.2139
SPESS-2	0.0000	0.0000	0.8102	0.8608	0.0000	0.0250	0.0007	0.0000	1.0115	0.2132
SPESS-3	0.0000	0.0000	0.8085	0.8481	0.0001	0.0259	0.0003	0.0000	0.9916	0.2185
SPESS-4	0.0000	0.0000	0.8155	0.8550	0.0000	0.0253	0.0001	0.0000	0.9977	0.2169
SPESS-5	0.0000	0.0000	0.8162	0.8646	0.0003	0.0240	0.0002	0.0000	1.0154	0.2158
AUGI-1	0.0107	0.0141	0.0279	1.2483	0.0004	0.5654	0.0116	0.0000	0.0200	0.9822
AUGI-2	0.0103	0.0146	0.0266	1.2562	0.0005	0.5634	0.0109	0.0000	0.0195	0.9838
AUGI-3	0.0117	0.0137	0.0271	1.2527	0.0000	0.5449	0.0113	0.0003	0.0196	1.0045
AUGI-4	0.0109	0.0143	0.0275	1.2454	0.0003	0.5595	0.0116	0.0003	0.0201	0.9952
Pertinent averages	1.0138	1.0000	1.0009	1.0048	0.9996	1.0004	0.9958	1.0077	1.0026	0.9914
Std Dev	0.0062	0.0031	0.0033	0.0032	0.0059	0.0036	0.0031	0.0031	0.0103	0.0105

85

KB2 Garnet-1	Coordinates		Weight Percent Oxides										Total
	X	Y	SiO ₂	TiO ₂	Al ₂ O ₃	Cr ₂ O ₃	FeO*	MnO	MgO	CaO	Na ₂ O	K ₂ O	
KB2-Grt1-1	-12700	-17476	37.95	0.10	20.81	0.02	34.51	0.28	4.12	3.09	0.00	0.00	100.88
KB2-Grt1-2	-12700	-17500	37.62	0.10	20.88	0.01	34.68	0.31	4.18	3.07	0.00	0.00	100.85
KB2-Grt1-3	-12700	-17525	37.87	0.09	20.91	0.01	34.76	0.41	3.90	3.48	0.00	0.00	101.43
KB2-Grt1-4	-12700	-17550	37.52	0.13	20.91	0.00	34.30	0.48	3.69	3.98	0.00	0.00	101.02
KB2-Grt1-5	-12702	-17575	37.77	0.08	21.00	0.01	33.86	0.52	3.56	4.54	0.00	0.00	101.33
KB2-Grt1-6	-12702	-17600	37.70	0.12	20.97	0.01	33.48	0.57	3.50	5.02	0.00	0.00	101.37
KB2-Grt1-7	-12702	-17625	37.71	0.07	20.84	0.01	33.55	0.57	3.44	5.00	0.00	0.00	101.20
KB2-Grt1-8	-12702	-17650	37.80	0.12	20.93	0.01	32.21	0.57	3.26	6.24	0.00	0.00	101.16
KB2-Grt1-9	-12702	-17675	37.79	0.10	20.77	0.01	32.09	0.55	3.16	6.18	0.00	0.00	100.67
KB2-Grt1-10	-12726	-17700	37.78	0.11	20.83	0.01	31.96	0.66	3.13	6.63	0.00	0.00	101.12
KB2-Grt1-11	-12720	-17725	37.62	0.13	21.00	0.01	31.72	0.68	2.97	6.88	0.00	0.00	101.00
KB2-Grt1-12	-12718	-17750	37.60	0.08	21.03	0.01	31.88	0.83	2.99	6.52	0.00	0.00	100.96
KB2-Grt1-13	-12718	-17775	37.55	0.12	20.89	0.02	32.23	0.88	2.92	6.40	0.00	0.00	101.00
KB2-Grt1-14	-12718	-17800	37.71	0.13	21.04	0.01	31.54	0.96	2.64	7.43	0.00	0.00	101.48
KB2-Grt1-15	-12718	-17825	37.68	0.11	20.90	0.01	32.32	1.02	2.60	6.71	0.00	0.01	101.36
KB2-Grt1-16	-12718	-17850	37.57	0.09	20.89	0.01	32.49	0.90	2.70	6.47	0.00	0.00	101.13
KB2-Grt1-17	-12718	-17875	37.40	0.08	20.94	0.01	33.19	0.63	2.97	5.63	0.00	0.00	100.85
KB2-Grt1-18	-12718	-17900	37.53	0.07	20.85	0.01	34.19	0.60	3.23	4.54	0.00	0.00	101.02
KB2-Grt1-19	-12703	-17925	37.52	0.10	20.98	0.03	34.19	0.59	3.34	4.60	0.00	0.00	101.34
KB2-Grt1-20	-12708	-17950	37.65	0.12	20.88	0.02	34.50	0.48	3.57	3.90	0.00	0.00	101.11
KB2-Grt1-21	-12708	-17975	37.57	0.09	21.05	0.00	35.07	0.42	3.81	3.43	0.00	0.00	101.44
KB2-Grt1-22	-12708	-18000	37.68	0.09	20.79	0.02	34.79	0.40	3.87	3.13	0.00	0.00	100.78
KB2-Grt1-23	-12708	-18025	37.93	0.09	21.18	0.02	35.05	0.35	4.14	3.15	0.00	0.00	101.90
KB2-Grt1-24	-12708	-18050	37.64	0.09	20.98	0.01	34.92	0.36	4.29	2.89	0.00	0.00	101.18
KB2-Grt1-25	-12674	-18083	37.15	0.07	21.06	0.01	36.03	0.34	4.74	1.83	0.00	0.00	101.25
KB2-Grt1-26	-12651	-18108	36.71	0.11	21.03	0.00	35.80	0.34	4.76	1.43	0.00	0.01	100.20

KB2 Garnet-2	Coordinates		Weight Percent Oxides										Total
	X	Y	SiO ₂	TiO ₂	Al ₂ O ₃	Cr ₂ O ₃	FeO*	MnO	MgO	CaO	Na ₂ O	K ₂ O	
KB2-Grt2-1	-10814	-19493	37.28	0.06	21.05	0.00	35.68	0.31	4.91	1.94	0.00	0.00	101.23
KB2-Grt2-2	-10788	-19494	37.31	0.06	20.77	0.00	35.24	0.31	4.92	2.07	0.00	0.00	100.68
KB2-Grt2-3	-10763	-19494	37.16	0.06	20.81	0.01	34.55	0.32	4.74	2.56	0.00	0.00	100.22
KB2-Grt2-4	-10734	-19499	37.21	0.07	20.94	0.00	35.00	0.33	4.75	2.35	0.00	0.00	100.66
KB2-Grt2-5	-10709	-19499	37.19	0.07	20.81	0.00	34.57	0.35	4.76	2.66	0.00	0.00	100.41
KB2-Grt2-6	-10684	-19496	37.44	0.06	20.72	0.00	34.14	0.34	4.41	3.23	0.00	0.00	100.35
KB2-Grt2-7	-10659	-19496	37.54	0.08	20.98	0.01	33.69	0.34	4.39	3.95	0.00	0.00	100.99
KB2-Grt2-8	-10634	-19506	37.40	0.07	20.83	0.01	32.64	0.32	4.08	4.92	0.00	0.00	100.26
KB2-Grt2-9	-10609	-19490	37.28	0.05	20.80	0.03	32.82	0.33	3.98	4.97	0.00	0.00	100.25
KB2-Grt2-10	-10584	-19490	37.40	0.08	20.79	0.02	32.60	0.31	3.99	5.19	0.00	0.00	100.36
KB2-Grt2-11	-10559	-19490	37.38	0.09	20.98	0.00	32.76	0.34	4.01	5.11	0.00	0.00	100.67
KB2-Grt2-12	-10534	-19490	37.38	0.07	20.68	0.00	33.06	0.31	4.04	4.77	0.00	0.00	100.33
KB2-Grt2-13	-10509	-19490	37.27	0.05	20.82	0.01	33.98	0.34	4.13	3.94	0.00	0.00	100.53
KB2-Grt2-14	-10484	-19508	37.38	0.04	20.91	0.00	35.51	0.34	4.48	2.39	0.00	0.00	101.05
KB2-Grt2-15	-10454	-19486	37.37	0.06	20.86	0.00	33.72	0.32	3.92	4.45	0.00	0.00	100.71
KB2-Grt2-16	-10429	-19471	37.21	0.06	20.94	0.00	33.75	0.32	4.08	4.30	0.00	0.01	100.66
KB2-Grt2-17	-10404	-19468	37.17	0.08	20.80	0.00	33.89	0.36	4.02	4.24	0.00	0.01	100.58
KB2-Grt2-18	-10379	-19459	37.47	0.06	20.83	0.02	33.41	0.33	4.06	4.61	0.00	0.00	100.79
KB2-Grt2-19	-10354	-19463	37.39	0.09	20.82	0.00	33.18	0.33	3.95	4.69	0.00	0.00	100.44
KB2-Grt2-20	-10329	-19463	37.26	0.07	20.87	0.01	33.74	0.36	4.08	4.24	0.00	0.00	100.62
KB2-Grt2-21	-10304	-19463	37.31	0.07	21.06	0.01	33.51	0.31	4.01	4.68	0.00	0.00	100.96
KB2-Grt2-22	-10279	-19454	37.27	0.08	20.92	0.00	33.11	0.31	4.08	4.60	0.00	0.00	100.36
KB2-Grt2-23	-10252	-19456	37.35	0.07	20.93	0.02	33.13	0.32	4.06	4.52	0.00	0.01	100.41
KB2-Grt2-24	-10227	-19457	37.62	0.08	20.84	0.03	33.00	0.30	3.98	4.90	0.00	0.00	100.75
KB2-Grt2-25	-10202	-19465	37.25	0.10	20.68	0.00	32.10	0.29	3.77	5.82	0.00	0.00	100.00
KB2-Grt2-26	-10177	-19479	37.77	0.08	20.87	0.01	32.49	0.30	3.94	5.36	0.00	0.00	100.81
KB2-Grt2-27	-10152	-19464	37.56	0.10	20.90	0.02	32.80	0.32	4.02	5.15	0.00	0.00	100.86
KB2-Grt2-28	-10127	-19464	37.34	0.09	20.94	0.00	33.10	0.33	4.06	4.94	0.00	0.00	100.80
KB2-Grt2-29	-10102	-19440	37.58	0.07	20.87	0.01	33.50	0.35	4.16	4.26	0.00	0.00	100.80
KB2-Grt2-30	-10074	-19440	37.36	0.10	20.95	0.01	33.11	0.33	4.18	4.38	0.00	0.00	100.43
KB2-Grt2-31	-10049	-19439	37.52	0.10	20.64	0.00	33.58	0.33	4.18	3.99	0.00	0.01	100.33
KB2-Grt2-32	-10024	-19451	37.63	0.07	20.81	0.01	34.49	0.34	4.49	2.87	0.00	0.00	100.71
KB2-Grt2-33	-9999	-19456	37.66	0.06	20.95	0.01	34.76	0.36	4.53	2.72	0.00	0.01	101.06
KB2-Grt2-34	-9974	-19460	37.75	0.07	21.05	0.02	34.48	0.27	4.61	2.72	0.00	0.00	100.97
KB2-Grt2-35	-9949	-19459	37.59	0.08	20.96	0.00	35.10	0.27	4.76	2.47	0.00	0.00	101.23
KB2-Grt2-36	-9924	-19455	37.59	0.25	21.09	0.00	35.33	0.28	4.83	1.85	0.00	0.00	101.22
KB2-Grt2-37	-9898	-19465	37.55	0.31	20.94	0.00	35.16	0.32	4.67	2.21	0.00	0.01	101.17
KB2-Grt2-38	-9873	-19465	37.68	0.06	20.93	0.00	35.31	0.29	4.62	2.33	0.00	0.00	101.21
KB2-Grt2-39	-9852	-19453	37.58	0.03	20.96	0.00	35.31	0.28	4.55	2.37	0.00	0.00	101.08

KB2 Garnet-3	Coordinates		Weight Percent Oxides										Total
	X	Y	SiO ₂	TiO ₂	Al ₂ O ₃	Cr ₂ O ₃	FeO*	MnO	MgO	CaO	Na ₂ O	K ₂ O	
KB2-Grt3-1	-10162	-19894	37.30	0.06	20.77	0.01	34.86	0.31	4.22	3.08	0.00	0.00	100.62
KB2-Grt3-2	-10163	-19919	37.61	0.07	20.81	0.01	34.82	0.27	4.24	3.14	0.00	0.00	100.98
KB2-Grt3-3	-10162	-19944	37.08	0.04	20.62	0.00	35.34	0.35	4.47	2.24	0.00	0.00	100.15
KB2-Grt3-4	-10166	-19969	37.55	0.08	20.74	0.01	34.81	0.41	4.14	3.20	0.00	0.00	100.94
KB2-Grt3-5	-10168	-19994	37.52	0.00	20.82	0.01	34.42	0.50	4.31	2.80	0.00	0.00	100.38
KB2-Grt3-6	-10168	-20019	37.76	0.08	20.92	0.00	33.91	0.49	4.02	3.84	0.00	0.00	101.04
KB2-Grt3-7	-10168	-20044	37.42	0.06	20.89	0.01	33.65	0.49	4.06	4.20	0.00	0.00	100.78
KB2-Grt3-8	-10146	-20069	37.62	0.08	21.06	0.01	33.18	0.44	3.92	4.81	0.00	0.00	101.12
KB2-Grt3-9	-10146	-20094	37.68	0.10	21.08	0.00	33.11	0.49	3.87	4.87	0.00	0.00	101.21
KB2-Grt3-10	-10165	-20119	37.83	0.10	20.99	0.00	31.91	0.50	3.51	6.19	0.00	0.00	101.03
KB2-Grt3-11	-10165	-20144	38.17	0.06	20.66	0.00	32.47	0.47	3.73	5.23	0.00	0.00	100.79
KB2-Grt3-12	-10139	-20169	37.74	0.10	20.90	0.01	31.78	0.48	3.49	6.36	0.00	0.00	100.85
KB2-Grt3-13	-10139	-20194	37.94	0.11	20.89	0.00	30.99	0.56	3.33	7.01	0.00	0.00	100.84
KB2-Grt3-14	-10157	-20219	37.60	0.13	20.98	0.00	31.59	0.48	3.45	6.58	0.00	0.01	100.81
KB2-Grt3-15	-10157	-20244	37.54	0.09	21.10	0.02	31.71	0.62	3.57	6.23	0.00	0.00	100.87
KB2-Grt3-16	-10157	-20269	37.52	0.01	21.10	0.01	35.01	0.53	4.11	2.88	0.00	0.01	101.19
KB2-Grt3-17	-10153	-20294	37.61	0.09	21.18	0.01	33.75	0.47	4.03	4.28	0.00	0.00	101.42
KB2-Grt3-18	-10158	-20319	37.52	0.07	21.18	0.01	34.36	0.44	4.32	3.38	0.00	0.01	101.30
KB2-Grt3-19	-10160	-20344	37.63	0.08	21.23	0.00	34.89	0.42	4.52	2.61	0.00	0.00	101.38
KB2-Grt3-20	-10160	-20369	37.65	0.05	21.34	0.01	35.71	0.35	4.59	2.03	0.00	0.00	101.72
KB2-Grt3-21	-10156	-20394	37.65	0.05	21.37	0.01	35.42	0.32	4.72	2.30	0.00	0.01	101.85
KB2-Grt3-22	-10156	-20419	37.70	0.05	21.23	0.01	35.43	0.29	4.82	1.91	0.00	0.00	101.43
KB2-Grt3-23	-10200	-20453	37.30	0.04	20.94	0.00	34.97	0.31	4.63	2.50	0.00	0.01	100.71
KB2-Grt3-24	-10212	-20478	37.23	0.03	20.98	0.01	34.94	0.30	4.54	2.51	0.00	0.02	100.57

KB2											
Atoms per 12 Oxygen											
Garnet-1	Si	Ti	Al	Cr	Fe	Mn	Mg	Ca	Na	K	Sum
KB2-Grt1-1	3.008	0.006	1.944	0.002	2.288	0.019	0.486	0.262	0.000	0.000	8.014
KB2-Grt1-2	2.988	0.006	1.954	0.001	2.303	0.021	0.494	0.261	0.000	0.000	8.029
KB2-Grt1-3	2.993	0.006	1.948	0.001	2.298	0.027	0.460	0.295	0.000	0.000	8.027
KB2-Grt1-4	2.980	0.008	1.958	0.000	2.279	0.033	0.437	0.339	0.000	0.000	8.033
KB2-Grt1-5	2.988	0.005	1.958	0.000	2.240	0.035	0.419	0.385	0.000	0.000	8.029
KB2-Grt1-6	2.982	0.007	1.955	0.001	2.214	0.038	0.413	0.425	0.000	0.000	8.034
KB2-Grt1-7	2.989	0.004	1.947	0.001	2.224	0.038	0.406	0.425	0.000	0.000	8.034
KB2-Grt1-8	2.989	0.007	1.951	0.001	2.129	0.039	0.385	0.529	0.000	0.000	8.028
KB2-Grt1-9	3.001	0.006	1.944	0.001	2.131	0.037	0.374	0.526	0.000	0.000	8.021
KB2-Grt1-10	2.990	0.007	1.943	0.001	2.115	0.045	0.370	0.562	0.000	0.000	8.031
KB2-Grt1-11	2.981	0.008	1.961	0.001	2.102	0.046	0.351	0.584	0.000	0.000	8.031
KB2-Grt1-12	2.982	0.005	1.965	0.001	2.114	0.056	0.353	0.554	0.000	0.000	8.031
KB2-Grt1-13	2.982	0.007	1.955	0.001	2.140	0.059	0.345	0.544	0.000	0.000	8.033
KB2-Grt1-14	2.978	0.008	1.959	0.001	2.084	0.064	0.311	0.629	0.000	0.000	8.034
KB2-Grt1-15	2.985	0.007	1.952	0.001	2.142	0.069	0.307	0.570	0.000	0.001	8.033
KB2-Grt1-16	2.984	0.005	1.955	0.001	2.158	0.061	0.320	0.551	0.000	0.000	8.034
KB2-Grt1-17	2.978	0.005	1.965	0.001	2.211	0.042	0.353	0.480	0.000	0.000	8.034
KB2-Grt1-18	2.987	0.004	1.955	0.000	2.275	0.040	0.383	0.387	0.000	0.000	8.032
KB2-Grt1-19	2.975	0.006	1.961	0.002	2.268	0.039	0.395	0.391	0.000	0.000	8.037
KB2-Grt1-20	2.989	0.007	1.954	0.001	2.290	0.032	0.422	0.332	0.000	0.000	8.027
KB2-Grt1-21	2.975	0.005	1.965	0.000	2.322	0.028	0.450	0.291	0.000	0.000	8.037
KB2-Grt1-22	2.998	0.006	1.949	0.001	2.315	0.027	0.459	0.266	0.000	0.000	8.022
KB2-Grt1-23	2.983	0.005	1.963	0.001	2.305	0.023	0.485	0.266	0.000	0.000	8.030
KB2-Grt1-24	2.981	0.005	1.959	0.001	2.313	0.024	0.506	0.245	0.000	0.000	8.034
KB2-Grt1-25	2.950	0.004	1.971	0.001	2.393	0.023	0.561	0.156	0.000	0.000	8.060
KB2-Grt1-26	2.944	0.007	1.988	0.000	2.401	0.023	0.569	0.123	0.000	0.001	8.056

KB2		Atoms per 12 Oxygen									
Garnet-2	Si	Ti	Al	Cr	Fe	Mn	Mg	Ca	Na	K	Sum
KB2-Grt2-1	2.956	0.003	1.967	0.000	2.366	0.021	0.580	0.165	0.000	0.000	8.058
KB2-Grt2-2	2.970	0.004	1.949	0.000	2.347	0.021	0.584	0.177	0.000	0.000	8.052
KB2-Grt2-3	2.969	0.004	1.960	0.001	2.309	0.022	0.565	0.219	0.000	0.000	8.047
KB2-Grt2-4	2.963	0.004	1.965	0.000	2.331	0.022	0.564	0.201	0.000	0.000	8.050
KB2-Grt2-5	2.967	0.004	1.956	0.000	2.306	0.023	0.566	0.227	0.000	0.000	8.051
KB2-Grt2-6	2.985	0.004	1.948	0.000	2.277	0.023	0.525	0.276	0.000	0.000	8.037
KB2-Grt2-7	2.973	0.005	1.958	0.001	2.231	0.023	0.518	0.335	0.000	0.000	8.043
KB2-Grt2-8	2.979	0.004	1.955	0.001	2.174	0.022	0.484	0.420	0.000	0.000	8.039
KB2-Grt2-9	2.974	0.003	1.955	0.002	2.190	0.023	0.474	0.424	0.000	0.000	8.044
KB2-Grt2-10	2.978	0.005	1.951	0.001	2.171	0.021	0.473	0.442	0.000	0.000	8.041
KB2-Grt2-11	2.968	0.006	1.963	0.000	2.175	0.023	0.475	0.435	0.000	0.000	8.045
KB2-Grt2-12	2.981	0.004	1.944	0.000	2.205	0.021	0.480	0.408	0.000	0.000	8.043
KB2-Grt2-13	2.972	0.003	1.956	0.001	2.266	0.023	0.491	0.337	0.000	0.000	8.047
KB2-Grt2-14	2.970	0.002	1.959	0.000	2.360	0.023	0.531	0.204	0.000	0.000	8.048
KB2-Grt2-15	2.974	0.004	1.957	0.000	2.244	0.021	0.465	0.380	0.000	0.000	8.044
KB2-Grt2-16	2.963	0.003	1.965	0.000	2.247	0.022	0.484	0.367	0.000	0.001	8.052
KB2-Grt2-17	2.966	0.005	1.956	0.000	2.261	0.024	0.477	0.363	0.000	0.001	8.052
KB2-Grt2-18	2.976	0.004	1.950	0.002	2.219	0.022	0.481	0.392	0.000	0.000	8.045
KB2-Grt2-19	2.978	0.005	1.954	0.000	2.210	0.022	0.469	0.401	0.000	0.000	8.040
KB2-Grt2-20	2.967	0.004	1.959	0.001	2.248	0.024	0.484	0.362	0.000	0.000	8.049
KB2-Grt2-21	2.960	0.004	1.970	0.001	2.224	0.021	0.474	0.397	0.000	0.000	8.051
KB2-Grt2-22	2.970	0.005	1.964	0.000	2.206	0.021	0.485	0.393	0.000	0.000	8.044
KB2-Grt2-23	2.974	0.004	1.964	0.001	2.206	0.022	0.482	0.385	0.000	0.001	8.040
KB2-Grt2-24	2.984	0.005	1.948	0.002	2.189	0.021	0.471	0.417	0.000	0.000	8.036
KB2-Grt2-25	2.977	0.006	1.948	0.000	2.145	0.020	0.449	0.498	0.000	0.000	8.043
KB2-Grt2-26	2.990	0.005	1.947	0.000	2.151	0.020	0.465	0.455	0.000	0.000	8.032
KB2-Grt2-27	2.976	0.006	1.952	0.001	2.173	0.022	0.474	0.437	0.000	0.000	8.041
KB2-Grt2-28	2.965	0.006	1.959	0.000	2.198	0.022	0.480	0.420	0.000	0.000	8.050
KB2-Grt2-29	2.982	0.005	1.952	0.000	2.223	0.023	0.492	0.362	0.000	0.000	8.038
KB2-Grt2-30	2.973	0.006	1.964	0.001	2.203	0.022	0.495	0.374	0.000	0.000	8.039
KB2-Grt2-31	2.991	0.006	1.939	0.000	2.239	0.023	0.497	0.341	0.000	0.001	8.034
KB2-Grt2-32	2.989	0.004	1.948	0.001	2.291	0.023	0.532	0.244	0.000	0.001	8.032
KB2-Grt2-33	2.983	0.004	1.956	0.001	2.302	0.024	0.535	0.231	0.000	0.001	8.036
KB2-Grt2-34	2.986	0.004	1.962	0.001	2.281	0.018	0.544	0.231	0.000	0.000	8.028
KB2-Grt2-35	2.974	0.005	1.955	0.000	2.322	0.018	0.562	0.210	0.000	0.000	8.045
KB2-Grt2-36	2.972	0.015	1.965	0.000	2.336	0.019	0.569	0.157	0.000	0.000	8.031
KB2-Grt2-37	2.973	0.018	1.954	0.000	2.327	0.021	0.551	0.187	0.000	0.001	8.033
KB2-Grt2-38	2.982	0.004	1.952	0.000	2.337	0.020	0.545	0.198	0.000	0.000	8.038
KB2-Grt2-39	2.980	0.002	1.958	0.000	2.341	0.019	0.538	0.201	0.000	0.000	8.039

KB2		Atoms per 12 Oxygen									
Garnet-3	Si	Ti	Al	Cr	Fe	Mn	Mg	Ca	Na	K	Sum
KB2-Grt3-1	2.976	0.004	1.953	0.001	2.325	0.021	0.502	0.264	0.000	0.000	8.044
KB2-Grt3-2	2.986	0.004	1.947	0.001	2.311	0.018	0.502	0.267	0.000	0.000	8.036
KB2-Grt3-3	2.975	0.002	1.950	0.000	2.371	0.024	0.534	0.193	0.000	0.000	8.049
KB2-Grt3-4	2.985	0.005	1.943	0.001	2.314	0.028	0.490	0.273	0.000	0.000	8.038
KB2-Grt3-5	2.992	0.000	1.957	0.001	2.295	0.034	0.513	0.239	0.000	0.000	8.030
KB2-Grt3-6	2.990	0.005	1.953	0.000	2.246	0.033	0.475	0.326	0.000	0.000	8.028
KB2-Grt3-7	2.974	0.004	1.957	0.001	2.237	0.033	0.481	0.358	0.000	0.000	8.043
KB2-Grt3-8	2.976	0.005	1.963	0.000	2.195	0.030	0.463	0.407	0.000	0.000	8.038
KB2-Grt3-9	2.977	0.006	1.963	0.000	2.188	0.033	0.455	0.412	0.000	0.000	8.035
KB2-Grt3-10	2.989	0.006	1.954	0.000	2.108	0.033	0.414	0.524	0.000	0.000	8.028
KB2-Grt3-11	3.020	0.004	1.926	0.000	2.149	0.032	0.440	0.444	0.000	0.000	8.013
KB2-Grt3-12	2.988	0.006	1.950	0.000	2.104	0.032	0.411	0.539	0.000	0.000	8.031
KB2-Grt3-13	2.998	0.006	1.946	0.000	2.048	0.038	0.393	0.594	0.000	0.000	8.023
KB2-Grt3-14	2.978	0.008	1.958	0.000	2.093	0.032	0.407	0.558	0.000	0.001	8.035
KB2-Grt3-15	2.972	0.006	1.969	0.001	2.100	0.042	0.421	0.528	0.000	0.000	8.038
KB2-Grt3-16	2.975	0.001	1.972	0.001	2.322	0.036	0.486	0.245	0.000	0.001	8.038
KB2-Grt3-17	2.969	0.005	1.970	0.001	2.228	0.032	0.475	0.362	0.000	0.000	8.040
KB2-Grt3-18	2.966	0.004	1.974	0.001	2.272	0.029	0.509	0.286	0.000	0.001	8.042
KB2-Grt3-19	2.971	0.005	1.975	0.000	2.304	0.028	0.532	0.221	0.000	0.000	8.036
KB2-Grt3-20	2.967	0.003	1.982	0.001	2.354	0.023	0.539	0.171	0.000	0.000	8.039
KB2-Grt3-21	2.961	0.003	1.981	0.000	2.330	0.021	0.553	0.193	0.000	0.001	8.045
KB2-Grt3-22	2.974	0.003	1.974	0.001	2.337	0.019	0.567	0.161	0.000	0.000	8.036
KB2-Grt3-23	2.969	0.003	1.964	0.000	2.328	0.021	0.550	0.213	0.000	0.001	8.048
KB2-Grt3-24	2.968	0.002	1.971	0.001	2.329	0.020	0.540	0.214	0.000	0.002	8.046

KB2 Garnet-1	K Numbers (=Ix/Istd)									
	Na	Mg	Al	Si	K	Ca	Ti	Cr	Mn	Fe
KB2-Grt1-1	0.0000	0.0497	0.8349	0.8724	0.0000	0.0886	0.0027	0.0003	0.0074	1.1655
KB2-Grt1-2	0.0000	0.0503	0.8366	0.8637	0.0000	0.0882	0.0027	0.0002	0.0082	1.1715
KB2-Grt1-3	0.0000	0.0470	0.8395	0.8714	0.0000	0.0999	0.0025	0.0002	0.0108	1.1744
KB2-Grt1-4	0.0000	0.0444	0.8413	0.8639	0.0001	0.1143	0.0035	0.0000	0.0129	1.1584
KB2-Grt1-5	0.0000	0.0429	0.8477	0.8718	0.0000	0.1304	0.0021	0.0001	0.0139	1.1426
KB2-Grt1-6	0.0000	0.0423	0.8481	0.8715	0.0002	0.1441	0.0031	0.0001	0.0152	1.1290
KB2-Grt1-7	0.0000	0.0416	0.8425	0.8718	0.0003	0.1437	0.0019	0.0001	0.0153	1.1317
KB2-Grt1-8	0.0000	0.0397	0.8521	0.8776	0.0000	0.1791	0.0033	0.0001	0.0153	1.0841
KB2-Grt1-9	0.0000	0.0384	0.8457	0.8777	0.0002	0.1775	0.0027	0.0002	0.0147	1.0799
KB2-Grt1-10	0.0000	0.0381	0.8491	0.8783	0.0000	0.1902	0.0030	0.0002	0.0176	1.0754
KB2-Grt1-11	0.0000	0.0362	0.8576	0.8748	0.0002	0.1974	0.0034	0.0001	0.0181	1.0670
KB2-Grt1-12	0.0000	0.0364	0.8576	0.8734	0.0000	0.1873	0.0022	0.0002	0.0222	1.0732
KB2-Grt1-13	0.0000	0.0354	0.8505	0.8723	0.0001	0.1839	0.0031	0.0002	0.0233	1.0855
KB2-Grt1-14	0.0000	0.0321	0.8616	0.8791	0.0000	0.2136	0.0035	0.0002	0.0254	1.0612
KB2-Grt1-15	0.0000	0.0315	0.8526	0.8768	0.0004	0.1929	0.0029	0.0001	0.0273	1.0889
KB2-Grt1-16	0.0000	0.0327	0.8509	0.8732	0.0002	0.1860	0.0024	0.0001	0.0240	1.0948
KB2-Grt1-17	0.0000	0.0359	0.8492	0.8661	0.0000	0.1619	0.0021	0.0001	0.0167	1.1191
KB2-Grt1-18	0.0000	0.0389	0.8410	0.8665	0.0002	0.1306	0.0018	0.0001	0.0160	1.1543
KB2-Grt1-19	0.0000	0.0402	0.8462	0.8658	0.0000	0.1321	0.0028	0.0004	0.0157	1.1545
KB2-Grt1-20	0.0000	0.0429	0.8402	0.8674	0.0000	0.1121	0.0031	0.0002	0.0127	1.1652
KB2-Grt1-21	0.0000	0.0458	0.8447	0.8633	0.0003	0.0987	0.0024	0.0000	0.0112	1.1853
KB2-Grt1-22	0.0000	0.0465	0.8335	0.8660	0.0000	0.0898	0.0025	0.0003	0.0108	1.1757
KB2-Grt1-23	0.0000	0.0498	0.8495	0.8713	0.0000	0.0905	0.0023	0.0002	0.0093	1.1847
KB2-Grt1-24	0.0000	0.0516	0.8398	0.8633	0.0000	0.0829	0.0023	0.0002	0.0097	1.1803
KB2-Grt1-25	0.0000	0.0568	0.8363	0.8473	0.0003	0.0527	0.0019	0.0002	0.0092	1.2199
KB2-Grt1-26	0.0000	0.0569	0.8340	0.8353	0.0008	0.0412	0.0029	0.0000	0.0092	1.2117

KB2 Garnet-2	K Numbers (=Ix/Istd)									
	Na	Mg	Al	Si	K	Ca	Ti	Cr	Mn	Fe
KB2-Grt2-1	0.0000	0.0589	0.8367	0.8506	0.0003	0.0558	0.0015	0.0000	0.0083	1.2073
KB2-Grt2-2	0.0000	0.0592	0.8258	0.8520	0.0000	0.0595	0.0015	0.0001	0.0084	1.1915
KB2-Grt2-3	0.0000	0.0572	0.8301	0.8496	0.0001	0.0734	0.0017	0.0001	0.0087	1.1671
KB2-Grt2-4	0.0000	0.0571	0.8344	0.8503	0.0000	0.0676	0.0019	0.0000	0.0089	1.1832
KB2-Grt2-5	0.0000	0.0574	0.8301	0.8507	0.0001	0.0764	0.0020	0.0000	0.0093	1.1677
KB2-Grt2-6	0.0000	0.0533	0.8300	0.8591	0.0000	0.0928	0.0016	0.0000	0.0090	1.1525
KB2-Grt2-7	0.0000	0.0532	0.8433	0.8631	0.0000	0.1133	0.0022	0.0002	0.0091	1.1363
KB2-Grt2-8	0.0000	0.0496	0.8413	0.8625	0.0000	0.1412	0.0019	0.0001	0.0085	1.0991
KB2-Grt2-9	0.0000	0.0484	0.8396	0.8598	0.0000	0.1425	0.0013	0.0003	0.0089	1.1055
KB2-Grt2-10	0.0000	0.0485	0.8403	0.8636	0.0000	0.1488	0.0020	0.0002	0.0081	1.0976
KB2-Grt2-11	0.0000	0.0488	0.8478	0.8624	0.0000	0.1466	0.0024	0.0001	0.0091	1.1033
KB2-Grt2-12	0.0000	0.0490	0.8339	0.8621	0.0003	0.1370	0.0019	0.0000	0.0083	1.1141
KB2-Grt2-13	0.0000	0.0498	0.8359	0.8567	0.0000	0.1132	0.0013	0.0002	0.0090	1.1467
KB2-Grt2-14	0.0000	0.0537	0.8334	0.8550	0.0001	0.0687	0.0010	0.0000	0.0092	1.2012
KB2-Grt2-15	0.0000	0.0474	0.8402	0.8609	0.0000	0.1279	0.0016	0.0000	0.0085	1.1372
KB2-Grt2-16	0.0000	0.0494	0.8421	0.8559	0.0004	0.1234	0.0015	0.0000	0.0085	1.1385
KB2-Grt2-17	0.0000	0.0485	0.8360	0.8553	0.0006	0.1219	0.0021	0.0000	0.0097	1.1435
KB2-Grt2-18	0.0000	0.0492	0.8394	0.8635	0.0000	0.1323	0.0017	0.0003	0.0088	1.1262
KB2-Grt2-19	0.0000	0.0479	0.8396	0.8619	0.0000	0.1347	0.0023	0.0000	0.0088	1.1181
KB2-Grt2-20	0.0000	0.0493	0.8390	0.8571	0.0002	0.1219	0.0018	0.0001	0.0095	1.1383
KB2-Grt2-21	0.0000	0.0486	0.8490	0.8592	0.0000	0.1342	0.0018	0.0002	0.0084	1.1300
KB2-Grt2-22	0.0000	0.0495	0.8432	0.8582	0.0000	0.1320	0.0020	0.0000	0.0083	1.1157
KB2-Grt2-23	0.0000	0.0493	0.8440	0.8602	0.0004	0.1296	0.0018	0.0003	0.0086	1.1164
KB2-Grt2-24	0.0000	0.0483	0.8417	0.8684	0.0000	0.1407	0.0022	0.0004	0.0081	1.1117
KB2-Grt2-25	0.0000	0.0459	0.8381	0.8618	0.0000	0.1668	0.0026	0.0000	0.0077	1.0799
KB2-Grt2-26	0.0000	0.0480	0.8451	0.8734	0.0000	0.1537	0.0022	0.0001	0.0080	1.0937
KB2-Grt2-27	0.0000	0.0488	0.8449	0.8674	0.0000	0.1476	0.0027	0.0002	0.0085	1.1047
KB2-Grt2-28	0.0000	0.0493	0.8449	0.8610	0.0001	0.1417	0.0024	0.0001	0.0087	1.1154
KB2-Grt2-29	0.0000	0.0504	0.8404	0.8655	0.0000	0.1221	0.0020	0.0001	0.0093	1.1296
KB2-Grt2-30	0.0000	0.0507	0.8441	0.8600	0.0001	0.1258	0.0027	0.0002	0.0088	1.1158
KB2-Grt2-31	0.0000	0.0506	0.8296	0.8636	0.0004	0.1144	0.0026	0.0000	0.0089	1.1324
KB2-Grt2-32	0.0000	0.0542	0.8327	0.8629	0.0003	0.0823	0.0019	0.0001	0.0090	1.1649
KB2-Grt2-33	0.0000	0.0546	0.8376	0.8631	0.0005	0.0780	0.0017	0.0001	0.0097	1.1745
KB2-Grt2-34	0.0000	0.0557	0.8424	0.8651	0.0001	0.0781	0.0019	0.0003	0.0072	1.1645
KB2-Grt2-35	0.0000	0.0574	0.8363	0.8601	0.0000	0.0710	0.0021	0.0000	0.0073	1.1863
KB2-Grt2-36	0.0000	0.0581	0.8402	0.8588	0.0000	0.0531	0.0066	0.0001	0.0074	1.1949
KB2-Grt2-37	0.0000	0.0562	0.8353	0.8593	0.0007	0.0634	0.0082	0.0000	0.0085	1.1886
KB2-Grt2-38	0.0000	0.0555	0.8348	0.8624	0.0000	0.0669	0.0017	0.0000	0.0078	1.1939
KB2-Grt2-39	0.0000	0.0547	0.8361	0.8599	0.0000	0.0681	0.0009	0.0000	0.0075	1.1938

KB2 Garnet-3	K Numbers (=Ix/Istd)									
	Na	Mg	Al	Si	K	Ca	Ti	Cr	Mn	Fe
KB2-Grt3-1	0.0000	0.0507	0.8306	0.8554	0.0002	0.0886	0.0016	0.0002	0.0082	1.1778
KB2-Grt3-2	0.0000	0.0510	0.8333	0.8635	0.0001	0.0903	0.0017	0.0002	0.0072	1.1762
KB2-Grt3-3	0.0000	0.0535	0.8207	0.8476	0.0000	0.0645	0.0010	0.0000	0.0095	1.1951
KB2-Grt3-4	0.0000	0.0497	0.8302	0.8625	0.0001	0.0920	0.0023	0.0001	0.0110	1.1761
KB2-Grt3-5	0.0000	0.0520	0.8334	0.8601	0.0000	0.0803	0.0000	0.0001	0.0134	1.1626
KB2-Grt3-6	0.0000	0.0486	0.8418	0.8693	0.0002	0.1104	0.0022	0.0000	0.0132	1.1445
KB2-Grt3-7	0.0000	0.0491	0.8407	0.8613	0.0000	0.1205	0.0016	0.0002	0.0131	1.1351
KB2-Grt3-8	0.0000	0.0476	0.8505	0.8680	0.0000	0.1380	0.0021	0.0001	0.0118	1.1185
KB2-Grt3-9	0.0000	0.0469	0.8522	0.8698	0.0000	0.1397	0.0027	0.0000	0.0130	1.1162
KB2-Grt3-10	0.0000	0.0429	0.8544	0.8777	0.0000	0.1776	0.0026	0.0000	0.0132	1.0736
KB2-Grt3-11	0.0000	0.0454	0.8375	0.8843	0.0001	0.1501	0.0016	0.0000	0.0126	1.0933
KB2-Grt3-12	0.0000	0.0426	0.8511	0.8760	0.0000	0.1824	0.0025	0.0001	0.0127	1.0689
KB2-Grt3-13	0.0000	0.0409	0.8544	0.8832	0.0001	0.2010	0.0028	0.0000	0.0149	1.0414
KB2-Grt3-14	0.0000	0.0421	0.8549	0.8728	0.0004	0.1887	0.0033	0.0000	0.0128	1.0623
KB2-Grt3-15	0.0000	0.0436	0.8585	0.8699	0.0000	0.1786	0.0025	0.0003	0.0164	1.0668
KB2-Grt3-16	0.0000	0.0494	0.8449	0.8603	0.0006	0.0827	0.0003	0.0001	0.0143	1.1837
KB2-Grt3-17	0.0000	0.0488	0.8532	0.8659	0.0000	0.1228	0.0024	0.0002	0.0126	1.1386
KB2-Grt3-18	0.0000	0.0522	0.8496	0.8611	0.0004	0.0970	0.0019	0.0002	0.0117	1.1606
KB2-Grt3-19	0.0000	0.0545	0.8489	0.8617	0.0000	0.0749	0.0023	0.0000	0.0111	1.1792
KB2-Grt3-20	0.0000	0.0551	0.8508	0.8602	0.0000	0.0582	0.0013	0.0002	0.0093	1.2084
KB2-Grt3-21	0.0000	0.0568	0.8529	0.8607	0.0007	0.0659	0.0014	0.0001	0.0085	1.1981
KB2-Grt3-22	0.0000	0.0580	0.8461	0.8612	0.0000	0.0547	0.0013	0.0001	0.0077	1.1983
KB2-Grt3-23	0.0000	0.0557	0.8352	0.8531	0.0008	0.0719	0.0011	0.0000	0.0084	1.1820
KB2-Grt3-24	0.0000	0.0547	0.8374	0.8514	0.0017	0.0721	0.0007	0.0002	0.0079	1.1808

KB20 Garnet-1	Coordinates		Weight Percent Oxides										Total
	X	Y	SiO ₂	TiO ₂	Al ₂ O ₃	Cr ₂ O ₃	FeO*	MnO	MgO	CaO	Na ₂ O	K ₂ O	
KB20-Grt-1-1	-15246	-3202	36.78	0.05	20.84	0.01	28.86	0.90	4.00	7.82	0.00	0.01	99.26
KB20-Grt-1-2	-15195	-3193	36.85	0.08	20.79	0.01	29.50	0.89	3.94	7.65	0.00	0.00	99.71
KB20-Grt-1-3	-15145	-3203	36.62	0.08	20.67	0.01	29.21	0.72	3.43	8.16	0.00	0.00	98.91
KB20-Grt-1-4	-15095	-3203	36.86	0.13	20.65	0.01	29.73	0.69	3.34	8.07	0.00	0.00	99.48
KB20-Grt-1-5	-15045	-3213	36.56	0.62	20.48	0.02	29.68	0.75	3.05	8.13	0.00	0.00	99.30
KB20-Grt-1-6	-14995	-3236	37.14	0.06	20.92	0.00	30.23	0.69	3.00	8.08	0.00	0.00	100.12
KB20-Grt-1-7	-14948	-3247	37.56	0.07	20.79	0.01	30.05	0.69	2.78	8.38	0.00	0.00	100.33
KB20-Grt-1-8	-14900	-3324	37.54	0.08	20.88	0.00	30.55	0.88	2.68	8.12	0.00	0.00	100.74
KB20-Grt-1-9	-14850	-3319	37.20	0.11	20.52	0.00	30.01	0.88	2.54	8.43	0.00	0.00	99.70
KB20-Grt-1-10	-14801	-3370	37.37	0.10	20.81	0.00	29.93	1.01	2.30	9.04	0.00	0.00	100.55
KB20-Grt-1-11	-14751	-3357	37.35	0.06	20.74	0.03	30.55	1.31	2.18	8.46	0.00	0.00	100.68
KB20-Grt-1-12	-14703	-3373	37.35	0.10	20.79	0.03	30.38	0.99	2.39	8.45	0.00	0.00	100.47
KB20-Grt-1-13	-14653	-3371	37.37	0.17	20.57	0.02	29.89	1.16	2.30	9.16	0.00	0.01	100.64
KB20-Grt-1-14	-14603	-3361	37.38	0.13	20.51	0.00	29.73	1.52	2.27	8.53	0.00	0.00	100.06
KB20-Grt-1-15	-14553	-3349	37.33	0.10	20.69	0.03	30.09	1.46	2.09	8.88	0.00	0.00	100.67
KB20-Grt-1-16	-14503	-3362	37.41	0.12	20.75	0.02	29.82	1.45	2.13	8.83	0.00	0.00	100.53
KB20-Grt-1-17	-14452	-3362	37.34	0.16	20.81	0.02	30.18	1.49	2.06	8.72	0.00	0.01	100.81
KB20-Grt-1-18	-14404	-3357	37.50	0.13	20.71	0.02	29.82	1.43	2.11	9.27	0.00	0.00	100.99
KB20-Grt-1-19	-14354	-3362	37.41	0.13	20.59	0.03	30.55	1.50	2.14	8.59	0.00	0.00	100.96
KB20-Grt-1-20	-14304	-3387	37.40	0.18	20.73	0.02	29.68	1.54	2.03	8.96	0.00	0.01	100.55
KB20-Grt-1-21	-14254	-3360	37.44	0.15	20.73	0.02	29.84	1.52	2.06	8.96	0.00	0.00	100.73
KB20-Grt-1-22	-14204	-3360	37.12	0.23	20.67	0.03	29.92	1.44	1.97	9.10	0.00	0.00	100.48
KB20-Grt-1-23	-14154	-3320	37.28	0.16	20.72	0.03	30.34	1.60	2.00	8.37	0.00	0.00	100.50
KB20-Grt-1-24	-14102	-3316	37.14	0.58	20.68	0.03	29.52	1.50	2.00	9.47	0.00	0.01	100.93
KB20-Grt-1-25	-14052	-3308	37.49	0.16	20.78	0.00	29.97	1.38	1.93	9.21	0.00	0.00	100.93
KB20-Grt-1-26	-14002	-3316	37.60	0.14	20.73	0.05	29.02	1.48	2.03	9.74	0.00	0.00	100.79
KB20-Grt-1-27	-13952	-3333	37.44	0.23	20.57	0.03	29.60	1.72	2.11	8.91	0.00	0.01	100.61
KB20-Grt-1-28	-13902	-3332	37.48	0.18	20.64	0.02	28.87	1.71	2.00	9.44	0.00	0.00	100.33
KB20-Grt-1-29	-13852	-3349	37.18	0.18	20.55	0.01	29.63	1.82	2.04	8.88	0.00	0.00	100.29
KB20-Grt-1-30	-13802	-3369	37.40	0.23	20.39	0.01	28.95	2.02	1.90	9.60	0.00	0.00	100.48
KB20-Grt-1-31	-13752	-3369	37.28	0.19	20.44	0.01	29.46	1.94	2.04	8.90	0.00	0.00	100.26
KB20-Grt-1-32	-13702	-3369	37.42	0.17	20.40	0.03	29.20	1.75	1.95	9.39	0.00	0.01	100.33
KB20-Grt-1-33	-13652	-3339	37.33	0.17	20.70	0.02	29.62	1.75	2.03	8.91	0.00	0.00	100.53
KB20-Grt-1-34	-13602	-3333	37.41	0.93	20.58	0.03	29.31	1.63	2.02	9.30	0.00	0.00	101.21
KB20-Grt-1-35	-13552	-3332	37.37	0.46	20.59	0.02	29.94	1.72	2.11	8.54	0.00	0.00	100.76
KB20-Grt-1-36	-13499	-3403	37.54	0.25	20.67	0.02	29.77	1.77	2.00	8.85	0.00	0.00	100.88
KB20-Grt-1-37	-13449	-3412	37.38	0.20	20.73	0.03	29.73	1.61	1.93	9.10	0.00	0.00	100.73
KB20-Grt-1-38	-13399	-3412	37.45	0.17	20.57	0.02	29.93	1.47	1.82	9.19	0.00	0.00	100.62
KB20-Grt-1-39	-13349	-3489	37.39	0.05	20.75	0.01	30.47	1.56	1.91	8.60	0.00	0.00	100.73
KB20-Grt-1-40	-13299	-3489	37.42	0.13	20.75	0.02	30.10	1.51	2.05	8.66	0.00	0.00	100.65
KB20-Grt-1-41	-13249	-3479	38.01	0.13	20.57	0.00	29.68	1.47	2.06	8.88	0.00	0.00	100.80
KB20-Grt-1-42	-13199	-3407	37.51	0.10	20.79	0.00	30.01	1.54	2.02	8.83	0.00	0.00	100.81
KB20-Grt-1-43	-13119	-3586	37.53	0.14	20.74	0.01	29.98	1.20	2.35	8.77	0.00	0.00	100.71
KB20-Grt-1-44	-13063	-3575	37.47	0.17	20.59	0.02	29.34	1.08	2.31	9.44	0.00	0.00	100.42
KB20-Grt-1-45	-13013	-3576	37.44	0.15	20.63	0.01	29.65	1.21	2.29	9.01	0.00	0.01	100.39
KB20-Grt-1-46	-12963	-3542	37.62	0.11	20.69	0.02	29.89	1.11	2.39	8.77	0.00	0.00	100.59
KB20-Grt-1-47	-12913	-3543	37.72	0.14	20.68	0.01	29.36	1.03	2.35	9.33	0.00	0.00	100.61
KB20-Grt-1-48	-12848	-3548	37.60	0.07	20.82	0.02	30.65	0.90	2.54	8.21	0.00	0.00	100.81
KB20-Grt-1-49	-12798	-3548	37.64	0.11	20.81	0.02	30.19	0.91	2.62	8.56	0.00	0.00	100.86
KB20-Grt-1-50	-12742	-3554	37.84	0.11	20.80	0.00	30.04	0.76	2.75	8.52	0.00	0.01	100.83
KB20-Grt-1-51	-12692	-3553	37.83	0.13	20.84	0.03	30.49	0.69	2.83	8.23	0.00	0.00	101.07
KB20-Grt-1-52	-12642	-3533	36.88	0.13	20.72	0.02	29.97	0.75	3.03	8.10	0.00	0.00	99.59
KB20-Grt-1-53	-12592	-3569	37.28	0.04	20.79	0.01	30.16	0.84	3.03	8.00	0.00	0.01	100.16
KB20-Grt-1-54	-12542	-3580	37.27	0.05	20.79	0.00	29.93	0.81	3.17	8.01	0.00	0.01	100.04
KB20-Grt-1-55	-12492	-3618	37.43	0.05	20.88	0.03	30.18	0.77	3.47	7.64	0.00	0.00	100.45
KB20-Grt-1-56	-12442	-3618	37.55	0.03	20.92	0.01	29.90	0.82	3.95	7.29	0.00	0.00	100.46
KB20-Grt-1-57	-12392	-3618	37.63	0.07	20.83	0.03	29.11	0.95	3.99	7.71	0.00	0.00	100.31
KB20-Grt-1-58	-12342	-3684	37.75	0.05	20.87	0.02	28.64	0.90	3.94	8.00	0.00	0.00	100.17
KB20-Grt-1-59	-12282	-3694	37.68	0.06	20.85	0.02	28.48	1.23	3.64	8.46	0.00	0.00	100.42

KB20													
Garnet-2	X	Y	Weight Percent Oxides										
			SiO ₂	TiO ₂	Al ₂ O ₃	Cr ₂ O ₃	FeO*	MnO	MgO	CaO	Na ₂ O	K ₂ O	Total
KB20-Grt2-1	-12246	5966	37.77	0.05	21.01	0.00	28.45	1.17	3.76	8.24	0.00	0.00	100.43
KB20-Grt2-2	-12196	5966	37.81	0.03	20.96	0.04	29.20	0.99	3.98	7.77	0.00	0.00	100.77
KB20-Grt2-3	-12146	5966	37.78	0.07	20.97	0.02	29.52	0.78	3.51	8.21	0.00	0.01	100.86
KB20-Grt2-4	-12096	5966	37.69	0.11	20.80	0.01	29.57	0.80	2.91	8.97	0.00	0.00	100.85
KB20-Grt2-5	-12046	5966	37.39	0.11	20.73	0.03	29.78	0.67	2.61	9.05	0.00	0.00	100.37
KB20-Grt2-6	-11991	5961	37.48	0.06	20.80	0.01	30.34	0.84	2.69	8.19	0.00	0.01	100.42
KB20-Grt2-7	-11941	5961	37.68	0.13	20.64	0.02	29.83	0.91	2.52	8.91	0.00	0.00	100.65
KB20-Grt2-8	-11891	5978	37.42	0.15	20.52	0.02	29.88	0.92	2.48	9.09	0.00	0.00	100.47
KB20-Grt2-9	-11841	5978	37.65	0.18	20.61	0.02	29.75	0.91	2.41	9.11	0.00	0.00	100.64
KB20-Grt2-10	-11791	5964	37.56	0.21	20.62	0.02	29.76	0.90	2.36	8.99	0.00	0.00	100.42
KB20-Grt2-11	-11726	5975	37.53	0.26	20.81	0.02	30.13	0.93	2.55	8.55	0.00	0.00	100.77
KB20-Grt2-12	-11676	5968	37.63	0.14	20.61	0.03	30.47	0.97	2.38	8.68	0.00	0.00	100.90
KB20-Grt2-13	-11626	5966	37.50	0.10	20.66	0.02	30.14	1.11	2.37	8.65	0.00	0.01	100.55
KB20-Grt2-14	-11576	5976	37.75	0.13	20.78	0.01	30.14	1.21	2.40	8.54	0.00	0.00	100.97
KB20-Grt2-15	-11526	6038	37.50	0.15	20.60	0.02	29.69	0.96	2.33	9.11	0.00	0.01	100.37
KB20-Grt2-16	-11476	5905	37.33	0.13	20.77	0.03	29.79	1.33	1.85	9.54	0.00	0.01	100.76
KB20-Grt2-17	-11423	5911	37.33	0.51	20.53	0.01	29.19	1.37	2.00	9.53	0.00	0.00	100.47
KB20-Grt2-18	-11373	5911	37.45	0.15	20.51	0.01	29.39	1.26	1.77	9.98	0.00	0.01	100.53
KB20-Grt2-19	-11323	5932	37.66	0.14	20.49	0.02	29.14	1.36	1.85	10.00	0.00	0.00	100.66
KB20-Grt2-20	-11273	5874	37.42	0.22	20.64	0.01	29.55	1.37	1.95	9.44	0.00	0.00	100.59
KB20-Grt2-21	-11223	5874	37.46	0.10	20.68	0.01	28.75	1.42	2.00	9.87	0.00	0.00	100.29
KB20-Grt2-22	-11173	5877	38.63	0.14	20.69	0.02	29.64	1.48	2.28	8.60	0.00	0.00	101.49
KB20-Grt2-23	-11123	5846	37.47	0.28	20.42	0.01	29.23	1.61	2.16	9.31	0.00	0.00	100.49
KB20-Grt2-24	-11073	5880	37.59	0.19	20.55	0.03	29.49	1.50	2.22	9.14	0.00	0.00	100.71
KB20-Grt2-25	-11037	5781	37.67	0.19	20.60	0.02	29.75	1.59	2.04	9.15	0.00	0.00	101.01
KB20-Grt2-26	-10987	5795	37.36	0.21	20.71	0.01	30.17	1.67	2.04	8.59	0.00	0.00	100.74
KB20-Grt2-27	-10937	5830	37.51	0.17	20.65	0.02	29.35	1.39	2.22	9.13	0.00	0.00	100.44
KB20-Grt2-28	-10875	5809	37.54	0.18	20.50	0.00	29.43	1.52	2.04	9.19	0.00	0.00	100.41
KB20-Grt2-29	-10825	5809	37.78	0.10	20.62	0.01	29.25	1.40	2.12	9.24	0.00	0.00	100.52
KB20-Grt2-30	-10785	5828	37.58	0.15	20.48	0.01	29.73	1.42	1.85	9.33	0.00	0.00	100.55
KB20-Grt2-31	-10735	5809	37.61	0.15	20.76	0.02	29.53	1.31	1.98	9.66	0.00	0.00	101.02
KB20-Grt2-32	-10685	5813	37.37	0.15	20.70	0.01	29.54	1.35	1.85	9.51	0.00	0.00	100.49
KB20-Grt2-33	-10621	5791	37.71	0.11	20.62	0.00	30.32	1.55	2.05	8.56	0.00	0.00	100.93
KB20-Grt2-34	-10570	5791	37.68	0.16	20.63	0.03	29.65	1.06	2.11	9.08	0.00	0.00	100.40
KB20-Grt2-35	-10520	5782	37.60	0.16	20.62	0.00	29.45	0.87	2.14	9.60	0.00	0.01	100.45
KB20-Grt2-36	-10470	5836	37.54	0.16	20.73	0.00	29.88	0.92	2.24	9.41	0.00	0.00	100.89
KB20-Grt2-37	-10420	5825	37.87	0.08	20.82	0.01	30.10	0.93	2.42	8.46	0.00	0.00	100.68
KB20-Grt2-38	-10370	5816	37.74	0.11	20.78	0.01	29.92	0.99	2.36	8.96	0.00	0.01	100.87
KB20-Grt2-39	-10320	5814	37.56	0.11	20.68	0.01	30.00	0.86	2.54	8.64	0.00	0.00	100.40
KB20-Grt2-40	-10270	5814	36.86	0.05	20.42	0.05	30.38	0.86	2.76	7.82	0.00	0.00	99.20
KB20-Grt2-41	-10220	5814	36.40	0.07	20.25	0.03	30.25	0.73	2.74	8.17	0.00	0.00	98.64
KB20-Grt2-42	-10170	5803	37.01	0.07	20.52	0.01	30.17	0.69	2.95	8.14	0.00	0.00	99.56
KB20-Grt2-43	-10120	5823	37.19	0.07	20.10	0.02	28.91	0.82	3.10	8.09	0.00	0.00	98.30
KB20-Grt2-44	-10070	5823	37.45	0.05	20.70	0.02	29.74	0.99	3.62	7.51	0.00	0.01	100.08
KB20-Grt2-45	-10020	5810	37.94	0.03	20.68	0.01	29.03	0.99	3.95	7.80	0.00	0.00	100.43

KB20 Garnet-3	Coordinates		Weight Percent Oxides										Total
	X	Y	SiO ₂	TiO ₂	Al ₂ O ₃	Cr ₂ O ₃	FeO*	MnO	MgO	CaO	Na ₂ O	K ₂ O	
KB20-Grt3-1	2863	8010	37.52	0.03	20.90	0.01	28.81	1.05	3.87	8.00	0.00	0.00	100.20
KB20-Grt3-2	2897	7975	37.62	0.03	20.84	0.02	29.50	0.78	3.36	8.30	0.00	0.01	100.46
KB20-Grt3-3	2932	7940	37.48	0.09	20.74	0.00	29.58	0.87	2.91	8.47	0.00	0.00	100.14
KB20-Grt3-4	2967	7905	37.20	0.10	20.45	0.02	29.68	0.71	2.90	8.59	0.00	0.01	99.65
KB20-Grt3-5	3021	7870	37.40	0.08	20.79	0.03	30.35	0.99	2.67	8.19	0.00	0.01	100.49
KB20-Grt3-6	3056	7835	37.24	0.12	20.56	0.02	29.86	1.05	2.58	8.71	0.00	0.01	100.15
KB20-Grt3-7	3107	7800	37.34	0.08	20.63	0.02	29.50	1.00	2.51	8.73	0.00	0.00	99.81
KB20-Grt3-8	3142	7745	37.12	0.17	20.55	0.01	29.90	1.18	2.26	8.58	0.00	0.00	99.75
KB20-Grt3-9	3177	7697	37.47	0.15	20.65	0.00	29.35	1.56	2.25	8.98	0.00	0.00	100.43
KB20-Grt3-10	3204	7660	37.43	0.09	20.57	0.00	29.57	1.63	2.14	8.85	0.00	0.00	100.30
KB20-Grt3-11	3290	7633	37.09	0.15	20.51	0.01	30.52	1.53	1.88	8.90	0.00	0.01	100.61
KB20-Grt3-12	3333	7598	36.91	0.05	20.65	0.00	30.57	1.93	2.03	7.95	0.00	0.01	100.11
KB20-Grt3-13	3359	7556	37.09	0.24	20.28	0.02	29.11	2.12	1.71	9.34	0.00	0.00	99.90
KB20-Grt3-14	3409	7485	37.01	0.22	20.42	0.03	29.34	2.12	1.94	8.99	0.00	0.00	100.07
KB20-Grt3-15	3455	7450	37.22	0.23	20.11	0.03	28.96	2.11	2.02	9.14	0.00	0.00	99.83
KB20-Grt3-16	3508	7415	37.06	0.08	20.56	0.00	29.74	2.22	2.09	8.12	0.00	0.00	99.87
KB20-Grt3-17	3543	7401	37.03	0.22	20.29	0.02	28.64	2.05	1.88	9.58	0.00	0.00	99.72
KB20-Grt3-18	3567	7345	37.16	0.23	20.37	0.03	29.07	2.12	2.03	8.99	0.00	0.00	99.99
KB20-Grt3-19	3602	7306	37.11	0.14	20.57	0.01	29.22	2.16	1.96	9.12	0.00	0.00	100.29
KB20-Grt3-20	3635	7271	37.20	0.31	20.40	0.01	29.12	2.09	2.30	8.70	0.00	0.00	100.12
KB20-Grt3-21	3670	7236	37.02	0.20	20.40	0.00	28.88	2.13	1.85	9.11	0.00	0.00	99.59
KB20-Grt3-22	3705	7208	37.24	0.26	20.28	0.01	28.52	2.12	2.16	9.39	0.00	0.00	99.98
KB20-Grt3-23	3740	7152	37.33	0.09	20.66	0.01	29.35	1.97	2.96	7.72	0.00	0.00	100.09
KB20-Grt3-25	3819	7082	33.79	16.14	13.09	0.02	17.63	1.24	1.59	16.31	0.01	0.00	99.81
KB20-Grt3-26	3854	7047	37.06	0.15	20.54	0.05	28.84	2.19	2.28	8.91	0.00	0.00	100.03
KB20-Grt3-27	3883	7012	36.96	0.17	20.55	0.03	28.97	2.06	2.17	8.86	0.00	0.01	99.77
KB20-Grt3-28	3929	6972	36.97	0.21	20.27	0.01	29.12	2.21	2.11	8.93	0.00	0.00	99.83
KB20-Grt3-29	3964	6937	36.79	0.39	20.40	0.02	29.62	2.21	1.96	8.46	0.00	0.00	99.86
KB20-Grt3-30	4014	6902	36.97	0.12	20.46	0.00	29.81	2.21	2.06	8.10	0.00	0.00	99.73
KB20-Grt3-31	4049	6867	37.03	0.24	20.23	0.03	28.06	2.10	1.96	9.92	0.00	0.01	99.57
KB20-Grt3-32	4080	6832	37.05	0.25	20.37	0.00	29.42	2.10	2.04	8.64	0.00	0.00	99.87
KB20-Grt3-33	4115	6751	37.05	0.27	20.17	0.04	28.84	2.04	1.97	9.52	0.00	0.00	99.90
KB20-Grt3-34	4148	6694	37.09	0.27	20.40	0.02	29.51	2.08	2.16	8.59	0.00	0.00	100.13
KB20-Grt3-35	4183	6596	36.85	0.10	20.44	0.00	30.22	2.09	2.31	7.79	0.00	0.00	99.81
KB20-Grt3-36	4218	6561	37.02	0.15	20.07	0.02	29.46	2.10	2.08	8.67	0.00	0.00	99.59
KB20-Grt3-37	4253	6525	36.79	0.15	20.22	0.03	29.68	1.94	2.10	8.54	0.00	0.00	99.45
KB20-Grt3-38	4288	6452	36.87	0.41	20.32	0.01	28.76	1.73	2.00	9.42	0.00	0.00	99.53
KB20-Grt3-39	4339	6416	36.71	0.23	20.30	0.01	28.98	1.50	2.12	9.41	0.00	0.00	99.26
KB20-Grt3-40	4373	6381	36.84	0.14	20.31	0.01	29.08	1.49	2.12	9.10	0.00	0.01	99.10
KB20-Grt3-41	4414	6332	36.80	0.11	20.37	0.03	29.51	1.46	1.99	9.12	0.00	0.00	99.38
KB20-Grt3-42	4449	6297	36.92	0.14	20.34	0.01	29.56	1.61	2.02	8.98	0.00	0.00	99.57
KB20-Grt3-43	4476	6262	36.90	0.12	20.43	0.01	29.39	1.46	2.14	8.88	0.00	0.00	99.33
KB20-Grt3-44	4515	6204	36.89	0.11	20.62	0.00	29.25	1.28	2.36	9.11	0.00	0.00	99.62
KB20-Grt3-45	4565	6171	36.85	0.21	20.38	0.00	29.20	1.12	2.37	9.32	0.00	0.00	99.46
KB20-Grt3-46	4603	6136	36.64	0.17	20.50	0.02	30.05	1.06	2.38	8.72	0.00	0.00	99.53
KB20-Grt3-47	4652	6101	36.95	0.06	20.56	0.01	29.72	1.01	2.58	8.43	0.00	0.00	99.33
KB20-Grt3-48	4719	6054	37.02	0.08	20.59	0.00	29.12	0.97	2.72	8.68	0.00	0.01	99.20
KB20-Grt3-49	4770	6001	36.84	0.09	20.67	0.00	29.92	1.09	2.63	8.31	0.00	0.00	99.56
KB20-Grt3-50	4836	5976	36.79	0.13	20.40	0.00	29.74	1.00	2.55	8.83	0.00	0.00	99.45
KB20-Grt3-51	4915	5941	37.01	0.13	20.41	0.00	30.05	0.81	2.47	9.02	0.00	0.01	99.93
KB20-Grt3-52	4947	5891	37.13	0.12	20.40	0.01	30.00	0.81	2.56	8.58	0.00	0.00	99.62
KB20-Grt3-53	4982	5856	36.87	0.09	20.50	0.04	30.36	0.71	2.78	8.05	0.00	0.00	99.39
KB20-Grt3-54	5017	5821	37.00	0.07	20.65	0.00	30.24	0.76	2.99	8.13	0.00	0.00	99.85
KB20-Grt3-55	5052	5786	37.06	0.06	20.59	0.01	29.39	0.76	3.05	8.33	0.00	0.00	99.25
KB20-Grt3-56	5087	5751	37.33	0.10	20.66	0.02	28.88	0.77	3.72	8.13	0.00	0.00	99.59

KB20											
Garnet-1	Atoms per 12 Oxygen										
	Si	Ti	Al	Cr	Fe	Mn	Mg	Ca	Na	K	Sum
KB20-Grt-L1-1	2.948	0.003	1.969	0.001	1.934	0.061	0.478	0.672	0.000	0.001	8.065
KB20-Grt-L1-2	2.947	0.005	1.959	0.001	1.973	0.060	0.469	0.656	0.000	0.000	8.069
KB20-Grt-L1-3	2.953	0.005	1.964	0.001	1.970	0.049	0.413	0.705	0.000	0.000	8.060
KB20-Grt-L1-4	2.959	0.008	1.953	0.001	1.996	0.047	0.399	0.694	0.000	0.000	8.057
KB20-Grt-L1-5	2.945	0.037	1.944	0.002	1.999	0.051	0.366	0.701	0.000	0.000	8.045
KB20-Grt-L1-6	2.964	0.004	1.968	0.000	2.018	0.047	0.357	0.691	0.000	0.000	8.048
KB20-Grt-L1-7	2.988	0.004	1.949	0.001	2.000	0.047	0.330	0.714	0.000	0.000	8.033
KB20-Grt-L1-8	2.981	0.005	1.954	0.000	2.029	0.059	0.317	0.691	0.000	0.000	8.036
KB20-Grt-L1-9	2.986	0.007	1.942	0.000	2.014	0.060	0.304	0.725	0.000	0.000	8.037
KB20-Grt-L1-10	2.977	0.006	1.953	0.000	1.993	0.068	0.273	0.772	0.000	0.000	8.041
KB20-Grt-L1-11	2.979	0.004	1.950	0.002	2.038	0.089	0.259	0.723	0.000	0.000	8.042
KB20-Grt-L1-12	2.978	0.006	1.954	0.002	2.026	0.067	0.284	0.722	0.000	0.000	8.038
KB20-Grt-L1-13	2.978	0.010	1.931	0.001	1.991	0.079	0.273	0.782	0.000	0.001	8.046
KB20-Grt-L1-14	2.993	0.008	1.935	0.000	1.991	0.103	0.271	0.732	0.000	0.000	8.032
KB20-Grt-L1-15	2.977	0.006	1.945	0.002	2.007	0.099	0.248	0.759	0.000	0.000	8.044
KB20-Grt-L1-16	2.983	0.007	1.950	0.001	1.989	0.098	0.253	0.754	0.000	0.000	8.035
KB20-Grt-L1-17	2.974	0.009	1.954	0.001	2.010	0.101	0.245	0.744	0.000	0.001	8.040
KB20-Grt-L1-18	2.979	0.008	1.939	0.001	1.981	0.097	0.250	0.789	0.000	0.001	8.044
KB20-Grt-L1-19	2.980	0.008	1.933	0.002	2.035	0.101	0.254	0.733	0.000	0.000	8.046
KB20-Grt-L1-20	2.982	0.011	1.948	0.001	1.979	0.104	0.241	0.766	0.000	0.001	8.033
KB20-Grt-L1-21	2.982	0.009	1.946	0.002	1.987	0.103	0.244	0.764	0.000	0.000	8.036
KB20-Grt-L1-22	2.968	0.014	1.947	0.002	2.001	0.097	0.235	0.780	0.000	0.000	8.044
KB20-Grt-L1-23	2.979	0.010	1.952	0.002	2.028	0.109	0.238	0.716	0.000	0.000	8.034
KB20-Grt-L1-24	2.955	0.035	1.939	0.002	1.964	0.101	0.237	0.807	0.000	0.001	8.041
KB20-Grt-L1-25	2.980	0.010	1.947	0.000	1.993	0.093	0.229	0.784	0.000	0.000	8.036
KB20-Grt-L1-26	2.986	0.008	1.941	0.003	1.927	0.100	0.240	0.829	0.000	0.000	8.034
KB20-Grt-L1-27	2.985	0.014	1.932	0.002	1.973	0.116	0.251	0.761	0.000	0.001	8.035
KB20-Grt-L1-28	2.990	0.011	1.940	0.001	1.926	0.116	0.237	0.807	0.000	0.000	8.028
KB20-Grt-L1-29	2.977	0.011	1.940	0.001	1.984	0.123	0.244	0.762	0.000	0.000	8.041
KB20-Grt-L1-30	2.987	0.014	1.919	0.001	1.934	0.136	0.226	0.822	0.000	0.000	8.039
KB20-Grt-L1-31	2.985	0.012	1.930	0.001	1.973	0.131	0.243	0.764	0.000	0.000	8.038
KB20-Grt-L1-32	2.992	0.010	1.922	0.002	1.953	0.118	0.233	0.804	0.000	0.001	8.036
KB20-Grt-L1-33	2.979	0.010	1.947	0.001	1.977	0.118	0.241	0.762	0.000	0.000	8.036
KB20-Grt-L1-34	2.963	0.055	1.921	0.002	1.942	0.109	0.239	0.789	0.000	0.000	8.020
KB20-Grt-L1-35	2.977	0.028	1.933	0.001	1.995	0.116	0.251	0.728	0.000	0.001	8.029
KB20-Grt-L1-36	2.985	0.015	1.937	0.002	1.980	0.120	0.237	0.754	0.000	0.000	8.031
KB20-Grt-L1-37	2.978	0.012	1.947	0.002	1.981	0.109	0.229	0.777	0.000	0.000	8.036
KB20-Grt-L1-38	2.989	0.010	1.934	0.001	1.997	0.100	0.217	0.785	0.000	0.000	8.033
KB20-Grt-L1-39	2.983	0.003	1.951	0.000	2.033	0.105	0.227	0.736	0.000	0.000	8.038
KB20-Grt-L1-40	2.983	0.008	1.950	0.002	2.007	0.102	0.244	0.739	0.000	0.000	8.034
KB20-Grt-L1-41	3.016	0.008	1.924	0.000	1.969	0.099	0.243	0.755	0.000	0.000	8.014
KB20-Grt-L1-42	2.985	0.006	1.950	0.000	1.997	0.104	0.240	0.753	0.000	0.000	8.034
KB20-Grt-L1-43	2.984	0.008	1.943	0.001	1.993	0.081	0.278	0.747	0.000	0.000	8.036
KB20-Grt-L1-44	2.985	0.010	1.933	0.001	1.955	0.073	0.274	0.806	0.000	0.000	8.038
KB20-Grt-L1-45	2.986	0.009	1.939	0.001	1.977	0.082	0.272	0.770	0.000	0.001	8.036
KB20-Grt-L1-46	2.992	0.007	1.940	0.001	1.988	0.075	0.284	0.747	0.000	0.000	8.032
KB20-Grt-L1-47	2.995	0.008	1.935	0.001	1.949	0.069	0.278	0.794	0.000	0.000	8.029
KB20-Grt-L1-48	2.986	0.004	1.948	0.001	2.036	0.061	0.301	0.699	0.000	0.000	8.035
KB20-Grt-L1-49	2.984	0.007	1.945	0.001	2.001	0.061	0.310	0.727	0.000	0.000	8.036
KB20-Grt-L1-50	2.995	0.007	1.941	0.000	1.989	0.051	0.324	0.722	0.000	0.001	8.028
KB20-Grt-L1-51	2.989	0.008	1.941	0.002	2.015	0.046	0.334	0.697	0.000	0.000	8.031
KB20-Grt-L1-52	2.960	0.008	1.961	0.001	2.012	0.051	0.362	0.697	0.000	0.000	8.051
KB20-Grt-L1-53	2.974	0.003	1.955	0.001	2.012	0.057	0.360	0.684	0.000	0.001	8.046
KB20-Grt-L1-54	2.973	0.003	1.955	0.000	1.998	0.055	0.377	0.685	0.000	0.002	8.047
KB20-Grt-L1-55	2.972	0.003	1.954	0.002	2.004	0.052	0.411	0.650	0.000	0.000	8.048
KB20-Grt-L1-56	2.974	0.002	1.952	0.000	1.980	0.055	0.466	0.619	0.000	0.000	8.048
KB20-Grt-L1-57	2.979	0.004	1.944	0.002	1.928	0.064	0.471	0.654	0.000	0.000	8.044
KB20-Grt-L1-58	2.987	0.003	1.946	0.001	1.896	0.061	0.465	0.679	0.000	0.001	8.037
KB20-Grt-L1-59	2.981	0.004	1.944	0.001	1.884	0.082	0.430	0.717	0.000	0.000	8.043

KB20 Garnet-2	Atoms per 12 Oxygen										Sum
	Si	Ti	Al	Cr	Fe	Mn	Mg	Ca	Na	K	
KB20-Grt2-1	2.983	0.003	1.955	0.000	1.879	0.078	0.443	0.697	0.000	0.000	8.037
KB20-Grt2-2	2.980	0.002	1.947	0.002	1.924	0.066	0.467	0.656	0.000	0.000	8.044
KB20-Grt2-3	2.980	0.004	1.950	0.001	1.947	0.052	0.412	0.694	0.000	0.001	8.041
KB20-Grt2-4	2.982	0.006	1.939	0.000	1.957	0.054	0.343	0.760	0.000	0.000	8.042
KB20-Grt2-5	2.977	0.007	1.946	0.002	1.983	0.045	0.310	0.772	0.000	0.000	8.042
KB20-Grt2-6	2.984	0.003	1.952	0.001	2.020	0.057	0.320	0.699	0.000	0.001	8.036
KB20-Grt2-7	2.993	0.008	1.932	0.001	1.981	0.061	0.299	0.758	0.000	0.000	8.033
KB20-Grt2-8	2.982	0.009	1.927	0.001	1.992	0.062	0.294	0.777	0.000	0.000	8.045
KB20-Grt2-9	2.991	0.011	1.930	0.002	1.977	0.061	0.286	0.776	0.000	0.000	8.033
KB20-Grt2-10	2.990	0.013	1.935	0.001	1.982	0.061	0.280	0.767	0.000	0.000	8.029
KB20-Grt2-11	2.978	0.016	1.947	0.001	1.999	0.063	0.302	0.727	0.000	0.000	8.032
KB20-Grt2-12	2.989	0.008	1.929	0.002	2.024	0.065	0.282	0.738	0.000	0.000	8.037
KB20-Grt2-13	2.988	0.006	1.939	0.001	2.008	0.075	0.281	0.739	0.000	0.001	8.037
KB20-Grt2-14	2.992	0.008	1.941	0.001	1.998	0.081	0.284	0.725	0.000	0.000	8.030
KB20-Grt2-15	2.989	0.009	1.935	0.001	1.979	0.065	0.277	0.778	0.000	0.001	8.034
KB20-Grt2-16	2.974	0.008	1.950	0.002	1.985	0.090	0.220	0.814	0.000	0.001	8.043
KB20-Grt2-17	2.976	0.031	1.930	0.001	1.947	0.093	0.238	0.814	0.000	0.000	8.028
KB20-Grt2-18	2.988	0.009	1.929	0.001	1.962	0.085	0.211	0.853	0.000	0.001	8.038
KB20-Grt2-19	2.997	0.009	1.922	0.001	1.939	0.092	0.219	0.853	0.000	0.000	8.032
KB20-Grt2-20	2.983	0.013	1.939	0.000	1.969	0.093	0.231	0.806	0.000	0.000	8.034
KB20-Grt2-21	2.988	0.006	1.944	0.001	1.918	0.096	0.238	0.844	0.000	0.000	8.034
KB20-Grt2-22	3.035	0.009	1.916	0.001	1.948	0.099	0.267	0.724	0.000	0.001	7.998
KB20-Grt2-23	2.988	0.017	1.919	0.001	1.949	0.109	0.257	0.796	0.000	0.000	8.035
KB20-Grt2-24	2.990	0.011	1.926	0.002	1.962	0.101	0.264	0.779	0.000	0.000	8.035
KB20-Grt2-25	2.991	0.011	1.928	0.001	1.975	0.107	0.241	0.779	0.000	0.000	8.033
KB20-Grt2-26	2.978	0.013	1.946	0.001	2.011	0.113	0.242	0.733	0.000	0.000	8.036
KB20-Grt2-27	2.988	0.010	1.939	0.002	1.956	0.094	0.264	0.779	0.000	0.000	8.032
KB20-Grt2-28	2.996	0.011	1.928	0.000	1.964	0.103	0.243	0.786	0.000	0.000	8.030
KB20-Grt2-29	3.005	0.006	1.933	0.001	1.946	0.094	0.251	0.788	0.000	0.000	8.023
KB20-Grt2-30	2.998	0.009	1.926	0.001	1.983	0.096	0.221	0.798	0.000	0.000	8.030
KB20-Grt2-31	2.984	0.009	1.941	0.001	1.959	0.088	0.234	0.821	0.000	0.000	8.036
KB20-Grt2-32	2.982	0.009	1.947	0.001	1.972	0.091	0.220	0.813	0.000	0.000	8.035
KB20-Grt2-33	2.998	0.007	1.932	0.000	2.016	0.105	0.243	0.729	0.000	0.000	8.029
KB20-Grt2-34	3.001	0.009	1.937	0.002	1.975	0.072	0.251	0.775	0.000	0.000	8.020
KB20-Grt2-35	2.993	0.010	1.935	0.000	1.961	0.059	0.254	0.819	0.000	0.001	8.031
KB20-Grt2-36	2.980	0.010	1.940	0.000	1.984	0.062	0.265	0.800	0.000	0.000	8.040
KB20-Grt2-37	3.003	0.005	1.946	0.000	1.996	0.062	0.287	0.719	0.000	0.000	8.019
KB20-Grt2-38	2.992	0.007	1.941	0.000	1.983	0.066	0.279	0.761	0.000	0.001	8.031
KB20-Grt2-39	2.991	0.006	1.940	0.001	1.997	0.058	0.302	0.737	0.000	0.001	8.033
KB20-Grt2-40	2.977	0.003	1.944	0.003	2.052	0.059	0.332	0.676	0.000	0.000	8.046
KB20-Grt2-41	2.962	0.005	1.942	0.002	2.058	0.050	0.333	0.712	0.000	0.000	8.062
KB20-Grt2-42	2.974	0.004	1.943	0.001	2.028	0.047	0.354	0.701	0.000	0.000	8.051
KB20-Grt2-43	3.011	0.004	1.918	0.001	1.958	0.056	0.374	0.702	0.000	0.000	8.025
KB20-Grt2-44	2.981	0.003	1.942	0.001	1.980	0.067	0.429	0.641	0.000	0.001	8.045
KB20-Grt2-45	2.998	0.002	1.926	0.001	1.919	0.067	0.465	0.661	0.000	0.000	8.037

KB20 Garnet-3	Atoms per 12 Oxygen										
	Si	Ti	Al	Cr	Fe	Mn	Mg	Ca	Na	K	Sum
KB20-Grt3-1	2.974	0.002	1.953	0.001	1.910	0.071	0.457	0.680	0.000	0.000	8.047
KB20-Grt3-2	2.982	0.002	1.947	0.001	1.956	0.052	0.397	0.705	0.000	0.001	8.043
KB20-Grt3-3	2.986	0.005	1.947	0.000	1.971	0.059	0.346	0.723	0.000	0.000	8.036
KB20-Grt3-4	2.983	0.006	1.933	0.001	1.990	0.048	0.346	0.738	0.000	0.001	8.045
KB20-Grt3-5	2.978	0.005	1.951	0.002	2.021	0.067	0.317	0.699	0.000	0.001	8.041
KB20-Grt3-6	2.978	0.007	1.938	0.002	1.997	0.071	0.307	0.746	0.000	0.001	8.046
KB20-Grt3-7	2.989	0.005	1.946	0.001	1.975	0.068	0.300	0.749	0.000	0.000	8.032
KB20-Grt3-8	2.982	0.010	1.945	0.000	2.009	0.080	0.270	0.739	0.000	0.000	8.035
KB20-Grt3-9	2.987	0.009	1.940	0.000	1.957	0.106	0.268	0.767	0.000	0.000	8.034
KB20-Grt3-10	2.991	0.006	1.938	0.000	1.976	0.111	0.255	0.758	0.000	0.000	8.035
KB20-Grt3-11	2.971	0.009	1.936	0.001	2.044	0.104	0.225	0.764	0.000	0.001	8.053
KB20-Grt3-12	2.970	0.003	1.958	0.000	2.057	0.131	0.244	0.685	0.000	0.001	8.049
KB20-Grt3-13	2.985	0.015	1.923	0.001	1.959	0.145	0.205	0.806	0.000	0.000	8.038
KB20-Grt3-14	2.974	0.013	1.934	0.002	1.972	0.144	0.233	0.774	0.000	0.000	8.045
KB20-Grt3-15	2.994	0.014	1.907	0.002	1.948	0.144	0.243	0.787	0.000	0.000	8.038
KB20-Grt3-16	2.982	0.005	1.950	0.000	2.001	0.151	0.251	0.700	0.000	0.000	8.039
KB20-Grt3-17	2.981	0.013	1.925	0.001	1.929	0.140	0.226	0.827	0.000	0.000	8.043
KB20-Grt3-18	2.983	0.014	1.927	0.002	1.952	0.144	0.243	0.774	0.000	0.000	8.038
KB20-Grt3-19	2.973	0.008	1.942	0.001	1.958	0.147	0.234	0.783	0.000	0.000	8.047
KB20-Grt3-20	2.980	0.019	1.926	0.001	1.951	0.142	0.274	0.747	0.000	0.000	8.038
KB20-Grt3-21	2.984	0.012	1.938	0.000	1.947	0.145	0.223	0.786	0.000	0.000	8.035
KB20-Grt3-22	2.986	0.015	1.917	0.000	1.913	0.144	0.258	0.807	0.000	0.000	8.040
KB20-Grt3-23	2.982	0.005	1.945	0.001	1.960	0.134	0.353	0.660	0.000	0.000	8.040
KB20-Grt3-25	2.691	0.967	1.229	0.002	1.174	0.084	0.189	1.392	0.002	0.000	7.728
KB20-Grt3-26	2.972	0.009	1.942	0.004	1.934	0.149	0.273	0.766	0.000	0.000	8.047
KB20-Grt3-27	2.972	0.010	1.947	0.002	1.948	0.140	0.260	0.763	0.000	0.001	8.043
KB20-Grt3-28	2.977	0.013	1.923	0.001	1.961	0.151	0.253	0.770	0.000	0.000	8.048
KB20-Grt3-29	2.965	0.024	1.938	0.002	1.996	0.151	0.236	0.730	0.000	0.000	8.042
KB20-Grt3-30	2.981	0.007	1.944	0.000	2.010	0.151	0.247	0.700	0.000	0.000	8.040
KB20-Grt3-31	2.982	0.014	1.920	0.002	1.890	0.143	0.236	0.856	0.000	0.001	8.043
KB20-Grt3-32	2.981	0.015	1.931	0.000	1.979	0.143	0.245	0.745	0.000	0.000	8.039
KB20-Grt3-33	2.980	0.016	1.912	0.002	1.940	0.139	0.236	0.821	0.000	0.000	8.046
KB20-Grt3-34	2.977	0.016	1.929	0.001	1.981	0.141	0.259	0.739	0.000	0.000	8.042
KB20-Grt3-35	2.972	0.006	1.942	0.000	2.038	0.143	0.277	0.673	0.000	0.000	8.052
KB20-Grt3-36	2.990	0.009	1.910	0.001	1.990	0.144	0.251	0.750	0.000	0.000	8.045
KB20-Grt3-37	2.977	0.009	1.928	0.002	2.008	0.133	0.253	0.740	0.000	0.000	8.050
KB20-Grt3-38	2.972	0.025	1.930	0.001	1.938	0.118	0.241	0.814	0.000	0.000	8.038
KB20-Grt3-39	2.968	0.014	1.934	0.001	1.960	0.102	0.256	0.816	0.000	0.000	8.051
KB20-Grt3-40	2.981	0.008	1.937	0.001	1.968	0.102	0.256	0.789	0.000	0.001	8.042
KB20-Grt3-41	2.974	0.007	1.940	0.002	1.995	0.100	0.240	0.790	0.000	0.000	8.048
KB20-Grt3-42	2.979	0.008	1.935	0.000	1.994	0.110	0.243	0.776	0.000	0.000	8.045
KB20-Grt3-43	2.980	0.007	1.944	0.000	1.985	0.100	0.258	0.768	0.000	0.000	8.042
KB20-Grt3-44	2.967	0.007	1.954	0.000	1.967	0.087	0.283	0.785	0.000	0.000	8.050
KB20-Grt3-45	2.969	0.013	1.935	0.000	1.967	0.077	0.284	0.805	0.000	0.000	8.050
KB20-Grt3-46	2.957	0.011	1.949	0.001	2.028	0.072	0.286	0.754	0.000	0.000	8.058
KB20-Grt3-47	2.977	0.004	1.952	0.001	2.002	0.069	0.310	0.728	0.000	0.000	8.043
KB20-Grt3-48	2.980	0.005	1.953	0.000	1.960	0.066	0.327	0.748	0.000	0.001	8.040
KB20-Grt3-49	2.964	0.005	1.961	0.000	2.013	0.074	0.316	0.716	0.000	0.000	8.050
KB20-Grt3-50	2.966	0.008	1.939	0.000	2.006	0.069	0.306	0.763	0.000	0.000	8.056
KB20-Grt3-51	2.971	0.008	1.931	0.000	2.018	0.055	0.296	0.776	0.000	0.001	8.056
KB20-Grt3-52	2.984	0.007	1.932	0.001	2.017	0.055	0.307	0.739	0.000	0.000	8.043
KB20-Grt3-53	2.971	0.005	1.947	0.002	2.046	0.048	0.334	0.695	0.000	0.000	8.049
KB20-Grt3-54	2.966	0.004	1.950	0.000	2.027	0.052	0.358	0.698	0.000	0.000	8.055
KB20-Grt3-55	2.979	0.004	1.951	0.001	1.975	0.052	0.365	0.717	0.000	0.000	8.043
KB20-Grt3-56	2.978	0.006	1.943	0.001	1.927	0.052	0.443	0.695	0.000	0.000	8.044

KB20		K Numbers (=Ix/Istd)								
Garnet-I	Na	Mg	Al	Si	K	Ca	Ti	Cr	Mn	Fe
KB20-Grt-L1-1	0.0000	0.0495	0.8526	0.8541	0.0004	0.2239	0.0013	0.0001	0.0239	0.9671
KB20-Grt-L1-2	0.0000	0.0485	0.8489	0.8559	0.0003	0.2194	0.0021	0.0001	0.0234	0.9895
KB20-Grt-L1-3	0.0000	0.0423	0.8471	0.8521	0.0002	0.2339	0.0021	0.0001	0.0191	0.9791
KB20-Grt-L1-4	0.0000	0.0410	0.8455	0.8583	0.0003	0.2315	0.0033	0.0002	0.0182	0.9974
KB20-Grt-L1-5	0.0000	0.0374	0.8390	0.8524	0.0000	0.2334	0.0161	0.0003	0.0199	0.9958
KB20-Grt-L1-6	0.0000	0.0368	0.8580	0.8653	0.0000	0.2317	0.0016	0.0000	0.0184	1.0148
KB20-Grt-L1-7	0.0000	0.0342	0.8549	0.8777	0.0000	0.2404	0.0017	0.0001	0.0184	1.0084
KB20-Grt-L1-8	0.0000	0.0328	0.8573	0.8767	0.0000	0.2332	0.0022	0.0000	0.0233	1.0261
KB20-Grt-L1-9	0.0000	0.0311	0.8435	0.8696	0.0003	0.2419	0.0028	0.0000	0.0234	1.0072
KB20-Grt-L1-10	0.0000	0.0281	0.8580	0.8754	0.0000	0.2596	0.0025	0.0000	0.0267	1.0045
KB20-Grt-L1-11	0.0000	0.0265	0.8526	0.8738	0.0000	0.2431	0.0015	0.0004	0.0347	1.0269
KB20-Grt-L1-12	0.0000	0.0292	0.8549	0.8731	0.0000	0.2426	0.0027	0.0003	0.0262	1.0204
KB20-Grt-L1-13	0.0000	0.0281	0.8473	0.8763	0.0005	0.2633	0.0044	0.0002	0.0308	1.0032
KB20-Grt-L1-14	0.0000	0.0278	0.8439	0.8753	0.0000	0.2450	0.0033	0.0000	0.0404	0.9985
KB20-Grt-L1-15	0.0000	0.0255	0.8522	0.8746	0.0000	0.2553	0.0026	0.0003	0.0388	1.0109
KB20-Grt-L1-16	0.0000	0.0260	0.8556	0.8766	0.0000	0.2536	0.0030	0.0003	0.0385	1.0015
KB20-Grt-L1-17	0.0000	0.0251	0.8572	0.8746	0.0007	0.2508	0.0041	0.0003	0.0396	1.0142
KB20-Grt-L1-18	0.0000	0.0258	0.8543	0.8800	0.0003	0.2664	0.0034	0.0002	0.0379	1.0012
KB20-Grt-L1-19	0.0000	0.0261	0.8463	0.8763	0.0003	0.2472	0.0034	0.0004	0.0398	1.0271
KB20-Grt-L1-20	0.0000	0.0248	0.8553	0.8770	0.0004	0.2576	0.0047	0.0003	0.0408	0.9967
KB20-Grt-L1-21	0.0000	0.0252	0.8550	0.8780	0.0002	0.2574	0.0040	0.0003	0.0403	1.0021
KB20-Grt-L1-22	0.0000	0.0240	0.8518	0.8702	0.0000	0.2618	0.0059	0.0004	0.0381	1.0050
KB20-Grt-L1-23	0.0000	0.0244	0.8523	0.8723	0.0001	0.2406	0.0042	0.0004	0.0425	1.0199
KB20-Grt-L1-24	0.0000	0.0245	0.8536	0.8723	0.0006	0.2724	0.0152	0.0004	0.0398	0.9909
KB20-Grt-L1-25	0.0000	0.0236	0.8580	0.8798	0.0003	0.2647	0.0043	0.0000	0.0365	1.0065
KB20-Grt-L1-26	0.0000	0.0249	0.8585	0.8841	0.0000	0.2797	0.0036	0.0007	0.0392	0.9734
KB20-Grt-L1-27	0.0000	0.0258	0.8478	0.8784	0.0005	0.2561	0.0060	0.0004	0.0456	0.9940
KB20-Grt-L1-28	0.0000	0.0245	0.8540	0.8808	0.0000	0.2711	0.0046	0.0003	0.0453	0.9684
KB20-Grt-L1-29	0.0000	0.0249	0.8467	0.8716	0.0000	0.2553	0.0048	0.0001	0.0481	0.9952
KB20-Grt-L1-30	0.0000	0.0232	0.8427	0.8798	0.0000	0.2761	0.0059	0.0001	0.0533	0.9717
KB20-Grt-L1-31	0.0000	0.0249	0.8424	0.8744	0.0001	0.2559	0.0050	0.0001	0.0513	0.9897
KB20-Grt-L1-32	0.0000	0.0239	0.8426	0.8795	0.0009	0.2698	0.0045	0.0004	0.0463	0.9801
KB20-Grt-L1-33	0.0000	0.0248	0.8534	0.8753	0.0000	0.2561	0.0045	0.0003	0.0464	0.9950
KB20-Grt-L1-34	0.0000	0.0247	0.8503	0.8799	0.0003	0.2674	0.0242	0.0003	0.0430	0.9840
KB20-Grt-L1-35	0.0000	0.0258	0.8474	0.8760	0.0003	0.2455	0.0121	0.0003	0.0456	1.0062
KB20-Grt-L1-36	0.0000	0.0244	0.8522	0.8808	0.0003	0.2544	0.0066	0.0003	0.0470	1.0003
KB20-Grt-L1-37	0.0000	0.0236	0.8555	0.8771	0.0000	0.2617	0.0053	0.0004	0.0427	0.9986
KB20-Grt-L1-38	0.0000	0.0222	0.8489	0.8795	0.0000	0.2641	0.0045	0.0002	0.0390	1.0051
KB20-Grt-L1-39	0.0000	0.0232	0.8541	0.8757	0.0000	0.2474	0.0012	0.0001	0.0414	1.0242
KB20-Grt-L1-40	0.0000	0.0250	0.8549	0.8764	0.0002	0.2488	0.0033	0.0003	0.0401	1.0114
KB20-Grt-L1-41	0.0000	0.0252	0.8496	0.8930	0.0000	0.2551	0.0033	0.0001	0.0389	0.9964
KB20-Grt-L1-42	0.0000	0.0247	0.8574	0.8792	0.0000	0.2538	0.0027	0.0000	0.0408	1.0083
KB20-Grt-L1-43	0.0000	0.0287	0.8542	0.8791	0.0000	0.2517	0.0036	0.0001	0.0319	1.0065
KB20-Grt-L1-44	0.0000	0.0284	0.8504	0.8796	0.0002	0.2710	0.0044	0.0002	0.0286	0.9841
KB20-Grt-L1-45	0.0000	0.0280	0.8507	0.8777	0.0007	0.2587	0.0038	0.0002	0.0320	0.9949
KB20-Grt-L1-46	0.0000	0.0293	0.8526	0.8813	0.0000	0.2517	0.0028	0.0002	0.0293	1.0033
KB20-Grt-L1-47	0.0000	0.0289	0.8546	0.8855	0.0000	0.2677	0.0036	0.0002	0.0272	0.9844
KB20-Grt-L1-48	0.0000	0.0310	0.8551	0.8788	0.0000	0.2358	0.0017	0.0002	0.0239	1.0298
KB20-Grt-L1-49	0.0000	0.0321	0.8562	0.8807	0.0000	0.2456	0.0029	0.0003	0.0240	1.0134
KB20-Grt-L1-50	0.0000	0.0338	0.8564	0.8854	0.0004	0.2442	0.0030	0.0000	0.0200	1.0082
KB20-Grt-L1-51	0.0000	0.0347	0.8563	0.8843	0.0000	0.2361	0.0035	0.0004	0.0182	1.0237
KB20-Grt-L1-52	0.0000	0.0371	0.8494	0.8591	0.0001	0.2325	0.0034	0.0002	0.0198	1.0056
KB20-Grt-L1-53	0.0000	0.0371	0.8523	0.8692	0.0005	0.2294	0.0012	0.0002	0.0222	1.0126
KB20-Grt-L1-54	0.0000	0.0390	0.8525	0.8686	0.0010	0.2296	0.0014	0.0000	0.0214	1.0046
KB20-Grt-L1-55	0.0000	0.0427	0.8545	0.8711	0.0000	0.2190	0.0013	0.0003	0.0205	1.0133
KB20-Grt-L1-56	0.0000	0.0487	0.8547	0.8726	0.0000	0.2088	0.0008	0.0001	0.0218	1.0033
KB20-Grt-L1-57	0.0000	0.0493	0.8533	0.8761	0.0000	0.2207	0.0018	0.0003	0.0251	0.9761
KB20-Grt-L1-58	0.0000	0.0489	0.8570	0.8801	0.0003	0.2290	0.0013	0.0002	0.0239	0.9596
KB20-Grt-L1-59	0.0000	0.0452	0.8576	0.8800	0.0000	0.2422	0.0016	0.0003	0.0325	0.9544

KB20 Garnet-2	K Numbers (=Ix/Istd)									
	Na	Mg	Al	Si	K	Ca	Ti	Cr	Mn	Fe
KB20-Grt2-1	0.0000	0.0467	0.8642	0.8813	0.0000	0.2358	0.0013	0.0000	0.0308	0.9531
KB20-Grt2-2	0.0000	0.0493	0.8591	0.8808	0.0000	0.2224	0.0009	0.0005	0.0261	0.9792
KB20-Grt2-3	0.0000	0.0433	0.8615	0.8816	0.0005	0.2352	0.0019	0.0003	0.0205	0.9900
KB20-Grt2-4	0.0000	0.0358	0.8568	0.8825	0.0000	0.2572	0.0028	0.0001	0.0213	0.9917
KB20-Grt2-5	0.0000	0.0321	0.8543	0.8752	0.0000	0.2597	0.0028	0.0004	0.0177	0.9988
KB20-Grt2-6	0.0000	0.0330	0.8544	0.8754	0.0005	0.2351	0.0015	0.0002	0.0223	1.0186
KB20-Grt2-7	0.0000	0.0310	0.8507	0.8832	0.0000	0.2558	0.0033	0.0003	0.0240	1.0009
KB20-Grt2-8	0.0000	0.0303	0.8447	0.8769	0.0003	0.2611	0.0039	0.0002	0.0243	1.0028
KB20-Grt2-9	0.0000	0.0296	0.8500	0.8832	0.0000	0.2616	0.0046	0.0003	0.0240	0.9981
KB20-Grt2-10	0.0000	0.0289	0.8505	0.8805	0.0000	0.2580	0.0055	0.0002	0.0239	0.9985
KB20-Grt2-11	0.0000	0.0313	0.8565	0.8780	0.0000	0.2454	0.0068	0.0002	0.0246	1.0114
KB20-Grt2-12	0.0000	0.0291	0.8474	0.8814	0.0000	0.2492	0.0036	0.0004	0.0257	1.0234
KB20-Grt2-13	0.0000	0.0289	0.8501	0.8781	0.0008	0.2485	0.0026	0.0002	0.0293	1.0120
KB20-Grt2-14	0.0000	0.0294	0.8557	0.8842	0.0002	0.2452	0.0033	0.0001	0.0320	1.0123
KB20-Grt2-15	0.0000	0.0286	0.8498	0.8794	0.0005	0.2615	0.0039	0.0002	0.0253	0.9961
KB20-Grt2-16	0.0000	0.0226	0.8581	0.8764	0.0006	0.2741	0.0034	0.0003	0.0351	0.9999
KB20-Grt2-17	0.0000	0.0245	0.8489	0.8774	0.0000	0.2738	0.0132	0.0002	0.0363	0.9793
KB20-Grt2-18	0.0000	0.0217	0.8489	0.8813	0.0004	0.2868	0.0038	0.0002	0.0333	0.9860
KB20-Grt2-19	0.0000	0.0226	0.8491	0.8870	0.0000	0.2872	0.0037	0.0003	0.0359	0.9772
KB20-Grt2-20	0.0000	0.0238	0.8530	0.8790	0.0001	0.2712	0.0057	0.0001	0.0363	0.9916
KB20-Grt2-21	0.0000	0.0246	0.8569	0.8808	0.0002	0.2835	0.0025	0.0001	0.0375	0.9638
KB20-Grt2-22	0.0000	0.0279	0.8551	0.9082	0.0003	0.2468	0.0038	0.0002	0.0392	0.9952
KB20-Grt2-23	0.0000	0.0265	0.8428	0.8803	0.0001	0.2676	0.0073	0.0002	0.0425	0.9809
KB20-Grt2-24	0.0000	0.0272	0.8477	0.8825	0.0000	0.2627	0.0049	0.0004	0.0397	0.9897
KB20-Grt2-25	0.0000	0.0249	0.8502	0.8847	0.0000	0.2630	0.0049	0.0003	0.0421	0.9990
KB20-Grt2-26	0.0000	0.0248	0.8523	0.8750	0.0000	0.2469	0.0056	0.0002	0.0443	1.0138
KB20-Grt2-27	0.0000	0.0272	0.8525	0.8800	0.0002	0.2621	0.0044	0.0003	0.0369	0.9849
KB20-Grt2-28	0.0000	0.0250	0.8465	0.8818	0.0000	0.2640	0.0047	0.0000	0.0403	0.9878
KB20-Grt2-29	0.0000	0.0260	0.8526	0.8875	0.0000	0.2654	0.0026	0.0002	0.0369	0.9813
KB20-Grt2-30	0.0000	0.0227	0.8459	0.8831	0.0002	0.2683	0.0039	0.0002	0.0375	0.9979
KB20-Grt2-31	0.0000	0.0242	0.8587	0.8841	0.0000	0.2774	0.0039	0.0002	0.0347	0.9910
KB20-Grt2-32	0.0000	0.0226	0.8558	0.8778	0.0002	0.2734	0.0039	0.0002	0.0357	0.9915
KB20-Grt2-33	0.0000	0.0250	0.8487	0.8842	0.0000	0.2461	0.0030	0.0000	0.0412	1.0192
KB20-Grt2-34	0.0000	0.0259	0.8523	0.8845	0.0000	0.2607	0.0040	0.0003	0.0281	0.9948
KB20-Grt2-35	0.0000	0.0263	0.8530	0.8833	0.0005	0.2756	0.0042	0.0000	0.0230	0.9876
KB20-Grt2-36	0.0000	0.0274	0.8558	0.8809	0.0000	0.2701	0.0042	0.0000	0.0244	1.0028
KB20-Grt2-37	0.0000	0.0297	0.8581	0.8866	0.0000	0.2428	0.0020	0.0001	0.0245	1.0103
KB20-Grt2-38	0.0000	0.0289	0.8571	0.8848	0.0004	0.2573	0.0030	0.0001	0.0262	1.0040
KB20-Grt2-39	0.0000	0.0312	0.8513	0.8792	0.0003	0.2481	0.0028	0.0001	0.0227	1.0067
KB20-Grt2-40	0.0000	0.0337	0.8357	0.8589	0.0000	0.2244	0.0014	0.0007	0.0228	1.0201
KB20-Grt2-41	0.0000	0.0335	0.8283	0.8481	0.0001	0.2346	0.0019	0.0004	0.0193	1.0153
KB20-Grt2-42	0.0000	0.0362	0.8407	0.8629	0.0000	0.2337	0.0018	0.0001	0.0183	1.0126
KB20-Grt2-43	0.0000	0.0381	0.8256	0.8685	0.0000	0.2319	0.0019	0.0002	0.0217	0.9687
KB20-Grt2-44	0.0000	0.0445	0.8466	0.8717	0.0006	0.2153	0.0013	0.0002	0.0263	0.9982
KB20-Grt2-45	0.0000	0.0489	0.8478	0.8850	0.0000	0.2233	0.0007	0.0001	0.0263	0.9733

KB20										
Garnet-3	K Numbers (=Ix/Istd)									
	Na	Mg	Al	Si	K	Ca	Ti	Cr	Mn	Fe
KB20-Grt3-1	0.0000	0.0479	0.8577	0.8741	0.0001	0.2292	0.0007	0.0002	0.0278	0.9657
KB20-Grt3-2	0.0000	0.0414	0.8559	0.8781	0.0007	0.2379	0.0009	0.0002	0.0206	0.9894
KB20-Grt3-3	0.0000	0.0358	0.8530	0.8760	0.0000	0.2428	0.0022	0.0000	0.0231	0.9924
KB20-Grt3-4	0.0000	0.0356	0.8401	0.8694	0.0004	0.2463	0.0025	0.0003	0.0187	0.9955
KB20-Grt3-5	0.0000	0.0327	0.8535	0.8733	0.0005	0.2351	0.0020	0.0004	0.0262	1.0192
KB20-Grt3-6	0.0000	0.0316	0.8455	0.8712	0.0004	0.2502	0.0031	0.0003	0.0278	1.0021
KB20-Grt3-7	0.0000	0.0308	0.8499	0.8738	0.0000	0.2505	0.0021	0.0003	0.0264	0.9894
KB20-Grt3-8	0.0000	0.0276	0.8453	0.8684	0.0000	0.2466	0.0044	0.0001	0.0312	1.0037
KB20-Grt3-9	0.0000	0.0276	0.8520	0.8787	0.0000	0.2580	0.0039	0.0000	0.0414	0.9851
KB20-Grt3-10	0.0000	0.0262	0.8481	0.8776	0.0003	0.2544	0.0025	0.0000	0.0432	0.9929
KB20-Grt3-11	0.0000	0.0229	0.8433	0.8693	0.0005	0.2562	0.0040	0.0001	0.0405	1.0260
KB20-Grt3-12	0.0000	0.0246	0.8469	0.8619	0.0004	0.2288	0.0013	0.0000	0.0512	1.0287
KB20-Grt3-13	0.0000	0.0208	0.8371	0.8717	0.0000	0.2688	0.0063	0.0002	0.0562	0.9774
KB20-Grt3-14	0.0000	0.0237	0.8413	0.8682	0.0000	0.2588	0.0056	0.0003	0.0560	0.9857
KB20-Grt3-15	0.0000	0.0247	0.8293	0.8746	0.0002	0.2628	0.0061	0.0003	0.0559	0.9723
KB20-Grt3-16	0.0000	0.0255	0.8449	0.8667	0.0000	0.2335	0.0020	0.0000	0.0588	0.9998
KB20-Grt3-17	0.0000	0.0231	0.8385	0.8704	0.0003	0.2756	0.0057	0.0003	0.0542	0.9610
KB20-Grt3-18	0.0000	0.0248	0.8396	0.8720	0.0000	0.2586	0.0060	0.0004	0.0562	0.9760
KB20-Grt3-19	0.0000	0.0240	0.8482	0.8705	0.0000	0.2623	0.0036	0.0001	0.0572	0.9815
KB20-Grt3-20	0.0000	0.0281	0.8399	0.8719	0.0000	0.2500	0.0080	0.0001	0.0553	0.9780
KB20-Grt3-21	0.0000	0.0226	0.8420	0.8688	0.0001	0.2618	0.0053	0.0001	0.0564	0.9694
KB20-Grt3-22	0.0000	0.0264	0.8375	0.8753	0.0000	0.2700	0.0067	0.0001	0.0561	0.9570
KB20-Grt3-23	0.0000	0.0363	0.8472	0.8711	0.0000	0.2215	0.0023	0.0002	0.0523	0.9858
KB20-Grt3-25	0.0008	0.0199	0.5530	0.8445	0.0002	0.4791	0.4116	0.0003	0.0319	0.5828
KB20-Grt3-26	0.0000	0.0279	0.8465	0.8683	0.0000	0.2561	0.0038	0.0007	0.0579	0.9683
KB20-Grt3-27	0.0000	0.0265	0.8468	0.8659	0.0005	0.2546	0.0044	0.0003	0.0545	0.9727
KB20-Grt3-28	0.0000	0.0257	0.8342	0.8671	0.0000	0.2568	0.0056	0.0001	0.0585	0.9781
KB20-Grt3-29	0.0000	0.0239	0.8386	0.8614	0.0000	0.2435	0.0102	0.0003	0.0586	0.9957
KB20-Grt3-30	0.0000	0.0250	0.8403	0.8645	0.0000	0.2330	0.0031	0.0000	0.0585	1.0024
KB20-Grt3-31	0.0000	0.0241	0.8374	0.8715	0.0004	0.2850	0.0062	0.0004	0.0554	0.9406
KB20-Grt3-32	0.0000	0.0249	0.8382	0.8682	0.0000	0.2485	0.0064	0.0001	0.0557	0.9884
KB20-Grt3-33	0.0000	0.0240	0.8325	0.8711	0.0000	0.2739	0.0070	0.0005	0.0541	0.9679
KB20-Grt3-34	0.0000	0.0264	0.8389	0.8690	0.0000	0.2472	0.0069	0.0002	0.0550	0.9917
KB20-Grt3-35	0.0000	0.0280	0.8368	0.8601	0.0002	0.2242	0.0025	0.0000	0.0556	1.0166
KB20-Grt3-36	0.0000	0.0254	0.8249	0.8680	0.0000	0.2494	0.0040	0.0003	0.0557	0.9899
KB20-Grt3-37	0.0000	0.0255	0.8304	0.8611	0.0002	0.2456	0.0038	0.0004	0.0515	0.9974
KB20-Grt3-38	0.0000	0.0245	0.8390	0.8658	0.0000	0.2709	0.0107	0.0001	0.0457	0.9647
KB20-Grt3-39	0.0000	0.0260	0.8370	0.8608	0.0001	0.2705	0.0059	0.0001	0.0396	0.9721
KB20-Grt3-40	0.0000	0.0260	0.8375	0.8634	0.0005	0.2615	0.0036	0.0002	0.0393	0.9755
KB20-Grt3-41	0.0000	0.0243	0.8391	0.8622	0.0000	0.2621	0.0028	0.0004	0.0386	0.9905
KB20-Grt3-42	0.0000	0.0246	0.8377	0.8653	0.0000	0.2581	0.0036	0.0001	0.0426	0.9924
KB20-Grt3-43	0.0000	0.0262	0.8413	0.8642	0.0003	0.2550	0.0030	0.0001	0.0386	0.9865
KB20-Grt3-44	0.0000	0.0290	0.8497	0.8635	0.0002	0.2617	0.0028	0.0001	0.0338	0.9811
KB20-Grt3-45	0.0000	0.0290	0.8399	0.8635	0.0000	0.2678	0.0055	0.0001	0.0297	0.9790
KB20-Grt3-46	0.0000	0.0290	0.8416	0.8560	0.0002	0.2507	0.0045	0.0002	0.0280	1.0089
KB20-Grt3-47	0.0000	0.0316	0.8448	0.8630	0.0003	0.2420	0.0016	0.0002	0.0268	0.9972
KB20-Grt3-48	0.0000	0.0335	0.8479	0.8652	0.0009	0.2489	0.0020	0.0000	0.0258	0.9761
KB20-Grt3-49	0.0000	0.0322	0.8486	0.8595	0.0001	0.2386	0.0023	0.0000	0.0289	1.0045
KB20-Grt3-50	0.0000	0.0312	0.8381	0.8602	0.0003	0.2536	0.0035	0.0001	0.0265	0.9980
KB20-Grt3-51	0.0000	0.0302	0.8389	0.8663	0.0005	0.2592	0.0035	0.0001	0.0215	1.0086
KB20-Grt3-52	0.0000	0.0314	0.8380	0.8681	0.0002	0.2463	0.0031	0.0001	0.0215	1.0068
KB20-Grt3-53	0.0000	0.0340	0.8397	0.8594	0.0000	0.2311	0.0023	0.0005	0.0188	1.0192
KB20-Grt3-54	0.0000	0.0367	0.8457	0.8625	0.0000	0.2333	0.0019	0.0000	0.0202	1.0153
KB20-Grt3-55	0.0000	0.0375	0.8459	0.8646	0.0000	0.2388	0.0015	0.0001	0.0201	0.9853
KB20-Grt3-56	0.0000	0.0461	0.8478	0.8700	0.0000	0.2327	0.0025	0.0002	0.0202	0.9675

WB159													
Garnet-1	Coordinates		Weight Percent Oxides										
	X	Y	SiO ₂	TiO ₂	Al ₂ O ₃	Cr ₂ O ₃	FeO*	MnO	MgO	CaO	Na ₂ O	K ₂ O	Total
WB159-Grt1b-1	-18263	34248	37.75	0.02	21.18	0.01	27.02	0.91	4.71	7.77	0.00	0.00	99.37
WB159-Grt1b-2	-18263	34224	37.30	0.05	20.94	0.01	29.08	0.50	2.46	9.23	0.00	0.00	99.58
WB159-Grt1b-3	-18263	34199	37.17	0.08	20.94	0.01	28.84	0.72	1.96	10.15	0.00	0.00	99.87
WB159-Grt1b-4	-18263	34174	37.23	0.12	20.79	0.01	28.19	1.24	1.57	10.28	0.00	0.00	99.42
WB159-Grt1b-5	-18263	34149	37.26	0.12	20.79	0.00	27.69	1.71	1.34	10.79	0.00	0.00	99.70
WB159-Grt1b-6	-18263	34124	37.10	0.11	20.78	0.00	27.42	1.98	1.41	10.67	0.00	0.00	99.48
WB159-Grt1b-7	-18263	34099	37.13	0.15	20.87	0.00	27.01	2.70	1.75	10.02	0.00	0.01	99.64
WB159-Grt1b-8	-18263	34074	37.57	0.12	21.06	0.01	25.10	2.61	3.36	9.90	0.00	0.00	99.73
WB159-Grt1b-9	-18263	34049	37.42	0.12	21.05	0.00	22.59	5.45	2.32	10.56	0.00	0.00	99.53
WB159-Grt1b-10	-18263	34024	37.08	0.21	20.79	0.01	20.49	7.27	1.83	11.55	0.00	0.00	99.23
WB159-Grt1b-11	-18263	33999	37.07	0.15	20.86	0.00	20.92	7.45	1.42	11.41	0.00	0.01	99.30
WB159-Grt1b-12	-18263	33974	37.55	0.09	21.13	0.01	25.27	1.94	3.62	10.09	0.00	0.00	99.70
WB159-Grt1b-13	-18263	33949	37.32	0.12	20.88	0.00	26.32	1.73	2.58	10.48	0.00	0.01	99.45
WB159-Grt1b-14	-18263	33924	37.22	0.08	20.96	0.00	27.30	1.28	2.10	10.67	0.00	0.01	99.62
WB159-Grt1b-15	-18263	33899	37.25	0.03	20.92	0.01	28.28	0.68	3.26	9.12	0.00	0.01	99.56
WB159-Grt1b-16	-18263	33874	37.48	0.06	21.33	0.00	27.04	0.87	4.61	8.22	0.00	0.00	99.62
WB159-Grt1b-17	-18229	33859	37.71	0.06	21.26	0.01	26.82	0.81	4.81	8.03	0.00	0.00	99.52

WB159		Atoms per 12 Oxygen									
Garnet-1	Si	Ti	Al	Cr	Fe	Mn	Mg	Ca	Na	K	Sum
WB159-Grt1b-1	2.986	0.001	1.975	0.001	1.788	0.061	0.556	0.659	0.000	0.000	8.025
WB159-Grt1b-2	2.984	0.003	1.975	0.000	1.945	0.034	0.294	0.791	0.000	0.000	8.026
WB159-Grt1b-3	2.974	0.005	1.974	0.000	1.929	0.049	0.233	0.870	0.000	0.000	8.034
WB159-Grt1b-4	2.991	0.007	1.968	0.001	1.894	0.084	0.188	0.885	0.000	0.000	8.018
WB159-Grt1b-5	2.988	0.007	1.965	0.000	1.857	0.116	0.160	0.928	0.000	0.000	8.022
WB159-Grt1b-6	2.983	0.007	1.969	0.000	1.844	0.135	0.169	0.919	0.000	0.000	8.026
WB159-Grt1b-7	2.979	0.009	1.973	0.000	1.812	0.184	0.209	0.861	0.001	0.000	8.027
WB159-Grt1b-8	2.979	0.007	1.968	0.000	1.664	0.176	0.397	0.841	0.000	0.000	8.031
WB159-Grt1b-9	2.983	0.007	1.978	0.000	1.506	0.368	0.276	0.902	0.001	0.000	8.021
WB159-Grt1b-10	2.973	0.013	1.965	0.001	1.374	0.494	0.219	0.993	0.000	0.000	8.031
WB159-Grt1b-11	2.977	0.009	1.975	0.000	1.405	0.507	0.170	0.982	0.001	0.000	8.026
WB159-Grt1b-12	2.972	0.005	1.972	0.001	1.673	0.130	0.427	0.856	0.000	0.000	8.036
WB159-Grt1b-13	2.980	0.008	1.965	0.000	1.757	0.117	0.308	0.896	0.001	0.000	8.031
WB159-Grt1b-14	2.976	0.005	1.974	0.000	1.825	0.087	0.251	0.914	0.001	0.000	8.032
WB159-Grt1b-15	2.972	0.002	1.967	0.001	1.887	0.046	0.387	0.779	0.001	0.000	8.042
WB159-Grt1b-16	2.963	0.004	1.987	0.000	1.788	0.058	0.544	0.696	0.000	0.000	8.040
WB159-Grt1b-17	2.977	0.004	1.978	0.000	1.771	0.054	0.566	0.679	0.000	0.000	8.030

WB159										
K Numbers (=Ix/Istd)										
Garnet-1	Na	Mg	Al	Si	K	Ca	Ti	Cr	Mn	Fe
WB159-Grt1b-1	0.0000	0.0592	0.8717	0.8778	0.0002	0.2217	0.0004	0.0001	0.0240	0.9033
WB159-Grt1b-2	0.0000	0.0304	0.8664	0.8733	0.0001	0.2645	0.0013	0.0001	0.0133	0.9742
WB159-Grt1b-3	0.0000	0.0241	0.8693	0.8731	0.0000	0.2911	0.0022	0.0001	0.0190	0.9660
WB159-Grt1b-4	0.0000	0.0193	0.8655	0.8763	0.0000	0.2951	0.0031	0.0001	0.0327	0.9440
WB159-Grt1b-5	0.0000	0.0165	0.8677	0.8791	0.0000	0.3099	0.0031	0.0000	0.0450	0.9271
WB159-Grt1b-6	0.0000	0.0174	0.8669	0.8746	0.0002	0.3064	0.0028	0.0000	0.0523	0.9184
WB159-Grt1b-7	0.0000	0.0215	0.8684	0.8739	0.0010	0.2876	0.0038	0.0000	0.0713	0.9052
WB159-Grt1b-8	0.0000	0.0422	0.8765	0.8823	0.0001	0.2832	0.0030	0.0001	0.0687	0.8389
WB159-Grt1b-9	0.0000	0.0291	0.8833	0.8840	0.0003	0.3028	0.0031	0.0000	0.1432	0.7556
WB159-Grt1b-10	0.0000	0.0230	0.8768	0.8803	0.0001	0.3319	0.0055	0.0001	0.1908	0.6849
WB159-Grt1b-11	0.0000	0.0178	0.8802	0.8803	0.0005	0.3282	0.0039	0.0000	0.1956	0.7001
WB159-Grt1b-12	0.0000	0.0455	0.8794	0.8811	0.0000	0.2885	0.0023	0.0001	0.0511	0.8438
WB159-Grt1b-13	0.0000	0.0322	0.8702	0.8781	0.0004	0.3001	0.0032	0.0000	0.0456	0.8799
WB159-Grt1b-14	0.0000	0.0261	0.8734	0.8760	0.0004	0.3059	0.0021	0.0000	0.0337	0.9132
WB159-Grt1b-15	0.0000	0.0404	0.8636	0.8706	0.0006	0.2610	0.0009	0.0001	0.0180	0.9465
WB159-Grt1b-16	0.0000	0.0580	0.8784	0.8718	0.0001	0.2347	0.0016	0.0000	0.0229	0.9041
WB159-Grt1b-17	0.0000	0.0606	0.8758	0.8772	0.0002	0.2290	0.0016	0.0001	0.0214	0.8963

WB163		Coordinates		Weight Percent Oxides											
Garnet-I	X	Y	SiO ₂	TiO ₂	Al ₂ O ₃	Cr ₂ O ₃	FeO*	MnO	MgO	CaO	Na ₂ O	K ₂ O	Total		
WB163-Grt1-1	-6132	27572	38.04	0.10	20.61	0.00	29.59	0.56	4.33	7.25	0.00	0.01	100.49		
WB163-Grt1-2	-6132	27522	37.89	0.08	20.69	0.00	29.93	0.62	4.15	7.22	0.00	0.00	100.57		
WB163-Grt1-3	-6142	27472	37.57	0.05	20.78	0.01	30.04	0.67	4.19	7.11	0.00	0.00	100.43		
WB163-Grt1-4	-6140	27422	37.61	0.07	20.71	0.00	29.92	0.70	3.90	7.37	0.00	0.00	100.28		
WB163-Grt1-5	-6140	27372	37.25	0.06	20.77	0.00	30.19	0.78	3.77	7.22	0.00	0.00	100.03		
WB163-Grt1-6	-6143	27322	37.43	0.15	20.64	0.00	29.88	0.79	3.66	7.51	0.00	0.00	100.07		
WB163-Grt1-7	-6082	27272	37.38	0.11	20.36	0.01	29.94	0.79	3.64	7.41	0.00	0.00	99.66		
WB163-Grt1-8	-6065	27222	37.32	0.08	20.70	0.00	30.24	0.92	3.77	6.69	0.00	0.00	99.72		
WB163-Grt1-9	-6086	27172	37.07	0.24	20.57	0.00	30.10	0.93	3.59	7.24	0.00	0.01	99.77		
WB163-Grt1-10	-6125	27122	37.26	0.10	20.37	0.01	30.02	1.03	3.57	7.22	0.00	0.00	99.57		
WB163-Grt1-11	-6125	27072	36.10	3.41	20.16	0.00	29.74	1.08	3.52	6.43	0.00	0.00	100.44		
WB163-Grt1-12	-6125	27022	37.12	0.07	20.69	0.00	30.88	1.17	3.60	6.55	0.00	0.00	100.09		
WB163-Grt1-13	-6125	26972	37.08	0.02	20.69	0.00	30.46	1.10	3.65	6.52	0.00	0.00	99.51		
WB163-Grt1-14	-6125	26922	37.03	0.09	20.72	0.00	30.66	0.96	3.67	6.76	0.00	0.00	99.89		
WB163-Grt1-15	-6104	26872	37.17	0.07	20.75	0.00	30.94	0.83	3.64	6.81	0.00	0.01	100.24		
WB163-Grt1-16	-6157	26822	37.19	0.13	20.56	0.00	30.54	0.80	3.69	6.85	0.00	0.01	99.78		
WB163-Grt1-17	-6157	26772	37.12	0.14	20.65	0.00	30.44	0.74	3.75	6.98	0.00	0.00	99.80		
WB163-Grt1-18	-6157	26722	37.05	0.17	20.75	0.00	30.19	0.95	3.61	7.25	0.00	0.00	99.96		
WB163-Grt1-19	-6170	26662	37.33	0.29	20.58	0.01	30.45	0.93	3.41	7.01	0.00	0.00	100.01		
WB163-Grt1-20	-6193	26612	37.17	0.12	20.69	0.00	30.45	0.90	3.34	7.15	0.00	0.00	99.84		
WB163-Grt1-21	-6144	26562	37.24	0.18	20.69	0.01	30.13	1.41	3.31	7.11	0.00	0.00	100.07		
WB163-Grt1-22	-6144	26512	37.07	0.12	20.62	0.01	30.05	1.78	2.92	7.40	0.00	0.00	99.97		
WB163-Grt1-23	-6137	26462	37.16	0.16	20.78	0.01	30.13	1.56	3.31	7.17	0.00	0.00	100.29		
WB163-Grt1-24	-6174	26408	37.34	0.12	20.63	0.00	30.33	1.43	3.22	7.11	0.00	0.00	100.19		
WB163-Grt1-25	-6189	26358	37.37	0.08	20.77	0.00	30.30	1.15	3.52	7.29	0.00	0.00	100.47		
WB163-Grt1-26	-6189	26291	37.35	0.09	20.67	0.00	30.53	1.32	3.51	6.73	0.00	0.00	100.20		
WB163-Grt1-27	-6189	26241	37.31	0.07	20.80	0.00	30.33	1.34	3.46	7.07	0.00	0.00	100.38		
WB163-Grt1-28	-6189	26191	37.27	0.05	20.77	0.02	30.25	1.27	3.41	7.11	0.00	0.01	100.16		
WB163-Grt1-29	-6217	26132	37.58	0.05	20.71	0.00	30.45	0.89	3.61	7.20	0.00	0.01	100.50		
WB163-Grt1-30	-6201	26082	37.39	0.06	20.73	0.01	30.26	0.93	3.53	7.30	0.00	0.00	100.20		
WB163-Grt1-31	-6201	26032	37.48	0.05	20.81	0.01	30.55	0.93	3.63	7.08	0.00	0.00	100.54		
WB163-Grt1-32	-6201	25982	37.32	0.06	20.85	0.00	30.43	0.99	3.61	6.97	0.00	0.00	100.23		
WB163-Grt1-33	-6190	25932	37.40	0.06	20.80	0.00	30.43	1.21	3.43	7.29	0.00	0.00	100.62		
WB163-Grt1-34	-6172	25882	37.46	0.06	20.87	0.00	29.83	1.46	3.27	7.57	0.00	0.01	100.52		
WB163-Grt1-35	-6172	25827	37.43	0.05	20.83	0.01	30.22	1.47	3.38	6.82	0.00	0.00	100.21		
WB163-Grt1-36	-6218	25777	37.55	0.05	20.74	0.00	30.80	0.94	3.66	6.64	0.00	0.00	100.37		
WB163-Grt1-37	-6193	25727	37.75	0.05	20.70	0.00	30.65	0.78	3.63	7.09	0.00	0.00	100.66		
WB163-Grt1-38	-6193	25677	37.71	0.07	20.98	0.00	30.73	0.80	3.71	6.83	0.00	0.01	100.84		
WB163-Grt1-39	-6193	25627	37.70	0.04	21.01	0.00	30.84	0.80	3.57	7.02	0.00	0.00	100.99		
WB163-Grt1-40	-6185	25575	37.71	0.06	20.83	0.00	30.92	0.99	3.41	7.05	0.00	0.00	100.96		
WB163-Grt1-41	-6185	25525	37.55	0.02	20.91	0.00	30.73	1.06	3.33	7.03	0.00	0.00	100.64		
WB163-Grt1-42	-6227	25475	37.47	0.06	20.81	0.00	30.51	1.01	3.48	7.28	0.00	0.00	100.62		
WB163-Grt1-43	-6227	25425	37.42	0.08	20.75	0.01	30.72	0.94	3.57	6.76	0.00	0.00	100.25		
WB163-Grt1-44	-6227	25375	37.40	0.04	20.88	0.01	30.19	1.00	3.47	7.25	0.00	0.00	100.25		
WB163-Grt1-45	-6210	25325	37.36	0.06	20.75	0.01	30.68	1.04	3.55	7.04	0.00	0.00	99.74		
WB163-Grt1-46	-6210	25275	37.39	0.07	20.82	0.01	30.44	1.15	3.49	7.04	0.00	0.00	100.42		
WB163-Grt1-47	-6210	25225	39.36	0.07	21.08	0.00	26.65	0.95	3.19	6.25	0.86	0.01	98.43		
WB163-Grt1-48	-6210	25175	37.37	0.08	20.91	0.00	29.67	1.00	3.48	7.48	0.00	0.00	99.98		
WB163-Grt1-49	-6210	25125	37.34	0.07	20.83	0.00	30.48	0.96	3.57	6.92	0.00	0.00	100.18		
WB163-Grt1-50	-6210	25075	37.58	0.08	20.70	0.00	30.03	0.87	3.61	7.25	0.00	0.00	100.10		
WB163-Grt1-51	-6210	25025	37.72	0.11	20.77	0.00	30.16	0.82	3.68	7.28	0.00	0.01	100.55		
WB163-Grt1-52	-6227	24973	37.58	0.08	20.76	0.00	30.31	0.76	3.81	7.26	0.00	0.00	100.57		
WB163-Grt1-53	-6227	24923	37.65	0.06	20.80	0.00	30.30	0.77	3.81	7.05	0.00	0.01	100.44		
WB163-Grt1-54	-6227	24873	37.64	0.06	20.61	0.01	30.21	0.79	3.66	7.19	0.00	0.01	100.18		
WB163-Grt1-55	-6195	24823	37.54	0.07	20.71	0.00	30.20	0.77	3.82	7.14	0.00	0.00	100.26		
WB163-Grt1-56	-6195	24773	37.68	0.09	20.87	0.00	29.76	0.73	3.83	7.40	0.00	0.01	100.37		
WB163-Grt1-57	-6195	24723	37.46	0.10	20.67	0.00	29.78	0.73	3.85	7.62	0.00	0.00	100.22		
WB163-Grt1-58	-6195	24673	37.61	0.08	20.71	0.00	29.67	0.69	3.83	7.56	0.00	0.00	100.14		
WB163-Grt1-59	-6195	24623	37.54	0.12	20.75	0.02	29.45	0.68	3.86	7.62	0.00	0.00	100.05		
WB163-Grt1-60	-6233	24573	37.66	0.16	20.87	0.01	29.42	0.63	3.96	7.59	0.00	0.00	100.29		
WB163-Grt1-61	-6233	24523	37.52	0.11	20.78	0.00	29.58	0.64	4.01	7.60	0.00	0.00	100.24		
WB163-Grt1-62	-6233	24473	37.46	0.17	20.85	0.01	29.51	0.67	4.05	7.49	0.00	0.01	100.22		
WB163-Grt1-63	-6233	24423	37.63	0.07	21.05	0.01	29.94	0.65	4.16	7.24	0.00	0.00	100.75		
WB163-Grt1-64	-6233	24373	37.58	0.06	21.02	0.00	29.69	0.60	4.22	7.42	0.00	0.00	100.60		
WB163-Grt1-65	-6205	24323	37.57	0.07	21.23	0.00	29.62	0.56	4.40	7.17	0.00	0.00	100.61		
WB163-Grt1-66	-6174	24273	37.57	0.06	21.35	0.00	29.38	0.54	4.40	7.28	0.00	0.00	100.58		

WB163 Garnet-2	Coordinates		Weight Percent Oxides										Total
	X	Y	SiO ₂	TiO ₂	Al ₂ O ₃	Cr ₂ O ₃	FeO*	MnO	MgO	CaO	Na ₂ O	K ₂ O	
WB163-Grt2-1	4948	35113	37.64	0.09	21.39	0.00	29.51	0.58	4.17	7.49	0.00	0.00	100.88
WB163-Grt2-2	4998	35119	37.73	0.11	21.27	0.00	29.33	0.59	4.14	7.61	0.00	0.00	100.79
WB163-Grt2-3	5048	35115	37.61	0.11	21.14	0.02	29.55	0.60	3.99	7.78	0.00	0.01	100.81
WB163-Grt2-4	5098	35115	37.59	0.11	21.26	0.02	29.35	0.63	3.92	7.66	0.00	0.00	100.55
WB163-Grt2-5	5148	35110	37.43	0.06	21.39	0.01	29.60	0.68	3.95	7.66	0.00	0.00	100.77
WB163-Grt2-6	5198	35103	37.42	0.10	21.18	0.00	29.36	0.68	3.72	7.79	0.00	0.00	100.26
WB163-Grt2-7	5248	35103	37.42	0.06	21.24	0.00	29.75	0.74	3.62	7.83	0.00	0.01	100.66
WB163-Grt2-8	5303	35103	37.41	0.07	21.16	0.00	29.73	0.74	3.65	7.96	0.00	0.00	100.71
WB163-Grt2-9	5337	35101	37.47	0.06	21.25	0.00	29.85	0.78	3.60	7.79	0.00	0.00	100.80
WB163-Grt2-10	5397	35107	37.23	0.04	21.30	0.00	29.85	0.78	3.53	7.82	0.00	0.00	100.55
WB163-Grt2-11	5447	35107	37.31	0.08	21.13	0.00	29.63	0.85	3.41	8.03	0.00	0.00	100.45
WB163-Grt2-12	5497	35092	37.45	0.11	21.06	0.00	29.54	0.85	3.41	8.03	0.00	0.00	100.44
WB163-Grt2-13	5547	35092	37.40	0.10	21.08	0.00	29.64	0.88	3.44	8.11	0.00	0.00	100.65
WB163-Grt2-14	5597	35092	37.55	0.11	21.25	0.02	29.72	0.82	3.43	8.01	0.00	0.00	100.91
WB163-Grt2-15	5647	35092	37.58	0.01	21.25	0.00	29.58	0.67	3.49	8.12	0.00	0.00	100.70
WB163-Grt2-16	5697	35105	37.52	0.07	21.28	0.00	29.50	0.66	3.67	7.94	0.00	0.01	100.64
WB163-Grt2-17	5747	35105	37.55	0.10	21.23	0.00	29.29	0.63	3.98	7.76	0.00	0.01	100.54
WB163-Grt2-18	5797	35105	37.69	0.07	21.28	0.02	29.57	0.57	4.22	7.40	0.00	0.01	100.83
WB163-Grt2-19	5847	35105	37.62	0.11	21.27	0.00	29.39	0.59	4.11	7.61	0.00	0.00	100.70
WB163-Grt2-20	5897	35114	37.32	0.03	21.24	0.00	29.98	0.92	3.53	7.53	0.00	0.00	100.55
WB163-Grt2-21	5947	35111	37.58	0.09	21.15	0.00	30.40	1.02	3.54	7.32	0.00	0.00	101.10
WB163-Grt2-22	5997	35115	37.60	0.07	21.10	0.02	30.34	1.04	3.57	7.11	0.00	0.00	100.84
WB163-Grt2-23	6047	35115	37.65	0.09	21.02	0.00	30.11	1.09	3.51	7.33	0.00	0.01	100.81
WB163-Grt2-26	6188	35096	37.78	0.11	21.02	0.01	29.81	1.01	3.45	7.66	0.00	0.00	100.83
WB163-Grt2-27	6238	35081	37.59	0.09	20.98	0.00	29.80	1.09	3.47	7.55	0.00	0.00	100.57
WB163-Grt2-28	6288	35084	37.53	0.07	21.09	0.01	30.07	1.04	3.50	7.57	0.00	0.00	100.89
WB163-Grt2-29	6338	35084	37.49	0.07	21.10	0.01	29.70	1.09	3.35	7.96	0.00	0.00	100.77
WB163-Grt2-30	6388	35084	37.81	0.11	21.00	0.00	29.90	1.00	3.37	7.77	0.00	0.00	100.96
WB163-Grt2-31	6438	35084	37.84	0.07	21.12	0.01	29.93	0.98	3.39	7.78	0.00	0.00	101.10
WB163-Grt2-32	6488	35095	37.91	0.02	21.13	0.02	29.15	0.66	3.71	8.01	0.00	0.00	100.60
WB163-Grt2-34	6602	35085	37.87	0.07	21.31	0.01	29.21	0.66	3.72	8.14	0.00	0.00	100.97
WB163-Grt2-35	6652	35103	37.81	0.10	21.18	0.00	29.66	0.65	3.74	8.08	0.00	0.01	101.22
WB163-Grt2-36	6702	35103	37.84	0.09	21.15	0.00	29.69	0.68	3.90	7.51	0.00	0.00	100.86
WB163-Grt2-37	6752	35100	37.72	0.04	21.28	0.01	29.67	0.66	4.16	7.26	0.00	0.00	100.80
WB163-Grt2-38	6802	35100	37.96	0.10	21.12	0.00	29.45	0.64	4.02	7.58	0.00	0.01	100.89
WB163-Grt2-39	6852	35100	38.01	0.12	21.10	0.02	29.50	0.63	4.11	7.63	0.00	0.00	101.12
WB163-Grt2-40	6902	35172	37.92	0.11	21.02	0.00	29.44	0.62	4.09	7.54	0.00	0.00	100.73
WB163-Grt2-41	6952	35177	38.15	0.07	21.15	0.00	29.62	0.58	4.38	7.19	0.00	0.00	101.13
WB163-Grt2-42	6989	35196	38.38	0.04	21.03	0.01	29.43	0.49	4.41	7.20	0.00	0.01	101.00
WB163-Grt2-43	7039	35233	38.57	0.08	21.09	0.00	29.42	0.61	4.43	7.22	0.00	0.01	101.43
WB163-Grt2-44	7067	35255	37.78	0.05	21.19	0.01	29.86	0.53	4.30	6.94	0.00	0.01	100.68

WB163 Garnet-1	Atoms per 12 Oxygen										
	Si	Ti	Al	Cr	Fe	Mn	Mg	Ca	Na	K	Sum
WB163-Grt1-1	3.001	0.006	1.916	0.000	1.952	0.038	0.509	0.613	0.000	0.001	8.035
WB163-Grt1-2	2.992	0.005	1.926	0.000	1.977	0.041	0.489	0.611	0.000	0.000	8.040
WB163-Grt1-3	2.975	0.003	1.940	0.001	1.990	0.045	0.495	0.603	0.000	0.000	8.052
WB163-Grt1-4	2.984	0.004	1.937	0.000	1.985	0.047	0.461	0.626	0.000	0.000	8.044
WB163-Grt1-5	2.969	0.004	1.951	0.000	2.013	0.053	0.448	0.616	0.000	0.000	8.052
WB163-Grt1-6	2.980	0.009	1.937	0.000	1.990	0.054	0.434	0.641	0.000	0.000	8.043
WB163-Grt1-7	2.990	0.007	1.920	0.001	2.003	0.054	0.434	0.635	0.000	0.000	8.043
WB163-Grt1-8	2.981	0.005	1.949	0.000	2.020	0.062	0.449	0.573	0.000	0.000	8.039
WB163-Grt1-9	2.966	0.015	1.940	0.000	2.015	0.063	0.429	0.621	0.000	0.001	8.050
WB163-Grt1-10	2.986	0.006	1.924	0.001	2.012	0.070	0.426	0.620	0.000	0.000	8.045
WB163-Grt1-11	2.871	0.204	1.890	0.000	1.978	0.073	0.417	0.548	0.000	0.000	7.980
WB163-Grt1-12	2.967	0.004	1.949	0.000	2.064	0.079	0.429	0.561	0.000	0.000	8.054
WB163-Grt1-13	2.974	0.001	1.956	0.000	2.043	0.075	0.436	0.560	0.000	0.000	8.046
WB163-Grt1-14	2.963	0.006	1.953	0.000	2.051	0.065	0.438	0.580	0.000	0.000	8.055
WB163-Grt1-15	2.965	0.004	1.951	0.000	2.064	0.056	0.433	0.582	0.000	0.001	8.056
WB163-Grt1-16	2.976	0.008	1.939	0.000	2.043	0.054	0.440	0.587	0.000	0.001	8.048
WB163-Grt1-17	2.968	0.008	1.946	0.000	2.035	0.050	0.447	0.598	0.000	0.000	8.051
WB163-Grt1-18	2.960	0.010	1.953	0.000	2.017	0.064	0.429	0.621	0.000	0.000	8.054
WB163-Grt1-19	2.980	0.017	1.936	0.001	2.033	0.063	0.406	0.599	0.000	0.000	8.035
WB163-Grt1-20	2.974	0.007	1.951	0.000	2.038	0.061	0.399	0.613	0.000	0.000	8.043
WB163-Grt1-21	2.974	0.011	1.947	0.001	2.012	0.095	0.395	0.609	0.000	0.000	8.042
WB163-Grt1-22	2.972	0.007	1.948	0.000	2.014	0.121	0.349	0.635	0.000	0.000	8.047
WB163-Grt1-23	2.964	0.010	1.954	0.000	2.010	0.106	0.394	0.613	0.000	0.000	8.050
WB163-Grt1-24	2.981	0.007	1.941	0.000	2.025	0.097	0.383	0.608	0.000	0.000	8.042
WB163-Grt1-25	2.971	0.005	1.946	0.000	2.014	0.077	0.417	0.621	0.000	0.000	8.052
WB163-Grt1-26	2.979	0.005	1.942	0.000	2.036	0.089	0.417	0.575	0.000	0.000	8.045
WB163-Grt1-27	2.970	0.004	1.952	0.000	2.020	0.090	0.410	0.604	0.000	0.000	8.050
WB163-Grt1-28	2.973	0.003	1.952	0.001	2.018	0.086	0.405	0.608	0.000	0.001	8.048
WB163-Grt1-29	2.983	0.003	1.937	0.000	2.021	0.060	0.428	0.612	0.000	0.001	8.045
WB163-Grt1-30	2.977	0.003	1.946	0.001	2.015	0.063	0.418	0.623	0.000	0.000	8.046
WB163-Grt1-31	2.975	0.003	1.947	0.001	2.028	0.062	0.430	0.602	0.000	0.000	8.048
WB163-Grt1-32	2.971	0.003	1.957	0.000	2.026	0.067	0.428	0.594	0.000	0.000	8.047
WB163-Grt1-33	2.971	0.004	1.947	0.000	2.022	0.082	0.406	0.621	0.000	0.000	8.052
WB163-Grt1-34	2.976	0.003	1.954	0.000	1.982	0.098	0.387	0.645	0.000	0.001	8.045
WB163-Grt1-35	2.982	0.003	1.956	0.001	2.013	0.099	0.402	0.582	0.000	0.000	8.037
WB163-Grt1-36	2.985	0.003	1.943	0.000	2.048	0.063	0.434	0.566	0.000	0.000	8.041
WB163-Grt1-37	2.990	0.003	1.933	0.000	2.030	0.052	0.429	0.602	0.000	0.000	8.040
WB163-Grt1-38	2.980	0.004	1.954	0.000	2.031	0.054	0.437	0.578	0.000	0.001	8.039
WB163-Grt1-39	2.978	0.003	1.956	0.000	2.037	0.054	0.421	0.594	0.000	0.000	8.042
WB163-Grt1-40	2.984	0.004	1.942	0.000	2.046	0.066	0.402	0.597	0.000	0.000	8.042
WB163-Grt1-41	2.980	0.001	1.956	0.000	2.040	0.071	0.394	0.598	0.000	0.000	8.040
WB163-Grt1-42	2.974	0.004	1.946	0.000	2.025	0.068	0.412	0.620	0.000	0.000	8.049
WB163-Grt1-43	2.980	0.005	1.947	0.001	2.046	0.063	0.423	0.577	0.000	0.000	8.042
WB163-Grt1-44	2.976	0.003	1.958	0.001	2.009	0.067	0.412	0.618	0.000	0.000	8.043
WB163-Grt1-45	2.964	0.003	1.960	0.001	2.036	0.070	0.420	0.599	0.000	0.000	8.052
WB163-Grt1-46	2.974	0.004	1.952	0.000	2.025	0.078	0.414	0.600	0.000	0.000	8.046
WB163-Grt1-47	3.118	0.004	1.968	0.000	1.766	0.064	0.377	0.530	0.132	0.001	7.960
WB163-Grt1-48	2.976	0.005	1.963	0.000	1.976	0.067	0.413	0.638	0.000	0.000	8.038
WB163-Grt1-49	2.975	0.004	1.955	0.000	2.030	0.065	0.424	0.591	0.000	0.000	8.044
WB163-Grt1-50	2.989	0.005	1.940	0.000	1.998	0.059	0.428	0.618	0.000	0.000	8.036
WB163-Grt1-51	2.987	0.006	1.939	0.000	1.998	0.055	0.434	0.618	0.000	0.001	8.038
WB163-Grt1-52	2.978	0.005	1.939	0.000	2.008	0.051	0.450	0.617	0.000	0.000	8.048
WB163-Grt1-53	2.985	0.004	1.943	0.000	2.009	0.052	0.450	0.599	0.000	0.001	8.041
WB163-Grt1-54	2.993	0.004	1.932	0.001	2.009	0.053	0.434	0.613	0.000	0.001	8.038
WB163-Grt1-55	2.982	0.004	1.939	0.000	2.006	0.052	0.453	0.607	0.000	0.000	8.044
WB163-Grt1-56	2.984	0.005	1.948	0.000	1.971	0.049	0.452	0.628	0.000	0.001	8.037
WB163-Grt1-57	2.976	0.006	1.935	0.000	1.979	0.049	0.456	0.649	0.000	0.000	8.051
WB163-Grt1-58	2.986	0.005	1.938	0.000	1.970	0.046	0.454	0.643	0.000	0.000	8.041
WB163-Grt1-59	2.981	0.007	1.942	0.001	1.956	0.045	0.458	0.649	0.000	0.000	8.040
WB163-Grt1-60	2.981	0.009	1.947	0.000	1.947	0.042	0.467	0.643	0.000	0.000	8.037
WB163-Grt1-61	2.975	0.006	1.942	0.000	1.962	0.043	0.474	0.645	0.000	0.000	8.048
WB163-Grt1-62	2.970	0.010	1.948	0.000	1.957	0.045	0.479	0.636	0.000	0.001	8.046
WB163-Grt1-63	2.968	0.004	1.957	0.000	1.975	0.044	0.489	0.612	0.000	0.000	8.049
WB163-Grt1-64	2.967	0.004	1.956	0.000	1.961	0.040	0.497	0.628	0.000	0.000	8.052
WB163-Grt1-65	2.961	0.004	1.972	0.000	1.952	0.038	0.517	0.605	0.000	0.000	8.049
WB163-Grt1-66	2.959	0.004	1.982	0.000	1.935	0.036	0.517	0.614	0.000	0.000	8.047

WB163		Atoms per 12 Oxygen									
Garnet-2	Si	Ti	Al	Cr	Fe	Mn	Mg	Ca	Na	K	Sum
WB163-Grt2-1	2.959	0.006	1.982	0.000	1.940	0.039	0.489	0.631	0.000	0.000	8.045
WB163-Grt2-2	2.967	0.007	1.971	0.000	1.929	0.040	0.486	0.641	0.000	0.000	8.041
WB163-Grt2-3	2.964	0.006	1.963	0.001	1.948	0.040	0.468	0.657	0.001	0.000	8.048
WB163-Grt2-4	2.966	0.007	1.977	0.001	1.937	0.042	0.461	0.648	0.000	0.000	8.038
WB163-Grt2-5	2.951	0.003	1.988	0.001	1.952	0.045	0.464	0.647	0.000	0.000	8.051
WB163-Grt2-6	2.965	0.006	1.978	0.000	1.945	0.046	0.440	0.662	0.000	0.000	8.041
WB163-Grt2-7	2.959	0.004	1.980	0.000	1.967	0.049	0.426	0.663	0.001	0.000	8.048
WB163-Grt2-8	2.958	0.004	1.972	0.000	1.966	0.050	0.430	0.675	0.000	0.000	8.053
WB163-Grt2-9	2.960	0.004	1.978	0.000	1.972	0.052	0.424	0.659	0.000	0.000	8.048
WB163-Grt2-10	2.951	0.002	1.989	0.000	1.978	0.052	0.417	0.664	0.000	0.000	8.053
WB163-Grt2-11	2.959	0.005	1.976	0.000	1.966	0.057	0.403	0.682	0.000	0.000	8.048
WB163-Grt2-12	2.968	0.007	1.967	0.000	1.958	0.057	0.403	0.682	0.000	0.000	8.042
WB163-Grt2-13	2.961	0.006	1.967	0.000	1.962	0.059	0.406	0.688	0.000	0.000	8.049
WB163-Grt2-14	2.963	0.006	1.976	0.001	1.961	0.055	0.403	0.677	0.000	0.000	8.043
WB163-Grt2-15	2.968	0.001	1.978	0.000	1.954	0.045	0.410	0.688	0.000	0.000	8.043
WB163-Grt2-16	2.962	0.004	1.981	0.000	1.948	0.044	0.432	0.671	0.001	0.000	8.043
WB163-Grt2-17	2.963	0.006	1.975	0.000	1.933	0.042	0.468	0.656	0.001	0.000	8.044
WB163-Grt2-18	2.964	0.004	1.972	0.001	1.945	0.038	0.494	0.624	0.001	0.000	8.045
WB163-Grt2-19	2.963	0.006	1.974	0.000	1.936	0.039	0.482	0.642	0.000	0.000	8.044
WB163-Grt2-20	2.958	0.002	1.984	0.000	1.987	0.062	0.417	0.639	0.000	0.000	8.049
WB163-Grt2-21	2.965	0.005	1.966	0.000	2.006	0.068	0.417	0.619	0.000	0.000	8.047
WB163-Grt2-22	2.972	0.004	1.965	0.001	2.006	0.070	0.421	0.602	0.000	0.000	8.041
WB163-Grt2-23	2.976	0.005	1.959	0.000	1.991	0.073	0.414	0.621	0.001	0.000	8.040
WB163-Grt2-26	2.982	0.006	1.956	0.000	1.968	0.068	0.405	0.648	0.000	0.000	8.033
WB163-Grt2-27	2.977	0.006	1.958	0.000	1.974	0.073	0.410	0.641	0.000	0.000	8.039
WB163-Grt2-28	2.966	0.004	1.965	0.000	1.988	0.070	0.413	0.641	0.000	0.000	8.047
WB163-Grt2-29	2.966	0.004	1.968	0.001	1.965	0.073	0.395	0.675	0.000	0.000	8.046
WB163-Grt2-30	2.983	0.007	1.953	0.000	1.972	0.067	0.397	0.656	0.000	0.000	8.034
WB163-Grt2-31	2.980	0.004	1.960	0.000	1.971	0.065	0.399	0.656	0.000	0.000	8.036
WB163-Grt2-32	2.988	0.002	1.962	0.001	1.921	0.044	0.436	0.676	0.000	0.000	8.029
WB163-Grt2-34	2.975	0.004	1.973	0.000	1.919	0.044	0.436	0.685	0.000	0.000	8.035
WB163-Grt2-35	2.969	0.006	1.961	0.000	1.948	0.044	0.438	0.680	0.001	0.000	8.045
WB163-Grt2-36	2.979	0.005	1.961	0.000	1.954	0.045	0.458	0.633	0.000	0.000	8.036
WB163-Grt2-37	2.968	0.003	1.974	0.001	1.953	0.044	0.488	0.612	0.000	0.000	8.042
WB163-Grt2-38	2.983	0.006	1.956	0.000	1.936	0.043	0.471	0.638	0.001	0.000	8.034
WB163-Grt2-39	2.980	0.007	1.950	0.001	1.935	0.042	0.481	0.641	0.000	0.000	8.037
WB163-Grt2-40	2.985	0.006	1.950	0.000	1.938	0.041	0.480	0.635	0.000	0.000	8.034
WB163-Grt2-41	2.987	0.004	1.951	0.000	1.939	0.038	0.511	0.603	0.000	0.000	8.034
WB163-Grt2-42	3.004	0.003	1.940	0.000	1.926	0.033	0.514	0.604	0.001	0.000	8.024
WB163-Grt2-43	3.005	0.005	1.937	0.000	1.917	0.040	0.514	0.602	0.001	0.000	8.022
WB163-Grt2-44	2.975	0.003	1.967	0.001	1.967	0.036	0.505	0.586	0.001	0.000	8.039

WB163											
Garnet-I	K Numbers (=Ix/Istd)										
	Na	Mg	Al	Si	K	Ca	Ti	Cr	Mn	Fe	Sum
WB163-Grtl-1	0.0000	0.0536	0.8421	0.8855	0.0005	0.2075	0.0027	0.0000	0.0149	0.9921	2.9989
WB163-Grtl-2	0.0000	0.0513	0.8451	0.8815	0.0002	0.2066	0.0021	0.0000	0.0163	1.0041	3.0072
WB163-Grtl-3	0.0000	0.0517	0.8476	0.8726	0.0000	0.2036	0.0012	0.0002	0.0178	1.0083	3.0030
WB163-Grtl-4	0.0000	0.0481	0.8465	0.8750	0.0002	0.2110	0.0018	0.0000	0.0185	1.0041	3.0052
WB163-Grtl-5	0.0000	0.0463	0.8475	0.8653	0.0000	0.2068	0.0015	0.0000	0.0206	1.0136	3.0016
WB163-Grtl-6	0.0000	0.0450	0.8441	0.8713	0.0000	0.2153	0.0038	0.0001	0.0210	1.0029	3.0035
WB163-Grtl-7	0.0000	0.0448	0.8317	0.8704	0.0002	0.2124	0.0030	0.0002	0.0209	1.0049	2.9885
WB163-Grtl-8	0.0000	0.0463	0.8441	0.8661	0.0000	0.1917	0.0022	0.0000	0.0244	1.0156	2.9904
WB163-Grtl-9	0.0000	0.0441	0.8395	0.8617	0.0005	0.2078	0.0063	0.0000	0.0248	1.0109	2.9956
WB163-Grtl-10	0.0000	0.0437	0.8312	0.8668	0.0000	0.2070	0.0026	0.0001	0.0272	1.0080	2.9866
WB163-Grtl-11	0.0000	0.0430	0.8209	0.8413	0.0000	0.1855	0.0896	0.0000	0.0286	0.9990	3.0079
WB163-Grtl-12	0.0000	0.0440	0.8414	0.8609	0.0000	0.1881	0.0019	0.0000	0.0310	1.0386	3.0059
WB163-Grtl-13	0.0000	0.0447	0.8424	0.8596	0.0000	0.1870	0.0006	0.0000	0.0292	1.0235	2.9870
WB163-Grtl-14	0.0000	0.0449	0.8433	0.8589	0.0000	0.1940	0.0024	0.0000	0.0254	1.0304	2.9993
WB163-Grtl-15	0.0000	0.0445	0.8448	0.8625	0.0004	0.1954	0.0019	0.0001	0.0221	1.0401	3.0118
WB163-Grtl-16	0.0000	0.0452	0.8375	0.8636	0.0008	0.1965	0.0034	0.0000	0.0213	1.0260	2.9943
WB163-Grtl-17	0.0000	0.0460	0.8413	0.8616	0.0000	0.2001	0.0036	0.0000	0.0196	1.0223	2.9945
WB163-Grtl-18	0.0000	0.0442	0.8468	0.8608	0.0000	0.2080	0.0044	0.0000	0.0251	1.0139	3.0032
WB163-Grtl-19	0.0000	0.0418	0.8400	0.8684	0.0002	0.2011	0.0075	0.0001	0.0247	1.0230	3.0068
WB163-Grtl-20	0.0000	0.0409	0.8449	0.8642	0.0002	0.2053	0.0032	0.0000	0.0238	1.0230	3.0055
WB163-Grtl-21	0.0000	0.0406	0.8452	0.8662	0.0000	0.2041	0.0046	0.0001	0.0373	1.0123	3.0104
WB163-Grtl-22	0.0000	0.0357	0.8430	0.8635	0.0000	0.2125	0.0032	0.0001	0.0473	1.0100	3.0153
WB163-Grtl-23	0.0000	0.0406	0.8488	0.8641	0.0000	0.2058	0.0043	0.0001	0.0414	1.0128	3.0179
WB163-Grtl-24	0.0000	0.0394	0.8427	0.8692	0.0003	0.2041	0.0030	0.0000	0.0380	1.0194	3.0161
WB163-Grtl-25	0.0000	0.0431	0.8483	0.8691	0.0001	0.2092	0.0021	0.0000	0.0305	1.0179	3.0203
WB163-Grtl-26	0.0000	0.0429	0.8422	0.8678	0.0000	0.1932	0.0024	0.0000	0.0351	1.0264	3.0100
WB163-Grtl-27	0.0000	0.0423	0.8489	0.8672	0.0000	0.2030	0.0018	0.0000	0.0356	1.0194	3.0182
WB163-Grtl-28	0.0000	0.0418	0.8480	0.8665	0.0007	0.2040	0.0014	0.0002	0.0337	1.0165	3.0128
WB163-Grtl-29	0.0000	0.0443	0.8455	0.8743	0.0007	0.2063	0.0014	0.0000	0.0236	1.0229	3.0190
WB163-Grtl-30	0.0000	0.0433	0.8470	0.8696	0.0002	0.2094	0.0015	0.0001	0.0246	1.0164	3.0121
WB163-Grtl-31	0.0000	0.0446	0.8492	0.8711	0.0001	0.2031	0.0014	0.0001	0.0246	1.0264	3.0206
WB163-Grtl-32	0.0000	0.0443	0.8509	0.8667	0.0000	0.1997	0.0014	0.0000	0.0263	1.0223	3.0116
WB163-Grtl-33	0.0000	0.0420	0.8494	0.8700	0.0000	0.2093	0.0017	0.0000	0.0321	1.0227	3.0272
WB163-Grtl-34	0.0000	0.0401	0.8548	0.8726	0.0006	0.2172	0.0015	0.0000	0.0388	1.0019	3.0275
WB163-Grtl-35	0.0000	0.0414	0.8506	0.8701	0.0000	0.1957	0.0013	0.0001	0.0390	1.0156	3.0138
WB163-Grtl-36	0.0000	0.0448	0.8452	0.8718	0.0000	0.1905	0.0012	0.0000	0.0248	1.0352	3.0135
WB163-Grtl-37	0.0000	0.0446	0.8450	0.8783	0.0002	0.2034	0.0014	0.0001	0.0206	1.0295	3.0231
WB163-Grtl-38	0.0000	0.0455	0.8560	0.8760	0.0010	0.1957	0.0020	0.0000	0.0213	1.0326	3.0301
WB163-Grtl-39	0.0000	0.0438	0.8579	0.8764	0.0000	0.2014	0.0011	0.0000	0.0213	1.0363	3.0382
WB163-Grtl-40	0.0000	0.0417	0.8502	0.8773	0.0000	0.2021	0.0015	0.0000	0.0262	1.0394	3.0384
WB163-Grtl-41	0.0000	0.0408	0.8542	0.8732	0.0000	0.2016	0.0006	0.0000	0.0280	1.0329	3.0313
WB163-Grtl-42	0.0000	0.0426	0.8497	0.8717	0.0000	0.2090	0.0016	0.0000	0.0268	1.0251	3.0265
WB163-Grtl-43	0.0000	0.0437	0.8458	0.8692	0.0003	0.1938	0.0020	0.0001	0.0248	1.0325	3.0122
WB163-Grtl-44	0.0000	0.0426	0.8538	0.8698	0.0000	0.2080	0.0011	0.0001	0.0265	1.0139	3.0158
WB163-Grtl-45	0.0000	0.0435	0.8550	0.8679	0.0001	0.2020	0.0015	0.0002	0.0276	1.0311	3.0289
WB163-Grtl-46	0.0000	0.0428	0.8500	0.8692	0.0000	0.2018	0.0018	0.0001	0.0306	1.0229	3.0192
WB163-Grtl-47	0.0522	0.0399	0.8740	0.9188	0.0010	0.1779	0.0019	0.0000	0.0251	0.8909	2.9817
WB163-Grtl-48	0.0000	0.0429	0.8565	0.8694	0.0000	0.2142	0.0021	0.0000	0.0264	0.9956	3.0071
WB163-Grtl-49	0.0000	0.0438	0.8498	0.8674	0.0002	0.1985	0.0018	0.0000	0.0256	1.0240	3.0111
WB163-Grtl-50	0.0000	0.0444	0.8462	0.8744	0.0000	0.2077	0.0020	0.0000	0.0231	1.0079	3.0057
WB163-Grtl-51	0.0000	0.0452	0.8492	0.8780	0.0005	0.2088	0.0028	0.0000	0.0217	1.0127	3.0189
WB163-Grtl-52	0.0000	0.0468	0.8478	0.8741	0.0000	0.2082	0.0020	0.0000	0.0202	1.0176	3.0167
WB163-Grtl-53	0.0000	0.0468	0.8491	0.8752	0.0005	0.2020	0.0017	0.0000	0.0204	1.0175	3.0132
WB163-Grtl-54	0.0000	0.0450	0.8421	0.8759	0.0004	0.2062	0.0015	0.0001	0.0209	1.0143	3.0064
WB163-Grtl-55	0.0000	0.0470	0.8453	0.8728	0.0000	0.2045	0.0019	0.0000	0.0205	1.0140	3.0060
WB163-Grtl-56	0.0000	0.0472	0.8541	0.8769	0.0004	0.2120	0.0023	0.0000	0.0194	0.9985	3.0108
WB163-Grtl-57	0.0000	0.0475	0.8450	0.8720	0.0000	0.2184	0.0025	0.0000	0.0194	0.9993	3.0041
WB163-Grtl-58	0.0000	0.0473	0.8473	0.8755	0.0000	0.2164	0.0022	0.0000	0.0182	0.9952	3.0021
WB163-Grtl-59	0.0000	0.0478	0.8497	0.8739	0.0001	0.2183	0.0032	0.0002	0.0179	0.9876	2.9987
WB163-Grtl-60	0.0000	0.0490	0.8549	0.8766	0.0000	0.2172	0.0041	0.0001	0.0167	0.9863	3.0049
WB163-Grtl-61	0.0000	0.0495	0.8499	0.8730	0.0003	0.2175	0.0028	0.0000	0.0169	0.9922	3.0021
WB163-Grtl-62	0.0000	0.0501	0.8528	0.8711	0.0005	0.2144	0.0043	0.0001	0.0179	0.9896	3.0008
WB163-Grtl-63	0.0000	0.0514	0.8599	0.8742	0.0000	0.2074	0.0018	0.0001	0.0173	1.0047	3.0168
WB163-Grtl-64	0.0000	0.0523	0.8594	0.8731	0.0000	0.2124	0.0016	0.0000	0.0159	0.9960	3.0107
WB163-Grtl-65	0.0000	0.0545	0.8676	0.8716	0.0000	0.2050	0.0017	0.0000	0.0149	0.9933	3.0086
WB163-Grtl-66	0.0000	0.0547	0.8734	0.8715	0.0000	0.2081	0.0017	0.0000	0.0143	0.9851	3.0088

WB163 Garnet-2	K Numbers (=Ix/Istd)										Sum
	Na	Mg	Al	Si	K	Ca	Ti	Cr	Mn	Fe	
WB163-Grt2-1	2.959	0.006	1.982	0.000	1.940	0.039	0.489	0.631	0.000	0.000	8.045
WB163-Grt2-2	2.967	0.007	1.971	0.000	1.929	0.040	0.486	0.641	0.000	0.000	8.041
WB163-Grt2-3	2.964	0.006	1.963	0.001	1.948	0.040	0.468	0.657	0.001	0.000	8.048
WB163-Grt2-4	2.966	0.007	1.977	0.001	1.937	0.042	0.461	0.648	0.000	0.000	8.038
WB163-Grt2-5	2.951	0.003	1.988	0.001	1.952	0.045	0.464	0.647	0.000	0.000	8.051
WB163-Grt2-6	2.965	0.006	1.978	0.000	1.945	0.046	0.440	0.662	0.000	0.000	8.041
WB163-Grt2-7	2.959	0.004	1.980	0.000	1.967	0.049	0.426	0.663	0.001	0.000	8.048
WB163-Grt2-8	2.958	0.004	1.972	0.000	1.966	0.050	0.430	0.675	0.000	0.000	8.053
WB163-Grt2-9	2.960	0.004	1.978	0.000	1.972	0.052	0.424	0.659	0.000	0.000	8.048
WB163-Grt2-10	2.951	0.002	1.989	0.000	1.978	0.052	0.417	0.664	0.000	0.000	8.053
WB163-Grt2-11	2.959	0.005	1.976	0.000	1.966	0.057	0.403	0.682	0.000	0.000	8.048
WB163-Grt2-12	2.968	0.007	1.967	0.000	1.958	0.057	0.403	0.682	0.000	0.000	8.042
WB163-Grt2-13	2.961	0.006	1.967	0.000	1.962	0.059	0.406	0.688	0.000	0.000	8.049
WB163-Grt2-14	2.963	0.006	1.976	0.001	1.961	0.055	0.403	0.677	0.000	0.000	8.043
WB163-Grt2-15	2.968	0.001	1.978	0.000	1.954	0.045	0.410	0.688	0.000	0.000	8.043
WB163-Grt2-16	2.962	0.004	1.981	0.000	1.948	0.044	0.432	0.671	0.001	0.000	8.043
WB163-Grt2-17	2.963	0.006	1.975	0.000	1.933	0.042	0.468	0.656	0.001	0.000	8.044
WB163-Grt2-18	2.964	0.004	1.972	0.001	1.945	0.038	0.494	0.624	0.001	0.000	8.045
WB163-Grt2-19	2.963	0.006	1.974	0.000	1.936	0.039	0.482	0.642	0.000	0.000	8.044
WB163-Grt2-20	2.958	0.002	1.984	0.000	1.987	0.062	0.417	0.639	0.000	0.000	8.049
WB163-Grt2-21	2.965	0.005	1.966	0.000	2.006	0.068	0.417	0.619	0.000	0.000	8.047
WB163-Grt2-22	2.972	0.004	1.965	0.001	2.006	0.070	0.421	0.602	0.000	0.000	8.041
WB163-Grt2-23	2.976	0.005	1.959	0.000	1.991	0.073	0.414	0.621	0.001	0.000	8.040
WB163-Grt2-26	2.982	0.006	1.956	0.000	1.968	0.068	0.405	0.648	0.000	0.000	8.033
WB163-Grt2-27	2.977	0.006	1.958	0.000	1.974	0.073	0.410	0.641	0.000	0.000	8.039
WB163-Grt2-28	2.966	0.004	1.965	0.000	1.988	0.070	0.413	0.641	0.000	0.000	8.047
WB163-Grt2-29	2.966	0.004	1.968	0.001	1.965	0.073	0.395	0.675	0.000	0.000	8.046
WB163-Grt2-30	2.983	0.007	1.953	0.000	1.972	0.067	0.397	0.656	0.000	0.000	8.034
WB163-Grt2-31	2.980	0.004	1.960	0.000	1.971	0.065	0.399	0.656	0.000	0.000	8.036
WB163-Grt2-32	2.988	0.002	1.962	0.001	1.921	0.044	0.436	0.676	0.000	0.000	8.029
WB163-Grt2-34	2.975	0.004	1.973	0.000	1.919	0.044	0.436	0.685	0.000	0.000	8.035
WB163-Grt2-35	2.969	0.006	1.961	0.000	1.948	0.044	0.438	0.680	0.001	0.000	8.045
WB163-Grt2-36	2.979	0.005	1.961	0.000	1.954	0.045	0.458	0.633	0.000	0.000	8.036
WB163-Grt2-37	2.968	0.003	1.974	0.001	1.953	0.044	0.488	0.612	0.000	0.000	8.042
WB163-Grt2-38	2.983	0.006	1.956	0.000	1.936	0.043	0.471	0.638	0.001	0.000	8.034
WB163-Grt2-39	2.980	0.007	1.950	0.001	1.935	0.042	0.481	0.641	0.000	0.000	8.037
WB163-Grt2-40	2.985	0.006	1.950	0.000	1.938	0.041	0.480	0.635	0.000	0.000	8.034
WB163-Grt2-41	2.987	0.004	1.951	0.000	1.939	0.038	0.511	0.603	0.000	0.000	8.034
WB163-Grt2-42	3.004	0.003	1.940	0.000	1.926	0.033	0.514	0.604	0.001	0.000	8.024
WB163-Grt2-43	3.005	0.005	1.937	0.000	1.917	0.040	0.514	0.602	0.001	0.000	8.022
WB163-Grt2-44	2.975	0.003	1.967	0.001	1.967	0.036	0.505	0.586	0.001	0.000	8.039

WB164 Garnet-1	Coordinates		Weight Percent Oxides										Total
	X	Y	SiO ₂	TiO ₂	Al ₂ O ₃	Cr ₂ O ₃	FeO*	MnO	MgO	CaO	Na ₂ O	K ₂ O	
WB164-Grt1-1	15296	-8916	37.25	0.04	21.06	0.00	29.85	1.06	3.62	7.43	0.00	0.01	100.32
WB164-Grt1-2	15346	-8916	37.18	0.08	20.67	0.02	30.70	0.90	3.34	6.93	0.00	0.00	99.82
WB164-Grt1-3	15396	-8916	37.59	0.07	20.69	0.00	31.77	1.07	2.95	6.83	0.00	0.01	100.97
WB164-Grt1-4	15446	-8916	37.24	0.08	20.53	0.00	33.18	0.95	2.97	5.51	0.00	0.01	100.46
WB164-Grt1-5	15496	-8916	37.16	0.07	20.75	0.01	33.29	1.01	2.90	5.60	0.00	0.00	100.79
WB164-Grt1-6	15546	-8916	37.18	0.06	20.78	0.01	32.93	1.04	2.88	5.95	0.00	0.01	100.85
WB164-Grt1-7	15596	-8916	37.13	0.07	20.62	0.02	32.93	1.04	2.99	5.86	0.00	0.00	100.66
WB164-Grt1-8	15646	-8916	37.28	0.10	20.66	0.00	32.72	1.05	3.00	5.91	0.00	0.00	100.72
WB164-Grt1-9	15701	-8911	37.22	0.06	20.79	0.02	33.01	1.02	3.31	5.23	0.00	0.00	100.66
WB164-Grt1-10	15751	-8911	37.47	0.08	20.54	0.01	32.52	0.96	3.04	6.08	0.00	0.00	100.69
WB164-Grt1-11	15801	-8924	37.26	0.07	20.72	0.02	32.90	1.01	2.97	5.86	0.00	0.00	100.82
WB164-Grt1-12	15851	-8884	37.37	0.11	20.53	0.00	32.99	0.96	2.86	6.11	0.00	0.01	100.93
WB164-Grt1-13	15901	-8896	37.56	0.09	20.49	0.02	32.96	0.89	2.68	6.16	0.00	0.00	100.84
WB164-Grt1-14	15963	-8896	37.29	0.11	20.62	0.01	32.78	1.06	2.65	6.32	0.00	0.00	100.84
WB164-Grt1-15	16013	-8896	37.55	0.09	20.50	0.02	32.93	1.04	2.62	6.29	0.00	0.00	101.05
WB164-Grt1-16	16063	-8907	37.46	0.10	20.51	0.02	33.04	1.10	2.55	6.15	0.00	0.00	100.93
WB164-Grt1-17	16113	-8907	37.48	0.11	20.44	0.02	32.98	1.15	2.51	6.13	0.00	0.01	100.83
WB164-Grt1-18	16163	-8892	37.47	0.09	20.44	0.02	32.28	1.19	2.48	6.64	0.00	0.00	100.60
WB164-Grt1-19	16213	-8892	37.48	0.13	20.53	0.00	32.30	1.10	2.58	6.78	0.00	0.00	100.90
WB164-Grt1-20	16263	-8898	37.63	0.09	20.58	0.02	32.42	1.22	2.60	6.30	0.00	0.00	100.85
WB164-Grt1-21	16313	-8898	37.69	0.09	20.55	0.00	33.03	1.15	2.68	5.95	0.00	0.00	101.14
WB164-Grt1-22	16363	-8901	37.46	0.09	20.72	0.01	33.19	1.09	2.70	6.15	0.00	0.00	101.40
WB164-Grt1-23	16413	-8887	37.65	0.10	20.63	0.02	32.83	0.99	2.67	6.22	0.00	0.00	101.12
WB164-Grt1-24	16463	-8887	37.70	0.13	20.51	0.01	32.25	0.96	2.64	6.79	0.00	0.00	100.99
WB164-Grt1-25	16513	-8887	37.57	0.12	20.67	0.00	32.34	0.93	2.66	6.73	0.00	0.00	101.03
WB164-Grt1-26	16563	-8887	37.52	0.14	20.67	0.02	32.73	0.89	2.61	6.57	0.00	0.00	101.14
WB164-Grt1-27	16613	-8887	37.59	0.10	20.69	0.00	33.23	0.93	2.66	6.08	0.00	0.00	101.27
WB164-Grt1-28	16663	-8887	37.54	0.12	20.68	0.00	33.04	0.94	2.72	6.05	0.00	0.00	101.09
WB164-Grt1-29	16713	-8887	37.63	0.13	20.78	0.00	33.11	0.96	2.72	6.14	0.00	0.00	101.47
WB164-Grt1-30	16763	-8888	37.66	0.11	20.83	0.01	32.74	1.10	2.78	6.01	0.00	0.00	101.24
WB164-Grt1-31	16813	-8888	37.79	0.06	20.71	0.01	32.83	1.06	2.86	5.92	0.00	0.00	101.24
WB164-Grt1-32	16863	-8873	37.81	0.07	20.95	0.00	32.72	1.08	2.98	5.64	0.00	0.00	101.26
WB164-Grt1-33	16913	-8895	37.59	0.07	20.77	0.00	33.48	1.02	2.97	5.40	0.00	0.00	101.31
WB164-Grt1-34	16963	-8907	37.84	0.04	20.84	0.01	33.18	1.00	2.91	5.72	0.00	0.01	101.54
WB164-Grt1-35	17013	-8915	38.25	0.08	20.74	0.00	32.28	1.05	3.07	6.36	0.00	0.00	101.82
WB164-Grt1-36	17063	-8934	38.24	0.06	20.90	0.00	31.02	1.04	2.99	7.41	0.00	0.01	101.65
WB164-Grt1-37	17113	-8934	38.48	0.09	20.84	0.01	30.78	1.00	3.43	6.99	0.00	0.00	101.60
WB164-Grt1-38	17163	-8972	38.77	0.06	20.75	0.04	29.92	0.84	3.51	7.53	0.00	0.00	101.42

WB164 Garnet-2	Coordinates		Weight Percent Oxides										
	X	Y	SiO ₂	TiO ₂	Al ₂ O ₃	Cr ₂ O ₃	FeO*	MnO	MgO	CaO	Na ₂ O	K ₂ O	Total
WB164-Grt2-1	10099	8195	38.51	0.03	21.30	0.00	29.08	0.88	4.09	7.36	0.00	0.00	101.24
WB164-Grt2-2	10131	8170	37.80	0.04	20.77	0.00	29.89	1.20	3.45	7.38	0.00	0.00	100.54
WB164-Grt2-3	10118	8145	37.56	0.06	20.91	0.02	30.13	1.41	3.53	7.22	0.00	0.00	100.84
WB164-Grt2-4	10118	8120	37.56	0.05	20.76	0.00	30.27	1.69	3.08	7.21	0.00	0.00	100.62
WB164-Grt2-5	10118	8095	37.21	0.07	20.51	0.00	29.40	3.04	2.51	7.45	0.00	0.00	100.20
WB164-Grt2-6	10118	8070	37.28	0.08	20.43	0.01	28.96	4.41	2.23	7.21	0.00	0.00	100.60
WB164-Grt2-7	10118	8045	37.20	0.13	20.39	0.00	27.98	5.16	2.18	7.32	0.00	0.00	100.36
WB164-Grt2-8	10100	8020	37.00	0.10	20.34	0.00	27.24	6.19	2.00	7.14	0.00	0.00	100.00
WB164-Grt2-9	10100	7995	36.85	0.15	20.33	0.01	26.80	6.92	1.90	7.24	0.00	0.00	100.21
WB164-Grt2-10	10100	7970	37.11	0.16	20.26	0.01	26.33	7.30	1.85	7.23	0.00	0.00	100.26
WB164-Grt2-11	10100	7945	37.09	0.13	20.30	0.00	26.48	7.07	2.04	7.20	0.00	0.00	100.31
WB164-Grt2-12	10100	7920	37.06	0.14	20.50	0.01	26.26	7.11	2.12	7.10	0.00	0.00	100.29
WB164-Grt2-13	10093	7887	37.33	0.25	20.47	0.00	27.03	6.48	2.46	6.65	0.00	0.00	100.66
WB164-Grt2-14	10077	7862	37.28	0.28	20.65	0.00	28.17	4.99	2.88	6.55	0.00	0.01	100.81
WB164-Grt2-15	10095	7837	37.11	0.14	20.50	0.02	27.56	5.87	2.25	6.86	0.00	0.00	100.31
WB164-Grt2-16	10095	7812	37.25	0.10	20.56	0.00	28.40	5.58	2.42	6.41	0.00	0.00	100.72
WB164-Grt2-17	10061	7787	37.37	0.18	20.48	0.00	28.47	4.77	2.46	7.05	0.00	0.00	100.78
WB164-Grt2-18	10058	7765	36.70	2.18	20.43	0.00	28.30	4.18	2.71	6.75	0.00	0.00	101.25
WB164-Grt2-19	10080	7740	37.25	0.20	20.61	0.00	28.83	4.23	2.73	6.65	0.00	0.00	100.51
WB164-Grt2-20	10080	7715	37.27	0.21	20.49	0.00	29.32	3.69	2.61	6.94	0.00	0.00	100.53
WB164-Grt2-21	10080	7690	37.47	0.11	20.75	0.01	29.50	3.24	2.65	7.04	0.00	0.01	100.78
WB164-Grt2-22	10080	7665	37.51	0.09	20.69	0.00	29.49	2.85	2.86	7.14	0.00	0.00	100.62
WB164-Grt2-23	10080	7640	37.54	0.06	20.80	0.00	29.31	2.39	3.50	7.04	0.00	0.00	100.65
WB164-Grt2-24	10080	7615	37.58	0.08	20.92	0.00	29.32	1.65	3.47	7.55	0.00	0.01	100.60
WB164-Grt2-25	10097	7590	37.74	0.03	21.10	0.01	29.08	1.18	4.16	7.32	0.00	0.00	100.63

WB164 Garnet-3	Coordinates		Weight Percent Oxides										
	X	Y	SiO ₂	TiO ₂	Al ₂ O ₃	Cr ₂ O ₃	FeO*	MnO	MgO	CaO	Na ₂ O	K ₂ O	Total
WB164-Grt3-1	9335	5137	37.31	0.05	21.15	0.00	29.11	1.02	4.30	7.33	0.00	0.00	100.26
WB164-Grt3-2	9361	5137	37.26	0.08	20.90	0.00	30.06	1.11	3.41	7.39	0.00	0.00	100.21
WB164-Grt3-3	9386	5137	37.00	0.08	20.80	0.00	30.51	1.32	3.14	7.12	0.00	0.01	99.97
WB164-Grt3-4	9411	5137	37.10	0.11	20.62	0.01	30.20	1.80	3.08	7.07	0.00	0.00	99.99
WB164-Grt3-5	9436	5137	36.83	0.10	20.55	0.01	30.09	2.38	2.64	7.17	0.00	0.00	99.76
WB164-Grt3-6	9461	5137	36.94	0.10	20.54	0.01	29.57	3.22	2.53	7.15	0.00	0.00	100.06
WB164-Grt3-7	9486	5137	36.93	0.10	20.51	0.00	28.92	3.93	2.53	7.11	0.00	0.00	100.02
WB164-Grt3-8	9511	5168	36.95	0.05	20.41	0.01	27.14	5.47	2.42	7.43	0.00	0.00	99.88
WB164-Grt3-9	9536	5147	37.23	0.04	20.54	0.00	27.44	5.97	2.50	6.99	0.00	0.00	100.72
WB164-Grt3-10	9561	5147	36.91	0.16	20.32	0.00	25.25	8.19	1.69	7.76	0.00	0.00	100.29
WB164-Grt3-11	9581	5151	37.10	0.16	20.37	0.02	24.85	8.47	1.62	7.87	0.00	0.00	100.45
WB164-Grt3-12	9610	5151	37.05	0.21	20.26	0.01	26.03	6.90	2.11	7.70	0.00	0.00	100.27
WB164-Grt3-13	9635	5186	37.19	0.26	20.33	0.02	25.99	6.56	2.17	7.80	0.00	0.00	100.32
WB164-Grt3-14	9663	5184	37.29	0.16	20.28	0.00	26.99	6.03	2.35	7.18	0.00	0.00	100.27
WB164-Grt3-15	9688	5184	37.46	0.12	20.43	0.00	27.80	4.63	2.55	7.61	0.00	0.00	100.60
WB164-Grt3-16	9713	5184	37.20	0.12	20.47	0.00	28.27	4.31	2.48	7.21	0.00	0.00	100.06
WB164-Grt3-17	9738	5184	37.38	0.09	20.36	0.00	29.09	3.80	2.45	7.41	0.00	0.00	100.58
WB164-Grt3-18	9763	5184	37.33	0.08	20.62	0.01	29.76	3.20	2.59	7.22	0.00	0.01	100.82
WB164-Grt3-19	9788	5174	37.70	0.07	20.68	0.01	30.12	2.00	2.82	7.40	0.00	0.00	100.80
WB164-Grt3-20	9813	5174	37.70	0.06	20.74	0.00	30.66	1.27	3.03	7.35	0.00	0.00	100.83
WB164-Grt3-21	9838	5174	37.81	0.05	20.94	0.00	30.37	0.93	3.32	7.49	0.00	0.00	100.90
WB164-Grt3-22	9859	5190	37.88	0.04	20.78	0.00	30.04	0.78	3.55	7.43	0.00	0.01	100.53

WB164 Garnet-1	Atoms per 12 Oxygen										
	Si	Ti	Al	Cr	Fe	Mn	Mg	Ca	Na	K	Sum
WB164-Grt1-1	2.960	0.002	1.972	0.000	1.984	0.072	0.429	0.632	0.000	0.001	8.052
WB164-Grt1-2	2.977	0.005	1.951	0.001	2.056	0.061	0.398	0.594	0.000	0.000	8.043
WB164-Grt1-3	2.986	0.004	1.937	0.000	2.111	0.072	0.349	0.581	0.000	0.001	8.041
WB164-Grt1-4	2.984	0.005	1.939	0.000	2.223	0.064	0.354	0.473	0.000	0.001	8.042
WB164-Grt1-5	2.970	0.004	1.955	0.000	2.225	0.068	0.346	0.480	0.000	0.000	8.049
WB164-Grt1-6	2.969	0.004	1.955	0.000	2.199	0.071	0.343	0.509	0.000	0.001	8.051
WB164-Grt1-7	2.970	0.004	1.944	0.001	2.204	0.071	0.357	0.502	0.000	0.001	8.053
WB164-Grt1-8	2.977	0.006	1.944	0.000	2.185	0.071	0.357	0.505	0.000	0.000	8.046
WB164-Grt1-9	2.971	0.004	1.956	0.001	2.204	0.069	0.394	0.448	0.000	0.000	8.046
WB164-Grt1-10	2.989	0.005	1.931	0.001	2.169	0.065	0.362	0.520	0.000	0.000	8.041
WB164-Grt1-11	2.974	0.005	1.949	0.001	2.196	0.068	0.354	0.501	0.000	0.000	8.047
WB164-Grt1-12	2.982	0.006	1.930	0.000	2.202	0.065	0.340	0.522	0.000	0.001	8.047
WB164-Grt1-13	2.997	0.005	1.926	0.001	2.199	0.060	0.319	0.527	0.000	0.000	8.034
WB164-Grt1-14	2.978	0.006	1.941	0.001	2.190	0.072	0.315	0.541	0.000	0.000	8.045
WB164-Grt1-15	2.993	0.005	1.925	0.002	2.195	0.071	0.312	0.537	0.000	0.000	8.039
WB164-Grt1-16	2.991	0.006	1.930	0.002	2.206	0.075	0.303	0.527	0.000	0.000	8.038
WB164-Grt1-17	2.996	0.006	1.926	0.002	2.204	0.078	0.299	0.525	0.000	0.001	8.035
WB164-Grt1-18	2.997	0.005	1.927	0.001	2.159	0.081	0.296	0.569	0.000	0.000	8.034
WB164-Grt1-19	2.989	0.008	1.929	0.000	2.154	0.074	0.306	0.579	0.000	0.000	8.039
WB164-Grt1-20	2.999	0.006	1.933	0.001	2.161	0.082	0.309	0.538	0.000	0.000	8.029
WB164-Grt1-21	2.999	0.005	1.927	0.000	2.198	0.078	0.317	0.508	0.000	0.000	8.032
WB164-Grt1-22	2.977	0.005	1.941	0.000	2.206	0.073	0.320	0.523	0.000	0.000	8.047
WB164-Grt1-23	2.995	0.006	1.934	0.001	2.184	0.067	0.316	0.530	0.000	0.000	8.032
WB164-Grt1-24	2.999	0.008	1.923	0.001	2.146	0.065	0.313	0.579	0.000	0.000	8.032
WB164-Grt1-25	2.988	0.007	1.937	0.000	2.151	0.063	0.315	0.574	0.000	0.000	8.036
WB164-Grt1-26	2.985	0.008	1.938	0.001	2.177	0.060	0.310	0.560	0.000	0.000	8.038
WB164-Grt1-27	2.988	0.006	1.938	0.000	2.209	0.063	0.315	0.518	0.000	0.000	8.037
WB164-Grt1-28	2.987	0.007	1.940	0.000	2.199	0.063	0.323	0.516	0.000	0.000	8.036
WB164-Grt1-29	2.984	0.008	1.942	0.000	2.196	0.065	0.321	0.522	0.000	0.000	8.037
WB164-Grt1-30	2.989	0.007	1.948	0.000	2.173	0.074	0.329	0.511	0.000	0.000	8.030
WB164-Grt1-31	2.998	0.004	1.937	0.001	2.178	0.071	0.338	0.503	0.000	0.000	8.030
WB164-Grt1-32	2.994	0.004	1.955	0.000	2.167	0.073	0.352	0.479	0.000	0.000	8.024
WB164-Grt1-33	2.986	0.004	1.944	0.000	2.224	0.069	0.352	0.460	0.000	0.000	8.038
WB164-Grt1-34	2.994	0.002	1.944	0.000	2.196	0.067	0.343	0.485	0.000	0.001	8.032
WB164-Grt1-35	3.009	0.005	1.923	0.000	2.123	0.070	0.360	0.536	0.000	0.000	8.025
WB164-Grt1-36	3.005	0.003	1.935	0.000	2.038	0.069	0.350	0.624	0.000	0.001	8.025
WB164-Grt1-37	3.016	0.005	1.925	0.000	2.017	0.066	0.401	0.587	0.000	0.000	8.017
WB164-Grt1-38	3.033	0.003	1.913	0.003	1.958	0.056	0.410	0.631	0.000	0.000	8.006

WB164 Garnet-2	Atoms per 12 Oxygen										
	Si	Ti	Al	Cr	Fe	Mn	Mg	Ca	Na	K	Sum
WB164-Grt2-1	3.005	0.002	1.959	0.000	1.898	0.058	0.476	0.615	0.000	0.000	8.014
WB164-Grt2-2	2.995	0.002	1.940	0.000	1.980	0.081	0.408	0.627	0.000	0.000	8.033
WB164-Grt2-3	2.973	0.004	1.950	0.001	1.995	0.095	0.417	0.613	0.000	0.000	8.047
WB164-Grt2-4	2.986	0.003	1.945	0.000	2.013	0.114	0.365	0.614	0.000	0.000	8.039
WB164-Grt2-5	2.983	0.004	1.938	0.000	1.971	0.207	0.300	0.640	0.000	0.000	8.044
WB164-Grt2-6	2.986	0.005	1.929	0.000	1.940	0.299	0.266	0.619	0.000	0.000	8.044
WB164-Grt2-7	2.986	0.008	1.929	0.000	1.878	0.351	0.261	0.630	0.000	0.000	8.042
WB164-Grt2-8	2.985	0.006	1.933	0.000	1.837	0.423	0.240	0.617	0.000	0.000	8.042
WB164-Grt2-9	2.973	0.009	1.933	0.000	1.808	0.473	0.228	0.626	0.000	0.000	8.051
WB164-Grt2-10	2.989	0.010	1.923	0.000	1.773	0.498	0.222	0.624	0.000	0.001	8.040
WB164-Grt2-11	2.984	0.008	1.925	0.000	1.782	0.482	0.245	0.620	0.000	0.000	8.046
WB164-Grt2-12	2.978	0.009	1.942	0.000	1.765	0.484	0.254	0.611	0.000	0.000	8.043
WB164-Grt2-13	2.984	0.015	1.929	0.000	1.807	0.439	0.293	0.570	0.000	0.000	8.036
WB164-Grt2-14	2.971	0.017	1.940	0.000	1.878	0.337	0.342	0.559	0.000	0.001	8.043
WB164-Grt2-15	2.981	0.008	1.940	0.002	1.851	0.399	0.269	0.591	0.000	0.000	8.040
WB164-Grt2-16	2.981	0.006	1.939	0.000	1.901	0.378	0.289	0.549	0.000	0.000	8.044
WB164-Grt2-17	2.984	0.011	1.928	0.000	1.901	0.322	0.293	0.603	0.000	0.000	8.041
WB164-Grt2-18	2.912	0.130	1.910	0.000	1.878	0.281	0.320	0.573	0.000	0.000	8.003
WB164-Grt2-19	2.977	0.012	1.941	0.000	1.927	0.287	0.325	0.570	0.000	0.000	8.040
WB164-Grt2-20	2.980	0.013	1.932	0.000	1.961	0.250	0.311	0.595	0.000	0.000	8.041
WB164-Grt2-21	2.983	0.007	1.948	0.001	1.964	0.219	0.315	0.601	0.000	0.001	8.036
WB164-Grt2-22	2.987	0.005	1.942	0.000	1.964	0.192	0.339	0.609	0.000	0.000	8.038
WB164-Grt2-23	2.978	0.004	1.945	0.000	1.945	0.161	0.414	0.599	0.000	0.000	8.045
WB164-Grt2-24	2.977	0.005	1.954	0.000	1.943	0.110	0.410	0.641	0.000	0.001	8.042
WB164-Grt2-25	2.976	0.002	1.960	0.001	1.917	0.079	0.489	0.619	0.000	0.000	8.042

WB164 Garnet-3	Atoms per 12 Oxygen										Sum
	Si	Ti	Al	Cr	Fe	Mn	Mg	Ca	Na	K	
WB164-Grt3-1	2.955	0.003	1.973	0.000	1.928	0.068	0.507	0.622	0.000	0.000	8.056
WB164-Grt3-2	2.968	0.005	1.962	0.000	2.002	0.075	0.405	0.631	0.000	0.000	8.047
WB164-Grt3-3	2.964	0.005	1.963	0.000	2.044	0.090	0.375	0.611	0.000	0.001	8.051
WB164-Grt3-4	2.973	0.007	1.947	0.001	2.023	0.122	0.368	0.607	0.000	0.000	8.047
WB164-Grt3-5	2.968	0.006	1.952	0.001	2.027	0.163	0.317	0.619	0.000	0.000	8.051
WB164-Grt3-6	2.970	0.006	1.947	0.000	1.988	0.220	0.303	0.616	0.000	0.000	8.050
WB164-Grt3-7	2.971	0.006	1.945	0.000	1.946	0.268	0.303	0.613	0.000	0.000	8.051
WB164-Grt3-8	2.977	0.003	1.937	0.001	1.828	0.373	0.290	0.641	0.000	0.000	8.051
WB164-Grt3-9	2.977	0.002	1.936	0.000	1.835	0.405	0.298	0.599	0.000	0.000	8.053
WB164-Grt3-10	2.975	0.010	1.930	0.000	1.702	0.559	0.203	0.670	0.000	0.000	8.050
WB164-Grt3-11	2.982	0.010	1.930	0.001	1.671	0.577	0.195	0.678	0.000	0.000	8.043
WB164-Grt3-12	2.979	0.012	1.920	0.001	1.750	0.470	0.253	0.663	0.000	0.001	8.049
WB164-Grt3-13	2.983	0.016	1.922	0.001	1.743	0.446	0.259	0.670	0.000	0.000	8.040
WB164-Grt3-14	2.992	0.010	1.918	0.000	1.812	0.410	0.281	0.617	0.000	0.000	8.039
WB164-Grt3-15	2.990	0.007	1.922	0.000	1.856	0.313	0.303	0.651	0.000	0.000	8.042
WB164-Grt3-16	2.986	0.008	1.937	0.000	1.898	0.293	0.297	0.620	0.000	0.000	8.038
WB164-Grt3-17	2.990	0.005	1.920	0.000	1.946	0.257	0.292	0.635	0.000	0.000	8.045
WB164-Grt3-18	2.977	0.005	1.938	0.001	1.985	0.216	0.308	0.617	0.000	0.001	8.049
WB164-Grt3-19	2.995	0.004	1.935	0.001	2.001	0.135	0.334	0.629	0.000	0.000	8.034
WB164-Grt3-20	2.991	0.004	1.939	0.000	2.034	0.085	0.358	0.625	0.000	0.000	8.036
WB164-Grt3-21	2.988	0.003	1.950	0.000	2.007	0.062	0.391	0.634	0.000	0.000	8.034
WB164-Grt3-22	2.998	0.002	1.938	0.000	1.989	0.053	0.419	0.630	0.000	0.001	8.030

WB164 Garnet-1	K Numbers (=Ix/Istd)									
	Na	Mg	Al	Si	K	Ca	Ti	Cr	Mn	Fe
WB164-Grt1-1	0.0000	0.0446	0.8613	0.8658	0.0005	0.2129	0.0010	0.0000	0.0282	1.0023
WB164-Grt1-2	0.0000	0.0408	0.8433	0.8637	0.0002	0.1987	0.0020	0.0003	0.0238	1.0318
WB164-Grt1-3	0.0000	0.0358	0.8433	0.8746	0.0005	0.1962	0.0019	0.0000	0.0285	1.0693
WB164-Grt1-4	0.0000	0.0357	0.8309	0.8626	0.0005	0.1584	0.0020	0.0000	0.0253	1.1190
WB164-Grt1-5	0.0000	0.0349	0.8401	0.8603	0.0002	0.1612	0.0018	0.0001	0.0269	1.1232
WB164-Grt1-6	0.0000	0.0348	0.8427	0.8617	0.0009	0.1713	0.0017	0.0001	0.0278	1.1103
WB164-Grt1-7	0.0000	0.0361	0.8352	0.8602	0.0003	0.1685	0.0018	0.0002	0.0278	1.1105
WB164-Grt1-8	0.0000	0.0362	0.8379	0.8643	0.0003	0.1699	0.0025	0.0000	0.0280	1.1031
WB164-Grt1-9	0.0000	0.0400	0.8408	0.8603	0.0000	0.1505	0.0016	0.0002	0.0271	1.1132
WB164-Grt1-10	0.0000	0.0368	0.8335	0.8697	0.0000	0.1747	0.0020	0.0001	0.0256	1.0956
WB164-Grt1-11	0.0000	0.0359	0.8402	0.8636	0.0000	0.1686	0.0020	0.0002	0.0268	1.1093
WB164-Grt1-12	0.0000	0.0345	0.8325	0.8675	0.0006	0.1757	0.0028	0.0000	0.0255	1.1124
WB164-Grt1-13	0.0000	0.0323	0.8321	0.8730	0.0000	0.1773	0.0023	0.0002	0.0236	1.1112
WB164-Grt1-14	0.0000	0.0319	0.8377	0.8661	0.0000	0.1820	0.0028	0.0002	0.0283	1.1052
WB164-Grt1-15	0.0000	0.0316	0.8329	0.8732	0.0000	0.1810	0.0024	0.0003	0.0278	1.1103
WB164-Grt1-16	0.0000	0.0307	0.8327	0.8705	0.0002	0.1771	0.0025	0.0003	0.0294	1.1143
WB164-Grt1-17	0.0000	0.0302	0.8303	0.8714	0.0004	0.1763	0.0028	0.0003	0.0308	1.1122
WB164-Grt1-18	0.0000	0.0300	0.8325	0.8723	0.0001	0.1909	0.0022	0.0002	0.0317	1.0876
WB164-Grt1-19	0.0000	0.0312	0.8362	0.8727	0.0002	0.1949	0.0034	0.0000	0.0292	1.0882
WB164-Grt1-20	0.0000	0.0314	0.8374	0.8752	0.0002	0.1811	0.0024	0.0002	0.0325	1.0926
WB164-Grt1-21	0.0000	0.0323	0.8343	0.8759	0.0000	0.1713	0.0023	0.0000	0.0307	1.1139
WB164-Grt1-22	0.0000	0.0326	0.8409	0.8699	0.0000	0.1769	0.0024	0.0001	0.0291	1.1195
WB164-Grt1-23	0.0000	0.0322	0.8389	0.8753	0.0000	0.1789	0.0026	0.0002	0.0264	1.1069
WB164-Grt1-24	0.0000	0.0319	0.8359	0.8783	0.0000	0.1952	0.0034	0.0002	0.0255	1.0862
WB164-Grt1-25	0.0000	0.0322	0.8421	0.8745	0.0002	0.1936	0.0032	0.0000	0.0247	1.0893
WB164-Grt1-26	0.0000	0.0315	0.8412	0.8727	0.0001	0.1889	0.0036	0.0002	0.0238	1.1029
WB164-Grt1-27	0.0000	0.0320	0.8402	0.8731	0.0001	0.1748	0.0025	0.0000	0.0248	1.1207
WB164-Grt1-28	0.0000	0.0329	0.8399	0.8717	0.0000	0.1740	0.0031	0.0000	0.0251	1.1141
WB164-Grt1-29	0.0000	0.0328	0.8442	0.8741	0.0000	0.1766	0.0034	0.0000	0.0256	1.1167
WB164-Grt1-30	0.0000	0.0336	0.8466	0.8745	0.0000	0.1727	0.0030	0.0001	0.0292	1.1038
WB164-Grt1-31	0.0000	0.0346	0.8414	0.8777	0.0000	0.1702	0.0017	0.0001	0.0282	1.1067
WB164-Grt1-32	0.0000	0.0361	0.8511	0.8771	0.0002	0.1622	0.0018	0.0000	0.0288	1.1033
WB164-Grt1-33	0.0000	0.0358	0.8409	0.8709	0.0002	0.1553	0.0019	0.0000	0.0273	1.1300
WB164-Grt1-34	0.0000	0.0351	0.8460	0.8780	0.0005	0.1645	0.0010	0.0001	0.0266	1.1192
WB164-Grt1-35	0.0000	0.0372	0.8449	0.8904	0.0000	0.1826	0.0021	0.0000	0.0279	1.0872
WB164-Grt1-36	0.0000	0.0365	0.8561	0.8927	0.0006	0.2127	0.0015	0.0000	0.0277	1.0428
WB164-Grt1-37	0.0000	0.0421	0.8525	0.8974	0.0000	0.2003	0.0023	0.0001	0.0264	1.0344
WB164-Grt1-38	0.0000	0.0434	0.8519	0.9065	0.0002	0.2155	0.0015	0.0006	0.0222	1.0042

WB164 Garnet-2	K Numbers (=Ix/Istd)									
	Na	Mg	Al	Si	K	Ca	Ti	Cr	Mn	Fe
WB164-Grt2-1	0.0000	0.0509	0.8753	0.8971	0.0000	0.2103	0.0007	0.0000	0.0232	0.9748
WB164-Grt2-2	0.0000	0.0425	0.8507	0.8809	0.0000	0.2116	0.0010	0.0000	0.0319	1.0036
WB164-Grt2-3	0.0000	0.0434	0.8543	0.8739	0.0000	0.2072	0.0016	0.0002	0.0374	1.0124
WB164-Grt2-4	0.0000	0.0377	0.8489	0.8750	0.0000	0.2070	0.0013	0.0000	0.0448	1.0178
WB164-Grt2-5	0.0000	0.0306	0.8399	0.8688	0.0002	0.2144	0.0017	0.0000	0.0808	0.9893
WB164-Grt2-6	0.0000	0.0270	0.8366	0.8716	0.0001	0.2076	0.0022	0.0001	0.1171	0.9758
WB164-Grt2-7	0.0000	0.0265	0.8366	0.8707	0.0000	0.2110	0.0033	0.0000	0.1370	0.9425
WB164-Grt2-8	0.0000	0.0242	0.8345	0.8662	0.0000	0.2059	0.0027	0.0000	0.1643	0.9181
WB164-Grt2-9	0.0000	0.0230	0.8345	0.8632	0.0000	0.2090	0.0039	0.0001	0.1838	0.9040
WB164-Grt2-10	0.0000	0.0225	0.8327	0.8706	0.0004	0.2088	0.0042	0.0001	0.1938	0.8879
WB164-Grt2-11	0.0000	0.0248	0.8337	0.8693	0.0000	0.2077	0.0033	0.0000	0.1875	0.8928
WB164-Grt2-12	0.0000	0.0258	0.8422	0.8677	0.0000	0.2048	0.0037	0.0001	0.1886	0.8852
WB164-Grt2-13	0.0000	0.0299	0.8387	0.8729	0.0001	0.1918	0.0065	0.0000	0.1720	0.9112
WB164-Grt2-14	0.0000	0.0350	0.8443	0.8694	0.0005	0.1885	0.0073	0.0000	0.1326	0.9493
WB164-Grt2-15	0.0000	0.0273	0.8403	0.8675	0.0000	0.1979	0.0037	0.0003	0.1559	0.9289
WB164-Grt2-16	0.0000	0.0294	0.8403	0.8693	0.0000	0.1847	0.0026	0.0000	0.1483	0.9581
WB164-Grt2-17	0.0000	0.0299	0.8388	0.8736	0.0000	0.2030	0.0048	0.0000	0.1265	0.9593
WB164-Grt2-18	0.0000	0.0329	0.8356	0.8585	0.0001	0.1948	0.0575	0.0000	0.1108	0.9529
WB164-Grt2-19	0.0000	0.0332	0.8423	0.8685	0.0003	0.1915	0.0054	0.0000	0.1124	0.9713
WB164-Grt2-20	0.0000	0.0317	0.8378	0.8696	0.0000	0.1998	0.0056	0.0000	0.0979	0.9873
WB164-Grt2-21	0.0000	0.0323	0.8497	0.8741	0.0004	0.2025	0.0029	0.0001	0.0860	0.9932
WB164-Grt2-22	0.0000	0.0349	0.8470	0.8749	0.0001	0.2053	0.0023	0.0000	0.0755	0.9923
WB164-Grt2-23	0.0000	0.0429	0.8502	0.8739	0.0000	0.2022	0.0017	0.0000	0.0635	0.9853
WB164-Grt2-24	0.0000	0.0428	0.8576	0.8757	0.0009	0.2166	0.0021	0.0000	0.0436	0.9845
WB164-Grt2-25	0.0000	0.0516	0.8637	0.8775	0.0000	0.2096	0.0007	0.0002	0.0312	0.9753

WB164 Garnet-3	K Numbers (=Ix/Istd)									
	Na	Mg	Al	Si	K	Ca	Ti	Cr	Mn	Fe
WB164-Grt3-1	0.0000	0.0533	0.8646	0.8659	0.0000	0.2097	0.0013	0.0000	0.0270	0.9763
WB164-Grt3-2	0.0000	0.0418	0.8548	0.8666	0.0000	0.2121	0.0021	0.0000	0.0295	1.0094
WB164-Grt3-3	0.0000	0.0383	0.8490	0.8599	0.0004	0.2045	0.0020	0.0000	0.0351	1.0256
WB164-Grt3-4	0.0000	0.0376	0.8420	0.8632	0.0000	0.2030	0.0028	0.0001	0.0477	1.0155
WB164-Grt3-5	0.0000	0.0320	0.8396	0.8576	0.0000	0.2062	0.0025	0.0001	0.0633	1.0124
WB164-Grt3-6	0.0000	0.0308	0.8399	0.8612	0.0000	0.2057	0.0027	0.0001	0.0856	0.9954
WB164-Grt3-7	0.0000	0.0307	0.8388	0.8613	0.0000	0.2046	0.0027	0.0000	0.1044	0.9740
WB164-Grt3-8	0.0000	0.0295	0.8375	0.8643	0.0000	0.2140	0.0014	0.0001	0.1452	0.9136
WB164-Grt3-9	0.0000	0.0304	0.8415	0.8702	0.0000	0.2015	0.0010	0.0000	0.1586	0.9250
WB164-Grt3-10	0.0000	0.0205	0.8373	0.8674	0.0002	0.2240	0.0043	0.0000	0.2173	0.8514
WB164-Grt3-11	0.0000	0.0198	0.8409	0.8728	0.0000	0.2274	0.0042	0.0002	0.2245	0.8376
WB164-Grt3-12	0.0000	0.0257	0.8336	0.8694	0.0004	0.2221	0.0054	0.0001	0.1828	0.8769
WB164-Grt3-13	0.0000	0.0265	0.8376	0.8731	0.0003	0.2247	0.0069	0.0003	0.1738	0.8748
WB164-Grt3-14	0.0000	0.0286	0.8323	0.8733	0.0000	0.2068	0.0042	0.0000	0.1600	0.9093
WB164-Grt3-15	0.0000	0.0311	0.8387	0.8771	0.0000	0.2190	0.0032	0.0000	0.1228	0.9356
WB164-Grt3-16	0.0000	0.0303	0.8392	0.8691	0.0001	0.2075	0.0033	0.0000	0.1143	0.9516
WB164-Grt3-17	0.0000	0.0298	0.8338	0.8741	0.0000	0.2134	0.0023	0.0000	0.1008	0.9795
WB164-Grt3-18	0.0000	0.0315	0.8433	0.8711	0.0009	0.2078	0.0021	0.0002	0.0851	1.0021
WB164-Grt3-19	0.0000	0.0344	0.8468	0.8800	0.0000	0.2125	0.0017	0.0002	0.0531	1.0130
WB164-Grt3-20	0.0000	0.0370	0.8486	0.8789	0.0000	0.2111	0.0017	0.0000	0.0337	1.0308
WB164-Grt3-21	0.0000	0.0407	0.8576	0.8811	0.0001	0.2148	0.0013	0.0000	0.0246	1.0200
WB164-Grt3-22	0.0000	0.0438	0.8509	0.8827	0.0004	0.2130	0.0011	0.0000	0.0208	1.0084

Pre-run Standards		Coordinates		Weight Percent Oxides									
Standard Name	X	Y	SiO₂	TiO₂	Al₂O₃	Cr₂O₃	FeO*	MnO	MgO	CaO	Na₂O	K₂O	Total
AMAB-1	7906	-19038	68.29	0.00	19.79	0.00	0.00	0.00	0.01	0.26	11.58	0.23	100.17
AMAB-2	7885	-18937	68.34	0.00	19.87	0.00	0.01	0.01	0.00	0.26	11.42	0.23	100.15
AMAB-3	7661	-18871	67.88	0.00	19.75	0.00	0.00	0.01	0.00	0.24	11.29	0.19	99.35
AMAB-4	7432	-18871	69.52	0.00	19.95	0.01	0.00	0.00	0.00	0.22	11.69	0.18	101.58
PHLSY-1	10010	-24052	43.74	0.03	11.48	0.00	0.05	0.01	27.64	0.00	0.00	11.05	94.00
PHLSY-2	10017	-24094	44.03	0.02	11.31	0.01	0.05	0.01	27.82	0.00	0.01	10.93	94.19
PHLSY-3	10783	-23814	42.89	0.02	12.19	0.00	0.02	0.00	27.88	0.00	0.00	11.16	94.18
PHLSY-4	10791	-23894	43.14	0.01	12.09	0.00	0.00	0.03	27.92	0.00	0.01	11.04	94.24
CLAB-1	15057	-16756	53.57	0.07	28.97	0.00	0.36	0.00	0.10	11.93	4.63	0.28	99.92
CLAB-2	15085	-16632	53.40	0.08	29.13	0.01	0.34	0.01	0.10	11.89	4.54	0.28	99.78
CLAB-3	15085	-16514	53.23	0.06	29.24	0.00	0.40	0.01	0.10	11.91	4.58	0.29	99.82
CLAB-4	14890	-16208	53.44	0.08	29.62	0.00	0.35	0.01	0.10	11.93	4.54	0.29	100.36
CLAB-5	14856	-16048	53.49	0.06	29.56	0.01	0.34	0.00	0.11	11.96	4.56	0.29	100.38
SGKF-1	16236	-19201	64.87	0.00	18.41	0.00	0.01	0.00	0.01	0.00	1.27	14.74	99.30
SGKF-2	16236	-19138	64.91	0.00	18.45	0.00	0.00	0.01	0.01	0.01	1.27	14.79	99.45
SGKF-3	16302	-19052	65.17	0.00	18.64	0.00	0.01	0.01	0.01	0.01	1.27	14.81	99.93
SGKF-4	16410	-19052	64.78	0.01	18.55	0.00	0.02	0.00	0.00	0.01	1.25	14.81	99.43
TTNG-1	18703	-28352	30.64	40.07	0.01	0.02	0.04	0.00	0.00	28.11	0.04	0.05	98.97
TTNG-2	18793	-28352	30.44	39.67	0.01	0.00	0.06	0.00	0.00	27.83	0.03	0.05	98.09
TTNG-3	18751	-28202	30.65	40.40	0.00	0.00	0.07	0.00	0.00	28.16	0.02	0.03	99.33
TTNG-4	18723	-28115	30.69	40.45	0.01	0.00	0.06	0.00	0.00	28.19	0.03	0.05	99.48
MGCR-1	14909	-30637	0.03	0.02	0.08	54.57	0.05	0.00	21.23	0.01	0.00	0.00	75.99
MGCR-2	14909	-30496	0.04	0.01	0.10	54.50	0.07	0.00	21.46	0.00	0.00	0.00	76.18
MGCR-3	14791	-30419	0.02	0.00	0.09	54.41	0.07	0.00	21.14	0.00	0.00	0.00	75.74
MGCR-4	14772	-30546	0.02	0.01	0.09	54.47	0.07	0.00	21.07	0.01	0.00	0.00	75.73
RDN-1	14541	-21313	46.56	0.01	0.01	0.01	13.12	35.98	0.26	4.30	0.00	0.00	100.26
RDN-2	14488	-21313	46.64	0.00	0.03	0.00	12.97	35.80	0.26	4.36	0.00	0.00	100.08
RDN-3	14475	-21208	46.47	0.00	0.01	0.00	13.20	36.11	0.25	4.23	0.00	0.00	100.27
RDN-4	14582	-21173	46.34	0.02	0.03	0.00	13.15	35.93	0.23	4.23	0.00	0.00	99.94
AUGL-1	9244	-21556	48.16	0.41	0.73	0.01	29.62	0.74	1.23	20.01	0.20	0.00	101.09
AUGL-2	9244	-21561	48.01	0.37	0.76	0.00	29.69	0.69	1.20	19.84	0.22	0.00	100.78
AUGL-3	9244	-21566	48.04	0.35	0.71	0.00	30.06	0.71	1.22	19.79	0.20	0.01	101.08
AUGL-4	9244	-21581	48.13	0.34	0.66	0.01	30.15	0.73	1.21	19.20	0.18	0.00	100.61

Pre-run Standards		10 Oxygen + 2(OH) basis					Atomic per Formula Unit				
Standard Name	Si	Ti	Al	Cr	Fe	Mn	Mg	Ca	Na	K	Sum
AMAB-1	4.100	0.000	1.401	0.000	0.000	0.000	0.001	0.016	1.348	0.018	6.883
AMAB-2	4.101	0.000	1.405	0.000	0.001	0.001	0.000	0.017	1.329	0.018	6.870
AMAB-3	4.103	0.000	1.407	0.000	0.000	0.000	0.000	0.016	1.323	0.015	6.862
AMAB-4	4.111	0.000	1.391	0.001	0.000	0.000	0.000	0.014	1.341	0.014	6.871
PHLSY-1	3.082	0.001	0.953	0.000	0.003	0.001	2.903	0.000	0.000	0.994	7.937
PHLSY-2	3.093	0.001	0.937	0.001	0.003	0.001	2.913	0.000	0.001	0.980	7.928
PHLSY-3	3.023	0.001	1.013	0.000	0.001	0.000	2.929	0.000	0.001	1.004	7.972
PHLSY-4	3.035	0.001	1.003	0.000	0.000	0.002	2.928	0.000	0.001	0.991	7.960
CLAB-1	3.341	0.003	2.129	0.000	0.019	0.000	0.009	0.797	0.560	0.022	6.882
CLAB-2	3.334	0.004	2.143	0.001	0.018	0.001	0.010	0.795	0.550	0.023	6.877
CLAB-3	3.325	0.003	2.152	0.000	0.021	0.000	0.010	0.797	0.554	0.023	6.885
CLAB-4	3.318	0.004	2.167	0.000	0.018	0.001	0.009	0.794	0.546	0.023	6.880
CLAB-5	3.320	0.003	2.163	0.001	0.018	0.000	0.010	0.796	0.549	0.023	6.882
SGKF-1	4.126	0.000	1.380	0.000	0.000	0.000	0.001	0.000	0.156	1.196	6.860
SGKF-2	4.124	0.000	1.382	0.000	0.000	0.000	0.001	0.001	0.157	1.198	6.863
SGKF-3	4.120	0.000	1.389	0.000	0.000	0.001	0.001	0.001	0.155	1.194	6.861
SGKF-4	4.118	0.000	1.390	0.000	0.001	0.000	0.000	0.001	0.155	1.201	6.865
TTNG-1	2.221	2.184	0.001	0.002	0.003	0.000	0.000	2.183	0.006	0.004	6.602
TTNG-2	2.225	2.180	0.001	0.000	0.003	0.000	0.000	2.180	0.005	0.005	6.599
TTNG-3	2.213	2.194	0.000	0.000	0.004	0.000	0.000	2.179	0.003	0.003	6.596
TTNG-4	2.213	2.193	0.001	0.000	0.003	0.000	0.000	2.178	0.005	0.004	6.598
MGCR-1	0.009	0.004	0.031	21.737	0.016	0.000	10.906	0.005	0.000	0.000	32.708
MGCR-2	0.014	0.003	0.039	21.436	0.020	0.000	10.887	0.001	0.000	0.000	32.400
MGCR-3	0.007	0.001	0.039	21.761	0.021	0.000	10.906	0.001	0.000	0.000	32.734
MGCR-4	0.006	0.004	0.035	21.855	0.019	0.000	10.906	0.003	0.000	0.000	32.828
RDN-1	3.669	0.001	0.001	0.001	0.865	2.402	0.031	0.363	0.000	0.000	7.331
RDN-2	3.676	0.000	0.003	0.000	0.855	2.390	0.031	0.368	0.000	0.000	7.323
RDN-3	3.664	0.000	0.001	0.000	0.871	2.412	0.030	0.357	0.000	0.000	7.335
RDN-4	3.665	0.001	0.003	0.000	0.870	2.407	0.027	0.359	0.000	0.000	7.332
AUGI-1	3.602	0.023	0.064	0.001	1.853	0.047	0.137	1.603	0.029	0.000	7.359
AUGI-2	3.603	0.021	0.067	0.000	1.863	0.044	0.135	1.595	0.032	0.000	7.359
AUGI-3	3.600	0.020	0.062	0.000	1.884	0.045	0.136	1.588	0.028	0.001	7.364
AUGI-4	3.618	0.019	0.058	0.001	1.896	0.047	0.136	1.546	0.027	0.000	7.348

Pre-run Standards

Standard Name	K Numbers (=Ix/Istd)									
	Na	Mg	Al	Si	K	Ca	Ti	Cr	Mn	Fe
AMAB-1	1.0076	0.0003	0.6570	1.3276	0.0153	0.0211	0.0000	0.0001	0.0000	0.0000
AMAB-2	0.9933	0.0000	0.6601	1.3290	0.0153	0.0214	0.0000	0.0000	0.0002	0.0004
AMAB-3	0.9811	0.0000	0.6562	1.3184	0.0124	0.0198	0.0000	0.0000	0.0001	0.0000
AMAB-4	1.0183	0.0001	0.6629	1.3559	0.0121	0.0182	0.0000	0.0001	0.0000	0.0000
PHLSY-1	0.0000	0.9966	0.3216	0.7931	0.7462	0.0000	0.0006	0.0000	0.0003	0.0017
PHLSY-2	0.0006	1.0033	0.3167	0.7988	0.7378	0.0000	0.0004	0.0002	0.0002	0.0015
PHLSY-3	0.0004	1.0068	0.3413	0.7738	0.7538	0.0000	0.0006	0.0000	0.0000	0.0006
PHLSY-4	0.0009	1.0081	0.3383	0.7787	0.7455	0.0000	0.0002	0.0000	0.0008	0.0000
CLAB-1	0.3776	0.0033	0.9908	1.0073	0.0192	1.0010	0.0018	0.0000	0.0001	0.0117
CLAB-2	0.3702	0.0034	0.9968	1.0031	0.0194	0.9977	0.0018	0.0001	0.0003	0.0109
CLAB-3	0.3733	0.0033	1.0002	0.9990	0.0195	0.9999	0.0015	0.0000	0.0002	0.0129
CLAB-4	0.3703	0.0033	1.0145	1.0027	0.0201	1.0016	0.0018	0.0000	0.0003	0.0112
CLAB-5	0.3720	0.0035	1.0123	1.0040	0.0201	1.0042	0.0015	0.0001	0.0000	0.0109
SGKF-1	0.1032	0.0004	0.6536	1.3371	0.9951	0.0000	0.0001	0.0000	0.0000	0.0002
SGKF-2	0.1037	0.0002	0.6553	1.3381	0.9983	0.0008	0.0000	0.0000	0.0002	0.0000
SGKF-3	0.1031	0.0002	0.6623	1.3433	1.0001	0.0011	0.0000	0.0000	0.0003	0.0003
SGKF-4	0.1021	0.0000	0.6587	1.3346	0.9999	0.0008	0.0002	0.0000	0.0001	0.0006
TTNG-1	0.0024	0.0000	0.0002	0.6566	0.0036	2.6332	0.9909	0.0003	0.0000	0.0014
TTNG-2	0.0020	0.0000	0.0003	0.6521	0.0038	2.6067	0.9804	0.0000	0.0000	0.0018
TTNG-3	0.0013	0.0000	0.0000	0.6567	0.0024	2.6399	0.9995	0.0001	0.0000	0.0022
TTNG-4	0.0021	0.0000	0.0004	0.6577	0.0037	2.6417	1.0008	0.0000	0.0000	0.0018
MGCR-1	0.0000	0.4871	0.0017	0.0005	0.0000	0.0015	0.0005	1.0087	0.0000	0.0018
MGCR-2	0.0000	0.4931	0.0022	0.0007	0.0000	0.0003	0.0004	1.0073	0.0000	0.0023
MGCR-3	0.0000	0.4849	0.0021	0.0003	0.0000	0.0002	0.0001	1.0055	0.0000	0.0023
MGCR-4	0.0000	0.4831	0.0019	0.0003	0.0000	0.0009	0.0005	1.0066	0.0000	0.0022
RDN-1	0.0000	0.0064	0.0004	0.9141	0.0000	0.3939	0.0003	0.0001	1.0016	0.4512
RDN-2	0.0000	0.0064	0.0009	0.9162	0.0000	0.3998	0.0000	0.0000	0.9960	0.4460
RDN-3	0.0000	0.0062	0.0002	0.9119	0.0000	0.3879	0.0000	0.0000	1.0055	0.4540
RDN-4	0.0000	0.0057	0.0008	0.9093	0.0000	0.3883	0.0006	0.0000	1.0001	0.4523
AUGI-1	0.0112	0.0317	0.0206	0.9623	0.0001	1.7839	0.0103	0.0002	0.0199	0.9862
AUGI-2	0.0124	0.0310	0.0215	0.9587	0.0000	1.7689	0.0093	0.0000	0.0185	0.9886
AUGI-3	0.0110	0.0314	0.0200	0.9589	0.0006	1.7649	0.0088	0.0000	0.0193	1.0015
AUGI-4	0.0103	0.0312	0.0187	0.9600	0.0002	1.7118	0.0086	0.0001	0.0199	1.0048
Pertinent Averages	1.0001	1.0037	1.0029	1.0032	0.9984	1.0009	0.9929	1.0070	1.0008	0.9953
Std Dev	0.0163	0.0051	0.0102	0.0030	0.0023	0.0024	0.0094	0.0013	0.0039	0.0092

Pre-run Standards

Atomic per 11 Oxygen atoms (10 Ox + 2(OH): original software calculation)

Standard Name	Si	Ti	Al	Cr	Fe	Mn	Mg	Ca	Na	K	Sum
AMAB-1	4.100	0.000	1.401	0.000	0.000	0.000	0.001	0.016	1.348	0.018	6.883
AMAB-2	4.101	0.000	1.405	0.000	0.001	0.001	0.000	0.017	1.329	0.018	6.870
AMAB-3	4.103	0.000	1.407	0.000	0.000	0.000	0.000	0.016	1.323	0.015	6.862
AMAB-4	4.111	0.000	1.391	0.001	0.000	0.000	0.000	0.014	1.341	0.014	6.871
PHLSY-1	3.082	0.001	0.953	0.000	0.003	0.001	2.903	0.000	0.000	0.994	7.937
PHLSY-2	3.093	0.001	0.937	0.001	0.003	0.001	2.913	0.000	0.001	0.980	7.928
PHLSY-3	3.023	0.001	1.013	0.000	0.001	0.000	2.929	0.000	0.001	1.004	7.972
PHLSY-4	3.035	0.001	1.003	0.000	0.000	0.002	2.928	0.000	0.001	0.991	7.960
CLAB-1	3.341	0.003	2.129	0.000	0.019	0.000	0.009	0.797	0.560	0.022	6.882
CLAB-2	3.334	0.004	2.143	0.001	0.018	0.001	0.010	0.795	0.550	0.023	6.877
CLAB-3	3.325	0.003	2.152	0.000	0.021	0.000	0.010	0.797	0.554	0.023	6.885
CLAB-4	3.318	0.004	2.167	0.000	0.018	0.001	0.009	0.794	0.546	0.023	6.880
CLAB-5	3.320	0.003	2.163	0.001	0.018	0.000	0.010	0.796	0.549	0.023	6.882
SGKF-1	4.126	0.000	1.380	0.000	0.000	0.000	0.001	0.000	0.156	1.196	6.860
SGKF-2	4.124	0.000	1.382	0.000	0.000	0.000	0.001	0.001	0.157	1.198	6.863
SGKF-3	4.120	0.000	1.389	0.000	0.000	0.001	0.001	0.001	0.155	1.194	6.861
SGKF-4	4.118	0.000	1.390	0.000	0.001	0.000	0.000	0.001	0.155	1.201	6.865
TTNG-1	2.221	2.184	0.001	0.002	0.003	0.000	0.000	2.183	0.006	0.004	6.602
TTNG-2	2.225	2.180	0.001	0.000	0.003	0.000	0.000	2.180	0.005	0.005	6.599
TTNG-3	2.213	2.194	0.000	0.000	0.004	0.000	0.000	2.179	0.003	0.003	6.596
TTNG-4	2.213	2.193	0.001	0.000	0.003	0.000	0.000	2.178	0.005	0.004	6.598
MGCR-1	0.009	0.004	0.031	21.737	0.016	0.000	10.906	0.005	0.000	0.000	32.708
MGCR-2	0.014	0.003	0.039	21.436	0.020	0.000	10.887	0.001	0.000	0.000	32.400
MGCR-3	0.007	0.001	0.039	21.761	0.021	0.000	10.906	0.001	0.000	0.000	32.734
MGCR-4	0.006	0.004	0.035	21.855	0.019	0.000	10.906	0.003	0.000	0.000	32.828
RDN-1	3.669	0.001	0.001	0.001	0.865	2.402	0.031	0.363	0.000	0.000	7.331
RDN-2	3.676	0.000	0.003	0.000	0.855	2.390	0.031	0.368	0.000	0.000	7.323
RDN-3	3.664	0.000	0.001	0.000	0.871	2.412	0.030	0.357	0.000	0.000	7.335
RDN-4	3.665	0.001	0.003	0.000	0.870	2.407	0.027	0.359	0.000	0.000	7.332
AUGI-1	3.602	0.023	0.064	0.001	1.853	0.047	0.137	1.603	0.029	0.000	7.359
AUGI-2	3.603	0.021	0.067	0.000	1.863	0.044	0.135	1.595	0.032	0.000	7.359
AUGI-3	3.600	0.020	0.062	0.000	1.884	0.045	0.136	1.588	0.028	0.001	7.364
AUGI-4	3.618	0.019	0.058	0.001	1.896	0.047	0.136	1.546	0.027	0.000	7.348

KB2	Coordinates		Weight Percent Oxides										Total
	X	Y	SiO ₂	TiO ₂	Al ₂ O ₃	Cr ₂ O ₃	FeO*	MnO	MgO	CaO	Na ₂ O	K ₂ O	
Mica-1													
KB2-M1-1	-10366	-17656	49.68	0.31	32.09	0.04	1.41	0.00	2.03	0.00	0.80	8.74	95.10
KB2-M1-2	-10366	-17684	49.96	0.32	32.26	0.03	1.36	0.00	2.08	0.00	0.74	8.75	95.50
KB2-M1-3	-10296	-17681	49.46	0.30	32.03	0.03	1.28	0.00	2.03	0.01	0.75	8.80	94.70
KB2-M1-4	-10245	-17675	49.93	0.30	32.08	0.02	1.35	0.00	2.16	0.00	0.77	8.81	95.43
KB2-M1-5	-10196	-17647	49.62	0.31	32.10	0.02	1.35	0.00	2.09	0.00	0.79	8.82	95.11
Mica-2													
KB2-M2-1	-10196	-18323	50.16	0.23	31.62	0.02	1.32	0.01	2.31	0.00	0.55	9.11	95.34
KB2-M2-2	-10166	-18323	50.07	0.25	31.89	0.03	1.30	0.00	2.27	0.00	0.60	9.06	95.48
KB2-M2-3	-10051	-18323	49.81	0.32	32.35	0.01	1.30	0.00	2.13	0.00	0.77	8.91	95.61
KB2-M2-4	-9992	-18328	49.76	0.29	32.51	0.00	1.30	0.00	2.12	0.00	0.72	8.68	95.40
KB2-M2-5	-9940	-18309	49.63	0.31	32.69	0.01	1.28	0.00	2.04	0.00	0.80	8.75	95.51
Mica-3													
KB2-M3-1	-10906	-18395	50.07	0.31	32.18	0.00	1.39	0.01	2.16	0.00	0.76	8.81	95.68
KB2-M3-2	-10843	-18384	49.65	0.32	32.22	0.04	1.37	0.00	2.05	0.00	0.79	8.83	95.27
KB2-M3-3	-10762	-18419	49.63	0.31	32.51	0.02	1.33	0.01	2.00	0.00	0.81	8.88	95.51
KB2-M3-4	-10705	-18435	49.58	0.30	32.46	0.01	1.33	0.00	1.98	0.00	0.82	8.86	95.34
KB2-M3-5	-10614	-18447	49.65	0.32	32.80	0.03	1.27	0.00	1.93	0.00	0.86	8.82	95.68
Mica-4													
KB2-M4-1	-10220	-18897	49.16	0.33	32.35	0.03	1.36	0.00	2.04	0.00	0.72	8.76	94.76
KB2-M4-2	-10180	-18898	49.48	0.33	32.33	0.01	1.37	0.00	2.12	0.00	0.75	8.76	95.13
KB2-M4-3	-10136	-18909	49.19	0.31	32.31	0.01	1.32	0.01	2.06	0.00	0.74	8.74	94.69
KB2-M4-4	-10086	-18901	49.62	0.31	32.37	0.02	1.34	0.01	2.05	0.00	0.78	8.72	95.22
KB2-M4-5	-10030	-18908	49.43	0.32	32.33	0.00	1.35	0.00	2.13	0.01	0.76	8.77	95.09
Mica-5													
KB2-M5-1	-12185	-18657	48.59	0.29	34.28	0.02	1.22	0.00	1.68	0.00	1.02	8.69	95.78
KB2-M5-2	-12147	-18657	48.80	0.32	33.55	0.03	1.24	0.01	1.81	0.00	0.92	8.64	95.31
KB2-M5-3	-12070	-18661	50.15	0.33	32.15	0.00	1.31	0.00	2.20	0.00	0.75	8.82	95.71
KB2-M5-4	-11949	-18650	50.01	0.32	32.35	0.00	1.33	0.00	2.13	0.00	0.75	8.80	95.69
KB2-M5-5	-11927	-18704	49.97	0.31	32.33	0.02	1.35	0.00	2.17	0.00	0.73	8.78	95.66
Chlorite-1													
KB2-Chl1-1	-16125	-26154	25.80	0.07	23.34	0.02	24.81	0.01	15.06	0.01	0.00	0.03	89.16
KB2-Chl1-2	-16088	-26120	25.70	0.08	23.45	0.02	24.58	0.04	15.57	0.00	0.00	0.03	89.46
KB2-Chl1-3	-16039	-26120	27.50	0.05	22.76	0.03	23.03	0.04	15.24	0.01	0.00	0.48	89.13
KB2-Chl1-4	-15978	-26123	25.42	0.07	23.57	0.02	24.59	0.03	15.60	0.01	0.00	0.00	89.31
KB2-Chl1-5	-15942	-26143	25.56	0.07	23.65	0.01	24.91	0.03	15.40	0.00	0.00	0.02	89.66

KB2		10 Oxygen + 2(OH) basis		Atomic per Formula Unit							
Mica-1	Si	Ti	Al	Cr	Fe	Mn	Mg	Ca	Na	K	Sum
KB2-M1-1	3.270	0.015	2.490	0.003	0.078	0.000	0.199	0.000	0.102	0.734	6.890
KB2-M1-2	3.272	0.016	2.490	0.003	0.074	0.000	0.203	0.000	0.094	0.731	6.883
KB2-M1-3	3.269	0.015	2.494	0.002	0.071	0.000	0.200	0.001	0.097	0.742	6.891
KB2-M1-4	3.274	0.015	2.480	0.002	0.074	0.000	0.211	0.000	0.098	0.737	6.890
KB2-M1-5	3.266	0.016	2.491	0.002	0.074	0.000	0.206	0.000	0.101	0.741	6.895
Mica-2		10 Oxygen + 2(OH) basis									
KB2-M2-1	3.295	0.011	2.447	0.002	0.073	0.001	0.226	0.000	0.071	0.763	6.889
KB2-M2-2	3.284	0.012	2.465	0.003	0.072	0.000	0.222	0.000	0.077	0.758	6.892
KB2-M2-3	3.261	0.016	2.497	0.001	0.071	0.000	0.208	0.000	0.098	0.744	6.896
KB2-M2-4	3.260	0.014	2.510	0.000	0.071	0.000	0.207	0.000	0.092	0.726	6.880
KB2-M2-5	3.250	0.016	2.523	0.001	0.070	0.000	0.199	0.000	0.101	0.731	6.890
Mica-3		10 Oxygen + 2(OH) basis									
KB2-M3-1	3.274	0.015	2.480	0.000	0.076	0.001	0.210	0.000	0.096	0.735	6.886
KB2-M3-2	3.264	0.016	2.496	0.003	0.076	0.000	0.201	0.000	0.101	0.740	6.896
KB2-M3-3	3.254	0.015	2.512	0.001	0.073	0.001	0.195	0.000	0.103	0.743	6.898
KB2-M3-4	3.256	0.015	2.512	0.001	0.073	0.000	0.194	0.000	0.104	0.742	6.897
KB2-M3-5	3.248	0.016	2.529	0.002	0.069	0.000	0.189	0.000	0.109	0.736	6.897
Mica-4		10 Oxygen + 2(OH) basis									
KB2-M4-1	3.248	0.016	2.520	0.003	0.075	0.000	0.201	0.000	0.092	0.739	6.894
KB2-M4-2	3.255	0.016	2.506	0.001	0.075	0.000	0.207	0.000	0.096	0.735	6.892
KB2-M4-3	3.251	0.016	2.517	0.001	0.073	0.000	0.203	0.000	0.094	0.737	6.892
KB2-M4-4	3.260	0.016	2.506	0.001	0.073	0.000	0.201	0.000	0.100	0.731	6.888
KB2-M4-5	3.253	0.016	2.508	0.000	0.074	0.000	0.209	0.001	0.097	0.736	6.894
Mica-5		10 Oxygen + 2(OH) basis									
KB2-M5-1	3.176	0.014	2.641	0.001	0.067	0.000	0.163	0.000	0.129	0.725	6.917
KB2-M5-2	3.204	0.016	2.596	0.002	0.068	0.000	0.177	0.000	0.117	0.724	6.905
KB2-M5-3	3.277	0.016	2.475	0.000	0.072	0.000	0.214	0.000	0.095	0.735	6.885
KB2-M5-4	3.268	0.016	2.492	0.000	0.073	0.000	0.207	0.000	0.095	0.734	6.885
KB2-M5-5	3.268	0.015	2.491	0.002	0.074	0.000	0.212	0.000	0.092	0.732	6.885
Chlorite-1		10 Oxygen + 8(OH) basis									
KB2-Chl1-1	2.651	0.005	2.828	0.002	2.133	0.001	2.308	0.001	0.000	0.004	9.934
KB2-Chl1-2	2.630	0.006	2.828	0.002	2.104	0.003	2.376	0.000	0.000	0.003	9.953
KB2-Chl1-3	2.797	0.004	2.728	0.004	1.959	0.003	2.310	0.001	0.000	0.062	9.869
KB2-Chl1-4	2.608	0.006	2.850	0.002	2.110	0.002	2.385	0.001	0.000	0.000	9.964
KB2-Chl1-5	2.614	0.005	2.852	0.001	2.131	0.003	2.349	0.000	0.000	0.002	9.957

KB2										
K Numbers (=Ix/Istd)										
Mica-1	Na	Mg	Al	Si	K	Ca	Ti	Cr	Mn	Fe
KB2-M1-1	0.0655	0.0704	1.1161	0.9136	0.5880	0.0000	0.0075	0.0006	0.0000	0.0456
KB2-M1-2	0.0607	0.0724	1.1227	0.9191	0.5889	0.0000	0.0077	0.0006	0.0001	0.0438
KB2-M1-3	0.0620	0.0708	1.1148	0.9093	0.5923	0.0010	0.0074	0.0004	0.0000	0.0412
KB2-M1-4	0.0631	0.0750	1.1157	0.9190	0.5925	0.0000	0.0074	0.0004	0.0000	0.0436
KB2-M1-5	0.0647	0.0728	1.1164	0.9124	0.5933	0.0000	0.0076	0.0004	0.0000	0.0435
Mica-2										
KB2-M2-1	0.0454	0.0805	1.1000	0.9263	0.6130	0.0000	0.0055	0.0004	0.0004	0.0426
KB2-M2-2	0.0496	0.0791	1.1095	0.9231	0.6097	0.0000	0.0061	0.0006	0.0000	0.0420
KB2-M2-3	0.0633	0.0742	1.1259	0.9161	0.5996	0.0000	0.0077	0.0002	0.0001	0.0420
KB2-M2-4	0.0593	0.0739	1.1321	0.9140	0.5840	0.0004	0.0070	0.0000	0.0000	0.0420
KB2-M2-5	0.0656	0.0709	1.1387	0.9110	0.5883	0.0000	0.0076	0.0002	0.0001	0.0414
Mica-3										
KB2-M3-1	0.0624	0.0751	1.1194	0.9217	0.5925	0.0000	0.0075	0.0000	0.0002	0.0447
KB2-M3-2	0.0649	0.0713	1.1206	0.9128	0.5941	0.0000	0.0078	0.0006	0.0000	0.0443
KB2-M3-3	0.0665	0.0695	1.1319	0.9120	0.5979	0.0000	0.0076	0.0003	0.0004	0.0430
KB2-M3-4	0.0671	0.0690	1.1303	0.9109	0.5960	0.0000	0.0072	0.0002	0.0001	0.0430
KB2-M3-5	0.0710	0.0672	1.1433	0.9117	0.5934	0.0000	0.0077	0.0005	0.0000	0.0409
Mica-4										
KB2-M4-1	0.0590	0.0710	1.1258	0.9018	0.5896	0.0003	0.0080	0.0006	0.0000	0.0439
KB2-M4-2	0.0616	0.0736	1.1244	0.9086	0.5893	0.0000	0.0080	0.0001	0.0000	0.0441
KB2-M4-3	0.0605	0.0716	1.1243	0.9026	0.5881	0.0001	0.0077	0.0002	0.0001	0.0424
KB2-M4-4	0.0644	0.0713	1.1265	0.9116	0.5866	0.0002	0.0077	0.0003	0.0002	0.0431
KB2-M4-5	0.0624	0.0742	1.1244	0.9075	0.5897	0.0006	0.0077	0.0000	0.0000	0.0436
Mica-5										
KB2-M5-1	0.0838	0.0583	1.1975	0.8853	0.5846	0.0002	0.0072	0.0003	0.0000	0.0394
KB2-M5-2	0.0757	0.0628	1.1705	0.8913	0.5814	0.0001	0.0078	0.0004	0.0002	0.0400
KB2-M5-3	0.0619	0.0765	1.1183	0.9236	0.5934	0.0000	0.0080	0.0000	0.0000	0.0422
KB2-M5-4	0.0616	0.0740	1.1262	0.9200	0.5923	0.0000	0.0078	0.0000	0.0001	0.0429
KB2-M5-5	0.0597	0.0755	1.1247	0.9192	0.5907	0.0000	0.0076	0.0004	0.0000	0.0435
Chlorite-1										
KB2-Chl1-1	0.0000	0.4247	0.6148	0.4173	0.0023	0.0007	0.0018	0.0003	0.0004	0.8260
KB2-Chl1-2	0.0000	0.4406	0.6164	0.4152	0.0018	0.0002	0.0021	0.0003	0.0010	0.8179
KB2-Chl1-3	0.0000	0.4362	0.6049	0.4487	0.0331	0.0011	0.0014	0.0006	0.0010	0.7647
KB2-Chl1-4	0.0000	0.4412	0.6193	0.4101	0.0000	0.0005	0.0019	0.0004	0.0007	0.8185
KB2-Chl1-5	0.0000	0.4348	0.6221	0.4127	0.0013	0.0002	0.0017	0.0002	0.0009	0.8295

KB2											
Atomic per 11 Oxygen atoms (10 Ox + 2(OH): original software calculation)											
Mica-1	Si	Ti	Al	Cr	Fe	Mn	Mg	Ca	Na	K	Sum
KB2-M1-1	3.270	0.015	2.490	0.003	0.078	0.000	0.199	0.000	0.102	0.734	6.890
KB2-M1-2	3.272	0.016	2.490	0.003	0.074	0.000	0.203	0.000	0.094	0.731	6.883
KB2-M1-3	3.269	0.015	2.494	0.002	0.071	0.000	0.200	0.001	0.097	0.742	6.891
KB2-M1-4	3.274	0.015	2.480	0.002	0.074	0.000	0.211	0.000	0.098	0.737	6.890
KB2-M1-5	3.266	0.016	2.491	0.002	0.074	0.000	0.206	0.000	0.101	0.741	6.895
Mica-2											
KB2-M2-1	3.295	0.011	2.447	0.002	0.073	0.001	0.226	0.000	0.071	0.763	6.889
KB2-M2-2	3.284	0.012	2.465	0.003	0.072	0.000	0.222	0.000	0.077	0.758	6.892
KB2-M2-3	3.261	0.016	2.497	0.001	0.071	0.000	0.208	0.000	0.098	0.744	6.896
KB2-M2-4	3.260	0.014	2.510	0.000	0.071	0.000	0.207	0.000	0.092	0.726	6.880
KB2-M2-5	3.250	0.016	2.523	0.001	0.070	0.000	0.199	0.000	0.101	0.731	6.890
Mica-3											
KB2-M3-1	3.274	0.015	2.480	0.000	0.076	0.001	0.210	0.000	0.096	0.735	6.886
KB2-M3-2	3.264	0.016	2.496	0.003	0.076	0.000	0.201	0.000	0.101	0.740	6.896
KB2-M3-3	3.254	0.015	2.512	0.001	0.073	0.001	0.195	0.000	0.103	0.743	6.898
KB2-M3-4	3.256	0.015	2.512	0.001	0.073	0.000	0.194	0.000	0.104	0.742	6.897
KB2-M3-5	3.248	0.016	2.529	0.002	0.069	0.000	0.189	0.000	0.109	0.736	6.897
Mica-4											
KB2-M4-1	3.248	0.016	2.520	0.003	0.075	0.000	0.201	0.000	0.092	0.739	6.894
KB2-M4-2	3.255	0.016	2.506	0.001	0.075	0.000	0.207	0.000	0.096	0.735	6.892
KB2-M4-3	3.251	0.016	2.517	0.001	0.073	0.000	0.203	0.000	0.094	0.737	6.892
KB2-M4-4	3.260	0.016	2.506	0.001	0.073	0.000	0.201	0.000	0.100	0.731	6.888
KB2-M4-5	3.253	0.016	2.508	0.000	0.074	0.000	0.209	0.001	0.097	0.736	6.894
Mica-5											
KB2-M5-1	3.176	0.014	2.641	0.001	0.067	0.000	0.163	0.000	0.129	0.725	6.917
KB2-M5-2	3.204	0.016	2.596	0.002	0.068	0.000	0.177	0.000	0.117	0.724	6.905
KB2-M5-3	3.277	0.016	2.475	0.000	0.072	0.000	0.214	0.000	0.095	0.735	6.885
KB2-M5-4	3.268	0.016	2.492	0.000	0.073	0.000	0.207	0.000	0.095	0.734	6.885
KB2-M5-5	3.268	0.015	2.491	0.002	0.074	0.000	0.212	0.000	0.092	0.732	6.885
Chlorite-1											
KB2-Ch11-1	2.083	0.004	2.222	0.002	1.676	0.001	1.813	0.001	0.000	0.004	7.805
KB2-Ch11-2	2.067	0.005	2.222	0.002	1.653	0.003	1.867	0.000	0.000	0.003	7.820
KB2-Ch11-3	2.198	0.003	2.144	0.003	1.539	0.002	1.815	0.001	0.000	0.049	7.754
KB2-Ch11-4	2.049	0.004	2.239	0.002	1.658	0.002	1.874	0.001	0.000	0.000	7.829
KB2-Ch11-5	2.054	0.004	2.241	0.001	1.674	0.002	1.845	0.000	0.000	0.002	7.824

KB20													
	Coordinates		Weight Percent Oxides										
White Mica-1	X	Y	SiO ₂	TiO ₂	Al ₂ O ₃	Cr ₂ O ₃	FeO*	MnO	MgO	CaO	Na ₂ O	K ₂ O	Total
K20B-Mica1-1	1460	6858	50.05	0.34	27.89	0.01	3.46	0.00	2.92	0.00	0.75	10.01	95.44
K20B-Mica1-2	1526	6858	50.28	0.36	27.76	0.01	3.48	0.00	2.92	0.00	0.75	10.09	95.65
K20B-Mica1-3	1585	6858	50.53	0.37	27.56	0.01	3.51	0.01	3.06	0.00	0.69	10.14	95.87
K20B-Mica1-4	1624	6854	50.43	0.35	27.98	0.01	3.58	0.01	2.93	0.00	0.73	10.12	96.14
K20B-Mica1-5	1668	6957	50.49	0.37	27.42	0.01	3.53	0.01	3.04	0.00	0.71	10.15	95.73
Omphacite-1													
K20B-AMP1-1	1745	7302	55.85	0.07	9.12	0.01	10.02	0.06	6.53	10.89	8.06	0.00	100.59
K20B-AMP1-2	1686	7284	55.90	0.10	9.30	0.00	9.70	0.05	6.63	11.41	7.83	0.01	100.92
K20B-AMP1-3	1648	7262	55.82	0.15	9.41	0.01	9.66	0.04	6.57	11.28	8.02	0.00	100.95
K20B-AMP1-4	1572	7219	55.89	0.10	9.65	0.00	9.69	0.06	6.48	11.22	7.98	0.01	101.07
K20B-AMP1-5	1510	7185	55.96	0.08	9.53	0.01	9.42	0.04	6.60	11.22	7.83	0.00	100.67
Omphacite-2													
K20B-AMP2-1	1304	7439	56.04	0.10	10.16	0.01	9.28	0.05	6.66	11.19	7.92	0.00	101.41
K20B-AMP2-2	1227	7440	55.65	0.08	9.07	0.00	10.34	0.05	6.36	11.70	7.41	0.01	100.67
K20B-AMP2-3	1175	7440	55.50	0.05	9.03	0.02	11.26	0.11	5.90	11.39	7.57	0.00	100.83
K20B-AMP2-4	1114	7446	55.89	0.07	9.57	0.01	11.46	0.11	5.44	10.60	8.03	0.01	101.20
K20B-AMP2-5	1043	7449	55.85	0.11	9.92	0.03	9.10	0.04	6.73	11.48	7.65	0.00	100.92
White Mica-2													
K20B-Mica2-1	1650	7608	50.03	0.52	28.60	0.03	3.52	0.00	2.88	0.00	0.83	9.75	96.15
K20B-Mica2-2	1650	7638	50.11	0.53	28.54	0.02	3.72	0.01	2.82	0.00	0.87	9.82	96.44
K20B-Mica2-3	1655	7669	49.87	0.53	28.61	0.02	3.84	0.00	2.78	0.00	0.85	9.88	96.38
K20B-Mica2-4	1702	7693	49.99	0.56	28.59	0.02	3.68	0.00	2.81	0.01	0.90	9.92	96.47
K20B-Mica2-5	1718	7729	49.77	0.53	28.59	0.01	3.62	0.00	2.82	0.00	0.87	9.86	96.08
White Mica-3													
K20B-Mica3-1	357	6195	50.61	0.39	26.82	0.00	3.59	0.01	3.39	0.02	0.52	10.33	95.69
K20B-Mica3-2	301	6184	50.24	0.41	27.62	0.02	3.52	0.01	3.09	0.01	0.62	10.31	95.83
K20B-Mica3-3	262	6184	50.04	0.39	27.68	0.02	3.53	0.01	3.06	0.00	0.73	10.23	95.69
K20B-Mica3-4	189	6168	49.60	0.49	28.14	0.03	3.61	0.00	2.86	0.01	0.78	9.92	95.46
K20B-Mica3-5	129	6146	50.28	0.40	27.98	0.01	3.47	0.00	3.03	0.02	0.70	10.08	95.98
White Mica-4													
K20B-Mica4-1	523	5287	49.55	0.53	28.30	0.02	3.32	0.00	2.83	0.01	0.89	9.87	95.32
K20B-Mica4-2	565	5290	49.61	0.55	28.42	0.02	3.23	0.01	2.82	0.01	0.84	9.89	95.41
K20B-Mica4-3	620	5278	49.87	0.49	28.12	0.01	3.38	0.00	2.95	0.00	0.79	9.84	95.46
K20B-Mica4-4	682	5293	50.13	0.43	27.91	0.02	3.53	0.00	3.09	0.01	0.82	9.77	95.70
K20B-Mica4-5	773	5286	49.69	0.55	28.34	0.02	3.47	0.00	2.85	0.00	0.87	9.76	95.55
Epidote													
K20B-Epd-1	1916	7558	38.65	0.16	25.85	0.00	10.43	0.05	0.06	23.04	0.00	0.01	98.25
K20B-Epd-2	1893	7551	38.54	0.13	25.93	0.01	10.18	0.06	0.05	23.16	0.00	0.00	98.06
K20B-Epd-3	1893	7643	38.75	0.12	25.74	0.01	10.44	0.10	0.04	23.00	0.00	0.00	98.19
K20B-Epd-4	1983	7671	38.80	0.12	26.41	0.01	9.79	0.07	0.07	23.07	0.00	0.00	98.35
Omphacite-3													
K20B-Amp3-1	1098	7253	55.86	0.09	9.80	0.02	9.43	0.05	6.47	10.86	7.99	0.00	100.59
K20B-Amp3-2	1176	7253	55.56	0.07	8.97	0.00	10.85	0.07	6.27	11.57	7.69	0.01	101.06
K20B-Amp3-3	1265	7255	55.60	0.04	9.55	0.00	11.02	0.07	5.63	10.79	8.01	0.00	100.72
K20B-Amp3-4	1359	7255	56.04	0.10	9.74	0.02	9.60	0.04	6.65	11.10	8.01	0.00	101.30
K20B-Amp3-5	1404	7284	55.72	0.09	10.13	0.02	9.27	0.02	6.70	11.23	7.61	0.01	100.81
Omphacite-4													
K20B-Amp4-1	1014	7133	55.54	0.09	9.89	0.02	9.61	0.04	6.47	11.33	7.78	0.00	100.77
K20B-Amp4-2	997	7091	55.46	0.07	9.22	0.00	10.18	0.05	6.51	11.71	7.38	0.00	100.59
K20B-Amp4-3	954	7091	55.74	0.07	9.93	0.01	10.08	0.05	6.05	10.67	7.98	0.00	100.59
K20B-Amp4-4	902	7091	55.78	0.08	9.86	0.01	9.38	0.03	6.54	11.02	7.90	0.00	100.60
K20B-Amp4-5	857	7100	55.81	0.09	9.67	0.02	9.85	0.04	6.43	10.83	8.07	0.00	100.82

KB20		10 Oxygen + 2(OH) basis		Atomic per Formula Unit							
White Mica-1	Si	Ti	Al	Cr	Fe	Mn	Mg	Ca	Na	K	Sum
K20B-Mica1-1	3.351	0.017	2.201	0.001	0.194	0.000	0.292	0.000	0.098	0.855	7.008
K20B-Mica1-2	3.360	0.018	2.187	0.001	0.195	0.000	0.290	0.000	0.097	0.860	7.007
K20B-Mica1-3	3.369	0.019	2.166	0.001	0.196	0.001	0.305	0.000	0.089	0.862	7.006
K20B-Mica1-4	3.354	0.017	2.193	0.001	0.199	0.001	0.290	0.000	0.094	0.858	7.009
K20B-Mica1-5	3.373	0.019	2.158	0.001	0.197	0.001	0.303	0.000	0.092	0.865	7.008
Omphacite-1	22 Oxygen + 2(OH) basis										
K20B-AMP1-1	7.760	0.007	1.493	0.002	1.164	0.007	1.351	1.621	2.170	0.000	15.574
K20B-AMP1-2	7.734	0.010	1.516	0.000	1.123	0.006	1.367	1.691	2.101	0.001	15.549
K20B-AMP1-3	7.722	0.016	1.534	0.001	1.118	0.004	1.354	1.672	2.151	0.001	15.572
K20B-AMP1-4	7.718	0.010	1.570	0.001	1.120	0.007	1.334	1.660	2.135	0.001	15.556
K20B-AMP1-5	7.742	0.008	1.555	0.001	1.090	0.004	1.361	1.663	2.099	0.001	15.524
Omphacite-2	22 Oxygen + 2(OH) basis										
K20B-AMP2-1	7.691	0.011	1.643	0.001	1.064	0.006	1.363	1.645	2.106	0.001	15.531
K20B-AMP2-2	7.741	0.008	1.487	0.000	1.203	0.006	1.320	1.743	1.997	0.001	15.507
K20B-AMP2-3	7.742	0.005	1.484	0.003	1.314	0.013	1.227	1.702	2.047	0.001	15.538
K20B-AMP2-4	7.756	0.007	1.565	0.002	1.330	0.013	1.126	1.576	2.161	0.003	15.539
K20B-AMP2-5	7.700	0.012	1.613	0.005	1.050	0.005	1.384	1.696	2.044	0.000	15.509
White Mica-2	10 Oxygen + 2(OH) basis										
K20B-Mica2-1	3.322	0.026	2.238	0.002	0.196	0.000	0.285	0.000	0.107	0.825	7.001
K20B-Mica2-2	3.323	0.026	2.230	0.001	0.206	0.000	0.279	0.000	0.112	0.831	7.009
K20B-Mica2-3	3.313	0.026	2.240	0.002	0.213	0.000	0.276	0.000	0.110	0.837	7.016
K20B-Mica2-4	3.316	0.028	2.235	0.001	0.204	0.000	0.278	0.000	0.116	0.840	7.018
K20B-Mica2-5	3.313	0.026	2.243	0.001	0.202	0.000	0.280	0.000	0.113	0.837	7.015
White Mica-3	10 Oxygen + 2(OH) basis										
K20B-Mica3-1	3.386	0.020	2.115	0.000	0.201	0.001	0.338	0.002	0.067	0.881	7.011
K20B-Mica3-2	3.356	0.021	2.174	0.001	0.197	0.000	0.308	0.001	0.080	0.878	7.016
K20B-Mica3-3	3.349	0.020	2.184	0.001	0.198	0.001	0.305	0.000	0.094	0.873	7.024
K20B-Mica3-4	3.325	0.025	2.224	0.003	0.203	0.000	0.286	0.001	0.102	0.848	7.016
K20B-Mica3-5	3.348	0.020	2.196	0.001	0.193	0.000	0.301	0.001	0.090	0.857	7.008
White Mica-4	10 Oxygen + 2(OH) basis										
K20B-Mica4-1	3.322	0.027	2.236	0.001	0.186	0.000	0.283	0.001	0.116	0.844	7.015
K20B-Mica4-2	3.321	0.028	2.242	0.002	0.181	0.000	0.282	0.001	0.109	0.844	7.009
K20B-Mica4-3	3.336	0.025	2.217	0.001	0.189	0.000	0.294	0.000	0.102	0.840	7.003
K20B-Mica4-4	3.345	0.022	2.195	0.001	0.197	0.000	0.307	0.000	0.106	0.832	7.006
K20B-Mica4-5	3.322	0.028	2.233	0.002	0.194	0.000	0.284	0.000	0.112	0.832	7.007
Epidote	12 Oxygen + 1(OH) basis										
K20B-Epd-1	3.082	0.009	2.429	0.000	0.695	0.004	0.007	1.968	0.000	0.000	8.195
K20B-Epd-2	3.077	0.008	2.440	0.001	0.680	0.004	0.006	1.981	0.000	0.000	8.197
K20B-Epd-3	3.091	0.007	2.420	0.001	0.696	0.007	0.005	1.966	0.000	0.000	8.193
K20B-Epd-4	3.079	0.007	2.470	0.001	0.650	0.005	0.009	1.961	0.000	0.000	8.180
Omphacite-3	22 Oxygen + 2(OH) basis										
K20B-Amp3-1	7.733	0.009	1.599	0.004	1.092	0.006	1.336	1.611	2.145	0.000	15.534
K20B-Amp3-2	7.725	0.007	1.469	0.000	1.262	0.008	1.300	1.724	2.074	0.002	15.571
K20B-Amp3-3	7.744	0.005	1.568	0.000	1.283	0.008	1.168	1.609	2.164	0.000	15.550
K20B-Amp3-4	7.715	0.010	1.580	0.004	1.105	0.005	1.364	1.638	2.137	0.000	15.557
K20B-Amp3-5	7.690	0.009	1.648	0.003	1.070	0.002	1.379	1.660	2.037	0.001	15.500
Omphacite-4	22 Oxygen + 2(OH) basis										
K20B-Amp4-1	7.691	0.010	1.614	0.004	1.113	0.005	1.335	1.681	2.088	0.000	15.540
K20B-Amp4-2	7.718	0.007	1.513	0.001	1.185	0.005	1.350	1.746	1.992	0.000	15.516
K20B-Amp4-3	7.732	0.007	1.624	0.002	1.169	0.006	1.251	1.585	2.147	0.001	15.524
K20B-Amp4-4	7.719	0.008	1.609	0.002	1.085	0.004	1.349	1.634	2.119	0.000	15.529
K20B-Amp4-5	7.726	0.010	1.578	0.003	1.140	0.005	1.328	1.606	2.165	0.001	15.561

KB20										
K Numbers (=Ix/Istd)										
	Na	Mg	Al	Si	K	Ca	Ti	Cr	Mn	Fe
White Mica-1										
K20B-Mica1-1	0.0600	0.0991	0.9469	0.9338	0.6772	0.0000	0.0083	0.0002	0.0001	0.1117
K20B-Mica1-2	0.0593	0.0988	0.9425	0.9396	0.6828	0.0001	0.0088	0.0001	0.0000	0.1127
K20B-Mica1-3	0.0548	0.1039	0.9347	0.9454	0.6861	0.0000	0.0090	0.0001	0.0003	0.1133
K20B-Mica1-4	0.0581	0.0992	0.9496	0.9423	0.6847	0.0000	0.0085	0.0001	0.0003	0.1159
K20B-Mica1-5	0.0563	0.1030	0.9295	0.9451	0.6869	0.0000	0.0090	0.0001	0.0004	0.1143
Omphacite-1										
K20B-AMP1-1	0.5925	0.1900	0.2697	1.0827	0.0000	0.9288	0.0016	0.0002	0.0015	0.3255
K20B-AMP1-2	0.5770	0.1938	0.2757	1.0850	0.0005	0.9731	0.0024	0.0000	0.0013	0.3152
K20B-AMP1-3	0.5916	0.1919	0.2789	1.0825	0.0002	0.9623	0.0038	0.0001	0.0009	0.3138
K20B-AMP1-4	0.5884	0.1895	0.2864	1.0833	0.0004	0.9569	0.0025	0.0001	0.0015	0.3149
K20B-AMP1-5	0.5787	0.1935	0.2833	1.0854	0.0003	0.9561	0.0019	0.0001	0.0010	0.3057
Omphacite-2										
K20B-AMP2-1	0.5874	0.1958	0.3024	1.0851	0.0003	0.9534	0.0026	0.0001	0.0013	0.3012
K20B-AMP2-2	0.5399	0.1856	0.2690	1.0817	0.0005	0.9993	0.0019	0.0000	0.0014	0.3361
K20B-AMP2-3	0.5464	0.1706	0.2671	1.0777	0.0002	0.9744	0.0012	0.0003	0.0029	0.3666
K20B-AMP2-4	0.5811	0.1567	0.2836	1.0831	0.0010	0.9059	0.0017	0.0002	0.0030	0.3734
K20B-AMP2-5	0.5671	0.1983	0.2956	1.0826	0.0000	0.9788	0.0027	0.0005	0.0011	0.2955
White Mica-2										
K20B-Mica2-1	0.0660	0.0976	0.9709	0.9311	0.6595	0.0000	0.0126	0.0004	0.0000	0.1139
K20B-Mica2-2	0.0691	0.0954	0.9680	0.9332	0.6648	0.0000	0.0129	0.0003	0.0002	0.1203
K20B-Mica2-3	0.0674	0.0939	0.9699	0.9279	0.6691	0.0001	0.0129	0.0004	0.0000	0.1241
K20B-Mica2-4	0.0715	0.0948	0.9695	0.9309	0.6719	0.0005	0.0136	0.0003	0.0000	0.1191
K20B-Mica2-5	0.0695	0.0954	0.9699	0.9258	0.6676	0.0003	0.0129	0.0002	0.0001	0.1171
White Mica-3										
K20B-Mica3-1	0.0409	0.1150	0.9072	0.9493	0.6991	0.0018	0.0095	0.0001	0.0003	0.1162
K20B-Mica3-2	0.0489	0.1047	0.9366	0.9397	0.6980	0.0007	0.0100	0.0003	0.0002	0.1139
K20B-Mica3-3	0.0576	0.1036	0.9382	0.9348	0.6923	0.0000	0.0095	0.0003	0.0004	0.1142
K20B-Mica3-4	0.0620	0.0967	0.9542	0.9235	0.6715	0.0012	0.0121	0.0005	0.0000	0.1168
K20B-Mica3-5	0.0557	0.1027	0.9496	0.9389	0.6825	0.0015	0.0099	0.0002	0.0000	0.1123
White Mica-4										
K20B-Mica4-1	0.0710	0.0960	0.9610	0.9220	0.6679	0.0008	0.0129	0.0003	0.0000	0.1072
K20B-Mica4-2	0.0670	0.0958	0.9660	0.9232	0.6692	0.0008	0.0135	0.0004	0.0001	0.1045
K20B-Mica4-3	0.0627	0.1001	0.9545	0.9290	0.6661	0.0001	0.0120	0.0002	0.0000	0.1092
K20B-Mica4-4	0.0653	0.1046	0.9451	0.9344	0.6609	0.0005	0.0106	0.0003	0.0000	0.1140
K20B-Mica4-5	0.0688	0.0966	0.9615	0.9246	0.6603	0.0000	0.0135	0.0003	0.0001	0.1121
Epidote										
K20B-Epd-1	0.0000	0.0017	0.8348	0.7187	0.0004	1.9998	0.0038	0.0000	0.0014	0.3390
K20B-Epd-2	0.0000	0.0015	0.8382	0.7164	0.0002	2.0096	0.0031	0.0002	0.0015	0.3308
K20B-Epd-3	0.0000	0.0013	0.8311	0.7207	0.0000	1.9964	0.0028	0.0001	0.0025	0.3392
K20B-Epd-4	0.0000	0.0022	0.8566	0.7210	0.0000	2.0001	0.0029	0.0002	0.0018	0.3179
Omphacite-3										
K20B-Amp3-1	0.5916	0.1896	0.2913	1.0817	0.0000	0.9258	0.0022	0.0004	0.0014	0.3063
K20B-Amp3-2	0.5586	0.1818	0.2651	1.0787	0.0007	0.9895	0.0016	0.0000	0.0018	0.3529
K20B-Amp3-3	0.5823	0.1625	0.2831	1.0771	0.0000	0.9217	0.0011	0.0000	0.0018	0.3586
K20B-Amp3-4	0.5920	0.1946	0.2891	1.0858	0.0000	0.9468	0.0024	0.0004	0.0010	0.3119
K20B-Amp3-5	0.5641	0.1974	0.3017	1.0786	0.0005	0.9567	0.0022	0.0003	0.0005	0.3010
Omphacite-4										
K20B-Amp4-1	0.5736	0.1895	0.2940	1.0755	0.0000	0.9664	0.0023	0.0004	0.0011	0.3120
K20B-Amp4-2	0.5395	0.1901	0.2736	1.0767	0.0000	1.0002	0.0017	0.0001	0.0012	0.3308
K20B-Amp4-3	0.5869	0.1763	0.2952	1.0785	0.0003	0.9099	0.0017	0.0002	0.0013	0.3277
K20B-Amp4-4	0.5847	0.1918	0.2933	1.0799	0.0000	0.9393	0.0020	0.0002	0.0008	0.3045
K20B-Amp4-5	0.5947	0.1877	0.2869	1.0804	0.0003	0.9235	0.0023	0.0003	0.0011	0.3199

KB20											
Atomic per 11 Oxygen atoms (10 Ox + 2(OH): original software calculation)											
White Mica-1	Si	Ti	Al	Cr	Fe	Mn	Mg	Ca	Na	K	Sum
K20B-Mica1-1	3.351	0.017	2.201	0.001	0.194	0.000	0.292	0.000	0.098	0.855	7.008
K20B-Mica1-2	3.360	0.018	2.187	0.001	0.195	0.000	0.290	0.000	0.097	0.860	7.007
K20B-Mica1-3	3.369	0.019	2.166	0.001	0.196	0.001	0.305	0.000	0.089	0.862	7.006
K20B-Mica1-4	3.354	0.017	2.193	0.001	0.199	0.001	0.290	0.000	0.094	0.858	7.009
K20B-Mica1-5	3.373	0.019	2.158	0.001	0.197	0.001	0.303	0.000	0.092	0.865	7.008
Omphacite-1											
K20B-AMP1-1	3.711	0.003	0.714	0.001	0.557	0.003	0.646	0.775	1.038	0.000	7.448
K20B-AMP1-2	3.699	0.005	0.725	0.000	0.537	0.003	0.654	0.809	1.005	0.001	7.436
K20B-AMP1-3	3.693	0.008	0.734	0.000	0.535	0.002	0.648	0.800	1.029	0.000	7.447
K20B-AMP1-4	3.691	0.005	0.751	0.000	0.536	0.003	0.638	0.794	1.021	0.001	7.440
K20B-AMP1-5	3.703	0.004	0.744	0.001	0.521	0.002	0.651	0.795	1.004	0.000	7.424
Omphacite-2											
K20B-AMP2-1	3.678	0.005	0.786	0.001	0.509	0.003	0.652	0.787	1.007	0.000	7.428
K20B-AMP2-2	3.702	0.004	0.711	0.000	0.575	0.003	0.631	0.834	0.955	0.001	7.416
K20B-AMP2-3	3.703	0.002	0.710	0.001	0.628	0.006	0.587	0.814	0.979	0.000	7.431
K20B-AMP2-4	3.709	0.003	0.749	0.001	0.636	0.006	0.538	0.754	1.034	0.001	7.432
K20B-AMP2-5	3.683	0.006	0.771	0.002	0.502	0.002	0.662	0.811	0.978	0.000	7.417
White Mica-2											
K20B-Mica2-1	3.322	0.026	2.238	0.002	0.196	0.000	0.285	0.000	0.107	0.825	7.001
K20B-Mica2-2	3.323	0.026	2.230	0.001	0.206	0.001	0.279	0.000	0.112	0.831	7.009
K20B-Mica2-3	3.313	0.026	2.240	0.002	0.213	0.000	0.276	0.000	0.110	0.837	7.016
K20B-Mica2-4	3.316	0.028	2.235	0.001	0.204	0.000	0.278	0.000	0.116	0.840	7.018
K20B-Mica2-5	3.313	0.026	2.243	0.001	0.202	0.000	0.280	0.000	0.113	0.837	7.015
White Mica-3											
K20B-Mica3-1	3.386	0.020	2.115	0.000	0.201	0.001	0.338	0.002	0.067	0.881	7.011
K20B-Mica3-2	3.356	0.021	2.174	0.001	0.197	0.000	0.308	0.001	0.080	0.878	7.016
K20B-Mica3-3	3.349	0.020	2.184	0.001	0.198	0.001	0.305	0.000	0.094	0.873	7.024
K20B-Mica3-4	3.325	0.025	2.224	0.003	0.203	0.000	0.286	0.001	0.102	0.848	7.016
K20B-Mica3-5	3.348	0.020	2.196	0.001	0.193	0.000	0.301	0.001	0.090	0.857	7.008
White Mica-4											
K20B-Mica4-1	3.322	0.027	2.236	0.001	0.186	0.000	0.283	0.001	0.116	0.844	7.015
K20B-Mica4-2	3.321	0.028	2.242	0.002	0.181	0.000	0.282	0.001	0.109	0.844	7.009
K20B-Mica4-3	3.336	0.025	2.217	0.001	0.189	0.000	0.294	0.000	0.102	0.840	7.003
K20B-Mica4-4	3.345	0.022	2.195	0.001	0.197	0.000	0.307	0.000	0.106	0.832	7.006
K20B-Mica4-5	3.322	0.028	2.233	0.002	0.194	0.000	0.284	0.000	0.112	0.832	7.007
Epidote											
K20B-Epd-1	2.712	0.008	2.138	0.000	0.612	0.003	0.006	1.732	0.000	0.000	7.211
K20B-Epd-2	2.708	0.007	2.147	0.001	0.598	0.003	0.005	1.743	0.000	0.000	7.214
K20B-Epd-3	2.720	0.006	2.130	0.001	0.613	0.006	0.004	1.730	0.000	0.000	7.210
K20B-Epd-4	2.709	0.006	2.173	0.001	0.572	0.004	0.008	1.726	0.000	0.000	7.199
Omphacite-3											
K20B-Amp3-1	3.698	0.005	0.765	0.002	0.522	0.003	0.639	0.771	1.026	0.000	7.430
K20B-Amp3-2	3.695	0.003	0.703	0.000	0.603	0.004	0.622	0.825	0.992	0.001	7.447
K20B-Amp3-3	3.704	0.002	0.750	0.000	0.614	0.004	0.559	0.770	1.035	0.000	7.437
K20B-Amp3-4	3.690	0.005	0.756	0.002	0.529	0.002	0.652	0.783	1.022	0.000	7.440
K20B-Amp3-5	3.678	0.004	0.788	0.002	0.512	0.001	0.660	0.794	0.974	0.001	7.413
Omphacite-4											
K20B-Amp4-1	3.678	0.005	0.772	0.002	0.532	0.002	0.639	0.804	0.999	0.000	7.432
K20B-Amp4-2	3.691	0.003	0.723	0.000	0.567	0.003	0.646	0.835	0.953	0.000	7.421
K20B-Amp4-3	3.698	0.004	0.777	0.001	0.559	0.003	0.598	0.758	1.027	0.000	7.425
K20B-Amp4-4	3.692	0.004	0.770	0.001	0.519	0.002	0.645	0.782	1.013	0.000	7.427
K20B-Amp4-5	3.695	0.005	0.755	0.001	0.545	0.002	0.635	0.768	1.035	0.000	7.442

WB159		Coordinates		Weight Percent Oxides									
Amphibole-1	X	Y	SiO ₂	TiO ₂	Al ₂ O ₃	Cr ₂ O ₃	FeO*	MnO	MgO	CaO	Na ₂ O	K ₂ O	Total
WB159-AMP1-1	-17428	33015	49.05	0.42	12.73	0.01	12.19	0.02	11.91	6.78	4.53	0.34	97.98
WB159-AMP1-2	-17428	32974	48.68	0.41	12.96	0.00	12.25	0.01	11.88	6.99	4.62	0.34	98.15
WB159-AMP1-3	-17444	32903	47.45	0.43	13.50	0.02	12.52	0.04	11.78	7.34	4.45	0.46	97.99
WB159-AMP1-4	-17444	32837	47.33	0.54	14.14	0.00	12.70	0.03	11.43	6.96	4.86	0.43	98.42
WB159-AMP1-5	-17419	32781	46.58	0.60	14.62	0.02	12.64	0.03	11.21	7.25	4.77	0.47	98.18
WB159-AMP1-6	-17476	32781	46.68	0.56	14.35	0.01	12.67	0.03	11.19	7.42	4.47	0.50	97.89
WB159-AMP1-7	-17450	32692	48.62	0.41	12.91	0.01	12.47	0.04	11.84	6.96	4.54	0.35	98.15
WB159-AMP1-8	-17450	32633	48.57	0.33	12.91	0.01	12.72	0.04	11.65	6.93	4.53	0.32	98.01
WB159-AMP1-9	-17465	32614	49.31	0.29	12.32	0.00	12.30	0.04	11.92	6.88	4.55	0.31	97.91
WB159-AMP1-10	-17506	32802	46.63	0.55	14.45	0.01	13.23	0.04	11.05	7.41	4.61	0.52	98.51
Omphacite-1													
WB159-OMP1-1	-17750	33356	55.76	0.10	10.71	0.00	7.50	0.03	7.17	11.81	7.38	0.01	100.46
WB159-OMP1-2	-17750	33326	55.61	0.12	10.53	0.01	7.43	0.01	7.26	11.80	7.28	0.01	100.05
WB159-OMP1-3	-17750	33260	55.44	0.14	10.94	0.02	7.48	0.04	7.14	11.82	7.20	0.00	100.20
WB159-OMP1-4	-17750	33130	55.80	0.07	10.56	0.03	8.38	0.03	6.63	10.88	7.79	0.01	100.18
WB159-OMP1-5	-17769	33045	55.78	0.11	10.70	0.02	8.12	0.04	6.72	11.00	7.71	0.00	100.20
Omphacite-2													
WB159-OMP2-1	-18412	34113	56.15	0.08	10.53	0.00	7.70	0.03	7.28	11.71	7.46	0.00	100.94
WB159-OMP2-2	-18425	34159	55.97	0.09	10.58	0.01	8.60	0.02	6.47	10.75	8.03	0.00	100.52
WB159-OMP2-3	-18398	34174	56.09	0.09	10.59	0.00	7.35	0.02	7.20	11.69	7.52	0.00	100.56
WB159-OMP2-4	-18398	34208	55.72	0.10	10.01	0.00	7.58	0.02	7.53	12.23	7.17	0.00	100.37
WB159-OMP2-5	-18408	34242	55.72	0.08	10.21	0.01	7.54	0.04	7.43	12.05	7.31	0.00	100.39
Omphacite-3													
WB159-OMP3-1	-18272	34314	55.64	0.06	9.67	0.01	7.94	0.04	7.55	12.15	7.14	0.00	100.20
WB159-OMP3-2	-18272	34355	55.64	0.11	10.52	0.00	7.55	0.01	7.27	11.91	7.24	0.00	100.25
WB159-OMP3-3	-18272	34416	55.71	0.10	10.31	0.01	7.55	0.02	7.46	12.03	7.01	0.00	100.21
WB159-OMP3-4	-18272	34450	55.83	0.10	10.69	0.02	7.28	0.02	7.30	11.85	7.22	0.01	100.30
WB159-OMP3-5	-18272	34486	55.81	0.08	10.50	0.00	7.27	0.03	7.42	11.85	7.30	0.01	100.29
Omphacite-4													
WB159-OMP4-1	-18214	34424	55.62	0.08	10.46	0.00	7.67	0.02	7.44	12.10	7.22	0.00	100.61
WB159-OMP4-2	-18214	34390	55.69	0.10	10.51	0.00	7.50	0.01	7.41	12.17	7.26	0.00	100.65
WB159-OMP4-3	-18209	34366	55.68	0.11	10.60	0.01	7.39	0.03	7.35	11.92	7.34	0.00	100.44
WB159-OMP4-4	-18209	34344	55.64	0.11	10.72	0.01	7.43	0.03	7.17	11.83	7.29	0.00	100.23
WB159-OMP4-5	-18186	34250	55.53	0.09	10.55	0.01	7.50	0.04	7.38	11.78	7.30	0.01	100.19
Amphibole-2													
WB159-AMP2-1	-18042	34497	46.62	0.47	14.17	0.01	12.96	0.06	11.20	7.34	4.41	0.48	97.73
WB159-AMP2-2	-18048	34459	46.22	0.59	14.71	0.01	12.66	0.05	11.10	7.34	4.58	0.49	97.75
WB159-AMP2-3	-17981	34408	48.36	0.39	13.04	0.00	12.26	0.05	11.77	7.07	4.52	0.37	97.82
WB159-AMP2-4	-17987	34332	47.27	0.46	14.01	0.00	12.31	0.02	11.42	7.15	4.55	0.39	97.58
WB159-AMP2-5	-17918	34220	46.91	0.51	14.20	0.01	12.50	0.03	11.29	7.24	4.52	0.44	97.66
WB159-AMP2-6	-17965	34063	48.44	0.42	12.88	0.00	12.20	0.03	11.94	6.86	4.55	0.35	97.67
WB159-AMP2-7	-17933	34039	47.90	0.45	13.53	0.00	12.31	0.03	11.62	7.03	4.53	0.40	97.79
WB159-AMP2-8	-17867	34025	46.93	0.47	14.40	0.01	12.47	0.04	11.14	7.32	4.42	0.49	97.67
WB159-AMP2-9	-18046	33809	47.92	0.47	13.63	0.02	12.15	0.04	11.56	7.00	4.66	0.37	97.84
WB159-AMP2-10	-18046	33710	47.10	0.52	14.12	0.01	12.51	0.02	11.39	7.25	4.62	0.42	97.94

WB159		22 Oxygen + 2(OH) basis		Atomic per Formula Unit							
Amphibole-1	Si	Ti	Al	Cr	Fe	Mn	Mg	Ca	Na	K	Sum
WB159-AMP1-1	7.004	0.045	2.142	0.001	1.456	0.003	2.535	1.037	1.254	0.063	15.539
WB159-AMP1-2	6.952	0.045	2.181	0.000	1.463	0.002	2.530	1.070	1.279	0.062	15.583
WB159-AMP1-3	6.823	0.046	2.288	0.003	1.506	0.005	2.524	1.131	1.240	0.084	15.650
WB159-AMP1-4	6.779	0.058	2.386	0.001	1.521	0.003	2.440	1.068	1.350	0.078	15.685
WB159-AMP1-5	6.700	0.065	2.478	0.003	1.521	0.004	2.404	1.117	1.330	0.086	15.707
WB159-AMP1-6	6.733	0.061	2.439	0.002	1.528	0.004	2.405	1.147	1.249	0.092	15.659
WB159-AMP1-7	6.951	0.044	2.175	0.001	1.491	0.005	2.524	1.065	1.259	0.065	15.579
WB159-AMP1-8	6.959	0.036	2.181	0.001	1.524	0.005	2.488	1.064	1.258	0.059	15.575
WB159-AMP1-9	7.049	0.031	2.075	0.000	1.470	0.005	2.540	1.053	1.261	0.056	15.541
WB159-AMP1-10	6.705	0.060	2.450	0.002	1.591	0.005	2.368	1.142	1.284	0.095	15.701
Omphacite-1	6 Oxygen basis										
WB159-OMP1-1	1.999	0.003	0.452	0.000	0.225	0.001	0.383	0.453	0.513	0.000	4.029
WB159-OMP1-2	2.001	0.003	0.446	0.000	0.224	0.000	0.389	0.455	0.508	0.001	4.027
WB159-OMP1-3	1.992	0.004	0.463	0.001	0.225	0.001	0.382	0.455	0.501	0.000	4.024
WB159-OMP1-4	2.011	0.002	0.449	0.001	0.252	0.001	0.356	0.420	0.545	0.000	4.037
WB159-OMP1-5	2.007	0.003	0.454	0.001	0.244	0.001	0.360	0.424	0.538	0.000	4.033
Omphacite-2	6 Oxygen basis										
WB159-OMP2-1	2.004	0.002	0.443	0.000	0.230	0.001	0.387	0.448	0.516	0.000	4.031
WB159-OMP2-2	2.012	0.002	0.448	0.000	0.259	0.001	0.346	0.414	0.560	0.000	4.042
WB159-OMP2-3	2.006	0.002	0.446	0.000	0.220	0.001	0.384	0.448	0.522	0.000	4.029
WB159-OMP2-4	2.003	0.003	0.424	0.000	0.228	0.001	0.403	0.471	0.500	0.000	4.033
WB159-OMP2-5	2.002	0.002	0.432	0.000	0.227	0.001	0.398	0.464	0.509	0.000	4.035
Omphacite-3	6 Oxygen basis										
WB159-OMP3-1	2.007	0.002	0.411	0.000	0.240	0.001	0.406	0.470	0.500	0.000	4.036
WB159-OMP3-2	1.999	0.003	0.445	0.000	0.227	0.000	0.389	0.459	0.505	0.000	4.027
WB159-OMP3-3	2.002	0.003	0.437	0.000	0.227	0.001	0.399	0.463	0.489	0.000	4.022
WB159-OMP3-4	2.001	0.003	0.452	0.001	0.218	0.001	0.390	0.455	0.501	0.000	4.022
WB159-OMP3-5	2.002	0.002	0.444	0.000	0.218	0.001	0.397	0.455	0.508	0.001	4.028
Omphacite-4	6 Oxygen basis										
WB159-OMP4-1	1.994	0.002	0.442	0.000	0.230	0.000	0.398	0.465	0.502	0.000	4.033
WB159-OMP4-2	1.995	0.003	0.444	0.000	0.225	0.000	0.396	0.467	0.504	0.000	4.033
WB159-OMP4-3	1.997	0.003	0.448	0.000	0.222	0.001	0.393	0.458	0.510	0.000	4.032
WB159-OMP4-4	1.998	0.003	0.454	0.000	0.223	0.001	0.384	0.455	0.507	0.000	4.026
WB159-OMP4-5	1.997	0.003	0.447	0.000	0.226	0.001	0.395	0.454	0.509	0.000	4.032
Amphibole-2	22 Oxygen + 2(OH) basis										
WB159-AMP2-1	6.742	0.052	2.415	0.002	1.568	0.008	2.415	1.138	1.235	0.088	15.662
WB159-AMP2-2	6.680	0.064	2.506	0.002	1.530	0.006	2.391	1.137	1.284	0.091	15.692
WB159-AMP2-3	6.935	0.042	2.204	0.000	1.470	0.006	2.517	1.086	1.256	0.068	15.583
WB159-AMP2-4	6.810	0.050	2.378	0.000	1.483	0.002	2.452	1.104	1.271	0.072	15.623
WB159-AMP2-5	6.767	0.055	2.415	0.003	1.508	0.004	2.428	1.119	1.263	0.081	15.645
WB159-AMP2-6	6.951	0.046	2.179	0.000	1.464	0.004	2.553	1.054	1.264	0.064	15.578
WB159-AMP2-7	6.876	0.049	2.290	0.000	1.478	0.003	2.486	1.081	1.260	0.073	15.597
WB159-AMP2-8	6.766	0.051	2.447	0.001	1.504	0.005	2.394	1.130	1.236	0.089	15.623
WB159-AMP2-9	6.874	0.051	2.304	0.004	1.458	0.005	2.472	1.076	1.295	0.068	15.608
WB159-AMP2-10	6.775	0.056	2.394	0.002	1.504	0.003	2.442	1.117	1.287	0.077	15.656

WB159										
K Numbers (=Ix/Istd)										
Amphibole-1	Na	Mg	Al	Si	K	Ca	Ti	Cr	Mn	Fe
WB159-AMP1-1	0.3281	0.3564	0.3651	0.9059	0.0237	0.5781	0.0106	0.0001	0.0006	0.3977
WB159-AMP1-2	0.3343	0.3550	0.3717	0.8978	0.0235	0.5967	0.0104	0.0000	0.0004	0.3996
WB159-AMP1-3	0.3204	0.3511	0.3869	0.8720	0.0315	0.6273	0.0107	0.0003	0.0011	0.4087
WB159-AMP1-4	0.3506	0.3395	0.4053	0.8673	0.0294	0.5951	0.0135	0.0001	0.0007	0.4147
WB159-AMP1-5	0.3432	0.3330	0.4197	0.8517	0.0323	0.6199	0.0151	0.0003	0.0008	0.4128
WB159-AMP1-6	0.3207	0.3329	0.4126	0.8554	0.0344	0.6345	0.0140	0.0002	0.0008	0.4138
WB159-AMP1-7	0.3278	0.3533	0.3700	0.8967	0.0244	0.5938	0.0103	0.0001	0.0010	0.4068
WB159-AMP1-8	0.3259	0.3468	0.3701	0.8955	0.0223	0.5922	0.0083	0.0001	0.0010	0.4152
WB159-AMP1-9	0.3292	0.3561	0.3530	0.9122	0.0212	0.5866	0.0073	0.0000	0.0011	0.4011
WB159-AMP1-10	0.3291	0.3269	0.4149	0.8540	0.0359	0.6344	0.0139	0.0002	0.0011	0.4323
Omphacite-1										
WB159-OMP1-1	0.5571	0.2146	0.3212	1.0799	0.0004	1.0040	0.0025	0.0000	0.0008	0.2428
WB159-OMP1-2	0.5493	0.2175	0.3157	1.0771	0.0009	1.0031	0.0028	0.0001	0.0003	0.2406
WB159-OMP1-3	0.5426	0.2138	0.3284	1.0726	0.0000	1.0048	0.0034	0.0003	0.0011	0.2422
WB159-OMP1-4	0.5840	0.1964	0.3159	1.0789	0.0006	0.9253	0.0018	0.0004	0.0007	0.2717
WB159-OMP1-5	0.5789	0.1995	0.3204	1.0785	0.0002	0.9358	0.0028	0.0004	0.0011	0.2631
Omphacite-2										
WB159-OMP2-1	0.5624	0.2175	0.3153	1.0884	0.0001	0.9956	0.0020	0.0000	0.0008	0.2495
WB159-OMP2-2	0.6014	0.1909	0.3161	1.0821	0.0000	0.9148	0.0022	0.0002	0.0006	0.2790
WB159-OMP2-3	0.5693	0.2156	0.3177	1.0873	0.0000	0.9935	0.0023	0.0000	0.0005	0.2381
WB159-OMP2-4	0.5398	0.2253	0.2996	1.0815	0.0001	1.0407	0.0024	0.0001	0.0005	0.2455
WB159-OMP2-5	0.5507	0.2223	0.3055	1.0805	0.0000	1.0248	0.0021	0.0001	0.0011	0.2442
Omphacite-3										
WB159-OMP3-1	0.5352	0.2252	0.2886	1.0802	0.0000	1.0340	0.0016	0.0001	0.0010	0.2572
WB159-OMP3-2	0.5458	0.2176	0.3154	1.0779	0.0000	1.0130	0.0027	0.0000	0.0003	0.2446
WB159-OMP3-3	0.5279	0.2236	0.3091	1.0804	0.0002	1.0234	0.0024	0.0002	0.0005	0.2444
WB159-OMP3-4	0.5455	0.2191	0.3210	1.0819	0.0005	1.0067	0.0024	0.0004	0.0005	0.2357
WB159-OMP3-5	0.5524	0.2227	0.3149	1.0816	0.0009	1.0072	0.0020	0.0000	0.0009	0.2353
Omphacite-4										
WB159-OMP4-1	0.5432	0.2226	0.3131	1.0777	0.0001	1.0291	0.0020	0.0000	0.0004	0.2486
WB159-OMP4-2	0.5476	0.2220	0.3150	1.0793	0.0000	1.0350	0.0024	0.0001	0.0004	0.2427
WB159-OMP4-3	0.5544	0.2203	0.3177	1.0785	0.0000	1.0138	0.0027	0.0001	0.0009	0.2394
WB159-OMP4-4	0.5501	0.2148	0.3218	1.0776	0.0003	1.0061	0.0027	0.0001	0.0007	0.2405
WB159-OMP4-5	0.5511	0.2208	0.3160	1.0747	0.0006	1.0016	0.0023	0.0001	0.0010	0.2429
Amphibole-2										
WB159-AMP2-1	0.3153	0.3326	0.4067	0.8539	0.0328	0.6280	0.0119	0.0002	0.0016	0.4234
WB159-AMP2-2	0.3292	0.3298	0.4228	0.8446	0.0340	0.6281	0.0147	0.0002	0.0014	0.4133
WB159-AMP2-3	0.3265	0.3517	0.3741	0.8913	0.0255	0.6033	0.0096	0.0000	0.0014	0.3998
WB159-AMP2-4	0.3288	0.3407	0.4025	0.8669	0.0270	0.6110	0.0116	0.0000	0.0004	0.4018
WB159-AMP2-5	0.3251	0.3363	0.4082	0.8595	0.0305	0.6189	0.0128	0.0003	0.0009	0.4081
WB159-AMP2-6	0.3290	0.3568	0.3692	0.8927	0.0239	0.5853	0.0106	0.0000	0.0009	0.3979
WB159-AMP2-7	0.3272	0.3469	0.3887	0.8807	0.0274	0.6002	0.0113	0.0000	0.0007	0.4017
WB159-AMP2-8	0.3182	0.3321	0.4146	0.8602	0.0335	0.6250	0.0118	0.0002	0.0010	0.4071
WB159-AMP2-9	0.3372	0.3452	0.3916	0.8811	0.0258	0.5979	0.0118	0.0004	0.0011	0.3965
WB159-AMP2-10	0.3327	0.3391	0.4055	0.8634	0.0288	0.6192	0.0129	0.0002	0.0006	0.4082

WB159

Atomic per 11 Oxygen atoms (10 Ox + 2(OH): original software calculation)

Amphibole-1	Si	Ti	Al	Cr	Fe	Mn	Mg	Ca	Na	K	Sum
WB159-AMP1-1	3.350	0.022	1.024	0.001	0.696	0.001	1.213	0.496	0.600	0.030	7.432
WB159-AMP1-2	3.325	0.021	1.043	0.000	0.700	0.001	1.210	0.512	0.612	0.030	7.453
WB159-AMP1-3	3.263	0.022	1.094	0.001	0.720	0.003	1.207	0.541	0.593	0.040	7.485
WB159-AMP1-4	3.242	0.028	1.141	0.000	0.727	0.002	1.167	0.511	0.646	0.037	7.501
WB159-AMP1-5	3.204	0.031	1.185	0.001	0.727	0.002	1.150	0.534	0.636	0.041	7.512
WB159-AMP1-6	3.220	0.029	1.167	0.001	0.731	0.002	1.150	0.548	0.597	0.044	7.489
WB159-AMP1-7	3.325	0.021	1.040	0.000	0.713	0.002	1.207	0.510	0.602	0.031	7.451
WB159-AMP1-8	3.328	0.017	1.043	0.000	0.729	0.002	1.190	0.509	0.602	0.028	7.449
WB159-AMP1-9	3.371	0.015	0.992	0.000	0.703	0.003	1.215	0.504	0.603	0.027	7.433
WB159-AMP1-10	3.207	0.029	1.172	0.001	0.761	0.002	1.132	0.546	0.614	0.046	7.509
Omphacite-1											
WB159-OMP1-1	3.664	0.005	0.829	0.000	0.412	0.002	0.702	0.831	0.940	0.000	7.387
WB159-OMP1-2	3.668	0.006	0.818	0.001	0.410	0.001	0.714	0.834	0.931	0.001	7.384
WB159-OMP1-3	3.652	0.007	0.849	0.001	0.412	0.002	0.701	0.834	0.919	0.000	7.377
WB159-OMP1-4	3.686	0.004	0.822	0.002	0.463	0.002	0.653	0.770	0.998	0.001	7.401
WB159-OMP1-5	3.680	0.006	0.832	0.002	0.448	0.002	0.661	0.778	0.986	0.000	7.393
Omphacite-2											
WB159-OMP2-1	3.674	0.004	0.812	0.000	0.422	0.002	0.710	0.821	0.946	0.000	7.390
WB159-OMP2-2	3.688	0.005	0.821	0.001	0.474	0.001	0.635	0.759	1.027	0.000	7.411
WB159-OMP2-3	3.678	0.005	0.818	0.000	0.403	0.001	0.704	0.821	0.956	0.000	7.387
WB159-OMP2-4	3.672	0.005	0.778	0.000	0.418	0.001	0.739	0.864	0.917	0.000	7.393
WB159-OMP2-5	3.670	0.004	0.792	0.000	0.415	0.002	0.729	0.850	0.933	0.000	7.397
Omphacite-3											
WB159-OMP3-1	3.679	0.003	0.754	0.000	0.439	0.002	0.744	0.861	0.916	0.000	7.399
WB159-OMP3-2	3.665	0.006	0.817	0.000	0.416	0.001	0.714	0.841	0.925	0.000	7.384
WB159-OMP3-3	3.671	0.005	0.801	0.001	0.416	0.001	0.732	0.850	0.896	0.000	7.373
WB159-OMP3-4	3.669	0.005	0.828	0.002	0.400	0.001	0.715	0.834	0.919	0.001	7.374
WB159-OMP3-5	3.670	0.004	0.814	0.000	0.400	0.002	0.728	0.835	0.931	0.001	7.385
Omphacite-4											
WB159-OMP4-1	3.657	0.004	0.810	0.000	0.422	0.001	0.729	0.852	0.920	0.000	7.395
WB159-OMP4-2	3.657	0.005	0.814	0.000	0.412	0.001	0.725	0.856	0.925	0.000	7.394
WB159-OMP4-3	3.661	0.005	0.821	0.001	0.407	0.002	0.721	0.840	0.935	0.000	7.392
WB159-OMP4-4	3.664	0.006	0.832	0.000	0.409	0.001	0.704	0.835	0.930	0.000	7.381
WB159-OMP4-5	3.661	0.005	0.820	0.000	0.414	0.002	0.725	0.832	0.934	0.001	7.392
Amphibole-2											
WB159-AMP2-1	3.225	0.025	1.155	0.001	0.750	0.004	1.155	0.544	0.591	0.042	7.491
WB159-AMP2-2	3.195	0.031	1.199	0.001	0.732	0.003	1.144	0.544	0.614	0.044	7.505
WB159-AMP2-3	3.317	0.020	1.054	0.000	0.703	0.003	1.204	0.519	0.601	0.032	7.453
WB159-AMP2-4	3.257	0.024	1.137	0.000	0.709	0.001	1.173	0.528	0.608	0.034	7.472
WB159-AMP2-5	3.237	0.027	1.155	0.001	0.721	0.002	1.161	0.535	0.604	0.039	7.482
WB159-AMP2-6	3.324	0.022	1.042	0.000	0.700	0.002	1.221	0.504	0.605	0.030	7.451
WB159-AMP2-7	3.289	0.023	1.095	0.000	0.707	0.002	1.189	0.517	0.603	0.035	7.459
WB159-AMP2-8	3.236	0.025	1.170	0.001	0.719	0.002	1.145	0.541	0.591	0.043	7.472
WB159-AMP2-9	3.288	0.024	1.102	0.002	0.697	0.003	1.182	0.515	0.620	0.033	7.465
WB159-AMP2-10	3.240	0.027	1.145	0.001	0.720	0.001	1.168	0.534	0.616	0.037	7.488

WB163													
	Coordinates		Weight Percent Oxides									Total	
	X	Y	SiO ₂	TiO ₂	Al ₂ O ₃	Cr ₂ O ₃	FeO*	MnO	MgO	CaO	Na ₂ O		K ₂ O
Amphibole-1													
WB163-Amp1-1	-6153	24225	37.48	0.06	20.15	0.01	22.05	0.25	4.36	9.13	3.99	1.04	98.52
WB163-Amp1-2	-6178	24225	41.53	0.11	14.67	0.00	21.34	0.16	6.81	8.32	4.40	0.82	98.18
WB163-Amp1-3	-6178	24239	37.61	0.08	20.18	0.00	22.06	0.26	4.37	9.05	4.20	1.00	98.81
WB163-Amp1-4	-6221	24267	40.17	0.08	17.65	0.00	21.16	0.18	5.60	8.40	4.55	1.01	98.80
WB163-Amp1-5	-6279	24310	40.73	0.07	16.54	0.00	21.62	0.18	6.01	8.35	4.59	0.90	99.00
Amphibole-2													
WB163-Amp2-1	-6070	27662	41.09	0.16	15.23	0.00	20.67	0.19	7.37	8.15	4.78	0.88	98.51
WB163-Amp2-2	-6088	27620	40.53	0.13	16.92	0.00	20.10	0.17	6.94	8.24	4.55	0.99	98.57
WB163-Amp2-3	-6013	27513	39.97	0.30	16.46	0.00	21.21	0.19	6.55	8.22	4.68	0.96	98.55
WB163-Amp2-4	-5982	27421	38.44	0.40	17.92	0.00	21.39	0.21	5.79	8.68	4.19	1.10	98.11
WB163-Amp2-5	-5768	27421	41.93	0.17	14.33	0.01	21.12	0.17	7.17	7.75	4.91	0.64	98.19
WB163-Amp2-6	-5698	27367	41.72	0.15	15.20	0.00	20.69	0.18	7.11	7.68	4.80	0.69	98.23
Omphacite-1													
WB163-MS1-1	-5219	27981	56.15	0.08	11.28	0.00	9.65	0.02	5.62	9.44	8.88	0.00	101.13
WB163-MS1-2	-5260	27908	56.23	0.11	11.34	0.00	9.29	0.04	5.53	9.43	8.76	0.01	100.75
WB163-MS1-3	-5297	27880	56.46	0.12	12.05	0.01	9.23	0.00	5.17	8.62	9.21	0.00	100.87
WB163-MS1-4	-5372	27811	56.33	0.10	11.53	0.01	9.41	0.02	5.41	9.27	9.06	0.01	101.15
WB163-MS1-5	-5396	27754	56.38	0.09	11.80	0.01	9.25	0.04	5.36	9.07	9.22	0.00	101.23
Omphacite-2													
WB163-mAmp1-1	-5692	27945	56.20	0.11	10.99	0.00	9.53	0.02	5.81	9.90	8.73	0.00	101.29
WB163-mAmp1-2	-5715	27865	56.02	0.11	11.44	0.00	9.38	0.02	5.59	9.49	9.00	0.00	101.05
WB163-mAmp1-3	-5739	27754	56.14	0.09	10.28	0.01	10.07	0.04	6.14	10.30	8.36	0.00	101.42
WB163-mAmp1-4	-5777	27708	56.21	0.07	10.88	0.00	9.65	0.02	5.88	9.73	8.67	0.00	101.11
WB163-mAmp1-5	-5787	27588	55.97	0.09	10.31	0.00	9.91	0.02	6.11	10.27	8.28	0.01	100.95
White Mica-1													
WB163-WhMica1-1	11805	36570	48.50	0.21	39.66	0.01	1.12	0.02	0.15	0.26	7.10	0.80	97.82
WB163-WhMica1-2	11855	36602	48.33	0.20	39.71	0.01	1.14	0.00	0.15	0.24	7.01	0.91	97.70
WB163-WhMica1-3	11902	36625	48.21	0.18	39.81	0.00	1.04	0.00	0.19	0.21	6.84	1.01	97.49
WB163-WhMica1-4	11978	36697	48.20	0.17	39.75	0.00	1.02	0.00	0.20	0.17	6.80	1.18	97.48
WB163-WhMica1-5	11999	36788	48.17	0.15	39.79	0.00	1.18	0.00	0.20	0.20	6.87	1.09	97.65
White Mica-2													
WB163-WhMica2-1	12256	37519	48.54	0.21	39.38	0.00	1.14	0.00	0.17	0.23	7.04	0.97	97.68
WB163-WhMica2-2	12293	37537	48.43	0.18	39.55	0.01	1.06	0.00	0.18	0.18	6.80	1.14	97.51
WB163-WhMica2-3	12293	37575	48.05	0.19	39.25	0.00	1.11	0.00	0.19	0.17	6.68	1.19	96.83
WB163-WhMica2-4	12320	37594	48.03	0.18	39.77	0.00	1.16	0.00	0.15	0.28	6.96	0.79	97.32
WB163-WhMica2-5	12400	37584	48.73	0.14	39.38	0.00	1.04	0.00	0.16	0.14	7.02	0.82	97.43
White Mica-3													
WB163-WhMica3-1	12686	37115	47.59	0.23	39.41	0.00	1.22	0.00	0.21	0.17	6.80	1.31	96.97
WB163-WhMica3-2	12724	37105	47.63	0.21	39.75	0.01	1.05	0.00	0.17	0.23	7.10	0.90	97.05
WB163-WhMica3-3	12754	37086	47.74	0.21	39.69	0.00	1.07	0.01	0.19	0.23	6.94	1.07	97.14
WB163-WhMica3-4	12842	37086	47.42	0.18	39.55	0.00	1.13	0.01	0.19	0.21	7.07	1.04	96.79
WB163-WhMica3-5	12921	37057	47.53	0.24	39.68	0.00	1.10	0.00	0.21	0.21	6.92	1.11	97.01
White Mica-4													
WB163-WhMica4-1	11717	36889	47.79	0.16	39.52	0.01	1.15	0.00	0.21	0.17	6.92	1.11	97.05
WB163-WhMica4-2	11688	36908	47.76	0.15	39.85	0.00	0.98	0.01	0.17	0.19	6.99	0.98	97.08
WB163-WhMica4-3	11653	36908	47.88	0.15	39.48	0.01	1.03	0.00	0.19	0.16	6.85	1.19	96.94
WB163-WhMica4-4	11626	36908	48.03	0.13	39.65	0.01	1.06	0.00	0.18	0.17	6.98	1.14	97.33
WB163-WhMica4-5	11599	36908	47.88	0.13	39.34	0.00	1.08	0.00	0.17	0.20	7.08	1.08	96.97
Omphacite-2													
WB163-Ms2-1	11939	33476	56.10	0.10	10.39	0.00	9.62	0.02	6.09	10.32	8.55	0.00	101.18
WB163-Ms2-2	11984	33476	56.01	0.11	10.35	0.00	9.65	0.03	6.15	10.48	8.47	0.00	101.24
WB163-Ms2-3	12022	33476	56.07	0.10	10.52	0.00	9.58	0.03	6.05	10.34	8.40	0.00	101.09
WB163-Ms2-4	12079	33523	55.99	0.08	10.05	0.00	9.87	0.01	6.30	10.58	8.28	0.00	101.16
WB163-Ms2-5	12123	33471	56.07	0.10	10.47	0.00	9.69	0.03	6.08	10.25	8.45	0.00	101.13
Omphacite-3													
WB163-Ms3-1	-6158	35723	55.82	0.10	10.28	0.00	9.80	0.04	5.96	10.10	8.54	0.00	100.63
WB163-Ms3-2	-6158	35643	55.94	0.11	10.82	0.01	9.66	0.02	5.82	9.77	8.65	0.00	100.79
WB163-Ms3-3	-6226	35643	55.96	0.11	10.69	0.01	9.70	0.04	5.79	9.72	8.72	0.00	100.74
WB163-Ms3-4	-6145	35476	55.90	0.10	10.39	0.00	9.63	0.00	5.99	10.30	8.47	0.00	100.79
WB163-Ms3-5	-6154	35381	55.81	0.08	10.09	0.00	9.65	0.03	6.28	10.55	8.29	0.00	100.78

WB163		22 Oxygen + 2(OH) basis			Atomic per Formula Unit						
Amphibole-1	Si	Ti	Al	Cr	Fe	Mn	Mg	Ca	Na	K	Sum
WB163-Amp1-1	5.742	0.007	3.639	0.001	2.825	0.033	0.994	1.498	1.185	0.204	16.128
WB163-Amp1-2	5.325	0.013	2.633	0.000	2.718	0.021	1.546	1.358	1.301	0.160	16.076
WB163-Amp1-3	5.743	0.010	3.632	0.000	2.818	0.033	0.995	1.480	1.245	0.194	16.151
WB163-Amp1-4	6.082	0.009	3.150	0.000	2.679	0.024	1.263	1.362	1.336	0.195	16.100
WB163-Amp1-5	6.164	0.008	2.950	0.000	2.737	0.023	1.356	1.355	1.347	0.174	16.114
Amphibole-2	22 Oxygen + 2(OH) basis										
WB163-Amp2-1	6.230	0.018	2.722	0.001	2.621	0.024	1.665	1.323	1.405	0.171	16.179
WB163-Amp2-2	6.120	0.015	3.010	0.000	2.538	0.021	1.562	1.333	1.333	0.191	16.123
WB163-Amp2-3	6.084	0.035	2.952	0.000	2.700	0.024	1.486	1.341	1.380	0.187	16.190
WB163-Amp2-4	5.898	0.046	3.240	0.000	2.744	0.028	1.325	1.426	1.246	0.215	16.168
WB163-Amp2-5	6.370	0.020	2.565	0.002	2.682	0.021	1.623	1.261	1.445	0.124	16.114
WB163-Amp2-6	6.316	0.017	2.713	0.000	2.620	0.023	1.604	1.246	1.409	0.134	16.082
Omphacite-1											
WB163-MS1-1	2.011	0.002	0.476	0.000	0.289	0.000	0.300	0.362	0.617	0.000	4.057
WB163-MS1-2	2.016	0.003	0.479	0.000	0.279	0.001	0.296	0.362	0.609	0.000	4.046
WB163-MS1-3	2.017	0.003	0.507	0.000	0.276	0.000	0.275	0.330	0.638	0.000	4.046
WB163-MS1-4	2.013	0.003	0.486	0.000	0.281	0.001	0.288	0.355	0.628	0.000	4.056
WB163-MS1-5	2.011	0.003	0.496	0.000	0.276	0.001	0.285	0.347	0.638	0.000	4.057
Omphacite-2											
WB163-mAmp1-1	2.011	0.003	0.463	0.000	0.285	0.001	0.310	0.380	0.606	0.000	4.058
WB163-mAmp1-2	2.006	0.003	0.483	0.000	0.281	0.000	0.298	0.364	0.625	0.000	4.062
WB163-mAmp1-3	2.013	0.002	0.434	0.000	0.302	0.001	0.328	0.396	0.581	0.000	4.058
WB163-mAmp1-4	2.014	0.002	0.459	0.000	0.289	0.001	0.314	0.374	0.602	0.000	4.055
WB163-mAmp1-5	2.014	0.003	0.437	0.000	0.298	0.001	0.328	0.396	0.578	0.000	4.054
White Mica-1	10 Oxygen + 2(OH) basis										
WB163-WhMica1-1	3.027	0.010	2.917	0.001	0.059	0.001	0.014	0.017	0.859	0.063	6.967
WB163-WhMica1-2	3.021	0.009	2.926	0.001	0.060	0.000	0.014	0.016	0.849	0.072	6.968
WB163-WhMica1-3	3.018	0.008	2.937	0.000	0.054	0.000	0.018	0.014	0.830	0.081	6.961
WB163-WhMica1-4	3.019	0.008	2.935	0.000	0.053	0.000	0.018	0.011	0.825	0.095	6.965
WB163-WhMica1-5	3.015	0.007	2.935	0.000	0.062	0.000	0.019	0.013	0.834	0.087	6.971
White Mica-2	10 Oxygen + 2(OH) basis										
WB163-WhMica2-1	3.035	0.010	2.902	0.000	0.060	0.000	0.016	0.016	0.853	0.077	6.969
WB163-WhMica2-2	3.032	0.008	2.918	0.001	0.056	0.000	0.017	0.012	0.825	0.091	6.959
WB163-WhMica2-3	3.031	0.009	2.917	0.000	0.059	0.000	0.018	0.012	0.817	0.096	6.958
WB163-WhMica2-4	3.012	0.009	2.940	0.000	0.061	0.000	0.014	0.019	0.847	0.064	6.964
WB163-WhMica2-5	3.048	0.007	2.903	0.000	0.054	0.000	0.015	0.009	0.852	0.065	6.953
White Mica-3	10 Oxygen + 2(OH) basis										
WB163-WhMica3-1	3.006	0.011	2.934	0.000	0.065	0.000	0.020	0.012	0.832	0.106	6.986
WB163-WhMica3-2	2.999	0.010	2.951	0.001	0.055	0.000	0.016	0.016	0.867	0.073	6.986
WB163-WhMica3-3	3.004	0.010	2.944	0.000	0.057	0.000	0.018	0.015	0.846	0.086	6.980
WB163-WhMica3-4	2.998	0.008	2.947	0.000	0.060	0.000	0.018	0.014	0.866	0.084	6.996
WB163-WhMica3-5	2.997	0.012	2.949	0.000	0.058	0.000	0.020	0.014	0.846	0.090	6.985
White Mica-4	10 Oxygen + 2(OH) basis										
WB163-WhMica4-1	3.011	0.008	2.935	0.001	0.061	0.000	0.020	0.012	0.846	0.089	6.982
WB163-WhMica4-2	3.004	0.007	2.954	0.000	0.051	0.001	0.016	0.013	0.853	0.079	6.978
WB163-WhMica4-3	3.019	0.007	2.933	0.001	0.054	0.000	0.018	0.011	0.837	0.096	6.975
WB163-WhMica4-4	3.016	0.006	2.935	0.000	0.056	0.000	0.016	0.011	0.850	0.091	6.981
WB163-WhMica4-5	3.019	0.006	2.924	0.000	0.057	0.000	0.016	0.014	0.866	0.087	6.989
Omphacite-2	6 Oxygen basis										
WB163-Ms2-1	2.013	0.003	0.439	0.000	0.289	0.001	0.326	0.397	0.595	0.000	4.062
WB163-Ms2-2	2.010	0.003	0.438	0.000	0.289	0.001	0.329	0.403	0.589	0.000	4.063
WB163-Ms2-3	2.012	0.003	0.445	0.000	0.288	0.001	0.324	0.398	0.584	0.000	4.054
WB163-Ms2-4	2.013	0.002	0.426	0.000	0.297	0.000	0.337	0.408	0.577	0.000	4.061
WB163-Ms2-5	2.013	0.003	0.443	0.000	0.291	0.001	0.325	0.394	0.588	0.000	4.058
Omphacite-3	6 Oxygen basis										
WB163-Ms3-1	2.016	0.003	0.438	0.000	0.296	0.001	0.321	0.391	0.598	0.000	4.062
WB163-Ms3-2	2.013	0.003	0.459	0.000	0.291	0.001	0.312	0.377	0.603	0.000	4.057
WB163-Ms3-3	2.015	0.003	0.454	0.000	0.292	0.001	0.311	0.375	0.609	0.000	4.060
WB163-Ms3-4	2.014	0.003	0.441	0.000	0.290	0.000	0.322	0.398	0.592	0.000	4.059
WB163-Ms3-5	2.013	0.002	0.429	0.000	0.291	0.001	0.337	0.408	0.580	0.000	4.060

WB163		K Numbers (=Ix/Istd)								
Amphibole-1	Na	Mg	Al	Si	K	Ca	Ti	Cr	Mn	Fe
WB163-Amp1-1	0.2562	0.1196	0.5800	0.6681	0.0737	0.7950	0.0016	0.0001	0.0069	0.7302
WB163-Amp1-2	0.2857	0.1875	0.4144	0.7539	0.0579	0.7232	0.0029	0.0000	0.0043	0.7055
WB163-Amp1-3	0.2704	0.1199	0.5803	0.6701	0.0704	0.7882	0.0022	0.0000	0.0070	0.7307
WB163-Amp1-4	0.2964	0.1544	0.5046	0.7230	0.0711	0.7293	0.0019	0.0000	0.0049	0.6997
WB163-Amp1-5	0.2978	0.1651	0.4699	0.7352	0.0635	0.7262	0.0018	0.0000	0.0049	0.7153
Amphibole-2										
WB163-Amp2-1	0.3132	0.2035	0.4296	0.7426	0.0621	0.7069	0.0041	0.0001	0.0050	0.6828
WB163-Amp2-2	0.3002	0.1931	0.4812	0.7296	0.0695	0.7141	0.0033	0.0000	0.0045	0.6637
WB163-Amp2-3	0.3045	0.1803	0.4658	0.7195	0.0678	0.7147	0.0077	0.0000	0.0051	0.7015
WB163-Amp2-4	0.2708	0.1594	0.5104	0.6887	0.0774	0.7550	0.0101	0.0000	0.0058	0.7075
WB163-Amp2-5	0.3201	0.1970	0.4031	0.7603	0.0449	0.6728	0.0044	0.0002	0.0045	0.6979
WB163-Amp2-6	0.3147	0.1964	0.4295	0.7545	0.0486	0.6664	0.0039	0.0000	0.0048	0.6836
Omphacite-1										
WB163-MS1-1	0.6618	0.1637	0.3366	1.0806	0.0000	0.8032	0.0020	0.0000	0.0004	0.3137
WB163-MS1-2	0.6542	0.1617	0.3392	1.0831	0.0008	0.8020	0.0027	0.0000	0.0012	0.3018
WB163-MS1-3	0.6917	0.1509	0.3611	1.0843	0.0001	0.7330	0.0029	0.0002	0.0000	0.2998
WB163-MS1-4	0.6775	0.1578	0.3445	1.0838	0.0005	0.7886	0.0024	0.0002	0.0006	0.3059
WB163-MS1-5	0.6914	0.1563	0.3531	1.0837	0.0003	0.7712	0.0023	0.0001	0.0010	0.3006
Omphacite-2										
WB163-mAmp1-1	0.6500	0.1697	0.3276	1.0835	0.0001	0.8431	0.0026	0.0000	0.0005	0.3097
WB163-mAmp1-2	0.6728	0.1630	0.3416	1.0773	0.0001	0.8073	0.0028	0.0000	0.0004	0.3048
WB163-mAmp1-3	0.6172	0.1789	0.3052	1.0846	0.0000	0.8780	0.0021	0.0002	0.0009	0.3273
WB163-mAmp1-4	0.6449	0.1714	0.3241	1.0835	0.0003	0.8286	0.0017	0.0000	0.0006	0.3135
WB163-mAmp1-5	0.6119	0.1781	0.3063	1.0810	0.0004	0.8750	0.0023	0.0000	0.0005	0.3221
White Mica-1										
WB163-WhMica1-1	0.6106	0.0050	1.3534	0.8432	0.0529	0.0215	0.0052	0.0001	0.0004	0.0362
WB163-WhMica1-2	0.6024	0.0048	1.3560	0.8400	0.0604	0.0201	0.0049	0.0001	0.0000	0.0368
WB163-WhMica1-3	0.5888	0.0064	1.3613	0.8375	0.0674	0.0171	0.0044	0.0000	0.0000	0.0335
WB163-WhMica1-4	0.5848	0.0065	1.3598	0.8378	0.0787	0.0139	0.0042	0.0000	0.0001	0.0328
WB163-WhMica1-5	0.5906	0.0067	1.3591	0.8368	0.0722	0.0162	0.0037	0.0000	0.0000	0.0381
White Mica-2										
WB163-WhMica2-1	0.6048	0.0056	1.3437	0.8450	0.0644	0.0194	0.0051	0.0000	0.0000	0.0369
WB163-WhMica2-2	0.5844	0.0060	1.3524	0.8429	0.0756	0.0148	0.0043	0.0001	0.0000	0.0343
WB163-WhMica2-3	0.5738	0.0065	1.3413	0.8358	0.0790	0.0145	0.0046	0.0000	0.0000	0.0358
WB163-WhMica2-4	0.5985	0.0049	1.3578	0.8332	0.0528	0.0234	0.0045	0.0000	0.0000	0.0373
WB163-WhMica2-5	0.6048	0.0053	1.3451	0.8480	0.0545	0.0115	0.0035	0.0000	0.0000	0.0335
White Mica-3										
WB163-WhMica3-1	0.5826	0.0071	1.3445	0.8266	0.0874	0.0144	0.0058	0.0001	0.0000	0.0395
WB163-WhMica3-2	0.6114	0.0056	1.3558	0.8252	0.0600	0.0195	0.0050	0.0002	0.0000	0.0338
WB163-WhMica3-3	0.5967	0.0064	1.3547	0.8283	0.0712	0.0188	0.0051	0.0000	0.0002	0.0347
WB163-WhMica3-4	0.6079	0.0062	1.3477	0.8216	0.0692	0.0174	0.0043	0.0000	0.0002	0.0366
WB163-WhMica3-5	0.5946	0.0071	1.3539	0.8241	0.0742	0.0172	0.0060	0.0000	0.0000	0.0356
White Mica-4										
WB163-WhMica4-1	0.5948	0.0069	1.3483	0.8295	0.0739	0.0142	0.0040	0.0002	0.0000	0.0372
WB163-WhMica4-2	0.6029	0.0056	1.3611	0.8280	0.0653	0.0155	0.0037	0.0000	0.0003	0.0315
WB163-WhMica4-3	0.5893	0.0064	1.3490	0.8317	0.0793	0.0130	0.0036	0.0001	0.0000	0.0331
WB163-WhMica4-4	0.6007	0.0058	1.3541	0.8342	0.0755	0.0140	0.0033	0.0001	0.0000	0.0341
WB163-WhMica4-5	0.6094	0.0058	1.3414	0.8315	0.0718	0.0170	0.0031	0.0000	0.0000	0.0350
Omphacite-2										
WB163-MS2-1	0.6344	0.1776	0.3089	1.0836	0.0000	0.8791	0.0025	0.0000	0.0005	0.3126
WB163-MS2-2	0.6282	0.1794	0.3078	1.0820	0.0000	0.8930	0.0028	0.0000	0.0007	0.3134
WB163-MS2-3	0.6230	0.1769	0.3134	1.0830	0.0000	0.8808	0.0025	0.0000	0.0008	0.3114
WB163-MS2-4	0.6123	0.1837	0.2982	1.0826	0.0000	0.9020	0.0020	0.0000	0.0002	0.3208
WB163-MS2-5	0.6269	0.1775	0.3114	1.0826	0.0000	0.8731	0.0024	0.0000	0.0007	0.3148
Omphacite-3										
WB163-MS3-1	0.6322	0.1734	0.3055	1.0773	0.0001	0.8607	0.0024	0.0000	0.0009	0.3184
WB163-MS3-2	0.6425	0.1696	0.3221	1.0780	0.0000	0.8320	0.0026	0.0002	0.0006	0.3139
WB163-MS3-3	0.6476	0.1684	0.3182	1.0785	0.0000	0.8283	0.0027	0.0001	0.0011	0.3153
WB163-MS3-4	0.6286	0.1748	0.3092	1.0794	0.0000	0.8780	0.0025	0.0000	0.0000	0.3128
WB163-MS3-5	0.6139	0.1832	0.2996	1.0787	0.0002	0.8991	0.0021	0.0000	0.0008	0.3133

WB163											
Atomic per 11 Oxygen atoms (10 O _x + 2(OH): original software calculation)											
	Si	Ti	Al	Cr	Fe	Mn	Mg	Ca	Na	K	Sum
Amphibole-1											
WB163-Amp1-1	2.746	0.003	1.740	0.001	1.351	0.016	0.476	0.716	0.567	0.098	7.713
WB163-Amp1-2	3.025	0.006	1.259	0.000	1.300	0.010	0.740	0.650	0.622	0.077	7.689
WB163-Amp1-3	2.747	0.005	1.737	0.000	1.348	0.016	0.476	0.708	0.595	0.093	7.724
WB163-Amp1-4	2.909	0.004	1.507	0.000	1.281	0.011	0.604	0.652	0.639	0.093	7.700
WB163-Amp1-5	2.948	0.004	1.411	0.000	1.309	0.011	0.649	0.648	0.644	0.083	7.707
Amphibole-2											
WB163-Amp2-1	2.979	0.009	1.302	0.000	1.253	0.011	0.796	0.633	0.672	0.082	7.738
WB163-Amp2-2	2.927	0.007	1.440	0.000	1.214	0.010	0.747	0.637	0.638	0.091	7.711
WB163-Amp2-3	2.910	0.017	1.412	0.000	1.291	0.012	0.711	0.641	0.660	0.090	7.743
WB163-Amp2-4	2.821	0.022	1.550	0.000	1.312	0.013	0.634	0.682	0.596	0.103	7.732
WB163-Amp2-5	3.047	0.010	1.227	0.001	1.283	0.010	0.776	0.603	0.691	0.059	7.707
WB163-Amp2-6	3.021	0.008	1.297	0.000	1.253	0.011	0.767	0.596	0.674	0.064	7.691
Omphacite-1											
WB163-MS1-1	3.686	0.004	0.873	0.000	0.530	0.001	0.550	0.664	1.131	0.000	7.439
WB163-MS1-2	3.697	0.006	0.879	0.000	0.511	0.003	0.542	0.664	1.116	0.001	7.417
WB163-MS1-3	3.697	0.006	0.930	0.001	0.505	0.000	0.505	0.605	1.169	0.000	7.418
WB163-MS1-4	3.691	0.005	0.890	0.001	0.516	0.001	0.529	0.651	1.151	0.001	7.436
WB163-MS1-5	3.688	0.005	0.910	0.001	0.506	0.002	0.522	0.635	1.169	0.000	7.438
Omphacite-2											
WB163-mAmp1-1	3.686	0.005	0.849	0.000	0.523	0.001	0.569	0.696	1.110	0.000	7.439
WB163-mAmp1-2	3.678	0.006	0.886	0.000	0.515	0.001	0.547	0.667	1.146	0.000	7.446
WB163-mAmp1-3	3.691	0.004	0.796	0.001	0.554	0.002	0.602	0.725	1.066	0.000	7.440
WB163-mAmp1-4	3.693	0.003	0.842	0.000	0.530	0.001	0.575	0.685	1.104	0.000	7.435
WB163-mAmp1-5	3.693	0.005	0.801	0.000	0.547	0.001	0.601	0.726	1.059	0.001	7.432
White Mica-1											
WB163-WhMica1-1	3.027	0.010	2.917	0.001	0.059	0.001	0.014	0.017	0.859	0.063	6.967
WB163-WhMica1-2	3.021	0.009	2.926	0.001	0.060	0.000	0.014	0.016	0.849	0.072	6.968
WB163-WhMica1-3	3.018	0.008	2.937	0.000	0.054	0.000	0.018	0.014	0.830	0.081	6.961
WB163-WhMica1-4	3.019	0.008	2.935	0.000	0.053	0.000	0.018	0.011	0.825	0.095	6.965
WB163-WhMica1-5	3.015	0.007	2.935	0.000	0.062	0.000	0.019	0.013	0.834	0.087	6.971
White Mica-2											
WB163-WhMica2-1	3.035	0.010	2.902	0.000	0.060	0.000	0.016	0.016	0.853	0.077	6.969
WB163-WhMica2-2	3.032	0.008	2.918	0.001	0.056	0.000	0.017	0.012	0.825	0.091	6.959
WB163-WhMica2-3	3.031	0.009	2.917	0.000	0.059	0.000	0.018	0.012	0.817	0.096	6.958
WB163-WhMica2-4	3.012	0.009	2.940	0.000	0.061	0.000	0.014	0.019	0.847	0.064	6.964
WB163-WhMica2-5	3.048	0.007	2.903	0.000	0.054	0.000	0.015	0.009	0.852	0.065	6.953
White Mica-3											
WB163-WhMica3-1	3.006	0.011	2.934	0.000	0.065	0.000	0.020	0.012	0.832	0.106	6.986
WB163-WhMica3-2	2.999	0.010	2.951	0.001	0.055	0.000	0.016	0.016	0.867	0.073	6.986
WB163-WhMica3-3	3.004	0.010	2.944	0.000	0.057	0.000	0.018	0.015	0.846	0.086	6.980
WB163-WhMica3-4	2.998	0.008	2.947	0.000	0.060	0.000	0.018	0.014	0.866	0.084	6.996
WB163-WhMica3-5	2.997	0.012	2.949	0.000	0.058	0.000	0.020	0.014	0.846	0.090	6.985
White Mica-4											
WB163-WhMica4-1	3.011	0.008	2.935	0.001	0.061	0.000	0.020	0.012	0.846	0.089	6.982
WB163-WhMica4-2	3.004	0.007	2.954	0.000	0.051	0.001	0.016	0.013	0.853	0.079	6.978
WB163-WhMica4-3	3.019	0.007	2.933	0.001	0.054	0.000	0.018	0.011	0.837	0.096	6.975
WB163-WhMica4-4	3.016	0.006	2.935	0.000	0.056	0.000	0.016	0.011	0.850	0.091	6.981
WB163-WhMica4-5	3.019	0.006	2.924	0.000	0.057	0.000	0.016	0.014	0.866	0.087	6.989
Omphacite-2											
WB163-Ms2-1	3.691	0.005	0.805	0.000	0.529	0.001	0.597	0.727	1.090	0.000	7.447
WB163-Ms2-2	3.685	0.006	0.803	0.000	0.531	0.001	0.603	0.739	1.081	0.000	7.448
WB163-Ms2-3	3.689	0.005	0.816	0.000	0.527	0.002	0.594	0.729	1.071	0.000	7.433
WB163-Ms2-4	3.691	0.004	0.780	0.000	0.544	0.001	0.619	0.747	1.059	0.000	7.444
WB163-Ms2-5	3.690	0.005	0.812	0.000	0.533	0.002	0.597	0.723	1.079	0.000	7.439
Omphacite-3											
WB163-Ms3-1	3.695	0.005	0.802	0.000	0.543	0.002	0.588	0.716	1.096	0.000	7.447
WB163-Ms3-2	3.690	0.005	0.841	0.001	0.533	0.001	0.572	0.690	1.106	0.000	7.439
WB163-Ms3-3	3.694	0.005	0.832	0.001	0.536	0.002	0.569	0.688	1.116	0.000	7.443
WB163-Ms3-4	3.692	0.005	0.809	0.000	0.532	0.000	0.590	0.729	1.085	0.000	7.442
WB163-Ms3-5	3.690	0.004	0.786	0.000	0.533	0.002	0.619	0.747	1.063	0.000	7.444

WB137 - Garnet Composition Data

Results in Oxide Weight Percent

Traverse Point	SiO ₂	Al ₂ O ₃	MgO	CaO	MnO	FeO	Sum
Garnet 1, Traverse 1							
36	38.545	22.19	7.734	4.103	0.961	25.964	99.497
37	38.344	22.134	7.417	4.925	0.864	25.725	99.409
38	38.082	22.036	6.609	5.092	0.773	27.224	99.816
39	37.984	21.821	6.031	5.031	0.624	28.031	99.521
40	38.107	21.671	5.754	5.266	0.6	27.835	99.233
41	2.465	1.721	0.308	0.709	0.054	2.53	7.787
42	37.829	21.933	5.843	5.03	0.598	28.168	99.401
43	38.206	22.007	5.894	5.149	0.583	28.047	99.885
44	38.042	21.935	5.887	5.292	0.622	27.899	99.677
45	37.949	21.996	5.988	5.273	0.716	27.269	99.192
46	37.654	21.525	5.576	5.456	0.803	27.832	98.845
47	19.015	14.676	2.038	4.048	0.73	24.71	65.217
48	37.749	21.953	5.219	5.433	1.131	28.194	99.678
49	38.114	21.881	5.154	5.312	1.208	28.445	100.114
50	38.064	21.906	5.026	5.523	1.229	28.193	99.941
51	37.984	21.876	4.98	5.702	1.212	28.026	99.779
52	38.048	21.862	5.144	5.25	1.263	28.542	100.108
53	37.537	21.699	5.298	5.123	1.142	28.234	99.034
54	37.997	21.817	5.56	5.114	0.971	27.938	99.396
55	38.079	21.734	5.642	5.423	0.791	27.328	98.996
56	38.01	21.766	5.826	5.268	0.669	27.614	99.153
57	100.13	-0.011	-0.003	-0.002	0.012	0.245	100.371
58	37.804	21.813	5.777	5.119	0.629	27.776	98.919
59	40.256	27.281	1.81	1.944	0.215	12.158	83.664
60	38.3	21.949	6.195	4.941	0.625	27.93	99.94
61	100.236	0.01	-0.002	0.029	0.031	0.52	100.823
62	100.037	-0.001	-0.009	0.014	0.02	0.405	100.465
63	41.376	20.291	3.584	5.353	1.823	28.055	100.482
64	47.784	33.037	1.371	0.038	0.018	3.13	85.378
65	38.737	22.531	7.708	4.502	0.931	25.928	100.336
Garnet 1, Traverse 2							
66	38.355	21.768	6.331	5.095	0.824	27.321	99.694
67	38.375	21.907	5.812	5.763	0.721	27.668	100.245
68	38.836	22.329	7.431	5.733	0.679	26.001	101.008
69	38.353	21.736	6.186	6.261	0.705	26.328	99.571
70	98.946	0.459	0.044	0.071	0.02	0.57	100.11
71	43.248	16.945	12.083	0.048	0.112	17.507	89.942
72	38.072	21.835	5.908	5.309	0.599	27.691	99.414
73	39.164	23.319	6.279	4.75	0.628	27.839	101.979
74	38.015	21.889	5.883	4.645	0.618	28.582	99.632
75	100.195	0.025	-0.004	0.019	0.028	0.447	100.709
76	37.912	21.983	5.97	5.236	0.677	27.763	99.54
77	100.539	0.026	0	0.011	0.002	0.31	100.888
78	38.012	22.01	6.196	5.6	0.75	27.219	99.788
79	90.178	1.203	0.205	0.326	0.095	1.756	93.764
80	38.102	21.828	5.63	5.795	0.961	27.619	99.935
81	37.774	21.803	5.189	5.453	1.149	28.648	100.016
82	37.976	21.957	5.302	5.141	1.154	28.589	100.12
83	37.707	21.696	5.211	5.444	1.075	27.986	99.12
84	38.143	21.948	5.412	5.311	1.095	28.171	100.08
85	32.985	18.831	1.291	3.991	1.052	28.381	86.532
86	37.636	21.752	5.806	4.577	1.056	28.529	99.355
87	99.939	-0.012	0.007	-0.004	0.02	0.359	100.31
88	99.918	-0.017	-0.001	0.001	-0.004	0.133	100.029
89	97.31	0.392	0.074	0.11	0.013	0.832	98.732
90	37.962	21.838	6.438	4.261	0.65	28.014	99.164
91	38.006	22.055	5.969	4.916	0.581	28.201	99.729
92	37.963	21.996	5.908	4.987	0.526	28.329	99.709
93	38.007	22.008	6.127	5.168	0.52	27.873	99.703
94	38.255	21.956	6.55	5.02	0.553	27.5	99.833
95	38.842	22.135	6.511	5.354	0.604	27.099	100.545

WB137 - Garnet Composition Data

Results in Oxide Weight Percent

Traverse Point	SiO ₂	Al ₂ O ₃	MgO	CaO	MnO	FeO	Sum
Garnet 2, Traverse 1							
96	38.985	22.466	8.205	4.458	0.582	25.655	100.35
97	39.026	22.661	7.421	4.143	0.494	27.432	101.178
98	38.433	22.198	6.98	4.001	0.467	28.083	100.162
99	38.273	21.98	6.371	5.184	0.415	27.619	99.842
100	38.29	21.894	6.281	4.833	0.463	28.091	99.853
101	37.904	21.921	6.365	4.591	0.438	28.525	99.744
102	38.621	22.299	6.397	4.614	0.478	28.285	100.694
103	37.972	22.165	6.325	4.844	0.53	27.981	99.817
104	37.942	21.99	6.066	5.098	0.535	27.785	99.417
105	37.968	21.971	6.071	4.792	0.599	28.136	99.537
106	38.074	22.105	5.956	4.604	0.665	28.848	100.252
107	38.03	21.815	5.665	5.055	0.736	28.519	99.819
108	37.908	21.798	5.417	5.524	0.792	28.025	99.463
109	38.506	22.093	5.308	5.725	0.863	28.611	101.107
110	38.111	21.695	5.339	5.583	0.844	27.982	99.554
111	37.878	21.71	5.213	5.213	0.983	28.466	99.464
112	38.045	21.765	5.11	5.198	1.161	28.698	99.978
113	46.511	39.819	0.102	0.335	0.014	1.271	88.052
114	100.714	0.003	-0.002	0.01	0.016	0.525	101.265
115	38.03	21.643	4.745	5.747	1.382	28.584	100.131
116	37.716	21.741	4.704	5.361	1.535	28.776	99.834
117	37.889	21.69	4.645	5.478	1.708	28.634	100.044
118	31.111	17.832	1.068	11.425	0.154	11.156	72.745
119	37.838	21.585	4.589	5.893	1.83	28.094	99.828
120	38.906	22.453	5.214	5.191	1.867	28.004	101.635
121	38.05	21.747	5.064	5.83	1.68	27.614	99.986
122	100.726	0.02	-0.002	0.022	0.033	0.474	101.274
123	39.09	22.194	5.043	5.112	1.666	28.1	101.205
124	38.168	21.718	5.031	5.517	1.459	28.751	100.643
125	37.917	21.734	4.338	5.772	2.743	27.566	100.07
126	37.937	21.425	4.317	5.762	2.737	27.443	99.621
127	38.339	21.923	3.998	5.478	2.737	26.531	99.006
128	37.793	21.517	4.475	6.019	2.5	27.474	99.778
129	38.023	21.675	4.705	5.64	2.389	27.475	99.907
130	37.838	21.458	4.208	5.574	2.86	27.948	99.886
131	37.616	21.345	4.081	5.717	2.907	28.045	99.711
132	36.977	24.602	0.096	20.251	0.296	11.056	93.277
133	37.605	21.715	4.053	5.662	2.752	27.824	99.611
134	37.576	21.404	4.071	5.661	2.776	27.963	99.451
135	37.732	21.625	4.199	5.496	2.795	28.193	100.039
136	37.841	21.243	4.102	5.616	2.711	28.456	99.969
137	37.866	21.477	4.09	5.499	2.766	28.361	100.059
138	37.622	21.269	4.061	5.615	2.697	27.882	99.145
139	37.702	21.46	4.088	5.748	2.71	27.629	99.337
140	37.605	21.554	4.106	5.747	2.703	28.012	99.727
141	37.472	21.362	4.229	5.841	2.505	27.541	98.95
142	37.753	21.58	5.009	5.57	2.082	27.402	99.396
143	37.708	21.632	4.876	5.767	2.107	27.478	99.567
144	51.458	18.743	5.293	4.136	1.274	23.832	104.735
145	100.19	0.065	0.004	0.034	0.036	0.53	100.86
146	100.375	0.111	0.034	0.04	0.009	0.522	101.09
147	37.785	21.593	5.486	5.865	1.495	27.156	99.38
148	85.332	0.929	0.278	0.255	0.048	0.956	87.798
149	37.828	20.32	6.134	5.625	1.179	26.244	97.33
150	38.129	21.905	5.264	5.959	1.124	27.355	99.736
151	37.923	21.756	5.243	5.634	1.08	28.084	99.72
152	38.194	21.827	5.71	5.656	0.859	27.403	99.65
153	38.636	21.992	6.561	5.884	0.827	25.982	99.882
154	38.279	21.956	6.2	5.483	0.782	27.021	99.721
155	38.17	21.802	5.715	5.734	0.658	27.455	99.533
156	100.3	0.01	-0.015	0.019	0.005	0.507	100.826
157	38.175	21.893	6.207	5.265	0.54	26.762	98.841
158	38.873	22.457	6.723	5.257	0.52	26.673	100.503
159	38.573	22.232	7.172	5.001	0.744	25.767	99.488
160	99.338	0.008	-0.017	0.009	-0.01	0.29	99.619
161	100.119	-0.008	-0.005	0.01	0.004	0.399	100.521
162	40.345	23.128	6.14	4.285	0.389	23.062	97.349
163	38.654	22.074	7.08	4.676	0.42	27.026	99.93
164	37.973	21.729	7.33	4.478	0.401	26.031	97.943
165	38.514	22.169	8.047	4.342	0.434	25.909	99.415

WB137 - Garnet Composition Data

Results in Oxide Weight Percent

Traverse Poin	SiO ₂	Al ₂ O ₃	MgO	CaO	MnO	FeO	Sum
Garnet 2, Traverse 2							
166	38.963	22.219	8.051	3.639	0.684	26.841	100.397
167	38.552	22.081	7.571	4.95	0.574	25.925	99.653
168	99.871	0.024	-0.011	0.011	-0.005	0.423	100.312
169	98.123	-0.003	-0.029	0.011	0	0.348	98.449
170	38.01	21.921	6.521	5.811	0.51	26.318	99.091
171	100.052	0.004	-0.012	0.009	-0.004	0.358	100.407
172	38.064	21.946	6.783	4.817	0.637	27.037	99.284
173	37.843	21.883	6.393	4.247	0.628	28.32	99.315
174	37.923	21.862	5.927	4.649	0.665	28.425	99.451
175	37.486	21.547	5.525	5.385	0.742	27.515	98.2
176	37.42	21.848	5.438	5.274	0.868	28.298	99.146
177	37.566	21.696	5.375	4.869	0.905	28.495	98.905
178	37.323	21.566	4.969	5.732	0.992	28.163	98.745
179	34.007	19.643	4.169	4.664	1.01	25.686	89.178
180	30.107	17.302	4.012	4.797	1.232	28.475	85.926
181	37.287	21.855	4.759	5.675	1.256	28.213	99.045
182	37.352	21.717	4.911	4.576	1.491	29.079	99.128
183	37.582	21.554	4.676	5.262	1.635	28.604	99.313
184	37.683	21.656	4.463	6.317	1.657	27.971	99.747
185	37.526	21.488	4.508	5.858	1.712	27.77	98.861
186	37.748	21.715	5.011	5.522	1.629	27.566	99.191
187	98.775	0.006	-0.012	0.001	0.019	0.241	99.03
188	98.854	0.012	-0.023	0.006	0.01	0.105	98.963
189	96.301	0.016	-0.014	0.009	0.009	0.191	96.512
190	3.713	2.113	0.363	0.805	0.207	3.429	10.63
191	99.601	0.025	-0.014	0.006	0.036	0.218	99.872
192	37.784	21.365	4.347	5.399	2.607	27.634	99.136
193	37.842	21.612	4.774	5.85	2.181	27.083	99.342
194	37.451	21.52	4.291	5.908	2.779	27.562	99.512
195	37.789	21.377	4.306	5.559	2.897	27.576	99.504
196	99.862	0.019	-0.023	0.005	0.007	0.242	100.113
197	43.851	19.174	4.591	3.659	2.233	27.925	101.434
198	37.539	21.478	4.291	5.606	2.85	27.532	99.295
199	37.653	21.74	4.742	4.62	2.654	28.157	99.567
200	36.465	23.478	0.155	19.42	0.421	10.927	90.866
201	37.605	21.361	4.056	5.75	2.635	27.658	99.065
202	37.589	21.297	4.048	5.495	2.941	27.654	99.024
203	37.522	21.575	4.206	5.325	2.453	28.245	99.326
204	37.467	21.43	4.125	5.595	2.554	27.969	99.141
205	37.52	21.502	4.186	5.362	2.525	28.526	99.622
206	37.459	21.297	4.176	5.649	2.426	28.234	99.24
207	37.525	21.455	4.394	5.676	2.232	27.978	99.261
208	24.276	21.888	15.697	0.036	0.188	20.911	82.997
209	38.079	21.907	4.533	5.613	2.11	28.315	100.556
210	37.599	21.56	4.331	5.512	2.107	28.734	99.843
211	37.372	21.325	4.515	5.401	2.006	28.246	98.865
212	37.833	21.465	4.559	5.888	2.072	27.515	99.333
213	37.788	21.515	4.525	5.962	1.972	27.853	99.616
214	37.75	21.391	4.407	5.593	1.859	28.453	99.452
215	37.897	21.606	4.537	5.697	1.836	28.083	99.654
216	100.454	0.015	-0.023	0.018	-0.012	0.462	100.914
217	38.099	21.553	4.517	6.189	1.635	27.843	99.836
218	100.239	0.021	-0.019	0.033	0.031	0.622	100.927
219	37.767	21.676	4.472	5.845	1.692	28.17	99.622
220	37.938	21.58	4.59	5.604	1.658	28.315	99.685
221	100.082	0.005	-0.016	0.028	0.013	0.593	100.705
222	37.973	21.805	5.503	5.845	1.496	27.176	99.798
223	36.593	21.098	6.14	5.415	1.009	25.013	95.267
224	37.804	21.657	4.733	5.579	1.475	28.414	99.661
225	37.747	21.59	4.898	5.523	1.388	28.334	99.48
226	37.72	21.707	4.858	5.489	1.308	28.333	99.415
227	37.957	21.671	4.998	5.279	1.186	28.539	99.63
228	37.866	21.587	5.075	5.355	1.044	28.497	99.425
229	38.028	21.768	5.216	5.433	0.925	28.236	99.607
230	37.924	21.797	5.288	5.446	0.848	28.547	99.849
231	26.508	25.153	15.482	0.081	0.113	22.33	89.666
232	47.854	38.374	0.35	0.127	0.013	2.034	88.753
233	27.299	15.848	3.732	3.893	0.477	22.478	73.727
234	38.107	21.98	5.901	5.205	0.569	28.071	99.834

WB137 - Garnet Composition Data

Results in Oxide Weight Percent

Traverse Poin	SiO ₂	Al ₂ O ₃	MgO	CaO	MnO	FeO	Sum
Garnet 3, Traverse 1							
396	38.448	22.083	6.966	4.895	0.35	27.106	99.849
397	38.302	22.057	6.847	3.965	0.349	28.218	99.738
398	38.214	21.72	6.579	5.066	0.336	27.521	99.436
399	38.227	22.112	7.176	4.702	0.436	26.19	98.841
400	42.294	24.612	7.758	5.141	0.417	27.04	107.262
401	38.386	22.078	6.476	5.569	0.412	27.055	99.976
402	38.303	22.123	6.945	4.7	0.882	27.115	100.067
403	38.137	21.89	6.26	5.683	0.457	26.788	99.217
404	38.272	21.966	6.231	5.142	0.477	27.656	99.743
405	38.41	22.143	6.089	5.139	0.476	27.918	100.175
406	38.286	22.034	6.094	4.395	0.624	28.543	99.976
407	38.258	21.873	5.787	5.359	0.64	27.953	99.871
408	36.845	21.027	6.028	5.494	0.634	28.056	98.084
409	100.792	0.015	-0.004	0.014	0.024	0.62	101.461
410	38.105	21.816	5.458	5.486	0.808	28.382	100.054
411	33.681	19.919	5.057	5.662	0.846	27.415	92.581
412	37.67	21.717	5.224	5.39	0.919	28.564	99.483
413	37.972	21.65	5.371	4.647	0.991	29.11	99.742
414	38.089	21.815	5.361	4.768	1.066	29.07	100.169
415	38.067	21.961	5.271	4.76	1.112	28.759	99.929
416	37.767	21.862	5.102	5.316	1.121	28.681	99.85
417	37.843	21.883	5.02	5.281	1.27	28.929	100.226
418	36.559	21.253	4.939	5.263	1.461	28.64	98.116
419	37.949	21.87	4.887	4.839	1.452	29.095	100.092
420	38.142	21.726	4.825	5.602	1.904	28.034	100.234
421	47.774	41.541	0.104	0.599	0.001	0.976	90.994
422	46.37	39.479	0.083	0.433	0.017	1.085	87.468
423	37.754	21.832	4.785	5.355	1.84	28.453	100.018
424	41.8	23.882	4.661	5.508	1.75	27.961	105.561
425	36.902	21.218	4.202	5.662	1.925	28.014	97.924
426	38.145	21.817	4.403	5.616	1.978	28.58	100.54
427	37.856	21.536	4.405	5.424	2.159	28.3	99.681
428	37.972	21.634	4.439	5.349	2.279	28.788	100.461
429	38.151	21.597	4.283	5.922	2.314	27.904	100.172
430	38.109	21.65	4.333	5.891	2.324	27.932	100.24
431	41.62	37.235	0.135	0.37	0.024	1.381	80.765
432	38.201	21.632	4.741	5.673	1.962	27.946	100.155
433	38.014	21.722	4.607	5.859	2.213	27.952	100.367
434	28.474	23.467	14.157	0.13	0.212	22.889	89.329
435	100.761	-0.002	-0.005	0.001	0.005	0.216	100.977
436	100.4	-0.003	-0.011	-0.001	-0.002	0.002	100.385
437	100.624	0.023	-0.011	0.001	-0.006	0.08	100.71
438	38.212	21.916	5.219	4.285	2.43	28.291	100.355
439	100.744	-0.004	-0.006	0.013	0.034	0.358	101.138
440	42.92	24.537	4.672	4.998	1.873	25.966	104.966
441	37.915	21.368	4.096	5.803	3.089	27.664	99.936
442	36.116	20.619	3.779	5.812	3.121	27.785	97.232
443	20.347	18.725	11.667	0.271	0.461	24.832	76.304
444	38.312	21.522	5.07	6.25	1.982	26.793	99.928
445	0.111	0.009	0.055	50.308	0.039	0.114	50.635
446	94.455	0.017	-0.01	1.472	0.012	0.021	95.967
447	100.497	-0.011	-0.006	0.017	0.003	0.021	100.521
448	100.585	0.011	0.007	0.003	0.002	0.033	100.641
449	102.366	0.004	-0.002	0.002	0.005	0.026	102.401
450	101.015	-0.003	-0.001	0.003	0.011	0.048	101.072
451	101.146	0.005	-0.009	0.01	0.004	0.047	101.202
452	101.281	0.002	0.003	0.007	-0.005	0.158	101.448
453	100.917	-0.002	-0.001	0.005	0.006	0.195	101.12
454	100.871	0.005	0.003	0.005	0.018	0.209	101.112
455	39.708	22.68	5.792	6.072	1.609	26.322	102.184
456	38.704	21.858	5.769	5.887	1.496	26.625	100.338
457	101.034	0.01	0	0.008	0.022	0.3	101.374
458	101.036	0.039	0.007	0.005	0.009	0.122	101.218
459	100.578	0.015	0.002	0.004	0.026	0.18	100.805
460	95.178	0.104	0.011	0.026	0.012	0.347	95.679
461	36.601	20.758	4.487	5.596	1.297	27.94	96.678
462	38.081	21.714	4.803	5.614	1.381	28.302	99.895
463	38.217	21.899	4.837	5.712	1.363	28.499	100.527
464	38.421	21.763	5.041	5.697	1.285	28.485	100.693

WB137 - Garnet Composition Data

Results in Oxide Weight Percent

Traverse Poin	SiO ₂	Al ₂ O ₃	MgO	CaO	MnO	FeO	Sum
Garnet 3, Traverse 1							
465	38.269	21.631	4.817	5.602	1.314	28.72	100.354
466	38.529	21.789	4.831	5.754	1.248	28.508	100.659
467	25.911	17.215	7.154	3.142	0.685	27.462	81.569
468	42.152	24.122	6.142	5.576	1.196	27.56	106.748
469	100.762	0.019	-0.002	0.01	0.028	0.379	101.197
470	101.132	0.002	0	0.006	0.004	0.35	101.494
471	38.346	21.611	5.145	5.374	1.116	28.71	100.302
472	38.617	21.876	5.467	5.15	1.084	28.611	100.805
473	38.538	21.872	5.33	5.15	1.047	29.117	101.053
474	38.395	21.794	5.304	5.432	1.017	28.054	99.995
475	38.744	21.973	5.346	5.765	0.938	27.943	100.709
Garnet 3, Traverse 2							
476	38.194	21.944	6.957	4.667	0.38	27.181	99.324
477	38.207	22.205	7.057	4.478	0.383	27.461	99.792
478	38.265	22.113	6.415	4.529	0.332	28.797	100.45
479	38.018	21.845	6.241	4.729	0.38	28.564	99.777
480	24.107	22.14	16.663	0.034	0.099	20.639	83.683
481	37.98	22.077	6.24	4.686	0.422	28.186	99.591
482	39.397	26.04	1.213	1.283	0.134	8.205	76.27
483	38.339	22.206	6.06	5.273	0.543	27.742	100.164
484	37.917	21.996	5.879	5.205	0.596	27.945	99.538
485	37.92	22.174	5.834	5.164	0.627	28.535	100.254
486	44.033	27.125	0.407	0.164	0.021	3.229	74.979
487	37.732	21.824	5.442	5.384	0.763	28.178	99.323
488	37.915	21.969	5.349	5.488	0.794	28.232	99.747
489	37.954	22.06	5.248	5.643	0.795	28.551	100.252
490	37.857	21.98	5.219	5.511	0.853	28.476	99.896
491	38.021	21.848	5.256	5.472	0.862	28.589	100.047
492	38.096	21.834	5.237	5.321	0.952	28.767	100.208
493	37.748	21.709	5.151	5.241	0.973	28.822	99.644
494	38.152	21.887	5.069	5.579	1.019	28.444	100.15
495	38.095	21.88	4.977	5.875	1.035	28.608	100.47
496	38.101	21.807	4.923	5.913	1.048	27.991	99.783
497	35.286	20.504	4.626	4.931	0.949	28.409	94.705
498	38.64	22.132	5.456	5.866	1.158	27.492	100.744
499	37.632	21.643	5.813	1.551	1.414	31.3	99.353
500	38.407	22.048	6.612	2.215	1.23	29.798	100.309
501	100.281	0.013	-0.007	-0.001	0.005	0.286	100.578
502	38.269	21.908	5.468	5.584	1.218	27.781	100.229
503	37.936	21.782	4.642	6.123	1.359	28.367	100.208
504	38	21.635	4.632	5.85	1.456	28.626	100.199
505	37.892	21.561	4.621	5.687	1.497	28.648	99.906
506	37.716	21.568	4.658	5.535	1.5	28.963	99.939
507	37.955	21.739	4.579	5.527	1.516	28.629	99.945
508	37.64	21.364	4.511	5.867	1.56	28.674	99.617
509	37.734	21.729	4.572	5.445	1.561	28.763	99.804
510	37.543	21.581	4.61	5.46	1.634	28.57	99.398
511	37.861	21.689	4.442	6.032	1.602	28.525	100.15
512	37.803	21.522	4.578	5.231	1.706	29.571	100.411
513	37.924	21.528	4.456	5.831	1.686	28.885	100.31
514	37.74	21.819	4.384	6.016	1.646	28.357	99.963
515	38.086	21.727	4.639	5.291	1.735	29.03	100.507
516	97.97	1.944	0.29	0.206	0.142	1.852	102.405
517	37.941	21.885	4.569	5.632	1.793	28.477	100.297
518	38.363	21.814	4.86	5.257	1.975	28.372	100.64
519	37.771	21.692	4.32	5.65	2.212	28.243	99.887
520	38.618	21.985	4.622	5.909	1.837	28.344	101.315
521	37.851	21.667	4.391	5.96	1.871	28.565	100.305
522	37.642	21.6	4.611	5.133	1.979	29.051	100.016
523	37.787	21.479	4.492	5.476	2.002	28.892	100.127
524	37.758	21.702	4.401	5.536	1.989	28.865	100.251
525	37.991	21.67	4.374	5.836	1.951	28.755	100.578
526	38.329	21.909	4.476	5.883	1.941	28.448	100.986
527	37.673	21.615	4.321	6.057	1.839	28.554	100.059
528	37.96	21.505	4.358	5.787	1.8	28.151	99.56
529	38.248	22.478	4.519	5.668	1.681	28.433	101.026
530	37.686	21.659	4.491	5.851	1.655	28.548	99.89
531	37.917	21.643	4.529	6.015	1.594	28.545	100.242
532	37.946	21.536	4.606	5.82	1.499	28.869	100.278

WB137 - Garnet Composition Data
Results in Oxide Weight Percent

Traverse Poin	SiO ₂	Al ₂ O ₃	MgO	CaO	MnO	FeO	Sum
Garnet 3, Traverse 2							
533	38.176	21.688	4.673	5.991	1.434	28.219	100.181
534	38.035	21.847	4.842	6.073	1.375	27.999	100.171
535	97.543	0.016	-0.001	0.012	0	0.178	97.747
536	100.446	-0.005	-0.008	0.006	0.014	0.013	100.466
537	101.084	0.012	-0.005	0.003	0.017	0.023	101.134
538	100.781	0.017	0.003	0.006	0.009	0.098	100.914
539	38.412	21.98	5.566	5.515	1.112	27.408	99.993
540	38.647	21.824	5.934	5.642	0.696	28.089	100.831
541	38.488	22.22	6.721	4.056	0.502	28.541	100.527
542	36.636	64.115	0.001	0.005	-0.008	0.978	101.727
543	30.541	56.044	1.55	-0.007	0.169	10.679	98.976
544	21.922	19.397	12.216	0.12	0.149	22.141	75.945
545	38.501	22.228	6.805	5.32	0.501	27.021	100.376
546	38.712	22.044	6.646	4.587	0.431	28.257	100.676
547	38.581	22.064	6.455	4.981	0.44	28.076	100.598
548	38.551	22.096	6.467	5.43	0.448	27.109	100.101
549	100.465	0.018	-0.011	0.014	0.008	0.359	100.853
550	38.686	22.103	6.831	4.543	0.339	27.957	100.459
551	38.383	22.111	6.658	4.715	0.407	27.759	100.033
552	38.668	22.394	6.973	4.777	0.376	27.131	100.319
553	38.59	22.183	7.06	4.616	0.324	27.471	100.244
554	38.837	22.239	7.392	4.32	0.402	27.247	100.437
555	39.113	22.92	8.117	4.009	0.45	26.398	101.008

Bibliography

- Aerden, D. and Sayab, M. (2008). From Adria-to Africa-driven orogenesis: Evidence from porphyroblasts in the Betic Cordillera, Spain. *Journal of Structural Geology*, 30(10):1272–1287.
- Anczkiewicz, R., Platt, J., Thirlwall, M., and Wakabayashi, J. (2004). Franciscan subduction off to a slow start: evidence from high-precision Lu–Hf garnet ages on high grade-blocks. *Earth and Planetary Science Letters*, 225:147–161.
- Andriessen, P. A. M., Hebeda, E. H., Simon, O. J., and Verschure, R. H. (1991). Tourmaline K-Ar ages compared to other radiometric dating systems in Alpine anatectic leucosomes and metamorphic rocks (Cyclades and southern Spain). *Chemical Geology*, 91(1):33–48.
- Arnaud, N. and Kelley, S. (1995). Evidence for excess argon during high pressure metamorphism in the Dora Maira Massif (western Alps, Italy), using an ultra-violet laser ablation microprobe ^{40}Ar - ^{39}Ar technique. *Contributions to Mineralogy and Petrology*, 121(1):1–11.
- Augier, R., Agard, P., Monie, P., Jolivet, L., and Robin, C. (2005a). Exhumation, doming and slab retreat in the Betic Cordillera (SE Spain): *in*

- situ* $^{40}\text{Ar}/^{39}\text{Ar}$ ages and P-T-d-t paths for the Nevado-Filabride complex. *Journal of Metamorphic Geology*, 23:357–381.
- Augier, R., Booth-Rea, G., Agard, P., Martínez-Martínez, J., Jolivet, L., and Azañón, J. (2005b). Exhumation constraints for the lower Nevado-Filabride Complex (Betic Cordillera, SE Spain): a Raman thermometry and Tweeku multiequilibrium thermobarometry approach. *Bulletin de la Societe Geologique de France*, 176(5):403.
- Azañón, J. and Goffé, B. (1997). Ferro- and magnesiocarpholite assemblages as record of the high-P, low-T metamorphism in the Central Alpujarrides, Betic Cordillera (SE Spain). *European Journal of Mineralogy*, 9:1035–1051.
- Bakker, H., de Jong, K., Helmers, H., and Biermann, C. (1989). The geodynamic evolution of the Internal Zone of the Betic Cordilleras (southeast Spain): a model based on structural analysis and geothermobarometry. *Journal of Metamorphic Geology*, 7(3):359–381.
- Balanya, J., García-Dueñas, V., and Azañón, J. (1997). Alternating contractional and extensional events in the Alpujarride nappes of the Alboran Domain (Betics, Gibraltar Arc). *Tectonics*, 16(2):226–238.
- Behr, W. M. and Platt, J. P. (2012). Kinematic and thermal evolution during two-stage exhumation of a Mediterranean subduction complex. *Tectonics*, 31(4):TC4025.

- Bezada, M. J., Humphreys, E. D., Toomey, D. R., Harnafi, M., Dávila, J. M., and Gallart, J. (2013). Evidence for slab rollback in westernmost Mediterranean from improved upper mantle imaging. *Earth and Planetary Science Letters*, 368(Complete):51–60.
- Blanco, M. J. and Spakman, W. (1993). The P-wave velocity structure of the mantle below the Iberian Peninsula: evidence for subducted lithosphere below southern Spain. *Tectonophysics*, 221(1):13–34.
- Briend, M., Montenat, C., and Ott, d. (1990). P.(1990) le bassin de huercal overa. *Doc. et Trav. IGAL*, pages 12–13.
- Calvert, A., Sandvol, E., Seber, D., Barazangi, M., Roecker, S., Mourabit, T., Vidal, F., Alguacil, G., and Jabour, N. (2000). Geodynamic evolution of the lithosphere and upper mantle beneath the Alboran region of the western Mediterranean: Constraints from travel time tomography. *Journal of Geophysical Research-Solid Earth*, 105(B5):10,871–10,898.
- Chalouan, A. and Michard, A. (1990). The ghomarides nappes, rif coastal range, morocco: A variscan chip in the alpine belt. *Tectonics*, 9(6):1565–1583.
- Comas, M., Platt, J., Soto, J. I., and Watts, A. (1999). The origin and tectonic history of the Alboran Basin: insights from Leg 161 results. *Proceedings of the Ocean Drilling Program. Scientific results*, 161:555–580.

- de Jong, K. (2003). Very fast exhumation of high-pressure metamorphic rocks with excess ^{40}Ar and inherited ^{87}Sr , Betic Cordilleras, southern Spain. *Lithos*, 70(3-4):91–110.
- de Jong, K., Féraud, G., Ruffet, G., and Amouric, M. (2001). Excess argon incorporation in phengite of the Mulhacén Complex: submicroscopic illitization and fluid ingress during late Miocene extension in the Betic Zone, south-eastern Spain. *Chemical Geology*, 178:159–195.
- De Roever, W. and Nijhuis, H. J. (1964). Plurifacial alpine metamorphism in the eastern betic cordilleras (se Spain), with special reference to the genesis of the glaucophane. *Geologische Rundschau*, 53(1):324–336.
- Dempster, T. J., Hay, D. C., Gordon, S. H., and Kelly, N. M. (2008). Microzircon: origin and evolution during metamorphism. *Journal of Metamorphic Geology*, 26(5):499–507.
- Duchêne, S. and Lardeaux, J. (1997). Exhumation of eclogites: insights from depth-time path analysis. *Tectonophysics*, 280(1):125–140.
- García-Dueñas, V., Martínez-Martínez, J., Orozco, M., and Soto, J. I. (1988). Plis-nappes, cisaillements syn- a post-metamorphiques et cisaillements ductiles-fragiles en distension dans les Nevado-Filabrides (Cordilleres Betiques, Espagne). *Comptes Rendus Academie Sciences, Paris*, 307:1389–1395.

- Glodny, J., Kühn, A., and Austrheim, H. (2007). Geochronology of fluid-induced eclogite and amphibolite facies metamorphic reactions in a subduction–collision system, Bergen Arcs, Norway. *Contributions to Mineralogy and Petrology*, 156(1):27–48.
- Glodny, J., Ring, U., and Kühn, A. (2008). Coeval high-pressure metamorphism, thrusting, strike-slip, and extensional shearing in the Tauern Window, Eastern Alps. *Tectonics*, 27(4):TC4004.
- Glodny, J., Ring, U., Kühn, A., Gleissner, P., and Franz, G. (2005). Crystallization and very rapid exhumation of the youngest alpine eclogites (tauern window, eastern alps) from Rb/Sr mineral assemblage analysis. *Contributions to Mineralogy and Petrology*, 149(6):699–712.
- Goffé, B., Michard, A., García-Dueñas, V., Gonzales-Lodeiro, F., Monie, P., Campos, J., Galindo-Zaldívar, J., Jabaloy, A., Martínez-Martínez, J., and Simancas, J. F. (1989). First evidence of high-pressure, low-temperature metamorphism in the Alpujarride nappes, Betic Cordilleras (S. E. Spain). *European Journal of Mineralogy*, 1(1):139.
- Gomez-Pugnaire, M. and Fernández-Soler, J. (1987). High-pressure metamorphism in metabasites from the Betic Cordilleras (SE Spain) and its evolution during the Alpine orogeny. *Contributions to Mineralogy and Petrology*, 95:231–244.
- Gomez-Pugnaire, M., Rubatto, D., Fernández-Soler, J. M., Jabaloy, A., Lopez Sanchez-Vizcaino, V., González-Lodeiro, F., Galindo-Zaldívar, J.,

- and Padrón-Navarta, J. A. (2012). Late Variscan magmatism in the Nevado-Filábride Complex: U-Pb geochronologic evidence for the pre-Mesozoic nature of the deepest Betic complex (SE Spain). *Lithos*, 146-147(C):93–111.
- Hacker, B. R. and Wang, Q. (1995). Ar/Ar geochronology of ultrahigh-pressure metamorphism in central China. *Tectonics*, 14(4):994–1006.
- Jabaloy, A., Galindo-Zaldívar, J., and González-Lodeiro, F. (1993). The Alpujarride-Nevado-Filábride extensional shear zone, Betic Cordillera, SE Spain. *Journal of Structural Geology*, 15(3-5):555–569.
- Johnson, C., Harbury, N., and Hurford, A. (1997). The role of extension in the Miocene denudation of the Nevado-Filabride Complex, Betic Cordillera (SE Spain). *Tectonics*, 16(2):189–204.
- Kullerud, L. (1991). On the calculation of isochrons. *Chemical Geology: Isotope Geoscience section*, 87(2):115–124.
- Kylander-Clark, A., Hacker, B. R., and Johnson, C. M. (2007). Coupled Lu–Hf and Sm–Nd geochronology constrains prograde and exhumation histories of high- and ultrahigh-pressure eclogites from western Norway. *Chemical Geology*, 242(1):137–154.
- Ludwig, K. (1999). Isoplot/Ex Ver 2.06: a geochronological toolkit for Microsoft Excel. *Berkeley Geochronology Center Special Publications*.
- Mancilla, F. d. L., Stich, D., Berrocoso, M., Martin, R., Morales, J., Fernandez-Ros, A., Paez, R., and Perez-Pena, A. (2013). Delamination

- in the Betic Range: Deep structure, seismicity, and GPS motion. *Geology*, 41(3):307–310.
- Martínez-Martínez, J. (1984). Las sucesiones Nevado-Filabrides en la Sierra de los Filabres y Sierra Nevada. Correlaciones. *Cuad Geol Univ Granada*, 12:127–144.
- Martínez-Martínez, J. (1986). Evolucion tectono-metamorfica del Complejo Nevado-Filabride en el sector de union entre Sierra Nevada y Sierra de Los Filabres (Cordilleras Beticas). *Cuad Geol Univ Granada*, 13:1–194.
- Martínez-Martínez, J., Soto, J. I., and Balanya, J. C. (2002). Orthogonal folding of extensional detachments: Structure and origin of the Sierra Nevada elongated dome (Betics, SE Spain). *Tectonics*, 21(3).
- Monie, P., Galindo-Zaldívar, J., González-Lodeiro, F., Goffé, B., and Jabaloy, A. (1991). $^{40}\text{Ar}/^{39}\text{Ar}$ geochronology of Alpine tectonism in the Betic Cordilleras (southern Spain). *Journal of the Geological Society, London*, 148(2):289.
- Monie, P., Torres-Roldan, R., and Garcia-Casco, A. (1994). Cooling and exhumation of the Western Betic Cordilleras, $^{40}\text{Ar}/^{39}\text{Ar}$ thermochronological constraints on a collapsed terrane. *Tectonophysics*, 238:353–379.
- Montenat, C. and Ott, d. (1999). The diversity of late neogene sedimentary basins generated by wrench faulting in the eastern betic cordillera, SE Spain. *Journal of Petroleum Geology*, 22:61–80.

- Mora, M. (1993). *Tectonic and sedimentary analysis of the Huércal-Overa region, SE Spain, Betic Cordillera*. PhD thesis, Oxford University, Oxford England.
- Müller, W., Mancktelow, N. S., and Meier, M. (2000). Rb–Sr microchrons of synkinematic mica in mylonites: an example from the DAV fault of the Eastern Alps. *Earth and Planetary Science Letters*, 180(3-4):385–397.
- Platt, J., Anczkiewicz, R., Soto, J. I., and Kelley, S. (2006). Early Miocene continental subduction and rapid exhumation in the western Mediterranean. *Geology*, 34(11):981–984.
- Platt, J., Argles, T., Carter, A., and Kelley, S. (2003a). Exhumation of the Ronda peridotite and its crustal envelope: constraints from thermal modelling of a P-T-time array. *Journal of the Geological Society, London*, 160:655–676.
- Platt, J. and Behrmann, J. H. (1986). Structures and fabrics in a crustal-scale shear zone, Betic Cordillera, SE Spain. *Journal of Structural Geology*, 8(1):15–33.
- Platt, J., Behrmann, J. H., Martínez-Martínez, J., and Vissers, R. (1984). A zone of mylonite and related ductile deformation beneath the Alpujarride Nappe Complex, Betic Cordilleras, S. Spain. *International Journal of Earth Sciences*, 73(2):773–785.

- Platt, J., Kelley, S., Carter, A., and Orozco, M. (2005). Timing of tectonic events in the Alpujarride Complex, Betic Cordillera, southern Spain. *Journal of the Geological Society, London*, 162:451–462.
- Platt, J., Soto, J. I., Whitehouse, M., Hurford, A., and Kelley, S. (1998). Thermal evolution, rate of exhumation, and tectonic significance of metamorphic rocks from the floor of the Alboran extensional basin, western Mediterranean. *Tectonics*, 17(5):671–689.
- Platt, J. and Vissers, R. (1989). Extensional collapse of thickened continental lithosphere; a working hypothesis for the Alboran Sea and Gibraltar Arc. *Geology*, 17(6):540–543.
- Platt, J., Whitehouse, M., Kelley, S., Carter, A., and Hollick, L. (2003b). Simultaneous extensional exhumation across the alboran basin: Implications for the causes of late orogenic extension. *Geology*, 31(3):251–254.
- Platt, J. P., Behr, W. M., Johanesen, K., and Williams, J. R. (2013). The Betic-Rif Arc and Its Orogenic Hinterland: A Review. *Annual Reviews in Earth and Planetary Sciences*, 41(1):130315140716009.
- Poisson, A., Morel, J., Andrieux, J., Coulon, M., Wernli, R., and Guernet, C. (1999). The origin and development of Neogene basins in the SE Betic Cordillera (SE Spain): A case study of the Tabernas-Sorbas and Huercal-Overa Basins. *Journal of Petroleum Geology*, 22(1):97–114.

- Priem, H., Boelrijk, N., Hebeda, E., and Verschure, R. (1966). Isotopic Age Determinations on Tourmaline Granite-gneisses and a Metagranite in the Eastern Betic Cordilleras, South-Eastern Sierra de Los Filabres, SE Spain. *Geologie en Mijnbouw*, 45:184–187.
- Puga, E. (1971). *Investigaciones petrológicas en Sierra Nevada Occidental, Cordilleras Béticas (España)*. PhD thesis, Departamento de Geología, Facultad de Ciencias Universidad de Granada.
- Puga, E. and Díaz de Federico, A. (1978). Metamorfismo polifásico y deformaciones alpinas en el complejo de sierra nevada (cordillera bética). implicaciones geodinámicas. *Reunión Geodinámica Cordilleras Béticas y Mar De Alborán*, pages 79–111.
- Puga, E., Nieto, J., Díaz de Federico, A., Bodinier, J., and Morten, L. (1999). Petrology and metamorphic evolution of ultramafic rocks and dolerite of the Betic Ophiolitic Association (Mulhacén Complex, SE Spain): evidence of eo-Alpine subduction following an ocean-floor metasomatic process. *Lithos*, 49:23–56.
- Raczek, I., Jochum, K. P., and Hofmann, A. W. (2003). Neodymium and Strontium Isotope Data for USGS Reference Materials BCR-1, BCR-2, BHVO-1, BHVO-2, AGV-1, AGV-2, GSP-1, GSP-2 and Eight MPI-DING Reference Glasses. *Geostandards Newsletter*, 27(2):173–179.
- Ring, U. and Layer, P. W. (2003). High-pressure metamorphism in the Aegean,

- eastern Mediterranean: Underplating and exhumation from the Late Cretaceous until the Miocene to Recent above the retreating Hellenic subduction zone. *Tectonics*, 22(3).
- Rosenbaum, G., Menegon, L., Glodny, J., Vasconcelos, P., Ring, U., Massironi, M., Thiede, D., and Nasipuri, P. (2012). Dating deformation in the Gran Paradiso Massif (NW Italian Alps): Implications for the exhumation of high-pressure rocks in a collisional belt. *Lithos*, 144145(0):130 – 144.
- Rubatto, D. (2002). Zircon trace element geochemistry: partitioning with garnet and the link between U–Pb ages and metamorphism. *Chemical Geology*, 184(1):123–138.
- Rubatto, D., Gebauer, D., and Fanning, M. (1998). Jurassic formation and Eocene subduction of the Zermatt–Saas-Fee ophiolites: implications for the geodynamic evolution of the Central and Western Alps. *Contributions to Mineralogy and Petrology*.
- Sanchez-Vizcaino, V., Rubatto, D., Gomez-Pugnaire, M., Trommsdorff, V., and Muntener, O. (2001). Middle Miocene high-pressure metamorphism and fast exhumation of the Nevado-Filabride Complex, SE Spain. *Terra Nova*, 13(5):327–332.
- Scherer, E., Cameron, K., and Blichert-Toft, J. (2000). Lu–Hf garnet geochronology: closure temperature relative to the Sm–Nd system and the effects of trace mineral inclusions. *Geochimica et Cosmochimica Acta*, 64(19):3413–3432.

- Sherlock, S. and Kelley, S. (2002). Excess argon evolution in HP–LT rocks: a UVLAMP study of phengite and K-free minerals, NW Turkey. *Chemical Geology*, 182(2-4):619–636.
- Sherlock, S., Kelley, S., Inger, S., Harris, N., and Okay, A. (1999). ^{40}Ar - ^{39}Ar and Rb-Sr geochronology of high-pressure metamorphism and exhumation history of the Tavsanli Zone, NW Turkey. *Contributions to Mineralogy and Petrology*, 137(1-2):46–58.
- Sosson, M., Morrillon, A.-C., Bourgois, J., Fraud, G., Poupeau, G., and Saint-Marc, P. (1998). Late exhumation stages of the Alpujarride Complex (western Betic Cordilleras, Spain): new thermochronological and structural data on Los Reales and Ojen nappes. *Tectonophysics*, 285(34):253 – 273. Extensional Tectonics and Exhumation of Metamorphic Rocks in Mountain Belts.
- Spakman, W. and Wortel, R. (2004). A tomographic view on western Mediterranean geodynamics. *The TRANSMED Atlas-The Mediterranean region from Crust to Mantle*, pages 31–52.
- Tubía, J., Cuevas, J., Navarro-Vil, F., Alvarez, F., and Aldaya, F. (1992). Tectonic evolution of the Alpujarride Complex (Betic Cordillera, southern Spain). *Journal of Structural Geology*, 14(2):193 – 203.
- Vergés, J. and Fernandez, M. (2012). Tethys–Atlantic interaction along the Iberia–Africa plate boundary: The Betic–Rif orogenic system. *Tectonophysics*, 579:144–172.

- Visser, R., Platt, J., and van der Wal, D. (1995). Late orogenic extension of the Betic Cordillera and the Alboran Domain: A lithospheric view. *Tectonics*, 14(4):786–803.
- Visser, R. L. M. (1981). *A structural study of the central Sierra de los Filabres (Betic Zone, SE Spain), with emphasis on deformational processes and their relation to the Alpine metamorphism*. PhD thesis, University of Amsterdam.
- Wright, T., Baker, J., and Willigers, B. (2002). Rb isotope dilution analyses by MC-ICPMS using Zr to correct for mass fractionation: towards improved Rb–Sr geochronology? *Chemical Geology*, 186(1):99–116.
- Weijermars, R., Roep, T., van den Eeckhout, B., Postma, G., and Kleverlaan, K. (1985). Uplift history of a Betic fold nappe inferred from Neogene–Quaternary sedimentation and tectonics (in the Sierra Alhamilla and Almería, Sorbas and Tabernas Basins of the Betic Cordilleras, SE Spain). *Geologie en Mijnbouw*, 64:397–411.
- Whitehouse, M. and Platt, J. (2003). Dating high-grade metamorphism—constraints from rare-earth elements in zircon and garnet. *Contributions to Mineralogy and Petrology*, 145(1):61–74.
- Wilson, S. (1997). Data compilation for USGS reference material BHVO-2, Hawaiian basalt. *US Geological Survey Open-File Report*.
- Zhang, L., Ai, Y., Li, X., Rubatto, D., Song, B., Williams, S., Song, S., Ellis, D., and Liou, J. (2007). Triassic collision of western Tianshan orogenic

belt, China: Evidence from SHRIMP U-Pb dating of zircon from HP/UHP eclogitic rocks. *Lithos*, 96:266–280.

Vita

Kory Lee Kirchner was born in the the Basin and Range Province of the southwestern United States. After graduating from Arcadia High School, in 2009, he moved to the San Francisco Volcanic Field. He attended Northern Arizona University and earned a Bachelor of Science in Geology. He spent most of his free time hiking and climbing on the American Southwest and paddling canoes across the Canadian Shield. He graduated from Northern Arizona University in 2012. He left the Colorado Plateau in 2012 to pursue graduate studies at the Jackson School of Geosciences at The University of Texas at Austin.

Permanent address: KoryKirchner@utexas.edu

This thesis was typeset with L^AT_EX[†] by the author.

[†]L^AT_EX is a document preparation system developed by Leslie Lamport as a special version of Donald Knuth's T_EX Program.